Rheinland-Pfälzische
Technische Universität
Kaiserslautern
Landau

Characterization of Mitochondrial Protein Import Machineries in Plasmodium falciparum

Vom Fachbereich Chemie der Rheinland-Pfälzischen Technischen Universität zur Erlangung des akademischen Grades

“Doktor der Naturwissenschaften" (Dr. rer. nat.)

genehmigte Dissertation

D 386

Vorgelegt von

Felix Alexander Ayelazuno

geboren in Mirigu, Ghana

Betreuer: Prof. Dr. Marcel Deponte

Datum der Promotionsaussprache: Kaiserslautern, den 24.09.2025

Erklärung

lch erkläre hiermit, dass diese Arbeit ausschließlich von mir selbst verfasst wurde und einen Originalbericht meiner Forschungsarbeit darstellt, die ich unter der Aufsicht von Prof. Dr. Marcel Deponte durchgeführt habe. Die experimentellen Ergebnisse stammen ausschließlich von mir. Kollaborative Beiträge, unterstützende Literatur und Ressourcen sowie jegliche Form der von Kollegen erhaltenen Hilfe wurden im Text deutlich gekennzeichnet, anerkannt und ordnungsgemäß referenziert. lch erkläre, dass diese Arbeit kein Material enthält, das für die Verleihung eines anderen Abschlusses oder Diploms bzw. einer Prüfungsarbeit an einer Universität oder anderen tertiären Bildungseinrichtung akzeptiert wurde.

Kaiserslautern, den 18.08.2025 _____

Referees:

Prof. Dr. Marcel Deponte

Prof. Dr. Antonio Pierik

Prof. Dr. Georg Manolikakes

Prof. Dr. Jörg Fahrer

Dedication

To my senior brother, Prof. Jasper Abembia Ayelazuno, your unwavering support, both intellectually and financially, made this academic journey possible. Your sacrifices, encouragement, and belief in my potential have been guiding forces in my life. To my beloved wife, your love, patience, and steadfast presence gave me strength during the most demanding moments of this journey. To my parents, your prayers, values, and lifelong example of resilience laid the foundation for all I have achieved. Furthermore, to my two wonderful daughters, Delewine and Awintoya, may this accomplishment serve as a reminder that no dream is too distant when pursued with purpose and the support of family.

Acknowledgments

Firstly, I would like to extend my sincere gratitude to my supervisor, Prof. Dr. Marcel Deponte, for his exceptional mentorship, patience, and insightful guidance throughout this doctoral journey. His unwavering support and scientific rigor have shaped the foundation of this thesis. I am also very thankful to him for the many letters he wrote to the German Embassy in Ghana and the DAAD to support my study in Germany, even at the peak of COVID-19. My sincere appreciation to him for the kind support he gave to me and my family during and after the birth of my two kids during my doctoral studies. Secondly, I would also like to thank my entire doctoral committee, Prof. Dr. Antonio Pierik, Prof. Dr. Georg Manolikakes, and Prof. Dr. Jörg Fahrer for taking on this task.

Special thanks also go to Prof. Dr. Stefanie Müller-Schüssele and Sadia Sayed Tamanna for their tremendous support in optimizing the microscopy experiments. I want to thank Dr. Markus Räschle for conducting my MS analyses and supporting the data analyses, and Dr. Susanne Zehner for recording the immunofluorescence microscopy images for my work. I would also like to thank my colleagues Lukas, Eileen, Britta, Lea, Laura, Philipp, Fabian, Luzia, and Sophie. Thank you so much for your support! My time in the lab was a lot of fun. Even though things were not always easy, I could always rely on your open ears, friendly conversations, and advice. I would also like to thank all the students I supervised during my time in the lab and who supported me with parts of my work (Ellie, Bucket, Sipedeh, and Elisavert). Special thanks go to my family and my partner Eva, who supported me even in difficult times, and I am infinitely grateful to have you by my side. I also wish to sincerely thank the DAAD for funding my doctoral studies in Germany. Special mention to Dr. Cletus Wezena and Dr. Prince Amposah for their excellent counsel.

Abstract

Malaria remains a significant global health threat, with an estimated 263 million cases and 597,000 related deaths annually, especially among children under five years old. It is caused by Plasmodium parasites, which are transmitted to vertebrates through the bite of infected female Anopheles mosquitoes. Of the five parasites known to cause malaria in humans, *P. falciparum* is the deadliest and accounts for most malaria-related illness and death. Although significant progress has been made in reducing malaria, challenges such as drug and insecticide resistance remain.

Malaria parasites contain a small mitochondrion during the merozoite stage, which develops into an elongated tubular network in the schizont stage after invading red blood cells. This development requires the de novo synthesis of mitochondrial components, including the import and sorting of mitochondrial proteins. Although all living organisms have their own mitochondrial genome, nearly 99% of mitochondrial proteins are encoded in the nucleus, synthesized on cytosolic ribosomes, and then imported into the mitochondria. The process of importing proteins into mitochondria is believed to be highly conserved among eukaryotes. However, recent studies have revealed that the import machinery itself has undergone significant changes in various major eukaryotic lineages. The differences between the mitochondrial import machinery of malaria parasites and their hosts make mitochondria a promising target for drug development. Nevertheless, our understanding of mitochondrial protein import in malaria parasites and related apicomplexan parasites relies on poorly characterized components of the import machinery. To date, studies on the mitochondrial protein import machinery of malaria parasites have primarily relied on bioinformatics, with little experimental evidence validating their composition, sub-organellar localization, or interaction networks.

This thesis examined the composition and localizations of the components of the mitochondrial protein import machineries in malaria parasites. It also analyzed the interactomes of validated core components of these machineries. The findings demonstrated, for the first time in malaria parasites, the production and mitochondrial localization of the core components of mitochondrial import machineries. Specifically, the core subunits of the TOM and SAM complexes, *Pf*Tom40 and *Pf*Sam50, respectively, were successfully confirmed through confocal microscopy and western blot analyses. Similarly, two subunits of the PAM complex (*Pf*Hsp70 and *Pf*Mge1) and the central subunit of the OXA pathway, *Pf*Oxa1, were shown to be produced and localized in the mitochondria of malaria parasites. Western blot analyses also suggested the possible formation of Tim8/Tim13 hexamers in *P. falciparum*. Confocal microscopy revealed that Tim8, Tim13, and Pam16 are localized to the mitochondria of malaria parasites. Interactome analysis of *Pf*Mge1 showed significant enrichment

in the pulldown assay; however, *Pf*Mge1's interacting partners were not significantly enriched overall in this study. Additionally, the pulldown experiments for *Pf*Tom40 and *Pf*Sam50 did not show significant enrichment in the MS analyses. Future studies could explore chemical crosslinking and denaturing affinity purification methods to capture transient interacting partners and improve solubilization of integral membrane proteins. Gene knockout attempts for *PFHSP70* and *PFTOM40* indicated that transfection with circular plasmids could result in unwanted insertions or single crossovers in the parasite's genome; linearized plasmids are recommended.

Zusammenfassung

Malaria ist mit schätzungsweise 263 Millionen Fällen und 597.000 Todesfällen pro Jahr, insbesondere bei Kindern unter fünf Jahren, weiterhin eine globale Bedrohung für Menschenleben. Malaria wird durch Plasmodium-Parasiten verursacht, die durch den Stich infektiöser weiblicher

Anopheles-Mücken auf den Wirbeltierwirt übertragen werden. Von den fünf bekannten Malaria-Erregern beim Menschen ist P. falciparum der tödlichste und für den Großteil der malariabedingten Morbidität und Mortalität verantwortlich. Obwohl im Kampf gegen die Ausbreitung von Malaria beachtliche Erfolge erzielt wurden, bleiben Herausforderungen wie Medikamenten- und Insektizidresistenzen bestehen.

Malariaparasiten beherbergen im Merozoitenstadium ein kleines Mitochondrium, das sich nach dem Eindringen in die roten Blutkörperchen zu einem langgestreckten röhrenförmigen Netzwerk des Schizontenstadiums entwickelt. Diese Entwicklung erfordert die De-novo-Biosynthese mitochondrialen Materials, einschließlich des Imports und der Sortierung mitochondrialer Proteine. Obwohl die Mitochondrien aller Lebewesen ein eigenes Genom besitzen, sind fast 99 % aller mitochondrialen Proteine im Zellkern kodiert und müssen an Ribosomen im Zytosol synthetisiert und anschließend in die Mitochondrien importiert werden – der Import von Proteinen in die Mitochondrien galt bei Eukaryoten als hochkonserviert. Neuere Studien haben jedoch gezeigt, dass der Importmechanismus selbst in verschiedenen wichtigen eukaryotischen Linien signifikant verändert ist. Die Unterschiede zwischen dem Importmechanismus von Malariaparasiten und dem ihrer Wirte machen die Mitochondrien zu einem vielversprechenden Ziel für Medikamente. Das Verständnis des Proteinimports in die Mitochondrien von Malariaparasiten und den mit ihnen verwandten Apicomplexa-Parasiten basiert jedoch auf unzureichend charakterisierten Komponenten des mitochondrialen Proteinimportmechanismus. Bislang wurde der mitochondriale Proteinimportmechanismus von Malariaparasiten hauptsächlich mithilfe bioinformatischer Methoden analysiert, ohne dass experimentelle Daten zur Validierung der Zusammensetzung, der suborganellen Lokalisierung und des Interaktoms des mitochondrialen Importmechanismus von Malariaparasiten vorlagen.

Diese Arbeit untersuchte die Zusammensetzung und Lokalisierung der Komponenten des mitochondrialen Proteinimportmechanismus von Malariaparasiten. Die Interaktome validierter Kernkomponenten des Importmechanismus wurden ebenfalls analysiert. Die Ergebnisse dieser Arbeit zeigten erstmals bei Malariaparasiten die Produktion und mitochondriale Lokalisierung der Kernkomponenten des mitochondrialen Importmechanismus. Die Kernuntereinheiten des TOM- und SAM-Komplexes, *Pf*Tom40 bzw. *Pf*Sam50, wurden erfolgreich mittels konfokaler Mikroskopie und Western Blot-Analysen validiert. Ebenso wurde gezeigt, dass zwei Untereinheiten des PAM-Komplexes (*Pf*Hsp70 und *Pf*Mge1) sowie die zentrale Untereinheit des OXA-Signalwegs, *Pf*Oxa1, im Mitochondrium von Malariaparasiten produziert und lokalisiert werden. Western Blot analysiert außerdem die potenzielle Produktion und Bildung von Tim8/Tim13-Hexameren in *P. falciparum*. Konfokalmikroskopie ergab außerdem, dass Tim8, Tim13 und Pam16 im Mitochondrium von

Malariaparasiten lokalisiert sind. Die Interaktomanalyse von *Pf*Mge1 zeigte, dass es im Pulldown-Test signifikant angereichert war. Die Interaktionspartner von *Pf*Mge1 waren jedoch nach der statistischen Analyse in dieser Arbeit nicht signifikant angereichert. Auch das Pulldown-Experiment für *PfT*om40 und *Pf*Sam50 schien in der MS-Analyse nicht angereichert zu sein. Zukünftige Experimente könnten chemische Vernetzungs- und denaturierende Affinitätsreinigungsmethoden erforschen, um vorübergehende Interaktionspartner zu erfassen und die Solubilisierung integraler Membranproteine zu erhöhen. Gen-Knockout-Versuche für *PFHSP70* und *PFTOM40* haben gezeigt, dass die Transfektion zirkulärer Plasmide möglicherweise zu unerwünschten Insertionen oder einzelnen Crossover-Ereignissen im Genom des Malariaparasiten führen kann. Daher wird die Verwendung linearisierter Plasmide empfohlen.

Table of Contents

List of figures

List of tables

Abbreviations

°C	degree Celsius
α	anti
µg	microgram
µl	microliter
µm	micrometer
µM	micromolar
AB	antibody
µ	micro; 10^{-6}
ADP	adenosine diphosphate
ATP	adenosine triphosphate
bp	base pair
BSA	bovine serum albumin
C-terminus	C-terminus/carboxy terminus
Cas9	CRISPR associated with protein 9
cm	centimeter
CRISPR	clustered regularly interspaced short palindromic repeats
Da	Dalton
DAPI	4',6-diamidino-2-phenylindole
H2O	Water(Millipore)
DHFR	dihydrofolate reductase
DHODH	dihydroorotate dehydrogenase
DMSO	dimethyl sulfoxide
DNA	deoxyribonucleic acid
dNTP	deoxyribonucleoside triphosphate
DTT	dithiothreitol
E. coli	*Escherichia coli*
EDTA	ethylenediaminetetraacetic acid
Erv	essential for respiratory and vegetative growth protein
FBS	fetal bovine serum
g	gravitational force equivalent; $g \approx 9.81$ m/s^2
g	gram

h	hour
HA	human influenza hemagglutinin
HEPES	4-(2-hydroxyethyl)-1-piperazineethanesulfonic acid
HiFi	high Fidelity
HPLC	high-performance liquid chromatography
HRP	horseradish peroxidase
iRBC	infected red blood cell
kb	kilobase pair
kDa	kilodalton
KO	knock-out
L	liter
LB	lysogeny broth (Luria Bertani)
m	meter
M	molar
mg	milligram
min	minute
ml	milliliter
mM	millimolar
MeOH	methanol
Mia40	mitochondrial intermembrane space import and assembly protein 40
MS	mass spectrometry
nLC	nano-liquid chromatography
N-terminus	amino terminus
nm	nanometer
nM	nanomolar
P. Pf	*P. falciparum*
P value	*probabilitas* (probability) value
PAGE	polyacrylamide gel electrophoresis
PBS	phosphate buffered saline
PCR	polymerase chain reaction
PDB	Protein Data Bank
pH	*pondus hydrogenii*
PVDF	polyvinylidene difluoride
RBC	red blood cell

RNA	ribonucleic acid
rpm	revolutions per minute
RT	room temperature
s	second
S. cerevisiae	*Saccharomyces cerevisiae*
SDS	sodium dodecyl sulfate
sgRNA	single guide ribonucleic acid
SLI	Selection-linked integration
STAGE	stop and go extraction
TAE	Tris-acetate-EDTA buffer
TALENs	transcription activator-like type II effector nucleases
TBS	tris(hydroxymethyl)aminomethane buffered saline
TBS-T	tris(hydroxymethyl)aminomethane buffered saline 0.05% (m/v) Tween 20
TEMED	*N,N,N',N'*-tetramethyl ethylenediamine
TIM	translocase of the inner mitochondrial membrane
TM	transmembrane
TOM	translocase of the outer mitochondrial membrane
Tris	tris(hydroxymethyl)aminomethane
Triton	Triton X-100
SAM	sorting and assembly machinery
v/*v*	volume per volume
WR	WR99210
w/*v*	weight per volume
WHO	World Health Organization
WT	wild-type
ydhodh	yeast dihydroorotate dehydrogenase gene
yfcu	yeast fusion cytosine deaminase and uridyl phosphoribosyl transferase
ZFNs	zinc-finger nucleases

1 Introduction

1.1 Malaria

Malaria is a disease caused by *Plasmodium* parasites. There are five species to date out of the over 120 existing species that are known to cause malaria infection in humans: *P. falciparum, P. malariae, P. ovale, P. vivax,* and *P. knowlesi. P. falciparum* is the most virulent among these species and is responsible for most of the malaria morbidity and mortality (Varo et al., 2020; Weiland, 2023). *P. vivax* is thought to cause uncomplicated malaria, even though there is evidence of its potential to cause severe malaria (Naing et al., 2014). Both *P. malariae* and *P. ovale* are known also to cause uncomplicated malaria, whilst *P. knowlesi* is transmitted to humans from primates and can cause severe manifestations. Malaria infection occurs after the bite of an infected female *Anopheles* mosquito, and on rare occasions, human-to-human transmissions may occur through blood transfusion, organ transplantation, and vertically from mother to newborn (Varo et al., 2020; Weiland, 2023). Symptoms include fever, chills, and headache that predominantly begin after 10 to 15 days (Bartoloni & Zammarchi, 2012).

1.2 The global burden of malaria

Malaria is currently endemic in 83 countries globally, putting nearly half of the world's population at risk of the disease (WHO,2023). This endemicity encompasses portions of the Eastern Mediterranean, Southeast Asia, Western Pacific, the Americas, and all countries of the sub-Saharan African region (WHO,2023). Annually estimated malaria cases remained stable between the year 2000 and 2019, varying between 227 million and 248 million across malaria-endemic countries (WHO, 2023). This led to an overall reduction of 60% in malaria-related deaths compared to previous years (WHO, 2023), renewing the enthusiasm of the global health community in the push to eradicate malaria. However, since 2020, there has been a stall in the progress of reducing malaria burden, with a set of countries progressing towards malaria eradication, whilst another set of countries are showing an alarming rate of malaria case incidents (WHO, 2023). In 2023, there was a global estimate of 263 million malaria cases in 83 malaria-endemic countries, an increase of about 11 million cases compared with 2022. From 2021 to 2023, deaths caused by malaria were estimated to be between 578000 and 569000, with 95% of deaths occurring in the African region (WHO, 2023). Children under the age of five bore the most significant burden of malaria, accounting for 67% of all malaria-related deaths (WHO, 2023). *P. falciparum* remains the most virulent, accounting for

approximately 99% of malaria cases in the African region. Also, in the western Pacific region, it accounts for 71% of malaria cases, 69% the eastern Mediterranean, and about 63% in Southeast Asia (WHO, 2023). *P vivax* remains the driving force for the burden of malaria in the Americas and Southeast Asia. The case is, however, different for Sub-Saharan Africans due to the absence of the Duffy binding antigen in the human population (Ashley et al., 2018). *P. ovale* and *P. malarae* are distributed globally; however, their overall prevalence is relatively low (Ashley et al., 2018)

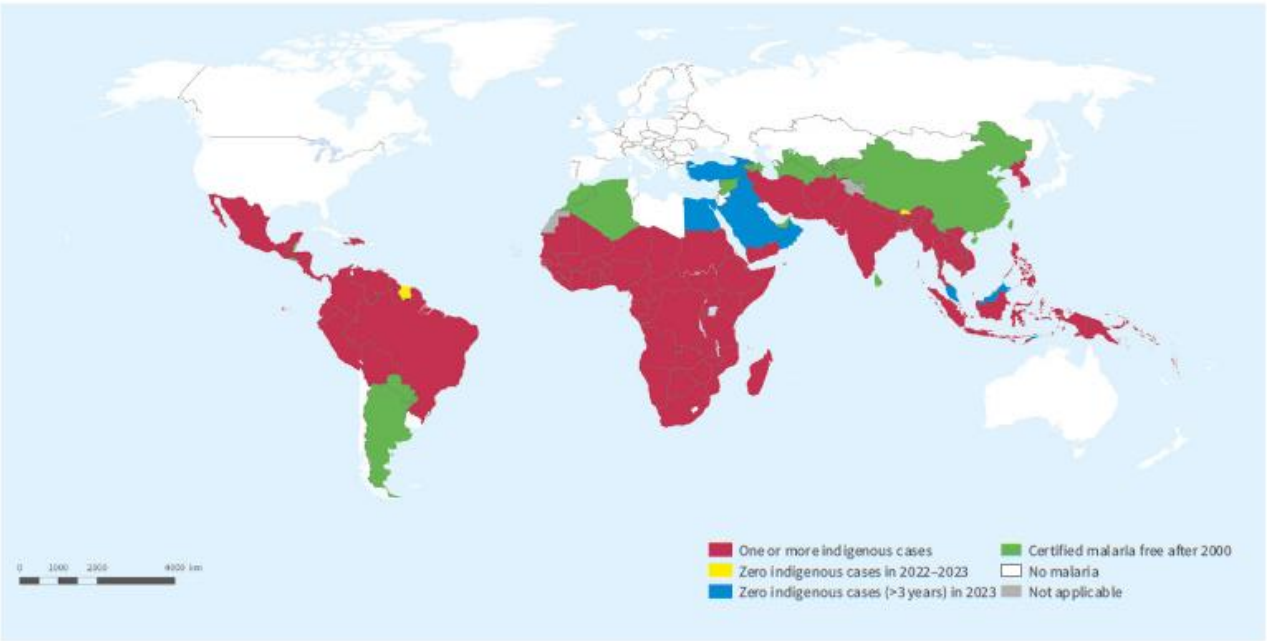

Figure 1 Distribution of malaria worldwide. Global distribution of malaria, with red zones having one or more indigenous cases, no malaria for white zones, and green zones being certified malaria-free for the last 2 decades (WHO, 2023).

1.3 The life cycle of *P. falciparum*

The complex life cycle of malaria parasites is characterized by successive rounds of asexual and sexual replication across various stages and tissues, in both the intermediate vertebrate host and the insect vector. In sexual reproduction, gametocytes are continuously formed in the red blood cells in the vertebrate host, while transmission to the insect host is required for gametogenesis and meiosis to occur. For most *Plasmodium* species, the highest number of cells is reached during asexual replication in circulating red blood cells of the vertebrate host, and a small proportion of the asexual parasites differentiate into sexual stages (Venugopal et al., 2020).

Transmission from mosquitoes to vertebrates occurs when *Plasmodium* sporozoites migrate from the salivary glands of an infected female *Anopheles* mosquito to the dermis of a vertebrate during a bite. The sporozoites actively invade the bloodstream and are transported to the liver, thereby evading the host immune system or clearance through the lymphatic system (Amino et al., 2006; Tavares et al., 2013). Once they arrive at the liver sinusoids, they cross the sinusoid barrier and

infect the hepatocytes and establish a parasitophorous vacuole where they differentiate in the first round of asexual replication (Mota et al., 1997; Tavares et al., 2013). For two to several days, depending on the *Plasmodium* species, a multinucleated exoerythrocytic schizont or meront harboring thousands of daughter merozoites is formed. Once they egress from the hepatocytes, the merozoites, clustered in membrane-bound vesicles called merosomes, are released into the bloodstream through the liver sinusoids. In the bloodstream, the merozoites invade the red blood cells and undergo erythrocytic schizogony, producing up to 32 merozoites per schizont over the course of 24 to 72 hours. Through repeated invasion cycles and replication, the parasites establish an acute infection that progresses to a chronic infection (Venugopal et al., 2020). Commonly, in *P. falciparum* infections, the parasites invade a high proportion of the red blood cells, leading to a high parasite burden, which is a characteristic feature of their capacity to cause severe malaria. In other *Plasmodium* species, such as P. vivax, their infection is restricted to reticulocytes, which make up a small proportion of red blood cells, therefore limiting the parasite burden. To initiate the sexual cycle, a proportion of the trophozoites are reprogrammed to differentiate into sexual stage male and female gametocytes that are infectious for a mosquito (Kafsack et al., 2014). The mature gametocytes circulate in the bloodstream for several days to increase their chances of being taken up by a mosquito. Once they are taken up and transported to the midgut of a female mosquito, the male and female gametocytes exit the red blood cells using proteases and differentiate into eight microgametes and one macrogamete, respectively. One microgamete fuses with a macrogamete to produce a zygote, which transforms into a motile ookinete capable of crossing the epithelial layer of the midgut wall to form an oocyst. The parasites then undergo a third round of asexual replication in the oocyst to produce several sporozoites. Hundreds of motile sporozoites are transported to the salivary glands, where they can be transmitted to the next human host during a blood meal of the female mosquito to continue the cycle (Cowman et al., 2016).

.

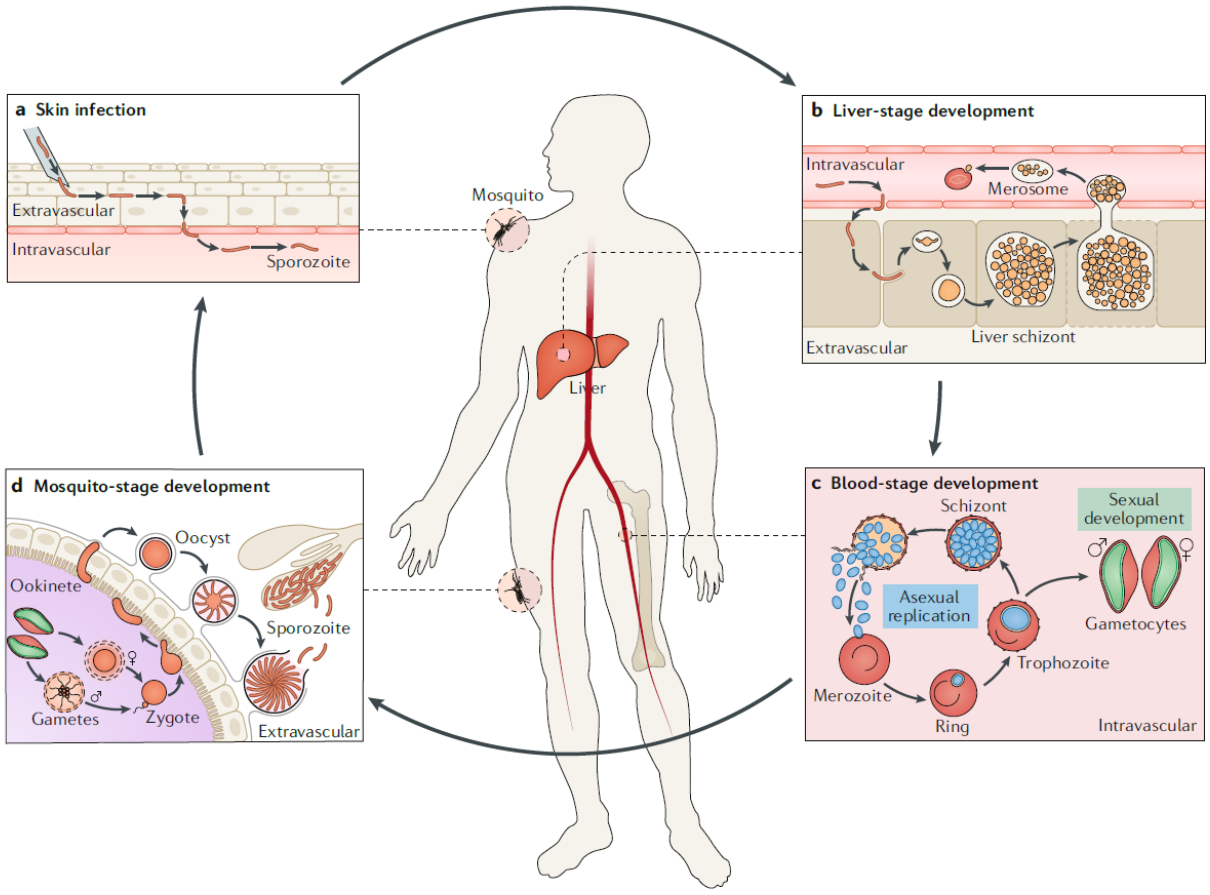

Figure 2 The life cycle of P. falciparum. (a) *P. falciparum* sporozoites (orange) are injected into the skin during the blood meal of an infected mosquito, where they migrate into the blood capillaries. (b) The sporozoites reach the liver sinusoids, where they leave the blood circulation to invade hepatocytes. In the hepatocytes, they undergo one asexual replication cycle that leads to the formation of liver schizonts containing thousands of merozoites (yellow). The merozoites enter the bloodstream in merosomes and are released to infect red blood cells (red) and initiate the intra-erythrocytic cycle. (c) *P. falciparum* parasites undergo cycles of asexual replication in the erythrocytes (blue). After the invasion of a red blood cell, they develop from ring stages to trophozoites and then to schizonts. Mature schizonts burst to release merozoites that initiate another replication cycle. A subpopulation of parasites commits to produce male and female sexual progeny or gametocytes (green). (d) A female *Anopheles* mosquito picks up gametocytes while feeding on an infected human. Male and female gametocytes undergo gametogenesis within the midgut of the mosquito. The gametes then fertilize to form a zygote (orange), which further develops into motile ookinetes. Ookinetes cross the midgut epithelium to form an oocyst beneath the basal lamina. Thousands of sporozoites are formed in the oocyst, which, upon bursting, enter the hemolymph to invade the salivary gland. From there, sporozoites are transmitted to the next human during the subsequent mosquito bite (Venugopal et al., 2020).

1.3.1 Asexual blood stages of *P. falciparum*

The red blood stage-invasion and subsequent replication of malaria parasites are mainly responsible for malaria pathogenesis and morbidity, which is typically characterized by fever and severe anemia (Autino et al., 2012). Erythrocytic schizogony of *P. falciparum* begins after the invasion of a red blood cell by a merozoite that is surrounded by a newly formed parasitophorous vacuole (Figure 3). The merozoite rapidly develops to a ring stage, which starts to remodel the host cell (Figure 3). This

stage usually lasts for about 18 hours (Grüring et al., 2011). The parasite then enters the metabolically active trophozoite stage, which is characterized by the presence of a food vacuole and knob formation on the surface of red blood cells (Leech et al., 1984). The schizont stage follows this at 34 hours post-invasion, which is characterized by asynchronous rounds of nuclear division followed by cytokinesis (Gerald et al., 2011), leading to the formation of daughter merozoites, which are released to invade new red blood cells after 48 hours (Bannister *et al.,* 2000).

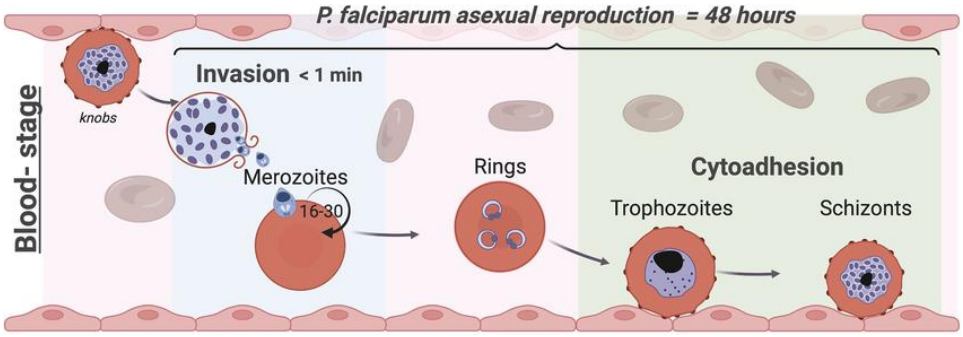

Figure 3 Asexual blood stages of *P. falciparum* . The asexual developmental cycle of *P. falciparum* in erythrocytes of the human host. Merozoites invade red blood cells to begin the erythrocytic asexual cycle. Each intracellular merozoite develops into an intra-erythrocytic ring stage, which matures into a trophozoite stage, and subsequently develops into a multinucleated schizont. 48 hours post-merozoite infection, 8–32 new merozoites egress from each schizont-infected erythrocyte, and a new erythrocytic cycle begins (Introini et al., 2022).

1.4 Malaria pathogenesis, immunity, and control

1.4.1 Malaria pathogenesis

The pathogenesis of malaria differs among different Plasmodium species due to variations in their genetic and physiological factors. In *P. falciparum* infection, the parasite secretes unique proteins that remodel the host red blood cell to present surface antigens that enable its adhesion to the endothelium, platelets, and neighboring uninfected erythrocytes. The cytoadhesion of *P. falciparum* parasites promotes clinical features of sequestration, tissue hypoxia, lactic acidosis, and microcirculation obstruction (Fairhurst & Wellems, 2006; Grau & Craig, 2012; Milner, 2018; Smith et al., 2013). Notably, the sequestration of infected RBCs temporarily removes the parasite from peripheral circulation, helping it to avoid parasite clearance and making it undetectable in blood smear diagnosis (Milner, 2018). *P. vivax* commonly requires the presence of the Duffy-binding antigen for the invasion of RBCs. Given that the Duffy-binding antigen is essentially not expressed in the population of Africa, malaria caused by *P. vivax* predominantly occurs in tropical and subtropical regions outside of Africa (Lo et al., 2015). Furthermore, *P. vivax* primarily infects reticulocytes, which form a small proportion of peripheral circulating RBCs, resulting in a lower parasitemia relative to other *Plasmodium* species infections, although *P. vivax* infection commonly

causes a higher systemic inflammatory response in the host (Dayananda et al., 2018; Hemmer et al., 2006; Moreno-Pérez et al., 2013). Another feature of *P. vivax* infection is the tendency for the parasites to form liver stage hypnozoites, a phenomenon that is also manifested in *P. ovale* infection. Hypnozoites have the potential to cause recurrent episodes of parasitemia months to years after the initial infection. *P. malariae* infections rank the lowest risk of severe malaria progression, with an approximate risk of 2% severe disease. However, infrequent complications that could sometimes arise include severe anemia, respiratory and renal insufficiency (Kotepui et al., 2020). Malaria caused by *P. knowlesi* is endemic to Southeast Asia, with the greater burden of human infection reported to occur in Malaysia. The usual hosts of this Simian parasite are reported to be long-tailed and pig-tailed macaques, and transmissions to human hosts take place when they are bitten by an infected mosquito that has previously fed on a macaque. Currently, there are no known cases of human-to-human transmission of *P. knowlesi* malaria (Cooper et al., 2020; Hussin et al., 2020; Kotepui et al., 2020).

1.4.2 Malaria immunity

Generally, there is no known data that supports complete immunity to malaria infection. However, there is evidence of acquired clinical immunity due to repeated episodes of malaria infection from exposure to infected mosquitoes. This acquired immunity usually protects the host from severe disease progression and mortality (Crompton et al., 2014). This is usually the case in areas of high malaria transmission, where children suffer from severe malaria while adults commonly exhibit an asymptomatic form of the disease. Mainly, these children acquire clinical immunity that protects them from suffering episodes of severe malaria after repeated exposures to mosquito bites. However, they might still suffer from malaria infections throughout their lifetime. To put this into perspective, there seems to be a complex relationship between the acquisition of natural immunity to malaria and transmission intensity. That is, if there is an incidence of high transmission, then the population is likely to suffer frequent malaria infection, leading to the acquisition of natural immunity, which protects them from severe malaria. However, if there is significantly low transmission intensity, the outcome is likely to be less frequent malaria infections, leading to loss of naturally acquired immunity against severe malaria progression (Fowkes et al., 2016). In addition, certain genetic and innate immunity factors also protect against severe disease progression, which is generally impacted by parasitemia, host age, immune response, chemoprophylaxis effects, and time of treatment. Important among these factors are some hemoglobinopathies that have demonstrated an advantage in the protection against malaria. Also, the absence of the Duffy-

binding antigen in the African population, as mentioned earlier, protects the population against *P. vivax* infection. It has also been reported that certain sickle-cell traits and sickle-cell disease protect individuals from malaria disease severity despite having a similar susceptibility profile as individuals without sickle-cell traits. There is also evidence that suggests malaria protection features of thalassemia, hemoglobin E disease, glucose-6-phosphate (G6PD) deficiency, and ovalocytosis (Kariuki & Williams, 2020; Leffler et al., 2017).

1.4.3 Clinical features of malaria

Typically, the incubation period of malaria parasites in a host varies between 7 and 30 days, depending on the *Plasmodium* species. Generally, shorter incubation periods have been observed to be associated with *P. falciparum* infections, with *P. malariae* exhibiting more extended incubation periods. Close to 95% of people who have been exposed to malaria parasites usually develop symptoms within 6 weeks (Crutcher *et al*., 1996). In endemic settings, it is common for some individuals to present an asymptomatic form of the disease with no clinical symptoms (Chen et al., 2016).

Most of the malaria infections usually result in mild disease outcomes, with approximately 1% of *P. falciparum* infections progressing to severe disease manifestations. The primary sign of malaria infection is an elevated body temperature, usually termed as fever. Additionally, the early symptoms of malaria are mostly nonspecific, and they include headache, fatigue, general malaise, nausea, myalgia, abdominal discomfort, arthralgia, and vomiting (Varo et al., 2020). A clinical diagnosis of malaria patients showing a parasitemia of greater than zero, where the conditions for severe malaria are not met, is usually defined as uncomplicated malaria. Severe malaria, on the other hand, is defined differently according to the age bracket of the population affected. Severe malaria in children is associated with a combination of three overlapping conditions: severe malaria anemia (SMA), cerebral malaria (CM), and acidosis/hyperlactatemia (WHO., 2014; Varo et al., 2020). Additional presentations include hyper parasitemia, repeated convulsions, pulmonary edema, acute kidney injury, hypoglycemia, jaundice, and significant bleeding. Although malaria clinical presentations differ between adults and children, recent discoveries showing high prevalence of acute kidney injury in children reveal that clinical manifestations that were associated with adults are also frequently observed in children (Conroy et al., 2016).

Generally, CM is presented as a severe impairment of consciousness commonly referred to as deep coma. CM is also sometimes characterized by repeated seizures and other neurological abnormalities and is associated with long-term cognitive and neurological defects in up to one-third

of survivors (John et al., 2010; Shikani et al., 2012; Zimmerman & Castro-Faria-Neto, 2010). In many instances, CM in both adults and children could potentially rise to a case fatality rate of 20% with brain swelling being a key pathogenetic event that explains the high percentages (Idro et al., 2005; Krishna et al., 1994; S. C. Murphy & Breman, 2001). Another feature of severe malaria is hyperlactemia or respiratory distress, which usually develops in up to 25% of adults and 40% of children (Taylor et al., 2012). This is typically presented with tachycardia, deep labored breathing, nasal flaring, and low chest indrawing. Severe malaria anemia is associated with malaria caused by all *Plasmodium* species and is thought to be the principal cause of malaria mortality worldwide (White, 2018).

1.4.4 Diagnosis of malaria

Malaria diagnosis has seen a lot of technological advancements in the past two decades; however, microscopy remains the gold standard for malaria diagnosis (Weiland, 2023). A combination of thin and thick smears is usually employed in the microscopy diagnosis of malaria. For parasite identification and estimation, a Giemsa-stained thick smear is usually performed, whilst thin smears are performed for species identification and evaluation of parasite growth stages. As a recommendation, two smears of each type should be made to amplify the diagnostic yield (Daily et al., 2022). Although light microscopy is sufficient in diagnosing malaria for a concentration of parasites above the range of 5 to 10 parasites per microliter, it is often interpreter-dependent (Murray et al., 2008). This gives rise to two significant limitations with the use of light microscopy regarding parasite density and the availability of experienced laboratory personnel (Weiland, 2023). The development and introduction of multiple malaria rapid diagnostic kits (RDTs) have aided in establishing quick diagnosis of malaria. These RDTs have been designed to detect *P. falciparum*-specific antigens and pan-malaria antigens, including histidine-rich protein 2(HRP-2), aldolase, and lactate dehydrogenase, which produce results within minutes (Moody, 2002; Murray et al., 2008). All RDTs are limited by their inability to detect mixed infections and to distinguish between species of *Plasmodium* causing the infection (Weiland, 2023). Even though some studies have reported the superiority of RDTs over microscopy (Stauffer et al., 2009). It is recommended that both should be used concurrently for malaria diagnosis (Murray et al., 2008).

1.4.5 Treatment of malaria

It is recommended to start the treatment for malaria as soon as the diagnosis is confirmed. Usually, admission to the hospital is advisable for most malaria cases with *P. falciparum*. Mostly uncomplicated malaria is treated with oral medications, whilst severe cases are treated with intravenous formulations (Weiland, 2023). For treatment of uncomplicated malaria caused by *P. falciparum* or when the species is unknown in a chloroquine-resistant geographic location, an artemisinin-based combination therapy (ACT), atovaquone-proguanil, or quinine plus doxycycline or clindamycin is recommended. However, if the infection was acquired in a chloroquine-sensitive area, chloroquine or hydroxychloroquine is recommended for children and adults by the CDC (CDC, 2025).WHO, on the contrary, recommends the use of ACTs over chloroquine or hydroxychloroquine for the treatment of all cases of uncomplicated malaria in children, adults, pregnant women (second and third trimester), and breastfeeding women (WHO, 2024). For treatment of uncomplicated malaria caused by *P. malariae* and *P. knowlesi*, either hydroxychloroquine or chloroquine is sufficient, as there is no reported resistance to date. A similar treatment regimen can be used for uncomplicated malaria caused by *P. vivax* or *P. ovale* in areas with no known chloroquine resistance. An ACT, atovaquone-proguanil, quinine plus doxycycline or clindamycin, or mefloquine, is usually recommended for treatment of *P. vivax* uncomplicated malaria in chloroquine-resistant areas (Weiland, 2023). The treatment for severe malaria can be either intravenous (IV) artesunate or IV quinine, although IV artesunate is thought to be more effective than IV quinine (Sinclair et al., 2012). In the absence of both regimens, oral artemether-lumefantrine is the preferred option, and treatment should begin as soon as the diagnosis is made.

1.4.6 Prevention of malaria

Vector control measures aimed at decreasing the population of mosquitoes to reduce the number of infective bites or the incidence of human-mosquito contact are thought to be the best control measures for malaria prevention (WHO, 2023). Two primary vector control measures have contributed to the significant global decline of malaria burden from 2000 to 2015: long-lasting insecticidal nets (LLINs) and indoor residual spraying (IRS) (Bhatt et al., 2015). Despite the reported success of these vector control measures, the emergence of pyrethroid-resistant mosquitoes has threatened the efficacy of these control measures (Ranson & Lissenden, 2016). Also, several mosquito behavioural modifications, such as shifting to outdoor or early biting and quick house

exiting immediately after feeding on a blood meal, have impacted the effectiveness of vector control measures (Killeen et al., 2017).

Chemoprophylaxis for malaria prevention includes measures such as intermittent preventive treatment, which involves administering different malaria drug regimens at separate times to at-risk groups to protect them from malaria. Many African countries endemic with P. falciparum malaria recommend implementing preventive treatment in pregnant women with sulfadoxine-pyrimethamine (SP). This regimen is reported to provide clear health benefits to both mother and newborn, and the WHO recommends at least three doses, spaced one month apart, during pregnancy. Seasonal malaria chemoprevention is another strategy to protect children under 5 years in regions with high seasonal transmission of malaria. This involves administering monthly doses of an artemisinin-free antimalarial, such as SP-Amodiaquine, to children during the transmission season. This strategy has demonstrated an 80% reduction in malaria episodes and nearly a 60% reduction in mortality when properly implemented. Another chemoprophylaxis approach is a fixed-term prophylaxis for individuals, especially children, traveling to malaria-endemic areas. This usually involves using suitable treatment regimens or drug combinations based on the destination. Commonly recommended drugs include atovaquone-proguanil, doxycycline, and mefloquine. Typically, the medication should be started before travel and continued for 1 to 4 weeks after returning to account for possible incubation periods of infections (Varo et al., 2020).

Malaria parasites display a high level of antigenic variability throughout their life cycle, which makes developing an effective vaccine difficult. The new malaria vaccine, R21/MATRIX-M, was reported to have an efficacy of over 75% against clinical malaria in a phase 2b trial with seasonal administration in Burkina Faso (Datoo et al., 2022). It was also reported that a booster dose of the vaccine at one year following the initial three-dose regimen maintained a high efficacy against first and multiple episodes of clinical malaria (Datoo et al., 2022). A phase 3 clinical trial on the R21/MATRIX-M vaccine showed an efficacy of 68% to 75% and was well-tolerated in African children aged 5-36 months (Datoo et al., 2024). This vaccine has received a WHO policy recommendation and has already been licensed by several African countries, offering a new hope to reduce the burden of malaria in sub-Saharan Africa (Datoo et al., 2024).

1.5 The mitochondrion and its biogenesis

According to the endosymbiont hypothesis, mitochondria evolved from an α-proteobacterium that was engulfed by a primordial eukaryotic cell (Dolezal et al., 2006). Mitochondria have a characteristic structure consisting of two membranes, an outer and an inner membrane, and two aqueous compartments. The mitochondrial inner membrane has a much larger surface area than

the outer membrane, forming invaginations called cristae. The oxidative phosphorylation system responsible for ATP synthesis is located on the membranes of the cristae. The two aqueous compartments are separated by the inner and outer membranes, forming the intermembrane space and the innermost compartment called the matrix. Initially, mitochondria were thought to be only necessary for energy conversion and ATP production via oxidative phosphorylation. However, they have been found to play essential roles in cellular metabolic processes such as the biosynthesis of lipids, heme, amino acids, and iron-sulfur (Fe-S) clusters. Additionally, mitochondria are involved in signaling pathways, quality control, and programmed cell death (Spinelli & Haigis, 2018). Although mitochondria have retained their own genome and protein synthesis machinery, most of the endosymbiont genes have been transferred to the nucleus. In humans, the mitochondrial genome encodes thirteen core subunits of the respiratory chain, along with seven subunits and one ribosomal protein in baker's yeast (Wiedemann & Pfanner, 2017). This indicates that approximately 99% of mitochondrial proteins are encoded by the nucleus and synthesized on cytosolic ribosomes. Precursor proteins synthesized on cytosolic ribosomes are subsequently imported into the mitochondria (Pfanner et al., 2019; Schmidt et al., 2010; Wiedemann & Pfanner, 2024). Precursor proteins synthesized on cytosolic ribosomes are subsequently imported into the mitochondria (Spinelli & Haigis, 2018).

1.5.1 The mitochondrion of *Plasmodium* parasites

Plasmodium parasites possess a single mitochondrion whose size significantly increases during reproduction, both in sporogony in the mosquito and exo- and intraerythrocytic schizogony in the vertebrate host, until a branched tubular mitochondrial network is formed (Figure 4) (Stanway et al., 2011; Van Dooren et al., 2005). *Plasmodium* parasites and related apicomplexan parasites possess a minimal mitochondrial genome that encodes many ribosomal RNAs and three proteins that are integral components of the electron transport chain in the mitochondrial inner membrane: cytochrome *b,* which forms a vital component of complex III, and the cytochrome *c* oxidase subunits I and III as vital components of complex IV (Vaidya & Mather, 2009). These three proteins have extreme hydrophobic properties, which are indicative of conserved genes in the mitochondrial genome (Keeling & Palmer, 2008).

Contrary to the human host, the *P. falciparum* mitochondrial matrix lacks a functional pyruvate dehydrogenase complex (Nair et al., 2023). Irrespective of this deficiency, the mitochondrion contains a functional citric acid cycle (Vaidya & Mather, 2009; Van Dooren et al., 2006). The biosynthesis of heme in *Plasmodium,* which is divided among the apicoplast, mitochondrion, and the cytosol, is considered essential to the blood stages of *Plasmodium* parasites despite the ability

to degrade hemoglobin in the food vacuole extensively. It is therefore suggested that succinyl-CoA is utilized to produce d-aminolevulinate, a precursor for the de novo biosynthesis of heme (Nagaraj, Arumugam, et al., 2010; Nagaraj, Prasad, et al., 2010; Vaidya & Mather, 2009; Van Dooren et al., 2006). The synthesis of ATP by oxidative phosphorylation is thought to be wholly absent or significantly reduced in *Plasmodium* (cultured) blood stage-parasites. This has been attributed to the presence of only a few to no tubular cristae in the mitochondrion of blood stage *Plasmodium* parasites, although this is species dependent (Aikawa et al., 1967; Fry & Beesley, 1991; Slomianny & Prensier, 1986). Despite the absence of oxidative phosphorylation, blood-stage *Plasmodium* parasites still require an electron transport chain to maintain a proton gradient across the inner membrane, which is a prerequisite for protein import in the matrix (Deponte, 2013). The presence of an electron transport chain is also vital for the *de novo* biosynthesis of nucleic acids in blood-stage *Plasmodium parasites* (Painter et al., 2007; Vaidya & Mather, 2009). Complex III serves as an electron sink for the essential biosynthesis of pyrimidines through the reduction of ubiquinone by dihydroorotate dehydrogenase on the outer side of the inner mitochondrial membrane(Painter et al., 2007).

The mitochondria of cultured gametocytes have been observed to contain more cristae with an increased enzymatic activity of the electron transport chain (Krungkrai et al., 2000). The electron transport chain and succinate dehydrogenase of *P. berghei* have been demonstrated to be essential for ookinete development *in vivo* (Hino et al., 2012).

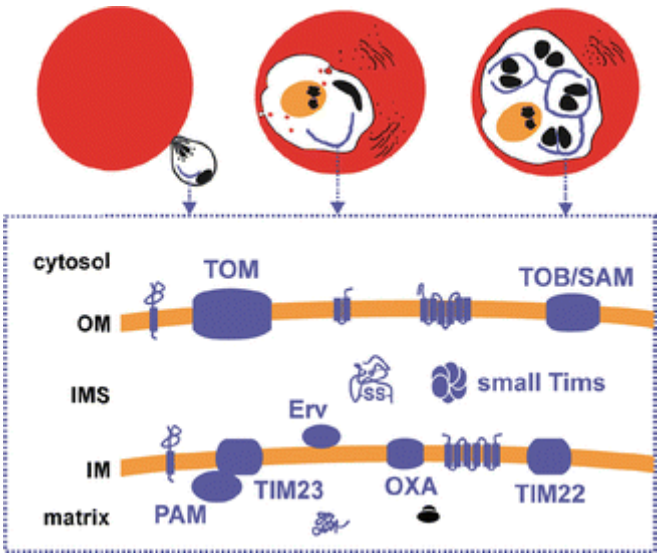

Figure 4 Mitochondrial protein import machineries of malaria parasites. After red blood cell invasion, the small mitochondrion of a merozoite-stage parasite grows into an elongated and branched mitochondrial tubular network of a schizont-stage parasite within 2 days. OM outer mitochondrial membrane, IMS mitochondrial intermembrane space, IM inner mitochondrial membrane (Deponte, 2013).

1.5.2 Mitochondrial protein import and overview

Nucleus-encoded mitochondrial proteins are synthesized on ribosomes in the cytosol and subsequently imported into the organelle (Dolezal et al., 2006). Until the beginning of the 21st century, there were only two known mitochondrial protein import pathways: the mitochondrial matrix and inner membrane import pathway (Schmidt et al., 2010). Currently, there are five known major protein import pathways characterized by unique targeting signals for each pathway (Wiedemann & Pfanner, 2017).

In the classical presequence import pathway, all proteins targeted to the matrix and many inner membrane proteins are synthesized with *N*-terminal presequences that serve as targeting signals (Abe et al., 2000; Vögtle et al., 2009). Preproteins carrying presequences are imported through the translocase of the outer membrane (TOM) and the translocase of the inner membrane (TIM 23) (Chacinska et al., 2005; Kiebler et al., 1990; Mokranjac & Neupert, 2015). The proteins are translocated into the matrix by the driving action of the presequence translocase-associated motor (PAM) (Horst et al., 1997; Kang et al., 1990). The presequence is cleaved off by mitochondrial processing peptidase (Hawlitschek et al., 1988). Contrary to the presequence pathway, the remaining four major import pathways do not possess cleavable presequences but rather unique internal targeting signals (Wiedemann & Pfanner, 2017). The second protein import pathway is the carrier pathway, which is characterized by the import of precursors of multi-spanning hydrophobic carrier proteins of the inner membrane by TOM, the carrier translocase of the inner membrane (TIM22), and the small Tim chaperones of the intermembrane space (Sirrenberg et al., 1996, 1998). The β-barrel pathway is the third known major protein import pathway. In this import pathway, β-barrel precursor proteins are inserted into the outer membrane by the sorting and assembly machinery (SAM) following translocation by TOM and small TIM chaperones (Wiedemann et al., 2003). The next major protein import pathway that was discovered involves the import of precursor proteins bearing cysteine motifs. The proteins are imported via the TOM and the import and assembly machinery (MIA) of the intermembrane space (Chacinska et al., 2004; Naoé et al., 2004). Several proteins with α-helical transmembrane segments of the outer membrane are imported via the fifth import pathway. The mitochondrial import (MIM) complex promotes the efficient import of outer-membrane proteins with an *N*-terminal signal-anchor sequence as well as multi-spanning (polytopic) outer-membrane proteins (Becker et al., 2008; Hulett et al., 2008; Popov-Čeleketić et al., 2008). Recent studies revealed an even higher complexity of mitochondrial protein sorting since novel import routes were identified that combine elements of different import and processing pathways (Ieva et al., 2014; Setoguchi et al., 2006; Stojanovski et al., 2012). For several precursor proteins, the import machinery has not been identified so far. Thus, it is likely that additional

mitochondrial protein import and assembly pathways may be discovered (Wiedemann & Pfanner, 2017).

1.5.3 Protein import into the mitochondrial outer membrane

Precursor proteins of the outer mitochondrial membrane do not share a unique import pathway, consistent with their different evolutionary origins, and recent studies have shown a large variety of protein-sorting pathways for protein import into the outer membrane. Two types of integral membrane proteins are found in the outer membrane: the β-barrel proteins that are integrated by multiple transmembrane β-barrel strands and the αhelical membrane proteins that are anchored by α-helical transmembrane segments. The α-helical proteins were introduced by eukaryotic cells, whereas the β-barrel proteins reflect the origin of the mitochondria from Gram-negative bacteria (Rapaport et al., 1997; Walther, Rapaport, et al., 2009; Wiedemann & Pfanner, 2017). The β-barrel precursor proteins are translocated via the TOM complex (Figure 5a) by a β-hairpin element-directed targeting signal (Jores et al., 2016). The β-hairpin consists of two adjacent β-strands, usually made up of the two most *C*-terminal beta-strands of the precursor proteins and the connecting loop. The precursor proteins are bound by the small TIM chaperones of the intermembrane space upon translocation through the TOM complex, protecting the hydrophobic β-barrel precursors of the outer membrane from aggregation in the aqueous intermembrane space (Wiedemann et al., 2003; Wiedemann & Pfanner, 2017). The SAM complex, which consists in opisthokonts of an integrated membrane protein, Sam50 (Tobb55), and two peripheral membrane proteins exposed to the cytosol, Sam35 and Sam37 (Figure 5a), performs the insertion of the β-barrel precursors into the outer membrane (Paschen et al., 2003; Wiedemann et al., 2003). The precursor proteins' most *C*-terminal β-strand functions as the β-signal that binds with Sam50-Sam35 and dictates insertion into the membrane (Kutik et al., 2008). It is proposed that the β-signal induces an opening of the lateral gate of Sam50, allowing the lateral release of the precursor polypeptide from the Sam50 channel into the membrane (Wiedemann & Pfanner, 2017). The Sam37 subunit of the SAM complex is known to interact directly with the cytosolic domain of Tom22 (Qiu et al., 2013; Wenz et al., 2015), causing the formation of a transient TOM-SAM super complex that promotes the β-barrel precursor transfer from TOM to SAM. Altogether, the Tom22-Sam37 interaction on the cytosolic side and the small TIM chaperones of the intermembrane space function for the efficient transfer of precursors to the SAM (Figure 5a). Finally, the formation of the β-barrel is achieved in association with Sam50-Sam35, leading to the release of a folded β-barrel protein into the lipid phase of the outer membrane (Wiedemann & Pfanner, 2017). The biogenesis of outer membrane α-helical proteins is

only partly understood (Dukanovic & Rapaport, 2011). There have been three main classifications of these proteins: tail-anchored proteins, signal-anchored proteins, and polytopic outer membrane α-helical proteins. The MIM complex, consisting of several copies of Mim1 and approximately one copy of Mim2, functions as a protein insertase for polytopic and signal-anchored outer membrane aα-helical proteins (Becker et al., 2008; Hulett et al., 2008; Popov-Čeleketić et al., 2008).

Although the biogenesis of β-barrel proteins seems to be conserved throughout evolution, and a homolog of Sam50/Tobb55 has been identified in apicomplexan parasites (Figure 5b). There are no clear homologs of the SAM complex receptor subunits Sam35 and Sam37 (Deponte et al., 2012; Eckers et al., 2012). Also, the import of several α-helical outer membrane precursor proteins depends on the outer membrane component Mim1 (Dudek et al., 2013a; Dukanovic & Rapaport, 2011) but there seems to be no homolog of Mim1 in *Plasmodium* parasites (Deponte et al., 2012). In the absence of these components and receptor homologs, it remains unclear how the β-barrel protein and several α-helical outer membrane proteins are imported in *P. falciparum* and other non-opistokonts (Deponte, 2013).

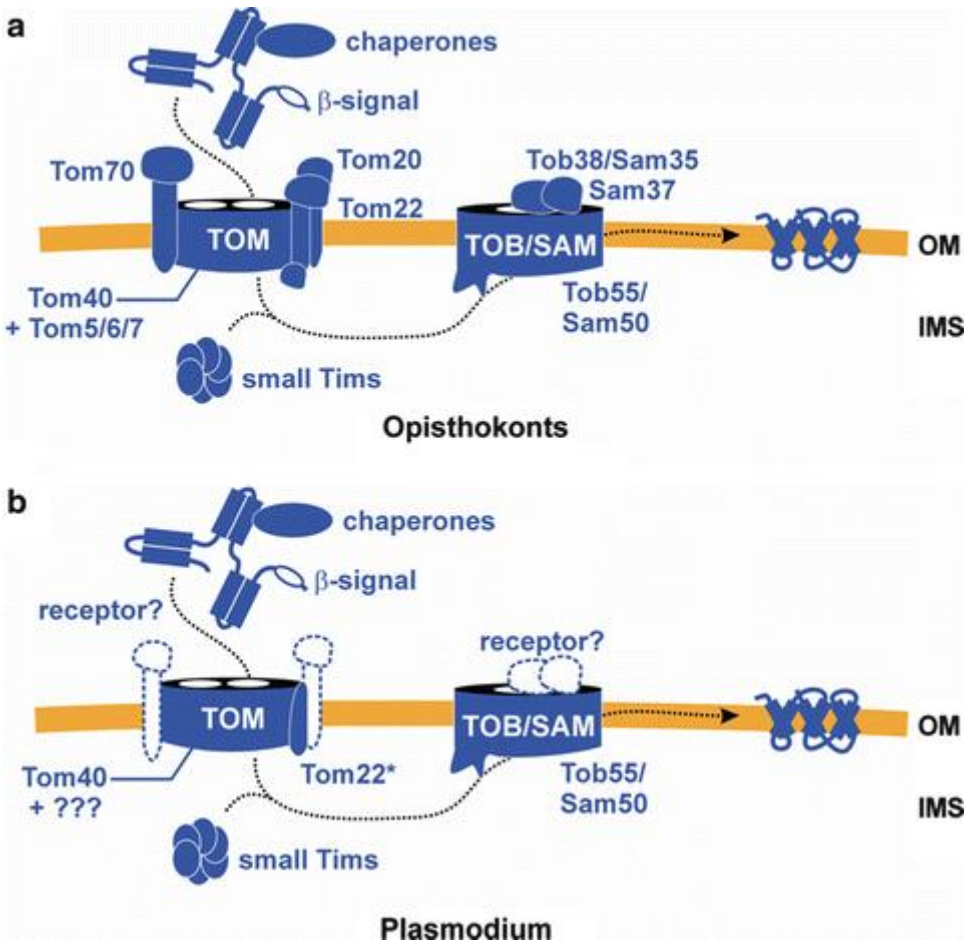

Figure 5 Comparison of the mitochondrial OM import pathways (**a**) Opisthokonts and (**b**) malaria parasites. Missing components are shown with dotted lines (Deponte, 2013).

1.5.4 Protein import into the mitochondrial intermembrane space

Several mitochondrial intermembrane space proteins are characterized by cysteine motifs that form intramolecular disulfide bonds. Previously, these precursor proteins were assumed to be in reduced states, like the majority of cytosolic and mitochondrial matrix proteins (Chacinska et al., 2004; Naoé et al., 2004). However, the identification of the oxidoreductase Mia40 revealed that the intermembrane space harbors an oxidative protein-folding machinery that catalyzes the formation of disulfide bonds in imported proteins (Chatzi et al., 2016; Fischer & Riemer, 2013).

Precursor proteins containing a characteristic signal with hydrophobic residues and a cysteine residue, called the intermembrane space sorting signal or mitochondrial intermembrane space sorting signal (MISS) (Milenkovic et al., 2009; Sideris et al., 2009), are translocated through the Tom40 channel and recognized by Mia40. Mia40 acts as a receptor in the intermembrane space and binds to the precursors via hydrophobic interactions, involving the formation of a transient intermolecular disulfide bond between the precursor proteins and Mia40 (Figure 6a). Electrons are then transferred from oxidized substrates via Mia40 to Erv1, and subsequently to cytochrome c of the electron transport chain (Bihlmaier et al., 2007; Bien et al., 2010; Dabir et al., 2007; Kawano et al., 2009). This process occurs through a transient interaction between the precursor proteins and a redox-active cysteine pair of Mia40, which is reoxidized by Erv1 (Figure 6a). The oxidation of Mia40 is facilitated by the zinc-binding protein Hot13, which maintains it in a zinc-free state (Curran et al., 2004; Mesecke et al., 2008).

Plasmodium parasites and other eukaryotic lineages are speculated to possess a similar flow of electrons for the import of mitochondrial intermembrane space proteins (Deponte, 2013). This speculation is because these organisms all have substrates of the oxidative folding pathway, including a homologue of Erv1/ALR, cytochrome *c*, and complex IV. Nevertheless, a homologue for Mia40 is missing in *Plasmodium* parasites and other non-opisthokonts (Figure 6b), and it therefore remains obscure which main component recognizes and oxidizes substrates containing cysteine residues during import into the mitochondrial intermembrane space (Deponte, 2013). Additionally, Erv1/ARL homologues of *P. falciparum* could not compensate for the loss of yeast Erv1 in a complementation assay, suggestive of a mechanistic difference between Erv1/ARL homologues that results in an incompatibility of redox partners (Deponte & Hell, 2009;Deponte et al., 2012; Eckers et al., 2012).

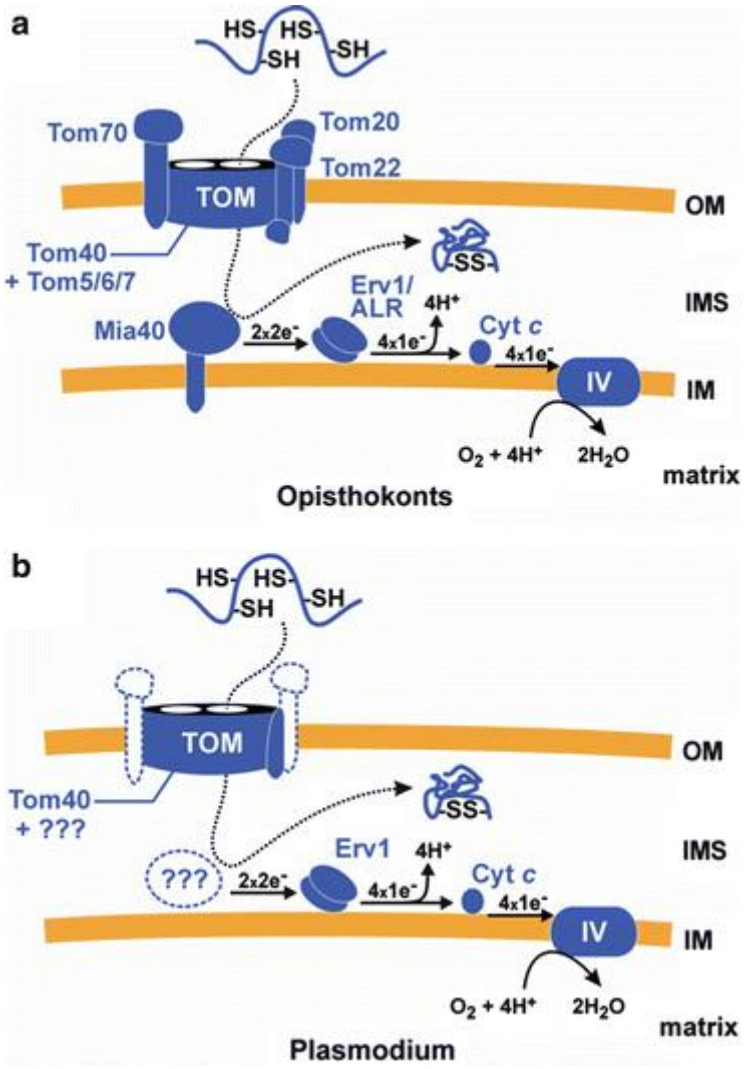

Figure 6 Comparison of the protein import pathway in the mitochondrial intermembrane space. Comparison of the oxidative-protein folding pathway in (**a**) Opisthokonts and (**b**) malaria parasites. Missing components are shown with dotted lines (Deponte, 2013).

1.5.5 Mitochondrial protein import into the matrix

Proteins targeted to the matrix are synthesized with positively charged *N*-terminal presequences that serve as targeting signals (Abe et al., 2000; Roise et al., 1986; Vögtle et al., 2009). The positively charged presequences are predicted to form amphipathic α-helixes and are imported through the TOM complex, which consists of the channel-forming protein, Tom40, Tom protein receptors, and three small Tom proteins (Hill et al., 1998; Kiebler et al., 1990; Mokranjac & Neupert, 2015; Shiota et al., 2015). In opisthokonts, the precursor proteins with positive *N*-terminal presequences are initially recognized and bound by Tom20 and handed over to Tom22 of the TOM complex (Chacinska et al., 2019; Dudek et al., 2013; Endo & Yamano, 2009; Gross & Bhattacharya, 2009; Lithgow & Schneider, 2010) (Figure 7a). The precursors are then translocated through the TOM pore to the

TIM 23 complex, which forms a super complex with the TOM complex that connects both the outer membrane and the inner membrane during protein translocation (Chacinska et al., 2009; Dudek et al., 2013b; Endo & Yamano, 2009; Gross & Bhattacharya, 2009; Lithgow & Schneider, 2010) (Figure 7a). The Tim50 receptor subunit at the TIM23 complex binds the positively charged presequence of the precursor proteins and transfers to the negatively charged area of Tim17 (Chacinska et al., 2009; Dudek et al., 2013; Endo & Yamano, 2009; Gross & Bhattacharya, 2009; Lithgow & Schneider, 2010). Through the combined action of an electrochemical potential gradient across the inner membrane and the ATP-consuming presequence translocase-associated motor (PAM) located at the inner membrane side of the matrix, the precursors are driven through the TIM pore into the matrix (Chacinska et al., 2009; Dudek et al., 2013; Endo & Yamano, 2009; Gross & Bhattacharya, 2009; Lithgow & Schneider, 2010). In the matrix, the precursors are trapped and folded by chaperones, and the presequence is cleaved by heterodimeric mitochondrial processing peptidases (Figure 7a) (Chacinska et al., 2009; Dudek et al., 2013; Endo & Yamano, 2009; Gross & Bhattacharya, 2009; Lithgow & Schneider, 2010).

Homologs of Tim17, Tim23, Tom40, Tim50, many PAM components, conserved chaperons, and processing peptidases have been identified in apicomplexan genomes, suggesting that the presequence import pathway is relatively conserved in *Plasmodium* parasites. Mechanistically, this has been assumed to be true, supported by the presence of the negatively charged substrate-interacting motif of Tim17 in homologs of malaria parasites. However, it is believed that modifications to the *N*-terminal presequences of *Plasmodium* proteins may occur due to their A/T-rich genome, making them difficult to predict. The Tom20 receptor subunit of the TOM complex is absent. In contrast, the Tom22 subunit appears to be significantly altered in *Plasmodium* parasites, leading to a loss of the negatively charged domain that is essential for precursor recognition. Consequently, it remains unclear how matrix-targeted precursors with N-terminal presequences are recognized by the modified TOM complex in *Plasmodium* parasites and directed into the mitochondria (Deponte et al., 2012; Eckers et al., 2012).

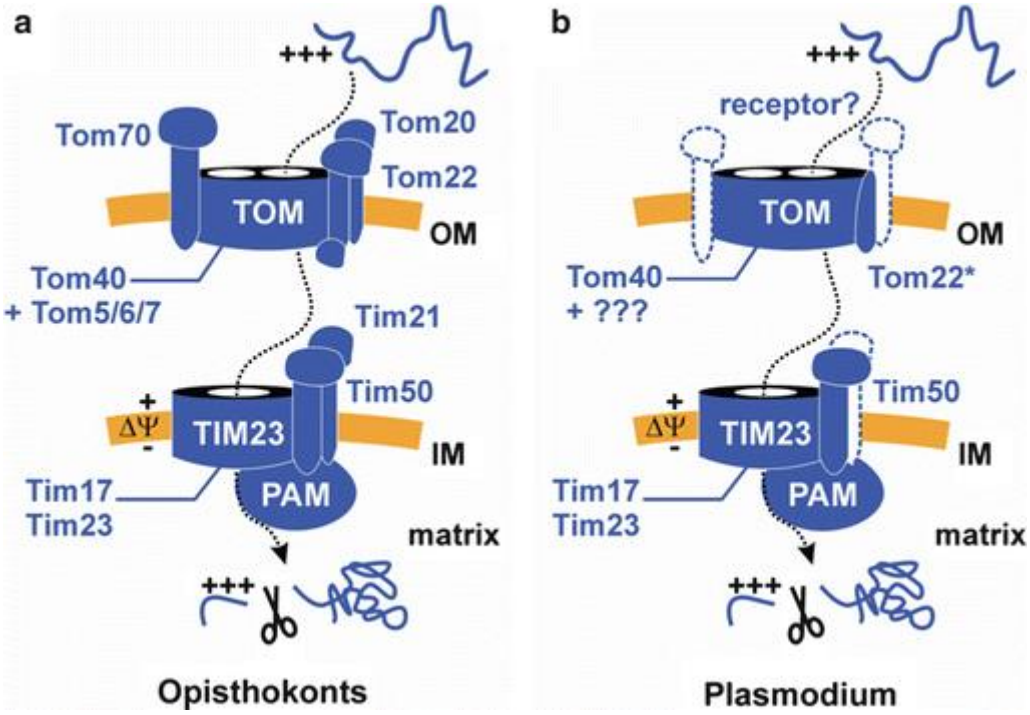

Figure 7 Comparison of mitochondrial import of matrix precursor proteins. Comparison of the TOM and TIM23 protein import machinery in (a) Opisthokonts and (b) malaria parasites. Missing components are shown with dotted lines (Deponte, 2013).

1.5.6 Protein import into the mitochondrial inner membrane

Three different import machineries are associated with the import of precursor proteins into the mitochondrial inner membrane of opisthokonts, namely, the TIM23 complex, the TIM22 complex, and the oxidase insertase assembly (OXA)complex (Chacinska et al., 2009; Dudek et al., 2013; Endo & Yamano, 2009; Gross & Bhattacharya, 2009; Lithgow & Schneider, 2010). The choice of a particular import machinery is dependent on the topology and number of transmembrane segments of the inner membrane precursor proteins. (Chacinska et al., 2009; Dudek et al., 2013; Endo & Yamano, 2009; Gross & Bhattacharya, 2009; Lithgow & Schneider, 2010)

The presequence signal pathway via the TIM23 complex, as described above (Figure 7a) is used for the import of mitochondrial inner membrane proteins having a single transmembrane segment with either an inside *N*-terminus or an outside *C*-terminus topology. (Chacinska et al., 2009; Dudek et al., 2013; Endo & Yamano, 2009; Gross & Bhattacharya, 2009; Lithgow & Schneider, 2010).Contrary to the mitochondrial matrix precursor proteins, the mitochondrial inner membrane substrates of the TIM23 complex carry a bipartite presequence. (Chacinska et al., 2009; Dudek et al., 2013; Endo & Yamano, 2009; Gross & Bhattacharya, 2009; Lithgow & Schneider, 2010). The initial part of the bipartite presequence (like the *N*-terminal presequence of the matrix-targeted precursor proteins) directs the N-terminus of the inner membrane precursor proteins to the matrix, where

they are proteolytically cleaved off. On the other hand, the second part of the bipartite presequence carries a hydrophobic sorting signal that is required to stop the translocation of the precursor protein across the TIM23 pore, causing it to be laterally released and inserted into the mitochondrial inner membrane (Figure 7a) (Chacinska et al., 2009; Dudek et al., 2013; Endo & Yamano, 2009; Gross & Bhattacharya, 2009; Lithgow & Schneider, 2010).

The OXA import machinery is vastly conserved throughout evolution. The machinery is closely matched with the YidC-dependent biogenesis of prokaryotic membrane proteins; it is sometimes, therefore, described as the conservative sorting pathway (Chacinska et al., 2009; Dudek et al., 2013; Endo & Yamano, 2009; Gross & Bhattacharya, 2009; Lithgow & Schneider, 2010). The substrates of OXA are inserted into the inner membrane from the matrix accordingly (Figure 8a). These substrates include proteins synthesized both on the mitochondrial ribosomes and nucleus-encoded proteins having multiple transmembrane segments. The nucleus-encoded inner membrane precursor proteins are first imported into the matrix via the TOM/TIM23 pathway as described above, and subsequently inserted into the inner mitochondrial membrane by Oxa1 (Figure 8b) (Chacinska et al., 2009; Endo & Yamano, 2009; Gross & Bhattacharya, 2009; Lithgow & Schneider, 2010). Mitochondrial metabolic carrier proteins are imported via the TIM22 import machinery (Figure 8c). These metabolic carrier proteins possess six transmembrane segments, although other substrates may have four transmembrane segments, such as the TIM23 complex subunits Tim23 and Tim17(Chacinska et al., 2009; Dudek et al., 2013; Endo & Yamano, 2009; Gross & Bhattacharya, 2009; Lithgow & Schneider, 2010). Metabolic carrier proteins do not carry presequence signals but possess internal signals for receptor recognition. These hydrophobic proteins in opistokonts are recognized at the TOM complex by the Tom70 receptor subunit in a chaperone-bound state (Chacinska et al., 2009; Dudek et al., 2013; Endo & Yamano, 2009; Gross & Bhattacharya, 2009; Lithgow & Schneider, 2010). The cytosolic-bound chaperones are removed, and the proteins are passed through the TOM pore into the intermembrane space, where they are bound by the small TIM proteins that form chaperone complexes for guiding the proteins to the TIM22 complex (Chacinska et al., 2009; Dudek et al., 2013; Endo & Yamano, 2009; Gross & Bhattacharya, 2009; Lithgow & Schneider, 2010). Upon arrival at the TIM22 complex, the small Tim proteins, Tim9/Tim10 and Tim8/ Tim13, recruit another small Tim, Tim12, which tethers the chaperon-protein complex with the help of Tim54 to the TIM22 complex (Chacinska et al., 2009; Dudek et al., 2013; Endo & Yamano, 2009; Gross & Bhattacharya, 2009; Lithgow & Schneider, 2010). The TIM22 complex central subunit, Tim22, is homologous to the Tim23 and Tim17 subunits of the TIM23 complex and forms the channel for insertion of the substrates into the mitochondrial inner membrane (Figure 8c)

(Chacinska et al., 2009; Dudek et al., 2013; Endo & Yamano, 2009; Gross & Bhattacharya, 2009; Lithgow & Schneider, 2010).

In *Plasmodium* parasites, important candidates that might be inserted into the inner mitochondrial membrane via the OXA import machinery include the three mitochondrial-encoded proteins and a few nucleus-encoded proteins, such as Oxa1 (Deponte, 2013). Although homologs of the insertase Oxa1 and the ribosome-interacting protein Mdm38 have been identified in apicomplexan parasites (Figure 8d), suggesting a conserved import mechanism, the inner membrane-associated ribosome receptor Mba1 appears to be absent in *Plasmodium* parasites (Deponte et al., 2012; Eckers et al., 2012). Also, while the import of mitochondrial inner membrane proteins via the TIM23 import machinery is conserved, the absence of a functional TOM complex receptor, as mentioned above (Figure 7b), raises further questions regarding how the substrates are recognized at the TOM complex in *Plasmodium* parasites (Deponte et al., 2012; Eckers et al., 2012). Mitochondrial inner membrane protein import via the TIM22 channel appears to be highly altered in *Plasmodium* parasites with missing homologs of Tom70 and Tim54 receptors at the TOM complex and TIM22 complex, respectively (Figure 8f). Additionally, Tim12, which serves as a tethering and assembly factor, is further missing in *Plasmodium* parasites. Thus, the homolog of Tim22 remains the only identified component of the predicted TIM22 complex-dependent import of inner membrane proteins in *Plasmodium* parasites (Deponte et al., 2012; Eckers et al., 2012).

Altogether, the central components of the OXA, TIM22, and TIM23 import machineries are conserved in *Plasmodium* parasites, suggesting a common principle in the biogenesis of inner mitochondrial membrane proteins of malaria parasites and their hosts (Figure 8d-f). Nevertheless, homologs of vital receptor subunits and other additional factors seem to be absent compared to the import machinery of opisthokonts. Therefore, the exact composition of these import machineries and their mechanism of action remains unclear in *Plasmodium* parasites (Deponte, 2013).

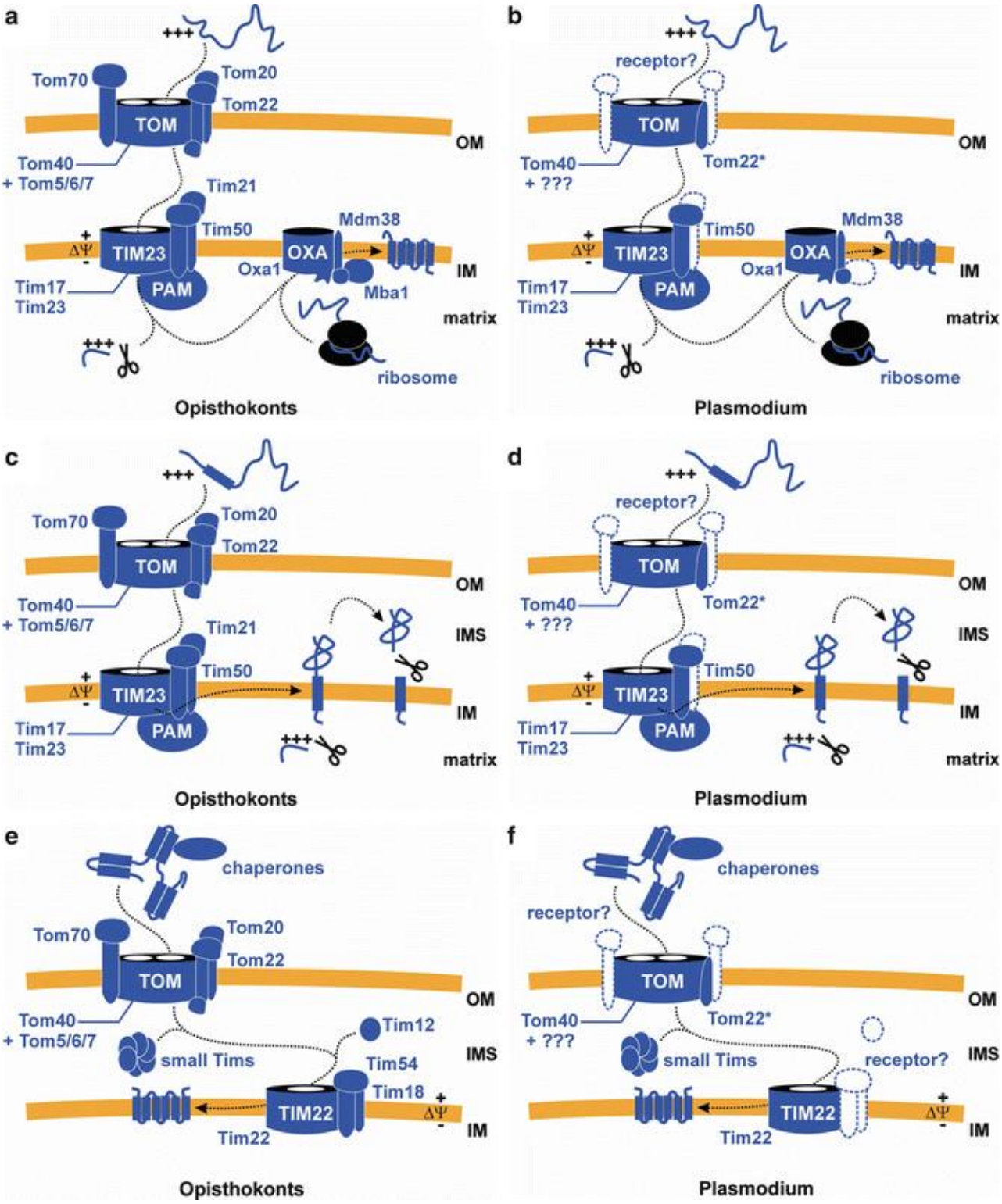

Figure 8 Comparison of mitochondrial protein import into the inner membrane. Comparison of the OXA (conservative sorting) pathway in (**a**) Opisthokonts and (**b**) malaria parasites. Comparison of the TIM23 stop transfer pathway in (**c**) Opisthokonts and (d) malaria parasites. Comparison of the TIM22 pathway in (e) Opisthokonts and (f) malaria parasites. Missing components are shown with dotted lines (Deponte, 2013).

1.6 Genetic manipulation of *P. falciparum*

1.6.1 Selection-linked integration system (SLI)

To overcome the low efficiency of homologous recombination in *P. falciparum*, Birnbaum *et al* developed a method permitting the selection of transgenic parasites with genomic integrations (Figure 9), which they termed the selection-linked integration system (SLI) (Birnbaum et al, 2017). Selection-linked integration allows rapid selection of genomic integration events. SLI also allows functional analyses of targets at the gene and protein level. In this technique, a sequence homologous to a part of the gene of interest is cloned into the plasmid to be integrated into the genome and fused with a tag-encoding sequence of choice. In addition to the tag, a T2A skip peptide and a selectable neomycin marker, termed the "SLI resistance", are fused at the *C*-terminus of the tag of choice. It is worth mentioning that the plasmid to be integrated already encodes human dihydrofolate reductase (*h*DHFR) as a selectable marker in its backbone to help with the initial selection of parasites that contain the episomal plasmid (Figure 9). Due to the absence of a promoter for the SLI resistance marker on the plasmid, the marker is only expressed after a successful integration of the plasmid, so that parasites with the integration can be selected with neomycin (Birnbaum et al., 2017). With this method, they generated GFP knockins in *P. falciparum,* obtaining cell lines with correct integration within 15-16 days of neomycin selection after transfection and initial selection for parasites bearing episomal plasmids (Birnbaum et al., 2017).

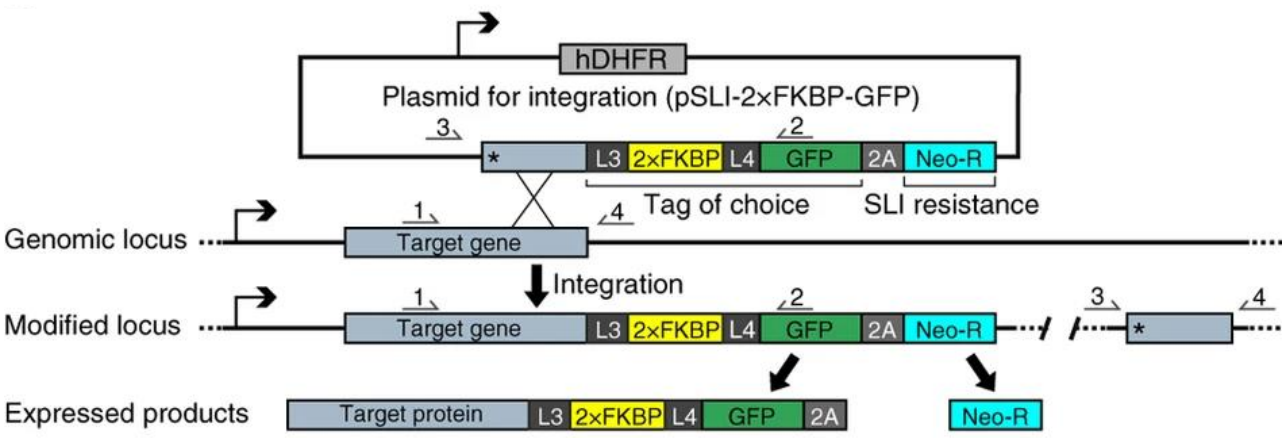

Figure 9 Selection-linked integration. Schematic of SLI strategy. L3 and L4 are linkers; 2A, T2A skip peptide; Neo-R, neomycin resistance gene; asterisks, stop codons; arrows, promoters (Birnbaum et al., 2017).

1.6.2 The CRISPR-Cas9 genome-editing strategy

In *P. falciparum*, conventional gene knockout attempts to obtain null mutants often take months and depend on spontaneous single- or double-crossover recombination using homologous sequence-containing plasmids to the target region. The zinc finger nuclease (ZFN) has been used to improve the generation of successful knockouts in *P. falciparum* (Singer et al., 2015; Straimer et al., 2012; Veiga et al., 2016). Although considered to be limited by excessive cost, complex design and implementation, and targeting capability. The method is also thought not to be suitable for genome-wide screening due to the large nature of ZNF vectors (Di Cristina & Carruthers, 2018). The adaptation of CRISPR-Cas9 to *P. falciparum* was first reported by two separate studies independently using the technology to manipulate the parasite's genome by expressing the gRNA via different approaches (Ghorbal et al., 2014; Wagner et al., 2014). Ghorbal *et al* in the first method, engineered a double plasmid system (Figure 10), one plasmid expressing the Cas9 endonuclease under the HSP86 promoter, and the single guide RNA (sgRNA) driven by the U6 promoter, along with homology region donors flanking selectable *h*DHFR in another vector (Ghorbal et al., 2014). In this method, both plasmids are co-transfected, and the drug selection is applied to achieve integration of DHFR at the target locus. The second plasmid (sgRNA/HR donor vector) also carries a negative selection marker, termed yeast cytosine deaminase and uridylyl phosphoribosyl transferase (yfcu), to eliminate parasites carrying copies of the plasmid. The mechanism of action of this system is the introduction of double-strand breaks at the target gene locus by the Cas9 endonuclease, which is directed by an sgRNA that binds to a 20-nucleotide protospacer sequence. This double-strand break is then repaired through a homologous-directed repair mechanism (Ghorbal et al., 2014). Ghorbal *et al,* first used the system to disrupt the transgene reporter eGFP and subsequently an essential endogenous gene for the knob-associated histidine-rich protein with a high level of efficiency over three weeks (Ghorbal et al., 2014). Wagner *et al* in the second study similarly used a two-plasmid system in which Cas9 and the sgRNA were expressed in one vector with a blasticidin-S deaminase (BSD) selection marker, and the HR donor was expressed in the second plasmid with neomycin resistance. The expression of the sgRNA in this system was driven by the expression of T7 polymerase under the control of the T7 promoter. Wagner *et al,* used this system to successfully demonstrate the disruption of *PFKHARP* and *PFEBA*-75 without a selectable marker integration (Wagner et al., 2014).

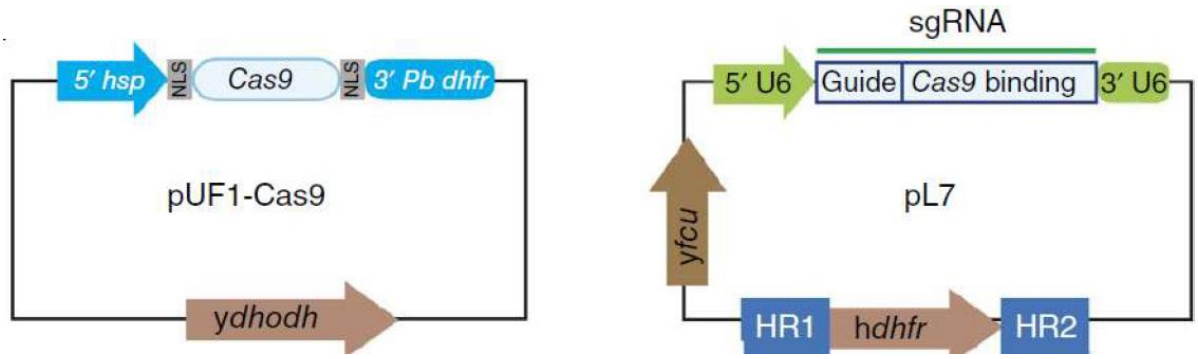

Figure 10 Two plasmids for targeted *P. falciparum* genome editing using sgRNA:Cas9. The pUF1-Cas9 expresses the Cas9 endonuclease using plasmodial regulatory elements. The Cas9 protein also bears nuclear localization signals (NLS). The pL7 episome contains the sgRNA expression cassette and 5′ and 3′ homologous regions (donor DNA). sgRNA is expressed from the *P. falciparum* U6 snRNA polymerase III promoter (5′ U6). The homologous region 1 (HR1) and homology region 2 (HR2) of the gene of interest (GOI) must surround a drug-selectable marker (H*DHFR*) to select gene disruption. 5′ *HSP*, heat shock protein 86 promoter region; 3′ *PB DHFR*, 3′ region of *P. berghei DHFR*; Y*DHODH*, yeast dihydroorotate dehydrogenase gene (Ghorbal et al., 2014).

1.7 Aim of the study

Mitochondrial protein import and the associated import machineries are essential for mitochondrial biogenesis and are crucial for the survival of malaria parasites. It has also been observed that mitochondrial metabolism in *Plasmodium* parasites differs significantly from that of their mammalian host, making the mitochondrion of *Plasmodium* parasites a promising target for intervention strategies (Deponte, 2012). Our understanding of mitochondrial protein import in *Plasmodium* parasites is currently based on poorly characterized import machineries. Although several core import components appear to be conserved, most import machineries in apicomplexan parasites seem to have undergone significant alterations compared to their hosts. To date, mitochondrial protein import machineries of malaria parasites have primarily been analyzed by comparative genomics studies (Deponte, 2013). Additionally, no study has demonstrated the composition, localization, and essentiality of the components of the import machineries of malaria parasites. This study, therefore, sought to characterize the mitochondrial protein import machineries of *P. falciparum* by validating their production and localization as well as their protein-protein interaction network via protein tagging with a 3xHA tag. In addition, this study also sought to determine the essentiality of the components of the mitochondrial protein import machineries to the blood-stage survival of *P. falciparum*. Table 1 shows candidate components of the mitochondrial protein import machineries of *P. falciparum,* which were addressed in this project.

Table 1 Candidate components of the mitochondrial protein import machinery of *P. falciparum*

Protein	PlasmoDB ID	Pathway
Tom40	PFF0825c	TOM complex
Tom22	PFE1230c	TOM complex
Tob55/Sam50	PFF0410w	SAM complex
Tim8	PF14_0208	Small Tim chaperon complex
Tim9	PF13_0358	Small Tim chaperon complex
Tim10	PFL0430w	Small Tim chaperon complex
Tim13	PFL2065c	Small Tim chaperon complex
Tim17	PF14_0328	TIM23 complex
Tim23	PF13_0300	TIM23 complex
Tim50	PF07_0110	TIM23 complex
Tim44	PF11_0265	PAM complex
mtHsp70 (Hsp70-3)	PF11_0351	PAM complex
Mge1	PF11_0258	PAM complex
Pam16	PFE0670w	PAM complex
Pam18	PF07_0103	PAM complex
Tim22	PFF1330c	TIM22 complex
Mdm38	PFD0835c	OXA pathway
Oxa1	MAL8P1.14	OXA pathway

Note. The TOM and SAM complexes belong to the outer mitochondrial membrane, the small Tim chaperon complex belongs to the intermembrane space, the Pam complex (Mge1 and Hsp70) belongs to the matrix, the Pam complex (Pam16 .) and the OXA pathway belong to the inner mitochondrial membrane.

2 Materials and methods

2.1 Materials

2.1.1 Equipment

Table 2 Laboratory equipment

Equipment	Manufacturer
Analytical balance	Kern
Benchtop centrifuge Micro 220/R	Hettich
Benchtop centrifuge Rotina 380/R	Hettich
Bright-field microscope Axio Lab.A1	Zeiss
CCD digital gel imaging system Fusion SL	Vilbert Lourmat
Cell counting chamber improved Neubauer	Marien Field
Horizontal agarose mini gel system	Biostep
Incubator (*E. coli*) INCU-Line	VWR
Incubator (*P. falciparum*)	Memmert
Incubator shaker Innova 44/44R	New Brunswick
Incubator shaker MaxQ4450	Thermo Scientific
Laminar flow hood for *P. falciparum* Safe 2020	Thermo Scientific
Laminar flow hood, *E. coli* MSC-Advantage	Thermo Scientific
Magnetic stirrer-hot plate Hei-Standard	Heidolph
Metal block thermostat MBT 250	Kleinfeld Labortechnik
Micropippette PIPETMAN (p2,P10, p20,p50,p200,p1000)	Gilson
Microwave	Severin
Mini-PROTEAN electrophoresis cell	Bio-Rad
Mini-PROTEAN Tetra Cell	Bio-Rad
Mini-Trans blot cell system	Bio-Rad
NanoDrop 1000 Spectrophotometer	Thermo Scientific
Personal-sized incubator	VWR
pH-meter PB-11	Sartorius
Pippette controler Accu-jet pro	Brand
Portable spectrophotometer Ultrospec 10	VWR

Power Supply Mini 300V	Major Science
Semi-Dry PerfectBlue system	VWR
Thermal Cycler Mastercycler Nexus	Eppendorf
Thermomixer shaker incubator block	Eppendorf
Transfection Device Nucleofector II/2b	Lonza
Vertical autoclave V-65	Systec
Vortex-mixer Genie 2	Heidolph

2.1.2 Disposables

Table 3 Disposables

Disposables	**Source**
Centrifuge tubes (15 and 50 mL)	Greiner
Cryovials 2 mL	Greiner
Durapore sterile filters PVDF (0.22 µm)	Merck
Electroporation Cuvettes plus 2 mm gap	BTX
Falcon 96 well black/clear flat bottom plate	Corning
Micro reaction tubes (1.5 and 2 mL)	Sarstedt
Parafilm	Bemis
PCR reaction tubes	Sarstedt
Petri dishes	Greiner
Pipette tips	Steinbrenner
PVDF membrane	Merck
Serological pipettes (1, 5, 10, and 25 mL)	Sarstedt
Sterile syringes	BD Plastipak
SuperFrost microscope slides	Buddeberg
Whatman paper	GE Healthcare

2.1.3 Chemicals

Table 4 Chemicals

Reagents	**Source**

Acetic acid	Merck
Acetone	Honeywell
Acrylamide/Bis Solution, 37.5:1 (30 % w/v)	Serva
Agarose	Serva
AlbuMAXII	Gibco
Ammonium persulfate (APS)	Sigma Aldrich
Ampicillin	AppliChem
Beta-Mercaptoethanol	Sigma Aldrich
Bromophenol blue	Waldeck
BSA	Serva
Calcium chloride	Merck
cOmplete EDTA-free protease Inhibitor	Roche
d-(+)-Glucose	Merck
d-(+)-Sorbitol	Sigma Aldrich
DAPI ≥ 98 %	Roth
Deoxyribonucleoside triphosphate (dNTPs)	Thermo Fisher Scientific
Dithiothreitol (DTT)	Sigma Aldrich
DNA ladder (100 bp, 1kb)	New England Biolabs
DNase I	Roche
DSM1	BEI Resources
Ethylenediaminetetraacetic acid (EDTA)	MERCK
Ethylene glycol-bis (β-aminoethylether)-N,N,N',N'-tetraacetic acid (EGTA)	AppliChem
Ethanol (absolute)	VWR
Fetal bovine serum (FBS heat-inactivated)	Gibco
Gel loading dye, purple 6x	New England Biolabs
Gel Loading Dye, Purple (6x), no SDS	New England Biolabs
GelRed® Nucleic Acid Strain 10000x in H2O	EMD Millipore Corp.
Gentamycin 50 mg/mL	C C pro
Giemsa stock solution	Carl Roth
Glycerol	AppliChem
Glycine 99 % for analyses	Thermo Scientific
HEPES	Calbiochem
Hydrochloric acid	VWR

Hypoxanthine 10 mM	c.c.pro
Isopropanol	Merck
Luria Bertani (LB) agar	Carl Roth
Luria Bertani (LB) medium	Carl Roth
Magnesium chloride	Merck
Methanol	Merck
Milk powder, skimmed, blotting grade	Carl Roth
PonceauS	Serva
Potassium hydroxide	Carl Roth
Roti-Lumin plus	Carl Roth
Prestained protein ladder	Thermo Scientific
Proteinase K	Roche
RNAse A	Sigma Aldrich
RPMI 1640 (HEPES, glutamine)	Gibco
Saponin	Sigma Aldrich
Sodium chloride	Sigma Aldrich
Sodium dihydrogen phosphate	Merck
Sodium dodecyl sulphate (SDS)	Serva
Sodium fluoride	Merck
Sodium hydrogen carbonate	Carl Roth
Sodium hydroxide	Carl Roth
Tetramethyl ethylenediamine (TEMED)	Serva
TRIS (tris(hydroxymethyl)aminomethane)	Carl Roth
Triton X-100	Merck
Trypan blue	Thermo Fisher Scientific
Tween-20	Sigma Aldrich
Urea	AppliChem
WR99210	Jacobus Pharmaceutical

2.1.4 Drugs used for selection

Table 5 Antibiotics

Drug	Stock	Working concentration	Supplier
Ampicillin	100 mg/ml in 50% ethanol	100 µg/mL	AppliChem
Gentamycin	50 mg/ml in ddH_2O	10 µg/mL	Gibco
WR99210	20 µM in RPMI medium (0.1% DMSO)	4 nM	Jacobus Pharmaceutical
DSM1	3.75 mM in 95% DMSO/ 5% PBS	900 nM	BEI Resources

2.1.5 Enzymes

Table 6 Enzymes

Enzyme	Concentration	Manufacturer
*Btgz*I	5,000 units/mL	New England Biolabs
EcoRI-HF	20,000 units/mL	New England Biolabs
*Nco*I-HF	20,000 units/mL	New England Biolabs
*Not*I-HF	20,000 units/mL	New England Biolabs
*Mlu*I-HF	20,000 units/mL	New England Biolabs
Phusion DNA polymerase	2,000 units/mL	New England Biolabs
*Spe*I-*HF*	20,000 units/mL	New England Biolabs
*Sac*II-*HF*	20,000 units/mL	New England Biolabs
*Sal*I-HF	20,000 units/mL	New England Biolabs
T4 DNA ligase	400,000 units/mL	New England Biolabs
Taq DNA polymerase	5,000 units/mL	New England Biolabs
*Xba*I	20,000 units/mL	New England Biolabs

2.1.6 Kits

Table 7 Kits

Kit	Manufacturer
Infusion cloning kits	Takara Bio
QIAprep Midiprep Kit	QIAGEN
QIAprep Spin Miniprep Kit	QIAGEN
Wizard SV Gel and PCR Clean-Up System	Promega

2.1.7 Software

Table 8 Software

Software/ Bioinformatics tools	Developer
Coreldraw	Corel
ImageJ	Wayne Rasband (NIH)
JustBio	https://www.justbio.com
MS Office	Microsoft
NCBI databases	https://www.ncbi.nlm.nih.gov/
Perseus	https://maxquant.net/perseus/
PlasmoDB	https://plasmodb.org/plasmo/app
PrimerX	https://www.bioinformatics.org/primerx/
ProtParam tool	https://web.expasy.org/protparam/
PyMOL by Schrödinger	https://www.pymol.org/

2.1.8 Antibodies

Table 9 Antibodies

Antibody	Host species	Source	Dilution
AlexaFluor™ 488 goat anti-rat IgG (H+L)	Goat	invitrogen	1:500
Anti-HA-Biotin, High Affinity (3F10)		Roche	1:2000

HA-Tag Rabbit mAB (C29F4)	Rabbit	Cell Signaling Technology	1:1000
Goat Anti-rabbit IgG (H+L)-HRP conjugate	Goat	Bio-rad	1:10000

2.1.9 Oligonucleotides

All primers were purchased from Metabion, desalted, and dissolved in ddH2O (100 µM).

Table 10 List of primers

Number	**Name**	**Sequence (5´ → 3´)**
Cloning primers		
P1	*PF*MGE1/S:	GATCGCGGCCGCTAAATAGAAACTAGTAAATTATATTG
P2	*PF*MGE1/AS:	GATCACGCGTATTTTTAACCACTCCAACTTTGG
P3	*PF*MTHSP70/S:	GATCGCGGCCGCTAACACCAGCACCAAGAGGTG
P4	*PF*MTHSP70/AS:	GATCACGCGTTGCATTATCTTTATTTTCTTCAGC
P5	*PF*OXA1/S:	GATCGCGGCCGCTAAAAAGAATAGCATCTTATCCTG
P6	*PF*OXA1/AS:	GATCACGCGTTTTTTTCCTTTTGATTAAATCATTC
P7	*PF*PAM16/S:	GATCGCGGCCGCTAAATATTATTATTAACATTCGAATTG
P8	*PF*PAM16/AS:	GATCACGCGTAATTTTAAATGCTGAAACAATATATC
P9	*PF*SAM50/S:	GATCGCGGCCGCTAATACATATATTAATATTAGTAATGG
P10	*PF*SAM50/AS:	GATCACGCGTTAAGATTCCCTTAAAATTCAAGC
P11	*PF*TIM8/S:	GATCGCGGCCGCTAAACATATTGAAGTGATGTTATG
P12	*PF*TIM8/AS:	GATCACGCGTCAAAATTTTCTGTTTTATTATTATCG
P13	*PF*TIM13/S:	GATCGCGGCCGCTAATGTGTTTCAAAAATTGGACC
P14	*PF*TIM13/AS:	GATCACGCGTTAAGTTTGTGTAGTCACTATTTG
P15	*PF*TOM40/S:	GATCGCGGCCGCTAAATATGGCAAGGAGCATGG
P16	*PF*TOM40/AS:	GATCACGCGTTGCTGCTGTCTGTGGTTGC
P17	3XHA TAG/S:	GATCACGCGTATCCTTATGATGTTCCAGATTATG
P18	3XHA TAG/AS:	GATCGTCGACTGCATAATCAGGAACATCATAAG
P19	*PF*TOM40/GRNA/S:	TAAGTATATAATATT**TAGATGGTAGTGTGAATGGT**GTTTTAGAGC TAGAA
P20	*PF*TOM40/GRNA/AS:	TTCTAGCTCTAAAAC**ACCATTCACACTACCATCTA**AATATTATATA CTTA
P21	*PF*TOM40/5HR/S:	GATCCCGCGGAaGGAGATAACAAACATTTTTAAG
P22	*PF*TOM40/5HR/AS:	GATCTCTAGAATATTTATTCGACTTATCATTAATAAG

P23	*PF*TOM40/3HR/S:	ATCGAATTCGTAAAAAGATTAATAATAATATTGATTG
P24	*PF*TOM40/3HR/AS:	GATCCCATGGCATACATATCACCTATTTGCGTC
P25	*PF*HSP70/GRNA/S:	TAAGTATATAATATTA**TTGCTGTATATGATTTAGG**GTTTTAGAGCTAGAA
P26	*PF*HSP70/GRNA/AS:	TTCTAGCTCTAAAAC**CCTAAATCATATACAGCAA**TAATATTATATACTTA
P27	*PF*HSP70/5HR/S:	GATCCCGCGGAaGGCATCACTCAATAAAAAGAAC
P28	*PF*HSP70/5HR/AS:	GATCTCTAGATACAGCAATAACTTTACCATCAC
P29	*PF*HSP70/3HR/S:	GATCGAATTCGATATTTCTATTTTAGAAATTTTAAG
P30	*PF*HSP70/3HR/AS:	GATCCCATGGTAAATCAAAAGAACCTAATAATTTG
P41	*PF*TIM9/5HR/S:	GATCCCGCGGGTTTGTATGTAGAATAAGTTAATC
P42	*PF*TIM9/5HR/AS:	GATCTCTAGAAATTATATGTATTCATAGTATCTTC
P43	*PF*TIM9/3HR/S:	GATCGAATTCAACGAATGCATAACATCCTTTC
P44	*PF*TIM9/3HR/AS:	GATCCCATGGATTTGTTATTTGTTATTTGTTATTTG
P45	*PF*TIM9/GRNA/S:	TAAGTATATAATATTCATATAATTCGATTGTGGAAGTTTTAGAGCTAGAA
P46	*PF*TIM9/GRNA/AS:	TTCTAGCTCTAAAACTTCCACAATCGAATTATATGAATATTATATACTTA
P47	PFTIM10/5HR/S:	GATCCCGCGGACATTTTTTTAATAAATTCATATAGG
P48	PFTIM10/5HR/AS:	GATCTCTAGACGTTTAAATAAGTCCGACATAC
P49	*PF*TIM10/3HR/S:	GATCGAATTCAAATGTATTCCGGATGTACATG
P50	*PF*TIM10/3HR/AS:	GATCCCATGGGAAGGATGAATAAGATCCATAC
P51	*PF*TIM10/GRNA/S:	TAAGTATATAATATTAACGTATGCAGAACACATGTGTTTTAGAGCTAGAA
P52	*PF*TIM10/GRNA/AS:	TTCTAGCTCTAAAACACATGTGTTCTGCATACGTTAATATTATATACTTA
P53	PFTIM13/5HR/S:	GATCCCGCGGTTTCCCATCTTTTCCATTTTGG
P54	*PF*TIM13/5HR/AS:	GATCTCTAGACACTTGAACTTAATTTTGGTCC
P55	*PF*TIM13/3HR/S:	GATCGAATTCGCAAATAGCTATTTTTATACTAAC
P56	*PF*TIM13/3HR/AS:	GATCCCATGGCAATTAAAAAGTAAGGAATATGTG
P57	*PF*TIM13/GRNA/S:	TAAGTATATAATATTCAAGTGAACAAAAATGTATAGTTTTAGAGCTAGAA
P58	*PF*TIM13/GRNA/AS:	TTCTAGCTCTAAAACTATACATTTTTGTTCACTTGAATATTATATACTTA

P59	*PF*MDM38/S:	GATCGCGGCCGCTAACAGAACTAGCCGAAAAAAAAC
P60	*PF*MDM38/S:	GATCACGCGTATTTTTTACATTCAAAGAATCGTC
P61	*PF*PAM18/S:	GATCGCGGCCGCTAATGGCCTGTTGTTATGTTAC
P62	*PF*PAM18/AS:	GATCACGCGTCTTCAATAATATGTCTTTAGCTTC
P63	*PF*TIM9/S:	GATCGCGGCCGCTAAGAGAAGTCTTTAGATTTGAG
P64	*PF*TIM9/AS:	GATCACGCGTTGTTTTTTTTTGCATTTCATTATTC
P65	*PF*TIM10/S:	GATCGCGGCCGCTAAGATAATATAAGCAAAGTAAATAG
P66	*PF*TIM10/AS:	GATCACGCGTGATTTGAGATTCTTGTAAATTTTTTC
P67	*PF*TIM17/S:	GATCGCGGCCGCTAACTACAAGAAAGAGATTTAGC
P68	*PF*TIM17/AS	GATCACGCGTTCTATTATTTTTTGTTGCCATTCT
P69	*PF*TIM23/S:	GATCGCGGCCGCTAATATATATGTATATATATTTGTGTG
P70	*PF*TIM23 /AS:	GATCACGCGTAATGTAACCTTTTTTAAATCCATAG
P71	*PF*TIM44/S:	GATCGCGGCCGCTAAGGGAAATTATTTGGTGAAAC
P72	*PF*TIM44/AS:	GATCACGCGTTGATGGAGTGTTTCCAATAATTG
P73	*PF*TIM50/S:	GATCGCGGCCGCTAAAGATTTTTTAAAGAATTATCAAG
P74	*PF*TIM50/AS:	GATCACGCGTCGAATTAAATGAAATGCCATTTG
P75	*PF*TOM22/S:	GATCGCGGCCGCTAACAGCACTATCAAAAATTATTAC
P76	*PF*TOM22/AS:	GATCACGCGTGTTTAATTGTGGAACATTGGCTG
Sequencing primers		
P31	PARL SENSE 55	GAGCGGATAACAATTTCAC
P32	PL7/GRNA SEQ/AS	TAGGAAATAATAAAAAAGCACC
P33	PL6 MCS1/AS	AACCAATAGATAAAATTTGTAGAG
P34	PL6 MCS2/AS	GCTTTCTTGAAACGGTTGTCC
Genotyping primers		
P35	HDHFR S	CATGGTTCGCTAAACTGCATC
P36	HDHFR AS	CCTTTCTCCTCCTGGACATC
P37	*PF*TOM40_5‘UTR/S	TTAACCTTAAGCATAAAGATGTATAGGAG
P38	*PF*TOM40_3‘UTR/AS	TGCCTTTAAAAAGGTATTACATATTTATTGG
P39	*PF*HSP70_5‘UTR/S	GTATTGTATGAATTGAAGATATATTTATGCC
P40	*PF*HSP70_3‘UTR/AS	CACCTCTTGGTGCTGGTGG

2.1.10 Plasmids

Table 11 Plasmids

Plasmid	Characteristics	Reference
pSLI-2xFKBP-GFP	AmpR. Selectable marker: *h*DHFR for plasmid selection and Neo-R for integrant selection in *P. falciparum*.	(Birnbaum et al. 2017)
pSLI-*PFTOM40*-3xHA	pSLI plasmid, *PFTOM40* HR with a *C*-terminally fused 3xHA tag for expressing *PFTOM40*-3xHA under the endogenous *PFTOM40* promoter.	This study
pSLI-*PFSAM50*-3xHA	pSLI plasmid, *PFSAM50* HR with a *C*-terminally fused 3xHA tag for expressing *PFSAM50*-3xHA under the endogenous *PFSAM50* promoter.	This study
pSLI-*PFTIM8*-3xHA	pSLI plasmid, *PFTIM8* HR with a *C*-terminally fused 3xHA tag for expressing *PFTIM8*-3xHA under the endogenous *PFTIM8* promoter.	This study
pSLI-*PFTIM13*-3xHA	pSLI plasmid, *PFTIM13* HR with a *C*-terminally fused 3xHA tag for expressing *PFTIM13*-3xHA under the endogenous *PFTIM13* promoter.	This study
pSLI-*PFOXA1*-3xHA	pSLI plasmid, *PFOXA1* HR with a *C*-terminally fused 3xHA tag for expressing *PFOXA1*-3xHA under the endogenous *PFOXA1* promoter.	This study
pSLI-*PFPAM16*-3xHA	pSLI plasmid, *FPAM16* HR with a *C*-terminally fused 3xHA tag for expressing *PFPAM16*-3xHA under the endogenous *PFPAM16* promoter.	This study
pSLI-*PFHSP70*-3xHA	pSLI plasmid, *PFHSP70* HR with a *C*-terminally fused 3xHA tag for expressing *PFHSP70*-3xHA under the endogenous *PFHSP70* promoter.	This study
pSLI-*PFMGE1*-3xHA	pSLI plasmid, *PFMGE1* HR with a *C*-terminally fused 3xHA tag for expressing *PFMGE1*-3xHA under the endogenous *PFMGE1* promoter.	This study
pUF1-*Cas9*	expression of Cas9 protein in *P. falciparum*, 5'hsp: 3'*Pb dhfr* regulatory elements. NLS, *ydhodh* - positive selection.	(Ghorbal et al., 2014a)

pL6	Expression of sgRNA in *P. falciparum*, 5' U6: 3' U6 regulatory elements, *hdhfr*- positive selection, *ycfu*- negative selection	(Ghorbal et al., 2014a)
pL7-*PFHSP70*	pL6 containing the guide sequence and HR for the generation of *PFHSP70* knockout strains	This study
pL7-*PFTOM40*	pL6 containing the guide sequence and HR for the generation of PFTOM40 knockout strains	This study

2.1.11 *P. falciparum* strains

Table 12 ***P. falciparum*** **strains**

P. falciparum **strain**	**Characteristics**	**Source/reference**
P. falciparum 3D7 Wild-type	Clonal line derived from NF54	(Walliker et al., 1987)
P. falciparum 3D7 Tom40-3xHA	*C*-terminal 3xHA-tagged *Pf*Tom40	This work
P. falciparum 3D7 Sam50-3xHA	*C*-terminal 3xHA-tagged *Pf*Sam50	This work
P. falciparum 3D7 Tim8-3xHA	*C*-terminal 3xHA-tagged *Pf*Tim8	This work
P. falciparum 3D7 Tim13-3xHA	*C*-terminal 3xHA-tagged *Pf*Tim13	This work
P. falciparum 3D7 Oxa1-3xHA	*C*-terminal 3xHA-tagged *Pf*Oxa1	This work
P. falciparum 3D7 Pam16-3xHA	*C*-terminal 3xHA-tagged *Pf*Pam16	This work
P. falciparum 3D7 Hsp70-3xHA	*C*-terminal 3xHA-tagged *Pf*Hsp70	This work
P. falciparum 3D7 Mge1-3xHA	*C*-terminal 3xHA-tagged *Pf*Mge1	This work
P. falciparum 3D7 ΔHsp70	*Pf*Hsp70 knockout strain	This work
P. falciparum 3D7 Δ*Pf*Tom40	*Pf*Tom40 knockout strain	This work

2.1.12 Bacterial strains

Table 13 Bacterial strains

E. coli **strain**	**Genotype**	**Source**
XL-1 blue	*recA1 endA1 gyrA96 thi-1 hsdR17 supE44 relA1 lac [F´ proAB lacIq ZΔM15 Tn10 (Tetr)]*	Stratagene
Stellar	*F–, endA1, supE44, thi-1, recA1, relA1, gyrA96,*	Clontech

	phoA, Φ80d lacZΔ M15, Δ (lacZYA - argF) U169,
	Δ(mrr - hsdRMS - mcrBC), ΔmcrA, λ–

2.2 Molecular biology methods

2.2.1 DNA amplification by polymerase chain reaction

Primers specific to target regions were designed with sticky-end restriction overhang sequences to amplify DNA fragments for cloning. All the primers were designed to start with a GATC nucleotide sequence, followed by the sequence for the restriction site. The annealing temperature of the designed primers was calculated using the formula: T_a = 4°C (G+C) + 2°C (A+T) – 5°C. Standard reaction mixture and cycling conditions were used for amplification of DNA fragments, as shown in Table 14.

Table 14 PCR conditions for the amplification of DNA fragments.

Reaction mixture

Component	**Volume (µL)**
H_2O (millipore)	36
5x Phusion HF Buffer	10
10 mM dNTPs	1
100 µM forward primer	0.5
100 µM reverse primer	0.5
Template DNA	1 (60 ng)
Phusion HF DNA Polymerase	1
Final volume	50

Thermocycling conditions

Temperature (°C)	**Time (s)**	
95	30	
95	30	
45-65	30	x 35 cycles
72	1 kb/20 s	
4	hold	

2.2.2 Agarose gel electrophoresis of DNA fragments

DNA fragments were resolved by agarose gel electrophoresis. Briefly, the agarose (1-2% (*w*/*v*)) was dissolved in TAE buffer by heating in a microwave. The dissolved agarose gel was allowed to cool for a short time, and GelRed® (1:10,000) was added and cast in a preinstalled gel chamber. The cured gel was transferred to an electrophoresis tank filled with TAE buffer. Samples were loaded in gel pockets after mixing with Gel Loading Dye, Purple (6x). A DNA ladder (1 kb or 100 bp) was loaded

alongside the samples for DNA fragment size reference. The gels were run at 90 to 120 V until the pink dye ran around two-thirds of the total gel length. The stained, separated DNA fragments were visualized using a UV light gel imaging system (Vilber).

TAE buffer: 40mM Tris, 20mM acetic acid, 1mM EDTA, pH = 8.0

2.2.3 Restriction digest of DNA fragments

Double digestion of DNA fragments using specific restriction enzymes was carried out either to obtain desired fragments for ligation or to verify the correct insertion of a target region into a plasmid. The digestion reactions were set up at 37 °C for a minimum of 2 h up to overnight. Digested plasmid products were first separated by agarose gel electrophoresis and then purified. Digested PCR products were directly purified. The reaction mixture is shown in Table 15.

Table 15 Reaction mixture for DNA digest

Reaction mixture

Component	Volume (µL)
H_2O (millipore)	39/28
10x Restriction Buffer	5
Vector/PCR product	4/15(1µg-2µg)
Enzyme 1	1 (20 units)
Enzyme 2	1 (20 units)
Final volume	50

2.2.4 Purification of DNA fragments

Digested plasmid and PCR products, as well as undigested PCR products, were purified using the Wizard SV Gel and PCR Clean-Up System (Promega) according to the manufacturer's protocol. For digested plasmid and PCR products, fragments were excised from agarose gels after separation and then purified according to the manual instructions. DNA was eluted (30 µl H_2O (Millipore)) and stored at -20 °C until ready to be used.

2.2.5 DNA quantification

The concentration of DNA was determined using a NanoDrop1000. The concentration was directly calculated by the software by measuring the absorbance at 280 nm. DNA quality was checked by determining the ratio of A260/A280 which should be between 1.7 and 2.0.

2.2.6 Ligation reaction of DNA fragments

Gel-purified digested plasmids and inserts were ligated using a standard reaction mixture (Table 16). To ligate purified DNA fragments, H_2O (Millipore), T4 DNA ligase buffer, vector, inserts, and T4 DNA ligase were added in that order in a 1.5 Eppendorf tube on ice. The mixture was then transferred to a cooling block shaker and incubated (16 °C for 2 hours to overnight). The reaction mixture was then transformed into chemically competent XL1-Blue cells.

Table 16 DNA ligation reaction mixture

Reaction mixture

Component	**Volume (µL)**
10x T4 Ligase Buffer	2
Inserts	4(38ng-75ng)
Vector	4 (50ng-100ng)
T4 DNA Ligase	1
H_2O(Millipore)	To final vol. 20

2.2.7 Sanger sequencing

DNA sequences were confirmed by Sanger sequencing performed by Microsynth Seqlab GmbH. Samples and primers were prepared according to the company's instructions.

2.2.8 Transformation of plasmids

Ligated plasmids were transformed into *E. coli* XL1-Blue chemically competent cells under sterile conditions to achieve plasmid amplification. To transform *E. coli* cells, ligated products (1 - 4 µL) were added to thawed chemically competent cells (50 µL) and incubated on ice for 30 min. The cells

were heat shocked (90 s at 42 °C) and transferred back to ice for 5 min. After the addition of LB medium (0.5 -1 mL), the cells were left to shake on an Eppendorf thermomixer (500 rpm) and incubated (37 °C for 1 h). The mixture was then plated on LB agar plates and incubated (37 °C overnight), and the colonies were stored at 4 °C.

LB medium 25 g LB medium powder in 1 L ddH_2O, autoclaved

LB agar 40 g LB agar powder in 1 L ddH_2O, autoclaved

2.2.9 Isolation and purification of plasmid DNA from *E. coli*

Plasmid DNA from transformed *E. coli* was isolated and purified using the alkaline lysis method(Bimboim & Doly, 1979). To isolate and purify plasmids, a single colony of transformed *E.coli* cells was picked and added to LB medium (3 mL) containing the required antibiotic under sterile conditions. The resulting culture was grown in a MaxQ4450 shaker (240 rpm, 37 °C overnight). The culture was transferred to a 2 mL Eppendorf tube and centrifuged (13000 x g for 30 s at 4 °C) to harvest cells. The pellet obtained after centrifugation was resuspended in ice-cold buffer P1 (100 µL), and cells were lysed with buffer P2 (200 µL) by inverting the tube (3 to 5 times) followed by incubation at room temperature (up to 5 min). The lysed cells were neutralized with ice-cold buffer P3 (150 µL) and centrifuged (13000 x g for 10 min at 4 °C). The supernatant was transferred to a new tube and plasmid DNA precipitated with 100% isopropanol (600 µL) by inverting the tube 3 to 5 times and centrifuging (13000 x g for 5 min at 4 °C). The precipitated plasmid DNA was washed with 70% ethanol (600 µL), air-dried under red light, and dissolved in H_2O (30 µL) (Millipore). Plasmid DNA was stored at −20 °C until use.

Buffer P1 50 mM Tris, 10 mM EDTA, 0.1 mg/mL RNase A, pH = 8

Buffer P2 0.2 M NaOH, 1% (*w*/*v*) SDS

Buffer P3 1.8 M potassium acetate, 11.5% (*w/v*) acetic acid, pH = 5.2

2.2.10 Midi-preparation of Plasmid DNA

For midi-preparation of plasmid DNA, a modified version of the method described in 2.2.9 was used. An overnight culture with a volume of 100 mL was prepared. All centrifugation steps were performed at 4 °C, 5000 × g for 30 min. The volume of the solutions used(buffer P1-P3) increased 40-fold. The DNA pellet was resuspended in 1 mL of water (Millipore).

2.2.10 Generation of CRISPR-Cas9 knockout constructs

To carry out gene knock-out studies for components of the mitochondrial protein import machineries in *P. falciparum*, the CRISPR-Cas9 method by Ghorbal *et al* was adopted. First, pL7 transfection plasmids containing the single guide RNA expression cassette and the 5'- and 3'-homology regions of the target gene were designed. Generation of the pL7 transfection plasmids required three cloning steps: the 5'- and 3'-homology regions of the target genes and cloning of the guide RNA. To clone the 3'-homology regions of my target genes, PCR products of the 3'-homology regions from genomic DNA and pL6 plasmid were digested with *EcoRI* and *Nco*I restriction enzymes. To clone the 5'-homology regions, the PCR products of the 5'-homology region of the target genes were digested with *SacII* and *XbaI*, while the pL6 plasmid was digested with *Sac*II and *Spe*I. For cloning of the guide RNA encoding sequence, synthesized oligonucleotides were heat annealed using PCR and cloned into the pL6 plasmid, digested with *AvrII* and *BtgzI,* using the infusion-cloning kits. All cloning steps were verified by colony PCR, analytical restriction digest, and Sanger sequencing.

2.2.11 Generation of SLI constructs

To adapt the SLI strategy, homology regions of the target genes and a 3xHA tag encoding sequence were cloned into the pSLI-2xFKBP-GFP plasmid. First, the 3xHA tag was cloned into the pSLI-2xFKBP-GFP plasmid using *Mlu*I and *Sal*II restriction sites. This was followed by cloning of the homology region using *Not*I and *Mlu*I restriction sites. Analytical restriction digests and Sanger sequencing verified successful cloning steps.

2.3 Cell culture of *P. falciparum* blood stages

2.3.1 Thawing of cryo-preserved *P. falciparum* strains

Cryo-preserved *P. falciparum* 3D7 wild-type parasites were thawed for continuous cultivation and generation of transgenic parasites. Cryo-vials containing a parasite culture (0.5 mL to 1 mL) were transferred from the liquid nitrogen tank to a water bath (37 °C) to thaw. The culture was then quickly transferred to a 15 mL Falcon tube, followed by a drop-wise addition of thawing solution I (0.2 volumes), incubation at room temperature (2 min). Thawing solution II (10 volumes) was slowly added and centrifuged (300 x g for 5 min). The supernatant was discarded, and the pellet was resuspended in thawing solution III (10 volumes) and centrifuged (300 x g for 5 min). The resulting pellet was washed with complete medium (10 mL) and resuspended (14 mL) in complete medium. The resuspended cells were then transferred to a new Petri dish, and fresh blood was added to set the hematocrit to 3.5. Continuous culture was maintained under standard conditions.

Thawing solution I	12% (*w*/*v*) NaCl in H_2O(Millipore)
Thawing solution II	1.6% (*w*/*v*) NaCl in H_2O(Millipore)
Thawing solution III	0.9% (*w*/*v*) NaCl, 0.2% (*w*/*v*) glucose in H_2O(Millipore)
Complete medium	RPMI 1640, 0.45% AlbuMAX II, 200 µM hypoxanthine, 5 µg/mL Gentamycin

2.3.2 Giemsa staining and parasitemia estimation

To analyze the parasite development and morphology and to estimate the parasitemia, blood smears were made and stained with Giemsa. To make blood smears, a 1 mL serological pipette was used to scrape red blood cells from the bottom of a culture-containing petri dish and to transfer them to a microscope slide. A second slide was used to smear the blood drop on the first slide to generate a thin blood cell monolayer. The smears were air-dried, fixed in methanol (100%) at room temperature (30 s), and dried again. Staining of the smear was conducted in a Giemsa solution (10% (v/v)) for a minimum of 30 min. The slides were washed with deionized H_2O and dried. The smears were analyzed using a light microscope with high magnification (100x, oil-immersion). Parasitemia was expressed as the percentage of infected red blood cells to the total number of red blood cells.

2.3.3 Continuous cultivation of *P. falciparum*

P. falciparum strains were cultivated using a modified standard protocol (Trager & Jensen, 1976). Cultures were maintained under standard conditions at 37 °C, 5% O_2, 5%CO_2, 90% N_2, and min. 90% humidity in complete medium RPMI 1640 containing 0.45% AlbuMAX II, 200 µM hypoxanthine, and 5 µg/mL gentamycin. Infected erythrocytes (A+) were suspended in 14 mL complete medium and cultured in petri dishes, and the hematocrit was adjusted to 3.5%. Parasitemia was kept between 0.1 and 10% to provide optimal growth conditions. The medium was changed by replacing 10 mL of culture medium with fresh prewarmed complete medium every one to two days. Cultures with parasitemia higher than 5% were usually diluted with red blood cells and complete medium, and the hematocrit was adjusted to 3.5%.

Complete medium	RPMI 1640, 0.45% AlbuMAX II, 200 µM hypoxanthine, 5 µg/mL Gentamycin

2.3.4 Cryo-preservation of *P. falciparum*

To preserve cultures for backups and future experiments, ring stages of parasitemia > 3% were cryo-preserved. A 14 mL standard culture was resuspended and centrifuged at 300 x g

for 5 min. The supernatant was discarded, and the cell pellet was dropwise resuspended in 500 µL freezing solution. After transferring to a cryovial, cells were immediately frozen in liquid nitrogen.

Freezing solution 28% (*v*/*v*) glycerol, 0.65% (*w*/*v*) NaCl, 3% (*w*/*v*) D-sorbitol in H_2O(Millipore)

2.3.5 Synchronization of *P. falciparum*

Parasites were synchronized to obtain uniform developmental stages for planned experiments. D-Sorbitol synchronization was done using a standard procedure by (Lambros & Vanderberg, 1979). D-Sorbitol treatment of infected red blood cells leads to osmotic lysis of red blood cells infected with mature parasite stages, leaving those infected with ring stage parasites intact. A parasite culture (14 mL) with a hematocrit of 3.5% and a minimum parasitemia of 0.5% was centrifuged (300 x g for 5 min). The cell pellet was resuspended in prewarmed D-sorbitol solution (5 mL) and incubated at room temperature (5 min). After centrifugation, the cell pellet was washed with complete medium (10 mL), resuspended in complete medium (14 mL), and continuously cultured.

Sorbitol solution 5% (*w*/*v*) D-sorbitol in ddH_2O

Complete medium RPMI 1640, 0.45% AlbuMAX II, 200 µM hypoxanthine, 5 µg/ml Gentamicin

2.3.6 Sterilization of plasmid DNA for *P. falciparum* transfections

Plasmid DNA used for generating transgenic *P. falciparum* parasites was first sterilized before being used for transfections. Purified plasmid DNA (100 µg) from a midi-preparation was acidified with sodium acetate (NaAc) buffer (0.1 volumes) and precipitated with 100% ethanol (2.5 volumes). For efficient precipitation, the mixture was stored at −20 °C overnight. After centrifugation (20000 x g for 30 min at 4 °C), the DNA was washed with 70% ethanol (500 µL). The supernatant was discarded under sterile conditions, and the DNA was dried for 10 min. The DNA was directly used to transfect *P. falciparum*.

NaAc buffer 3 M sodium acetate/acetic acid, pH = 4.7

2.3.7 Transfection of *P. falciparum*

To generate transgenic *P. falciparum* parasites, a transfection protocol by Deitsch *et al*. 2001 was adopted with modifications. Parasites were transfected by the spontaneous uptake of plasmid DNA from preloaded red blood cells. Transfections for both the CRISPR-Cas 9 knockout and SLI protein were carried out in 3D7 wild-type parasites. Parasites used for transfections were first d-sorbitol-synchronized to obtain a uniform trophozoite/schizont parasites. Synchronized parasites with a parasitaemia of 1% were centrifuged (300 x g for 5 min). After centrifugation, infected red blood cells (100 µL) were transferred to a petri dish and resuspended in complete medium (8 mL). Fresh red blood cells (2 mL) were washed twice by centrifugation (300 x g for 5 min) in ice-cold cytomix (with 6 mL). This was followed by mixing of washed red blood cells (400 µL) with sterilised plasmid DNA (100 µg) dissolved in cytomix (400 µL). The mixture was transferred to two prechilled electroporation cuvettes and incubated on ice (5 min). Transfection was carried out by electroporation using program U-033 of the Lonza Nucleofector 2b, followed by incubation on ice (5 min). Red blood cells loaded with plasmid DNA after electroporation were transferred to a 15 mL Falcon tube by rinsing each cuvette with complete medium (4 mL). After centrifugation (300 x g for 5 min), the supernatant was discarded and the remaining cell pellet resuspended in complete medium (6 mL) and mixed with infected red blood cells. Blood smears were prepared the following day to check for successful invasion. The infected erythrocytes were then washed with complete medium (10 mL), resuspended in complete medium (14 mL), and transferred to a new petri dish. The haematocrit was adjusted to 3.5% and the drug for plasmid selection was applied. For *h*DHFR selection, 2.7 nM WR99210 for the pL7 plasmid and 5 nM WR99210 for the pSLI plasmid were applied.

Cytomix 120 mM KCl, 0.15 mM $CaCl_2$, 2 mM EGTA, 5 mM $MgCl_2$, 10 mM K_2HPO_4, 10 mM KH_2PO_4, 25 mM HEPES, pH = 7.6 (KOH)

Complete medium RPMI 1640, 0.45% AlbuMAX II, 200 µM hypoxanthine, 5 µg/ml Gentamicin

2.3.8 Extraction of genomic DNA from *P. falciparum*

To isolate genomic DNA from *P. falciparum,* a fast and low-cost protocol was used(Seesui et al., 2018). This protocol does not result in pure genomic DNA. However, it resulted in DNA that led to reproducible results for genotyping PCR. A standard parasite culture (14 mL) with a parasitemia of 1-3% was centrifuged (300 x g for 5 min). After discarding the medium, infected red blood cells (100 µL) were resuspended in EDTA solution (1.9 mL). To lyse the red blood cells, the suspension was vortexed vigorously, incubated on ice (10 min), and centrifuged (12000 x g for 5 min). The supernatant was discarded, and the remaining pellet was resuspended in TE buffer (40 µL). Parasite lysis and release of DNA were initiated by the addition of proteinase K solution (10 µL). The mixture was shaken on an Eppendorf shaker (400 rpm at 56 °C for 1 h), and Proteinase K was inactivated (80°C for 10 min). After centrifugation (12000 x g for 5 min), the supernatant was transferred to a new tube and centrifuged again to remove insoluble material. The supernatant containing genomic DNA was stored at −20 °C until further use.

EDTA solution	500 µM EDTA in H_2O(Millipore)
TE buffer	10 mM Tris, 1 mM EDTA, pH = 7.6 (HCl)
Proteinase K solution	22 mg/mL proteinase K in TE buffer

2.3.9 Magnetic column isolation of *P. falciparum* and protein extraction

Mature stage parasites were enriched for mitochondrial isolation and western blot sample collection using VarioMACS. Mature parasites in the trophozoite or schizont stage possess iron-containing hemozoin in their food vacuoles, making it possible to isolate and enrich the parasites using a magnetic column. A parasite culture (14 mL) with high parasitemia > 5% was synchronized with 5% d-sorbitol and promptly expanded to a 40mL culture. On the day of parasite enrichment, the magnetic column was filled with incomplete RPMI medium via the three-way stopcock. Care was taken to ensure that there were no air bubbles in the syringe or the magnetic column. The column was placed in the VarioMACS, clamped, and equilibrated (5 min) with complete RPMI medium at room temperature. The culture (40 mL) was resuspended and successively applied to the magnetic column. The three-way cock was adjusted to allow a flow rate of 1 drop/s, and the flow-through was discarded. The column was washed with incomplete RPMI medium (20 mL) and transferred from the VarioMACS

magnetic clamp to a tripod clamp. The bound red cells containing the mature parasites were eluted with incomplete RPMI medium (10 mL) at maximum flow rate. The magnetic column was then washed with incomplete RPMI medium (20 mL) and was thus equilibrated for further extraction. Finally, the column was washed with autoclaved, degassed H_2O (Millipore) and stored in the same way. The column was never allowed to run dry. The eluate was centrifuged (10 min at 755 x g) at room temperature, and the supernatant was discarded. To estimate the parasitemia of the enriched parasites, 2 µL was taken directly from the pellet and added to PBS buffer (5 µL), spread on a slide, and stained with Giemsa. For Laemmli lysis, the remaining pellet (~2 µL) was mixed with PBS buffer (80 µL) containing cOmplete EDTA-free protease Inhibitor (one tablet dissolved in 50 mL PBS). To lyse the cells, the cell suspension (80 µL) was mixed with 5x Laemmli (20 µL) and boiled at 95 °C for 5 min. The lysate was stored at − 80 °C until use. In a second extraction method, the remaining pellet (~2 µL) was resuspended in 0.03% saponin (4 mL) and incubated on ice (10-30 min). The lysate was centrifuged (8.000 × g for 10 min), and the pellet was then washed repeatedly with PBS (5-10 volumes) until the supernatant lost its red coloration. The supernatant was removed, and cOmplete EDTA-free protease Inhibitor (one tablet dissolved in 50 mL PBS) was added (2–8 µL) and resuspended in parasite lysis buffer 1 (50–200 µL). To perform carbonate extraction, the remaining pellet (~2 µL) was incubated with 100 mM sodium carbonate (pH = 11.5) (100-150µL) on ice (1 h). After incubation, the samples were analyzed by immunoblotting.

Parasite lysis buffer 1	4% SDS, 0.5% Triton X-100
PBS	1.84 mM KH2PO4, 10 mM Na2HPO4, 137 mM, NaCl 2.7 mM KCl, pH 7.4
Saponin	0.0015 g saponin in 50 ml 1x PBS

2.4 Protein biochemistry methods

2.4.1 Sodium dodecyl sulfate polyacrylamide gel electrophoresis (SDS-PAGE)

Proteins were separated by SDS-polyacrylamide gel electrophoresis using the Bio-Rad Mini-PROTEAN system. The gels were cast to a 1 mm thickness following the manufacturer's instructions. Varying percentages of acrylamide were used in preparing the gels depending on

the expected sizes of the analyzed protein. The separating gel was first prepared and carefully poured into the glass gel casting chambers. The gel was overlaid with 100% isopropanol and allowed to polymerize. The isopropanol was removed after polymerization, and the stacking gel was carefully poured on top of the resolving gel. Well combs were inserted in the stacking gel and allowed to polymerize. The gel was used directly or stored at 4°C. To separate the proteins, gels were placed in an electrophoresis tank filled with SDS running buffer. Parasite lysate previously boiled in Laemmli buffer was thawed and boiled again for 5 min at 95 °C. Samples were then centrifuged (2 min at 21380 x g) and the supernatant loaded on the SDS gel. The gels were run at room temperature (200 V and 25 A per gel for 1 h). Table 17 Shows the SDS PAGE gel recipes.

Table 17 Recipe for SDS gels

	Separating gel			**Stacking gel**
	10%	**12%**	**15%**	**4%**
30% Acrylamide/bisacrylamide	3.3 mL	4.0 mL	5 mL	0.33 mL
1.5 M Tris-HCl, pH = 6.8	-	-		0.25 mL
1 M Tris-HCl, pH = 8.8	2.5 mL	2.5 mL	2.5 mL	-
10% SDS	100 µL	100 µL	100 µL	20 µL
10% APS	100 µL	100 µL	100 µl	20 µl
TEMED	4 µl	4 µl	4 µl	4 µl
ddH_2O	10 ml	10 ml	10 ml	2 ml

5x Laemmli buffer: 250 mM Tris/HCl pH 6.8, 10% (*w*/*v*) SDS, 25% (*v*/*v*) glycerol, 0.1% (*w*/*v*) bromophenol blue

SDS running buffer: 25 mM Tris/HCl, 250 mM glycine, 0.1% (*w*/*v*) SDS, pH = 8.3

2.4.2 Immunodetection of proteins by western blotting

To conduct immunodetection of HA-tagged proteins, gel-resolved proteins were blotted on PVDF membranes and probed with HA antibodies. Proteins were blotted using the Mini-PROTEAN wet blotting system (Bio-Rad) for high molecular weight proteins and the semi-dry blotting system for low molecular weight proteins. In the wet blot procedure, PVDF membranes were activated in 100% methanol (30 s). The activated membranes, SDS gels, and Whatman papers were then soaked in blotting buffer to equilibrate (10 min). A sandwich construction was then made with pre-soaked fiber pads, Whatman papers, gels, and membranes, and placed in a blotting cassette according to the manufacturer's instructions. The proteins were transferred (overnight at 4°C and a constant voltage of 15 V/gel). For the semi-dry transfer method, proteins separated by SDS-PAGE were transferred onto PVDF membranes using the HEP-1 Peqlab semi-dry blotter (20cm x 20cm). PVDF membranes were activated in 100% methanol (30 s). The activated membranes, SDS gels, and Whatman papers were then soaked in blotting buffer to equilibrate (5 min). A sandwich construction was then made with pre-soaked fiber pads, Whatman papers(3 on each side of the sandwich), gels, and membranes, and placed in a blotting cassette according to the manufacturer's instructions. Transfer was performed at 20 V for 45 minutes(or ~0.5–1.0 mA/cm² of gel area). To check the transfer efficiency and loading control, the membranes were stained with Ponceau S solution (2 min). The stained membranes were washed with H_2O (Millipore) to remove background staining and subsequently imaged with a scanner. After imaging, the membranes were completely destained by washing several times with TBS buffer. To prevent nonspecific binding of antibodies to the membranes, they were treated with a blocking solution at room temperature (1 h). The membranes were incubated with HA primary antibodies in blocking solution (4 °C overnight) on a rocking platform. The membranes were washed twice with TBS-T buffer (10 min) and once with TBS buffer (10 min) to remove unbound primary antibodies. After washing, the membranes were incubated with HRP-coupled secondary antibodies in blocking solution at room temperature (1 h). Thereafter, the membranes were washed with TBS (10 mins) followed by two washing steps with TBS-T (10 min). The membranes were probed for western blot signals using a 1:1 ratio of ECL solution 1 and 2. The chemiluminescent signals were immediately recorded with ECL CHEMOSTAR.

10x blotting buffer 247.6 mM Tris base, 1.93 M

	glycine
1x blotting buffer	10% (*v*/*v*) 10x blotting buffer,20% (*v*/*v*) methanol in ddH_2O
Ponceau solution	0.1% (*w*/*v*) Ponceau S, 1% (*v*/*v*) acetic acid
TBS buffer	20 mM Tris base, 150mM NaCl, pH 7.4
TBS-TT	20 mM Tris Base, 150.58 mM NaCl, 0.2% Triton X-100, 0.05% Tween20, pH = 7.4 (HCl)
Blocking solution	5% milk powder in TBS buffer
Chemiluminescence developer solution 1 (ECL Tom I)	40 mL ddH_2O, 5 mL 1 M Tris pH = 8.5, 0.5 mL 2.5 mM luminol, 0.22 ml 0.4 mM p-coumaric acid, H_2O (Millipore) to 50 mL
Chemiluminescence developer solution 2 (ECL Tom II)	40 mL ddH_2O, 5 mL1 M Tris pH = 8.5, 30 µL 30% H_2O_2, H_2O (Millipore) to 50 mL
Luminol stock solution	0.44 g luminol in 10 mL DMSO, p-coumaric acid: 0.15 g in 10 mL DMSO

2.4.3 Pulldown assay for identification of protein-interacting partners

To prepare samples for mass spectrometry analysis, a pulldown assay was conducted. Briefly, four large petri dishes containing 10% late trophozoite-schizont stage parasites were harvested and centrifuged at 300 x g for 5 minutes. The supernatant was discarded, and approximately 1 mL of cells was lysed with 0. 03% saponin (10 mL per plate) on ice for 15-30

minutes to remove erythrocytes and the parasitophorous vacuole. The saponin cell lysates were then centrifuged at 8, 8.000 × g for 10 minutes, and the supernatant was discarded. The parasite pellets (~50 µL) were washed three times with 1× PBS (10 mL) to remove hemoglobin contamination before lysis. The pellets were pooled (~200 µL) and resuspended in lysis buffer 2 (700 µL; 150 mM NaCl, 2 mM EDTA, 50 mM Tris- HCl pH 7. 4, 1% (w/v) n- dodecyl- β- D-maltoside (βDDM), protease inhibitor) for outer membrane proteins, or in lysis buffer 3 (700 µL; same composition but 1. 1.5% (w/v) βDDM) for matrix- soluble proteins, and incubated on a rotor at 4 ° C for 2 hours. Samples were then centrifuged at 16, 000 × g for 30 minutes at 4 ° C to separate soluble and insoluble material. The supernatant, containing solubilized proteins, was collected for western blot analysis (50 µL) and pulldown assay (650 µL). For the pulldown assay, anti- HA magnetic beads (Pierce) were aliquoted (50 µL, 0. 0.50mg) and washed twice with wash buffer (150 mM NaCl, 2 mM EDTA, 50 mM Tris- HCl pH 7. 7.4, 0. 5% (w/v) βDDM) (400 µL and 1 mL, respectively) by gentle inversion. The tube was then placed on a magnetic stand to collect the beads on its side. The supernatant was discarded. The samples containing solubilized HA-tagged proteins as bait were added to the washed beads (650 µL) and incubated overnight at 4 ° C on a mixing rotor. The next day, the beads were washed four times with 600 µL of wash buffer by gentle mixing, then collected on a magnetic stand. Bound proteins were then eluted with 50 mM NaOH (100 µL) and neutralized with 50 µL of neutralization buffer. The eluates were used for western blot analysis (50 µL) and mass spectrometry analysis (100 µL).

Saponin	0.0015 g saponin in 50 ml 1x PBS
Lysis buffer 2	150mM NaCl, 2mM EDTA, 50mM Tris-HCl pH = 7.4, 1% (*w*/*v*) βDDM
Lysis buffer 3	150mM NaCl, 2mM EDTA, 50mM Tris-HCl pH = 7.4, 1.5% (*w*/*v*) βDDM
Wash buffer	150mM NaCl, 2mM EDTA, 50mM Tris-HCl pH = 7.4, 0.5% (*w*/*v*) βDDM
Elution buffer	50mM NaOH
Neutralization buffer	1 M Tris, pH = 8.5

2.4.4 Single-pot solid-phase-enhanced sample preparation (SP3)

To perform protein clean-up and digestion, the Single-Pot Solid-Phase-enhanced Sample Preparation (SP3) protocol (Hughes et al., 2019) was adopted. This method utilizes

paramagnetic beads via a hydrophilic interaction mechanism to efficiently remove components used during cell or tissue lysis and protein solubilization, such as detergents, chaotropes, salts, buffers, acids, and solvents, prior to downstream proteomic analyses (Hughes et al., 2019). Here, a 1:1 slurry of the two types of Sera-Mag Beads (Thermo Scientific, 4515-2105-050250, 6515-2105-050250) was prepared by mixing equal amounts of both bead types in a 1.5 mL tube (4 µL from 50 µg/µL bead stock). The beads were separated from the supernatant by placing the tube on a magnetic stand. The beads were washed once with H_2O (HLPC grade) (20 µL) by gentle mixing, collected by placing the tube on a magnetic stand, and the supernatant was discarded. The beads were resuspended in H_2O (HLPC grade) to a final concentration of 50 µg/µL (8 µL). The pulldown eluates (100 µL) were then mixed with the washed beads (4 µL), followed by the addition of 100% ethanol (100 µL) to induce protein binding to the beads. The binding of proteins was achieved by shaking the mixture at room temperature (10 mins at 1000 rpm). The tube was then placed on a magnetic stand to collect the beads, and the supernatant was discarded. The beads were then washed three times with 80% ethanol (200 µL) by gentle mixing, collecting the beads on a magnetic stand, and discarding the supernatant. Proteins bound to the beads were digested with a digestion buffer(100 µL) on a shaker (overnight at 37°C, 1000 rpm). The following day, the beads were centrifuged briefly (1 min at 20,000 g). The beads were collected by placing the tube on a magnetic stand, and the supernatant containing the digested peptides was collected in a fresh tube (~100 µL).

Digestion buffer 100mM HEPES, pH=8.4, 0.8µg trypsin, 1.25nM TCEP, 5mM CAA

2.4.5 Purification of peptides on C18 stage tips

The C18 stage tipping was carried out in the Lab of Prof. Dr. Zuzana Storchová. Digested peptides (100 µL) were first diluted with buffer A(100 µL) and acidified with 0.9% trifluoroacetic acid (TFA)(20 µL of 10% TFA stock). After which, the pH was measured to ensure that it was below 2.0. The stage tips were prepared by punching the C18 membrane layers together with a large, blunt needle and placing them into white tips. The stage tips were activated with 100% methanol (100 µL) and washed 2 times with Buffer A (100 µL) by quick centrifugation with a microcentrifuge. The acidified peptides were loaded onto the stage tips

and washed with Buffer A (100 µL) by quick centrifugation with a microcentrifuge. The peptides were eluted with Buffer B (40 µL). Thereafter, the samples were evaporated in a Speedvac at room temperature (20 min), and Buffer A (1 µL) was added to an end volume of about 4 µL, and the mixture was sent for MS analysis. Dr. Markus Räschle conducted the MS analysis.

Buffer A: 0.1% (*v*/*v*) formic acid

Buffer B: 0.1% (*v*/*v*) formic acid in 80% (*v*/*v*) acetonitrile

2.5 Immunofluorescence microscopy

2.5.1 Sample preparation for immunofluorescence microscopy

Immunofluorescence imaging was carried out to validate the localization of HA-tagged proteins to the different compartments of the mitochondrion of *P. falciparum* parasites. To this end, a modified immunofluorescence assay (IFA) protocol from the group of Dr. Julien Guizetti of the Heidelberg University Hospital was used. An 8-well ibidi µ-Slide was coated with Concanavalin A (5 mg/mL, 80 µL) and incubated (37 °C for 20 min). Concanavalin A was removed after incubation, and the coated wells were washed twice with prewarmed PBS (300 µL), pH = 7.4. Thereafter, resuspended parasite cultures (150 µL) of parasitemia > 5% were aliquoted into 1.5 mL Eppendorf tubes and centrifuged (800 x g for 30 s). The supernatant was discarded, and the infected red blood cells were washed twice with prewarmed RPMI (200 µL), resuspended in RPMI (150 µL), pipetted into the ibidi wells, and incubated (37 °C for 10 min) for cells to settle. The wells were washed several times (5-8 times) by gently adding and removing RPMI medium (300 µL) until a visible monolayer was observed. The wells were then incubated with 100 nM MitoTrackerTM Orange CMTM Ros in prewarmed complete RPMI medium (300 µL) (20 min at 37 °C). The wells were washed four times with complete RPMI medium (300 µL) and three times with PBS (300 µL). The parasites were fixed with 4% paraformaldehyde in PBS buffer (200 µL) (20 min at 37 °C). After fixation, the wells were washed twice with PBS (300 µL) and stored overnight at 4 °C in the dark. The following day, the parasites were permeabilized with 0.1% Triton X-100 in PBS (300 µL) at room temperature (15 min). The parasites were washed 3 times with PBS (300 µL) and treated with 3% bovine

serum albumin solution (BSA) in PBS blocking solution at room temperature (1 h). The parasites were subsequently incubated with α-HA-Biotin High Affinity (3F10) in 3% BSA/PBS blocking solution at room temperature on a rocking platform (2 h). After incubation, the parasites were washed three times (10 min) with 0.5% Tween-20 in PBS buffer on a rocking platform. Afterwards, the parasites were probed with Alexa 488 Goat α Rat IgG (H+L) (dilution: 1:500) and 300 nM DAPI in 3% BSA/PBS at room temperature (1 h). The parasites were then washed twice (10 min) with 0.5% Tween-20 in PBS and once (10 min) with PBS. The parasites were fixed with 4% PFA solution in PBS (200 µL) at room temperature (20 min) and washed twice with PBS buffer (300 µL) and stored at 4 °C in the dark.

Complete RPMI medium	hypoxanthine 200 µM, gentamycin 2.7 g/mL, 0.45% (*w*/*v*) AlbuMAX II in RPMI only
Concanavalin A	5 mg/mL, in ddH_2O
PBS buffer	1.84 mM KH_2PO_4, 10 mM Na_2HPO_4, 137 mM NaCl, 2.7-mM KCl, pH = 7.4 (HCl)
BSA solution	3% BSA in PBS buffer pH = 7.4
Triton X-100 solution	0.1% Triton X-100 in PBS buffer pH = 7.4
Tween-20 solution	0.5% Tween-20 in PBS buffer pH = 7.4
PFA solution	4% PFA in PBS buffer pH = 7.4
DAPI	300 nM in 3% BSA solution
MitoTrackerTM Orange CMTM ROS	100 nM in complete RPMI medium

2.5.2 Microscopy and image evaluation

To carry out *P. falciparum* mitochondria localization studies, a ZEISS LSM880 Axio Observer confocal laser scanning microscope equipped with a Zeiss C-Apochromat 40x/1.2 autocorr water immersion objective from the working group of Prof. Dr. Frankenberg-Dinkel was used to acquire all images. The initial imaging method was developed by Prof. Dr. Stefanie Müller-Schüssele and undertaken by M.Sc. Sadia Sayed Tamanna. Thereafter, all strains were imaged by Dr. rer. nat. Susanne Zehner. The detection of HA-tagged proteins was achieved by ALEXA-488 labeling. Fluorescence was excited at 488 nm, and emission was detected from 499-

563 nm. The parasitized red blood cells were visualized in transmission light mode (Argon laser 488 1.5%, ex. 488 nm, em. 500-553 nm) and detected on a T-PMT detector. The parasites' nuclei were detected with DAPI staining (Diode laser 410 1.0%, ex: 405 nm, em: 410-496 nm) while the mitochondria were detected with Mito Tracker Orange CMTM Ros staining (helium neon laser 543, ex: 543 nm 3.0%, em: 562-685 nm). Images were obtained with 4x averaging, and Z-stacks were performed with 0.44 µm overlap. Images of ring, trophozoite, and schizont stages were recorded. The microscopy images were saved in .lsm file format. The Fiji ImageJ program was used for evaluation.

2.6 Mass spectrometry and data analyses

Statistical and bioinformatic analyses were performed with Perseus software (version 1.6.15.0). For statistical comparison, four groups were established, each containing three biological replicates for the pull-down samples (*Pf*3D7 WT, *Pf*Mge1-3xHA, *Pf*Tom40-3xHA, *Pf*Sam50-3xHA). The data were log-transformed and filtered to retain only proteins with at least 3 valid values across at least one group. Missing data points were filled using imputation by creating a Gaussian distribution of random numbers with a standard deviation of 33% relative to the standard deviation of the measured values and using 3 and 1.8 SD downshift of the means to simulate the distribution of low signal values statistical *t*-test FDR<0.01, S0 = 1 for class A interactors (high confidence) and t-test, FDR<0.05, S0 1 for class B interactors (low confidence) for creating Hawaii volcano plots. The different protein subnetworks were based on the results from the STRING database (Search Tool for the Retrieval of Interacting Genes/Proteins). The data analyses were carried out with the help of Dr. Markus Räschle

3 Results

3.1 *In silico* analyses of *N*-terminal presequences of the components of mitochondrial import machineries in *P. falciparum*

To adapt the SLI system to generate *P. falciparum* 3D7 SLI parasites with chromosomally encoded core components of the mitochondrial import machineries carrying a *C*-terminal 3xHA tag, the candidates were analyzed for the presence of mitochondrial targeting sequence at either the *C*- or *N*-terminus. The choice of the 3xHA tag's position was therefore influenced by the presence or absence of a cleavable mitochondrial targeting sequence at either the *N*- or *C*-terminus. Candidates that possessed *N*-terminal targeting sequences were *C*-terminally tagged to avoid impairment of their import into the mitochondria. Other candidates that did not have predicted targeting sequences at either the *N*- or *C*-terminus were also tagged at the *C*-terminus based on their predicted import pathway into the mitochondria. The Mitopro II software was employed in the targeting sequence prediction analyses. The results of the prediction analyses are shown in Table 18. In this work, four candidates were identified to possess a mitochondrial targeting sequence, all of which were located at the N-terminus (*Pf*Mge1, *Pf*Pam16, *Pf*Pam18, and *Pf*Tom40). All four candidates identified to possess mitochondrial targeting sequences were *C*-terminally tagged. Surprisingly, *Pf*mtHsp70 was not predicted to possess an *N*-terminal mitochondrial targeting sequence, although it is matrix-targeted (Voos, 2009). Nevertheless, it was *C*-terminally tagged since it is a known matrix-soluble protein and likely to possess a pre-sequence targeting it to the matrix. Similarly, Oxa1 was also tagged *C*-terminally based on the successful import of *C*-terminally tagged yeast Oxa1(Stoldt et al., 2012). For the remaining candidates, the predictions showed the absence of *N*- or *C*-terminal mitochondrial targeting pre-sequences. Notwithstanding this, these candidates may possess internal signals or targeting sequences that could not be predicted from the Mitoprot II analyses. These candidates were also *C*-terminally tagged.

Table 18 Predicted *N*-terminal presequence of *P. falciparum* components.

Protein candidate	Gene ID	Cleaved sequence	Cleavage site	Predicted import probability	Transmembrane segment
*Pf*Mge1	PF3D7_1124700	MRYSTNIIKKGILSRY	17	0.9715	
*Pf*Pam 16	PF3D7_0513500	MLPFRPLSQFVFQF	15	0.7306	1
*Pf*PAM18	PF3D7_0724400	MWPVVMLLFGGGVLFVKKGLNYVKNQGIQLNGKRSFFPSGFNK	44		
*Pf*mtHSP70	PF3D7_1134000	Not predictable			
*Pf*Oxa1	PF3D7_0828400	Not predictable		0.1110	4
*Pf*Tim8	PF3D7_1421500	Not predictable		0.0760	
*Pf*Tim9	PF3D7_1368600	Not predictable		0.0189	
*Pf*Tim10	PF3D7_1208600	Not predictable		0.0856	
*Pf*Tim13	PF3D7_1242900	Not predictable		0.0318	
*Pf*Tim22	PF3D7_0627400	Not predictable			
*Pf*Tim23	PF3D7_1356200	Not predictable		0.0822	2
*Pf*Tim17	PF3D7_1434700	Not predictable		0.0211	3
*Pf*Tim50	PF3D7_0726900	Not predictable		0.9355	
*Pf*Tim44	PF3D7_1125400	Not predictable		0.8940	
*Pf*Tom22	PF3D7_0524700	Not predictable		0.0766	1
*Pf*Tom40	PF3D7_0617000	MEITNIFKKLLCRQ	15	0.6733	
*Pf*Sam50	PF3D7_0608310	Not predictable		0.0389	
*Pf*Mdm38	PF3D7_0417300	Not predictable		0.4507	1

Table 19 List of successfully 3xHA tagged constructs

Protein candidate	PCR of the homology region (HR) of candidate genes	Cloning of the 3xHA tag sequence into the pSLI plasmid	Cloning of HRs into the pSLI-3xHA plasmid	Sequencing of pSLI-3xHA plasmids
*Pf*Tom40	completed	completed	completed	completed
*Pf*Tom22	completed	completed	completed	completed
*Pf*Sam50	completed	completed	completed	completed
*Pf*Tim9	completed	completed	completed	completed
*Pf*Tim10	completed	completed	completed	completed
*Pf*Tim8	completed	completed	completed	completed
*Pf*Tim13	completed	completed	completed	completed
*Pf*Tim17	completed	completed	completed	completed
*Pf*Tim23	completed	completed	completed	completed
*Pf*Tim50	completed	completed	completed	completed
*Pf*Tim44	completed	completed	completed	completed
*Pf*mtHsp70	completed	completed	completed	completed
*Pf*Mge1	completed	completed	completed	completed
*Pf*Pam16	completed	completed	completed	completed
*Pf*Pam18	completed	completed	completed	completed
*Pf*Oxa1	completed	completed	completed	completed
*Pf*Mdm38	completed	completed	completed	completed
*Pf*Erv1	completed	completed	completed	completed

3.2 Characterization of tagged components of the *P. falciparum* mitochondrial protein import machineries

To generate transgenic *P. falciparum* parasites producing *C*-terminally tagged 3xHA fusion proteins of components of the predicted mitochondrial import machinery, SLI vectors containing homologous sequences to the 3' region of the candidate genes fused with a 3xHA tag encoding sequence were transfected into the *P. falciparum* 3D7 wild-type strain. WR99210 drug selection was used to select parasites with initial plasmid uptake, followed by Neomycin (G418) selection to obtain parasites with genomic integrations. Western blot analyses were then conducted to validate the integration of the SLI vectors and subsequent endogenous expression of the predicted candidates of the *P. falciparum* mitochondrial protein import machineries. To this end, transgenic parasites producing 3xHA fusion proteins were harvested and lysed to obtain protein samples for western blot analyses. Differential protein extraction methods were used to obtain proteins in different mitochondrial sub-compartments and of different natures. Protein samples were resolved on SDS-PAGE gels of varying percentages depending on the molecular weight of the protein candidates to be analyzed. The separated proteins were transferred to PVDF membranes and decorated with α-HA antibodies to detect 3xHA fusion proteins.

3.2.1 Detection and Analyses of OM Components in *P. falciparum*

3.2.1.1 *Pf*Tom40 subunit of the TOM complex

Tom40 is the central subunit of the TOM complex, which serves as the primary entry gate for protein import into the mitochondria (Gabriel et al., 2003). It is the pore-forming subunit that serves as a sorting station for the translocation of proteins into the TIM23 complex, insertion into the outer membrane, and translocation into the intermembrane space (Gabriel et al., 2003). Structurally, Tom40 is a 19-transmembrane β-barrel forming channel with the first and last β-strands (β1 and β19) associating with each other to form a parallel β-sheet closing the barrel (Araiso & Endo, 2022). The predicted AlphaFold structures of *P. falciparum* Tom40 and human Tom40 are shown in Figure 11a and b, respectively. Comparing the human host Tom40 to the *P. falciparum* Tom40, a pairwise sequence alignment showed a low sequence identity

of 16% (62/396 residues) and similarity of 33% (134/396 residues) (Figure 11d). On the other hand, a structural alignment of the human Tom40 and the *P. falciparum* Tom40 showed a high structure similarity (Figure 11c) with a Root Mean Square Deviation (RMSD) score of 1.094, indicating a relatively conserved structure similarity despite the low sequence identity. In *P. falciparum* parasites, the Tom40 subunit has only been identified by a comparative genomic approach as putative to the TOM complex. To demonstrate the production of *P. falciparum*, Tom40, transgenic parasites producing *Pf*Tom40-3xHA fusion proteins were enriched with a MACS column and lysed with saponin to remove the erythrocytes and the parasitophorous vacuole. The resulting lysate after centrifugation was treated with parasite lysis buffer containing 4% SDS, 0.5% Triton X-100, and subsequently mixed with SDS loading buffer. The samples were resolved on a 15% SDS PAGE gel and transferred to a PVDF membrane. The membrane was decorated with rabbit α-HA antibody. The western blot analyses revealed a signal at ~48kDa (Figure 11e). The calculated molecular weight of the full-length *Pf*Tom40 is 44kDa, while the processed protein (N-terminal presequence cleaved off) has a calculated molecular weight of 42kDa. On the other hand, the calculated molecular weight of the full-length tagged *Pf*Tom40 (*Pf*Tom40-3xHA) was 47kDa, and the processed *Pf*Tom40-3xHA has a calculated molecular weight of 45kDa. Therefore, the western blot signal detected is likely to correspond to the calculated molecular weight of the full-length *Pf*Tom40-3xHA of 47kDa. This finding confirmed the successful genomic integration of the *PFTOM40-3xHA* SLI vector and validated the production of the *P. falciparum* Tom40 subunit of the TOM complex.

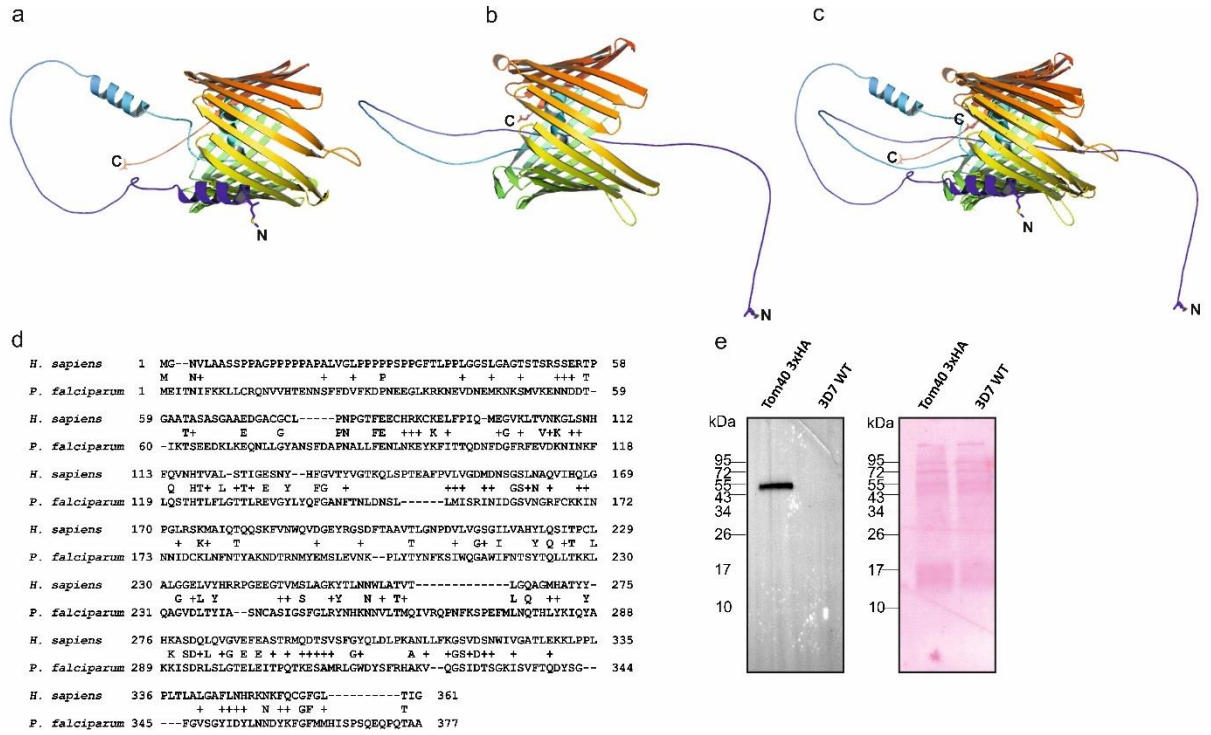

Figure 11 Analyses of *P. falciparum* Tom40. (a) Predicted AlphaFold structure of *Pf*Tom40. (b) Predicted AlphaFold structure of *Hs*Tom40. (c) Structural alignment of *Pf*Tom40 and *Hs*Tom40. (d) Sequence alignment of *Pf*Tom40 and *Hs*Tom40 (e) Left: Western blot detection of *PFTOM40-3xHA* SLI construct that was successfully integrated into the endogenous locus of *Pf*Tom40 and expressed in blood-stage parasites. Proteins were separated using a 15% SDS PAGE gel and transferred to a PVDF membrane, and probed with rabbit anti-HA antibody. Right: Ponceau S staining of PVDF membrane as a loading control.

3.2.1.2 *Pf*Sam50 subunit of the SAM complex

The SAM complex of yeasts, which mediates the insertion of β-barrel proteins into the outer mitochondrial membrane, consists of an integral membrane protein, Sam50, and two peripheral cytosol-exposed proteins, Sam35 and Sam37 (Becker et al., 2008; Paschen et al., 2003; Wiedemann et al., 2003). Sam50 is predicted to be present in *P. falciparum,* while both Sam35 and Sam37 are missing (Deponte et al., 2012; Eckers et al., 2012). Sam50 forms the principal component of the SAM complex and forms a 16-stranded β-barrel channel (Ulrich et al., 2014; Walther, Papic, et al., 2009) (Figure 12a), which is sensitive to the internal β-barrel signals close to the *C*-terminus *of* β-barrel precursor proteins (Kutik et al., 2008). The predicted AlphaFold structures of *P. falciparum* Sam50 and human Sam50 are shown in Figure 12a and b, respectively. A pairwise sequence alignment of the human host Sam50 and the *P. falciparum* Sam50 showed a low sequence identity of 20% (103/515 residues) and similarity of 36% (190/515 residues) (Figure 12d). Similarly, a structural alignment of the human Sam50 and the *P. falciparum* Sam50 produced a relatively low structure similarity (Figure 12c) with an

RMSD score of 3.502, corroborating the low sequence identity. The results of the sequence and structural alignments indicate a potential modification of the *Pf*Sam50. To confirm the production of *P. falciparum* Sam50, transgenic parasites producing *PfSam50-3xHA* fusion proteins were enriched using a MACS column and lysed with saponin to remove the erythrocytes and the parasitophorous vacuole. The resulting lysate after centrifugation was treated with parasite lysis buffer containing 4% SDS, 0.5% Triton X-100, and subsequently mixed with SDS loading buffer. The samples were resolved on a 15% SDS PAGE gel and transferred to a PVDF membrane. The membrane was decorated using a rabbit α-HA antibody. The western blot analyses revealed a signal slightly above 55kDa (Figure 12 e). The calculated molecular weight of the full-length *Pf*Sam50 is 54kDa, while the calculated molecular weight of the full-length tagged *Pf*Sam50 (*Pf*Sam50-3xHA) was 57kDa. Therefore, the detected western blot signal likely corresponds to the calculated molecular weight of the full-length *Pf*Sam50-3xHA of 57kDa, confirming the successful genomic integration of the *PFSAM50-3xHA* SLI vector and validating the production of the *P. falciparum* Sam50 subunit of the SAM complex.

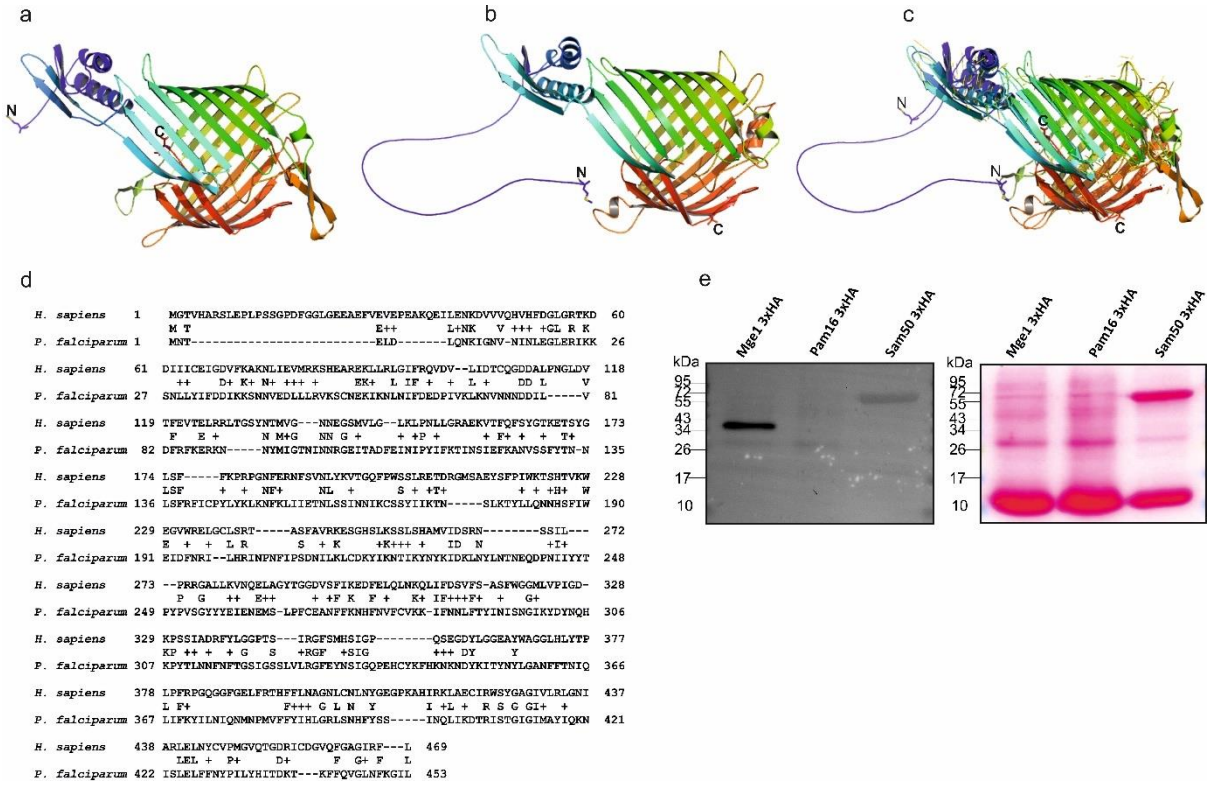

Figure 12 Analyses of *P. falciparum* Sam50. (a) Predicted AlphaFold structure of *Pf*Sam50. (b) Predicted AlphaFold structure of *Hs*Sam50. (c) Structural alignment of *Pf*Sam50 and *Hs*Tom40. (d) Sequence alignment of *Pf*Sam50 and *Hs*Sam50 (e) Left: Western blot detection of *PFSAM50-3xHA* SLI construct that was successfully integrated into the endogenous locus of

*Pf*Sam50 and expressed in blood-stage parasites. Proteins were separated using a 15% SDS PAGE gel and transferred to a PVDF membrane, and probed with rabbit anti-HA antibody. Right: Ponceau S staining of PVDF membrane as loading control.

3.2.2 Detection and analyses of tagged components of the PAM complex in *P. falciparum*

3.2.2.1 Mitochondrial Hsp70 (mtHsp70) chaperone

The Hsp70 class of chaperones is characterized by their high conservation and ubiquitous nature in all organisms (Mayer & Bukau, 2005). Typically, the Hsp70 family of chaperones is made up of three domains: a *N*-terminal nucleotide-binding domain preceding a domain that provides a groove for the interaction of substrate polypeptides and a variable *C*-terminal domain that covers the substrate-binding site (Voos, 2013). In Opisthokonts, mtHsp70 has been identified as an essential protein that is required for the import of precursor proteins from the cytosol into the mitochondrial matrix (Kang et al., 1990). The predicted AlphaFold structures of *P. falciparum* Hsp70 and human Hsp70 are shown in Figure 13a and b, respectively. A pairwise sequence alignment of the human host Hsp70 and the *P. falciparum* Hsp70 showed a relatively high sequence identity of 60% (409/679 residues) and similarity of 75% (513/679 residues) (Figure 13d). Similarly, a structural alignment of the human Hsp70 and the *P. falciparum* Hsp70 produced a relatively high structure similarity (Figure 13c) with an RMSD score of 0.313, corroborating the high sequence identity. The results of the sequence and structural alignments may indicate that Hsp70 is highly conserved between the human host and *P. falciparum*. To assess the production of *P. falciparum* mtHsp70, transgenic parasites producing *PfmHsp70-3xHA* fusion proteins were enriched with a MACS column to obtain a fraction of late-stage parasites. The enriched late-stage parasite fraction was directly lysed by boiling in Laemmli buffer and frozen until later use. The proteins were separated on a 10% SDS PAGE gel, transferred to a PVDF membrane, and probed with a rabbit α-HA antibody. The western blot analyses detected a signal slightly above 72 kDa (Figure 13e). The calculated molecular weight of the full-length *Pf*Hsp70 is 72kDa. At the same time, the calculated molecular weight of the full-length tagged *Pf*Hsp70 (*Pf*Hsp70-3xHA) was 75kDa. Therefore, the detected western blot signal likely corresponds to the predicted molecular weight of the full-length *Pf*mtHsp70-3xHA of 75kDa. This finding confirmed the successful

genomic integration of the *PFmtHSP70*-3xHA SLI vector and validated the production of *P. falciparum Pf*mtHsp70.

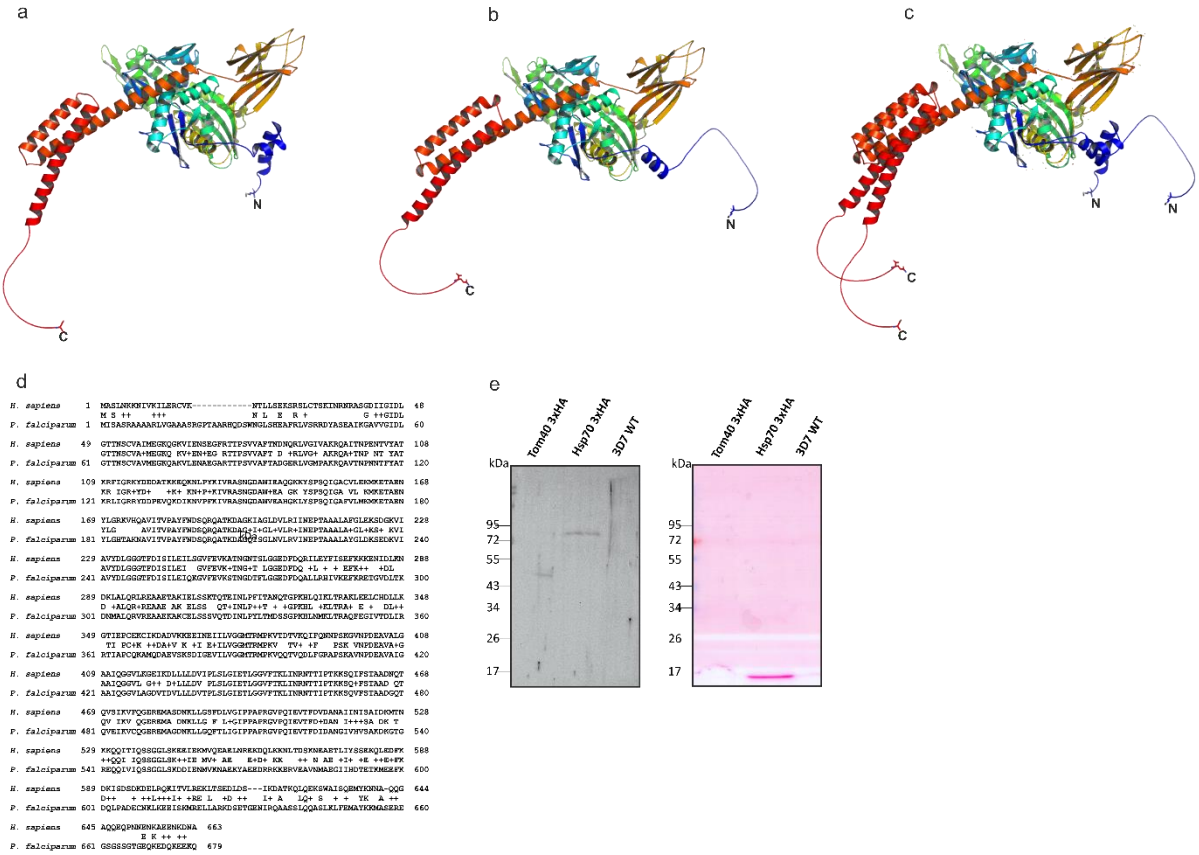

Figure 13 Analyses of *P. falciparum* mtHsp70. (a) Predicted AlphaFold structure of *Pf*Hsp70. (b) Predicted AlphaFold structure of *Hs*Hsp70. (c) Structural alignment of *Pf*Hsp70 and *Hs*Tom40. (d) Sequence alignment of *Pf*Hsp70 and *Hs*Hsp70 (e) Left: Western blot detection of *PFHSP70-3xHA* SLI construct that was successfully integrated into the endogenous locus of *Pf*Hsp70 and expressed in blood-stage parasites. Proteins were separated using a 10% SDS PAGE gel and transferred to a PVDF membrane and probed with rabbit anti-HA antibody. Right: Ponceau S staining of PVDF membrane as loading control.

.

3.2.2.2 Mitochondrial GrpE protein homolog1 (Mge1)

Mge1 is the nucleotide-exchange factor for mtHsp70 that is required for the exchange of ATP for ADP on mtHsp70, thereby promoting a faster substrate affinity for nucleotide-regulated recycling of mtHsp70 (Laloraya et al., 1994; Schneider et al., 1996; Voos et al., 1994; Westermann et al., 1995). In *E. coli*, the GrpE-Hsp70 complex crystal structure shows that GrpE exists as a homodimer attached to mtHsp70. Each molecule of GrpE in the homodimer is made up of an *N*-terminal a-helix domain, a central two-helix bundle domain, and a *C*-terminal b-sheet domain (Wu et al., 2012). The predicted AlphaFold structures of *P. falciparum* Mge1 and

human Mge1 are shown in Figure 14a and b, respectively. A pairwise sequence alignment of the human host Mge1 and the *P. falciparum* Mge1 showed a relatively low sequence identity of 29% (87/313 residues) and a moderate similarity of 40% (122/313 residues) (Figure 14d). Similarly, the structural alignment of the human Mge1 and the *P. falciparum* Mge1 produced a relatively high structure similarity (Figure 14c) with an RMSD score of 0.779, indicating high structural similarity despite the low sequence identity. The results of the sequence and structural alignments may indicate that Mge1 is highly conserved structurally between the human host and *P. falciparum.* To validate the production of *Pf*Mge1, transgenic parasites producing *Pf*Mge1-3xHA fusion proteins were enriched with a MACS column to obtain a parasite fraction containing late-stage parasites. The enriched late-stage parasites were directly lysed by boiling in Laemmli buffer and subsequently stored at – 80 °C until later use. The proteins were separated on a 15% SDS PAGE gel and transferred to a PVDF membrane. The membrane was probed with a rabbit α-HA antibody. The western blot analyses showed a signal above 34 kDa (Figure 14e). The calculated molecular weight of the full-length *Pf*Mge1 is 35kDa, while the processed protein (N-terminal presequence cleaved off) has a calculated molecular weight of 33kDa. On the other hand, the calculated molecular weight of the full-length tagged *Pf*Mge1 (*Pf*Mge1-3xHA) was 38kDa, and the processed *Pf*Tom40-3xHA has a calculated molecular weight of 36kDa. Therefore, the detected western blot signal likely corresponds to the calculated molecular weight of *Pf*Mge1-3xHA of 38kDa. This result confirms the successful genomic integration of the *PFMGE1-3xHA* SLI vector and validates the production of *Pf*Mge1-3xHA.

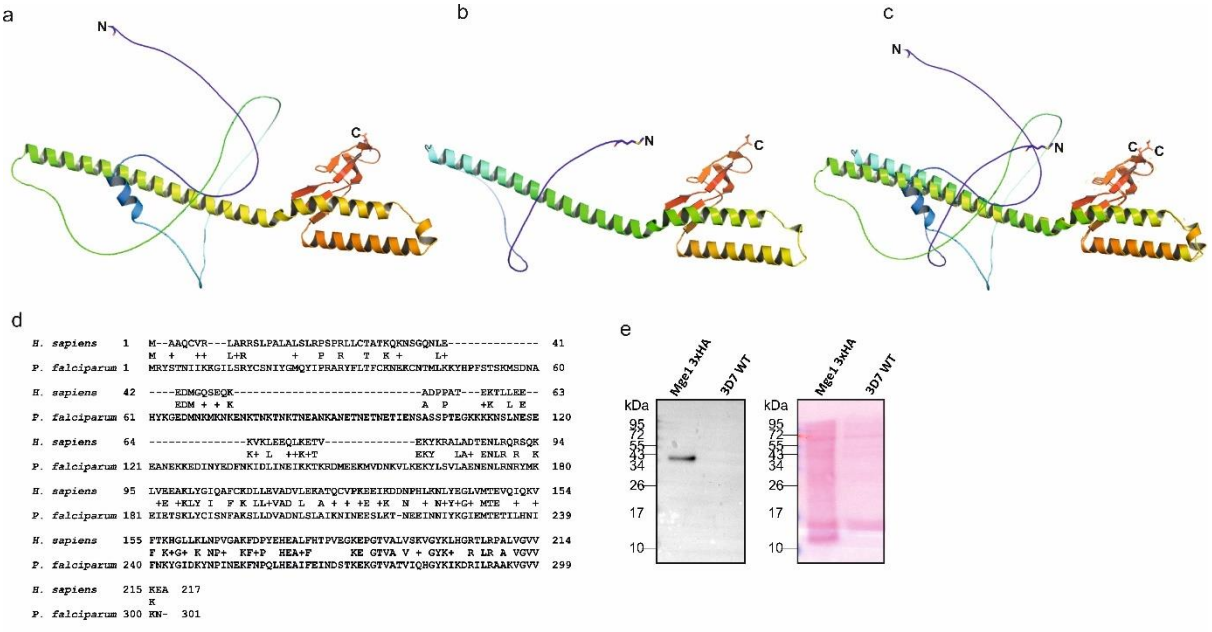

Figure 14 Analyses of *P. falciparum* Mge1. (a) Predicted AlphaFold structure of *Pf*Mge1. (b) Predicted AlphaFold structure of *Hs*Mge1. (c) Structural alignment of *Pf*Mge1 and *Hs*Mge1. (d) Sequence alignment of *Pf*Mge1 and *Hs*Mge1 (e) Left: Western blot detection of *PFMGE1-3xHA* SLI construct that was successfully integrated into the endogenous locus of *Pf*Mge1 and expressed in blood-stage parasites. Proteins were separated using a 15% SDS PAGE gel and transferred to a PVDF membrane, and probed with rabbit anti-HA antibody. Right: Ponceau S staining of PVDF membrane as a loading control.

3.2.2.3 Presequence translocase-associated protein import motor 16 (PAM16)

In *Saccharomyces cerevisiae*, Pam16 was identified as a 16 kDa protein containing an *N*-terminal mitochondrial targeting signal (Frazier et al., 2004). Pam16 has been noted to contain the three-characteristic α-helical segments of J-proteins, thereby showing substantial similarity to the J-proteins. However, Pam16 lacks the J-protein signature motif His-Pro-Asp (HPD) (Frazier et al., 2004). Functionally, Pam16 interacts with Pam18 for the formation of the mtHsp70-Tim44 complex needed for a functional PAM reaction cycle. Pam16 mediates the translocation of precursor proteins into the matrix but is not required for the insertion of precursor proteins into the inner membrane (Frazier et al., 2004). The predicted AlphaFold structures of *P. falciparum* Pam16 and human Pam16 are shown in Figure 15a and b, respectively. A pairwise sequence alignment of the human host Pam16 and the *P. falciparum* Pam16 showed a relatively low sequence identity of 21% (30/146 residues) and a moderate similarity of 39% (43/146 residues) (Figure 15d). However, the structural alignment of the human Pam16 and the *P. falciparum* Pam16 produced a relatively low structure similarity (Figure 15c) with an RMSD score of 7.612, indicating significant differences in their native structure despite the moderate sequence similarity. The results of the sequence and structural alignments may indicate that Pam16 is not conserved structurally between the human host and *P. falciparum.* To assess the production of *Pf*Pam16, transgenic parasites producing *Pf*Pam16-3xHA fusion proteins were enriched using a MACS column, followed by differential protein extraction methods to obtain protein samples for western blot analyses. In the first extraction method, parasites were treated with saponin to remove the erythrocytes and the parasitophorous vacuole, and the resulting lysate was centrifuged, followed by lysis of the pellet fraction in a buffer containing 4% SDS and 0.5% Triton X-100. The solubilized proteins were then mixed with SDS loading buffer. In a second approach, enriched late-stage parasites

were directly lysed by boiling in Laemmli buffer and stored at – 80 °C until later use. A third extraction method involved carbonate lysis of the enriched parasite fraction, followed by mixing with SDS loading buffer. All extracted samples were separated on a 20% SDS-PAGE gel, transferred to PVDF membranes, and probed with a rabbit α-HA antibody. Western blot analyses failed to detect a clear band at the expected molecular weight of *Pf*Pam16 compared to the positive controls of *Pf*Mge1 and *Pf*Sam50 (Figure 15e and f). The calculated molecular weight of the full-length *Pf*Pam16 is 15kDa, while the processed protein (N-terminal presequence cleaved off) has a calculated molecular weight of 13kDa. On the other hand, the calculated molecular weight of the full-length tagged *Pf*Pam16 (*Pf*Pam16-3xHA) was 18kDa, and the processed *Pf*Pam16-3xHA has a calculated molecular weight of 16kDa. No western blot signal was detected for any of the calculated molecular weights of *Pf*Pam16. Therefore, the production of *Pf*Pam16-3xHA could not be validated by western blot analyses.

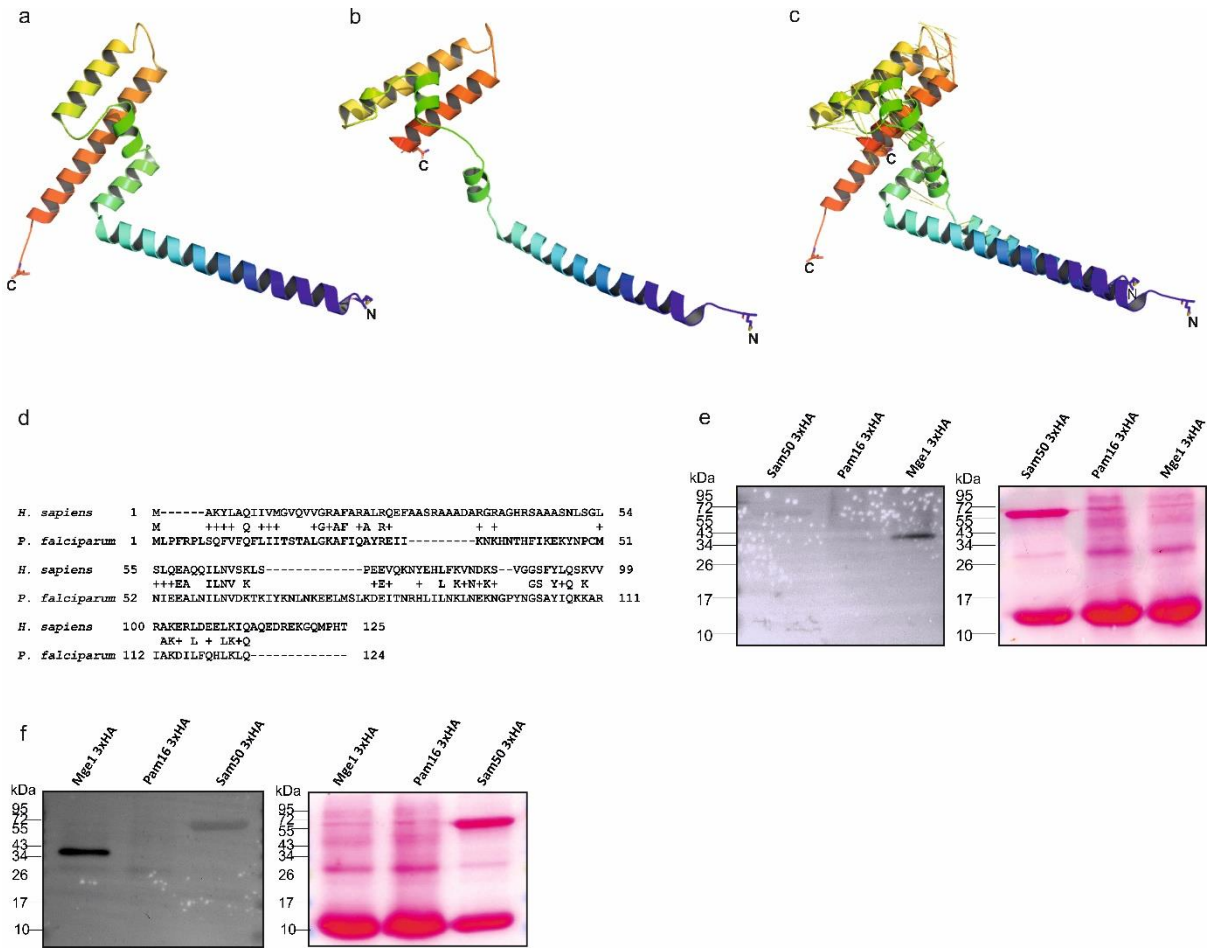

Figure 15 Analyses of *P. falciparum* Pam16. (a) Predicted AlphaFold structure of *Pf*Pam16. (b) Predicted AlphaFold structure of *Hs*Pam16. (c) Structural alignment of *Pf*Pam16 and *Hs*Pam16. (d) Sequence alignment of *Pf*Pam16 and *Hs*Pam16 (e) Left: Western blot detection of *PFPAM16-3xHA* SLI construct that was successfully integrated into the endogenous locus of

*Pf*Pam16 and expressed in blood-stage parasites. Proteins were separated using a 20% SDS PAGE gel and transferred to a PVDF membrane, and probed with rabbit anti-HA antibody. Right: Ponceau S staining of PVDF membrane as loading control.
.

3.2.3 Detection and analyses of inner mitochondrial membrane tagged components in *P. falciparum*

3.2.3.1 Oxidase assembly insertase 1 (Oxa1)

Oxa1 was identified in yeast as conserved and essential for cytochrome c biogenesis, respiratory growth, and the export and assembly of the mitochondrially encoded Cox2 subunit (Bauer et al., 1994; Bonnefoy et al., 1994). Oxa1 has five transmembrane segments that span the inner mitochondrial membrane with the *C*-terminus exposed into the matrix. (Homberg et al., 2023). Oxa1 forms the vital component of the OXA pathway, also known as the conservative sorting pathway, as it is highly conserved throughout evolution. The OXA pathway shares similarity with the YidC-dependent incorporation of membrane proteins in prokaryotes and is presumed to facilitate the insertion and assembly of substrates in a YidC-like manner (Chacinska et al., 2009; Dudek et al., 2013; Endo & Yamano, 2009; Gross & Bhattacharya, 2009; Lithgow & Schneider, 2010). Homologs of the Oxa1 subunit of the OXA pathway have been predicted to be present in the genome of apicomplexan parasites (Deponte et al., 2012; Eckers et al., 2012). In *Plasmodium* parasites, the OXA pathway is thought to insert important substrate candidates such as the three mitochondrially encoded proteins and a few nuclear encoded proteins, including the Oxa1 subunit itself (Deponte, 2013). Despite the conservation of the OXA pathway and the identification of the Oxa1 subunit in the genomes of apicomplexan parasites by comparative genomic studies, the presence of Oxa1 has not been demonstrated in apicomplexan parasites. The predicted AlphaFold structures of *P. falciparum* Oxa1 and human Oxa1 are shown in Figure 16a and b, respectively. A pairwise sequence alignment of the human host Oxa1 and the *P. falciparum* Oxa1 showed a relatively low sequence identity of 13% (81/645 residues) and a moderate similarity of 26% (172/645 residues) (Figure 16d). However, the structural alignment of the human Oxa1 and the *P. falciparum* Oxa1 produced a relatively low structure similarity (Figure 16c) with an RMSD score of 2.085 for the aligned atoms, indicating a moderately similar structure. The results of the sequence and structural alignments may indicate that the structure of Oxa1 is conserved

between the human host and *P. falciparum,* despite the very low sequence identity. To assess the endogenous production of *Pf*Oxa1, transgenic parasites producing *Pf*Oxa1-3xHA fusion proteins were enriched using a MACS column and treated with saponin to remove the erythrocytes and the parasitophorous vacuole. The resulting lysate was centrifuged, and the pellet fraction was subjected to carbonate lysis and mixed with SDS loading buffer. The samples were resolved on a 10% SDS PAGE gel and transferred to a PVDF membrane. The membrane was probed with a rabbit α-HA antibody. The Western blot analyses of two biological replicates revealed two distinct bands in each lane: an upper band migrating between 72 kDa and 95 kDa, and a lower band between 43 kDa and 55 kDa (Figure 16e). The calculated molecular weight of the full-length *Pf*Oxa1 is 70kDa, while the calculated molecular weight of the full-length tagged *Pf*Oxa1 (*Pf*Oxa1-3xHA) was 73kDa.The upper band likely corresponds to the calculated molecular weight of *Pf*Oxa1-3xHA of 75kDa. In contrast, the presence of the lower, which corresponds to a band size of ~50kDa, suggests a possible dual production of the tagged *Pf*Oxa1, potentially due to alternative splicing or initiation from an alternative translation start site at position 154 of the amino acid sequence (Figure 27).

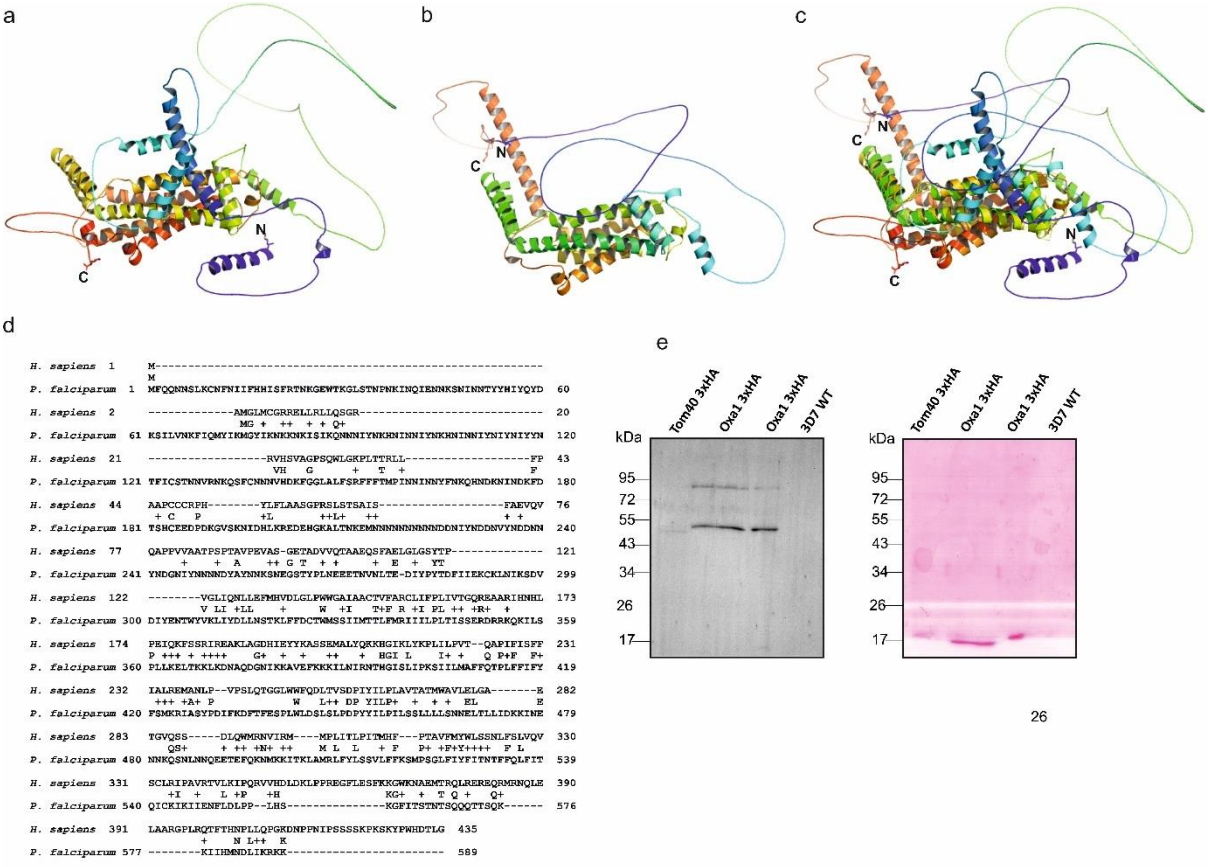

Figure 16 Analyses of *P. falciparum* Oxa1. (a) Predicted AlphaFold structure of *Pf*Oxa1. (b) Predicted AlphaFold structure of *Hs*Oxa1. (c) Structural alignment of *Pf*Oxa1 and *Hs*Oxa1. (d) Sequence alignment of *Pf*Oxa1 and *Hs*Oxa1 (e) Left: Western blot detection of *PFOXA1-3xHA* SLI construct that was successfully integrated into the endogenous locus of *Pf*Oxa1 and expressed in blood-stage parasites. Proteins were separated using a 15% SDS PAGE gel and transferred to a PVDF membrane and probed with rabbit anti-HA antibody. Right: Ponceau S staining of PVDF membrane as a loading control.

.

3.2.4 Detection of mitochondrial intermembrane space small Tim proteins in *P. falciparum*

3.2.4.1 Small Translocase of the inner membrane (Tim) proteins

The small Tim proteins belong to a set of chaperones in the intermembrane space of the mitochondria that assist in the import of proteins with internal targeting signals to the mitochondrial inner membrane (Joseph T Smith et al., 2018). The proteins are characterized by their conserved twin CxC motif separated by 11-16 residues (Koehler, 2000; Paschen & Neupert, 2001). In opisthokonts, the small Tim protein family consists of Tim8, Tim9, Tim10, Tim12, and Tim13 (Gentle et al., 2007; M. P. Murphy et al., 2001). Small Tim proteins form chaperone complexes that bind to the hydrophobic segments of mitochondrial inner membrane proteins with multiple transmembrane segments to aid their interaction with the TIM22 complex and subsequent insertion into the inner membrane (Curran et al., 2002a; Kovermann et al., 2002; Truscott et al., 2002). Tim9 and Tim10 form a 3B3 hexameric complex that binds to hydrophobic regions of imported substrates to facilitate their translocation to the TIM22 complex, while Tim8 forms a similar hexameric complex with Tim13 that aids in the import of Tim23 (Curran et al., 2002; Hoppins & Nargang, 2004; Paschen et al., 2000).

Although homologs of the small Tim proteins (Tim9/Tim10 and Tim8/Tim13) have been identified in the genome of *P. falciparum*, their production has not been demonstrated in *P. falciparum*. The predicted AlphaFold structures of *P. falciparum* Tim8 and Tim13 and human Tim8 and Tim13 are shown in Figure 17a and b, and 17d and e, respectively. A pairwise sequence alignment of the human host Tim8 and Tim13 and the *P. falciparum* Tim8 and Tim13 showed a relatively low sequence identity of 21% (26/125 residues) and 25% (28/110 residues) respectively and a moderate similarity of 36% (45/125 residues) and 40% (44/110 residues) respectively (Figure 17g and h). However, the structural alignment of the human Tim8 and Tim13 and the *P. falciparum* Tim8 and Tim13 produced a relatively low structure

similarity (Figure 17c and f), respectively, with an RMSD score of 4.548 and 4.924, respectively, for the aligned atoms. The results of the sequence and structural alignments may indicate that the structure of Tim8 and Tim13 is not conserved between the human host and *P. falciparum,* despite the moderate sequence similarity. To investigate the production of *P. falciparum* small Tim proteins, transgenic parasites expressing *P*fTim*8*-3xHA and *P*fTim13-3xHA fusion proteins were enriched using a MACS column and treated with saponin to remove the erythrocytes and the parasitophorous vacuole. The resulting lysate was centrifuged, then subjected to three different extraction protocols: (1) treatment with parasite lysis buffer containing 4% SDS and 0.5% Triton X-100 followed by mixing with SDS loading buffer, (2) direct lysis of enriched late-stage parasites by boiling in Laemmli buffer, and (3) carbonate lysis followed by addition of SDS loading buffer. All extracted samples were resolved on a 20% SDS-PAGE gel, transferred to PVDF membranes, and probed with a rabbit α-HA antibody. Western blot analyses detected multiple signals between 10kDa and 17kDa, 26kDa and 34kDa, and 55kDa for *Pf*Tim8-3xHA and *Pf*Tim13-3xHA compared to no signals in the negative control (3D7 WT) (Figure 17i and j). The calculated molecular weight of the full-length *Pf*Tim8 and *Pf*Tim13 is 13kDa and 11kDa, respectively, while the calculated molecular weights of the full-length tagged *Pf*Tim8 (*Pf*Tim8-3xHA) and *Pf*Tim13 (*Pf*Tim13-3xHA) were 17kDa and 14kDa, respectively. The western blot signals detected between 10kDa and 17kDa are likely to correspond to full-length untagged proteins for *Pf*Tim8 (13kDa) and PfTim13 (11kDa). In contrast, the detected signals between 26kDa and 34kDa could reflect the formation of *Pf*Tim8-3xHA/*Pf*Tim13-3xHA hexamers of 31kDa. The higher band signals detected may likely be false positives or signals corresponding to the HA antibody chain. The results likely confirm the production of *Pf*Tim8-3xHA and *Pf*Tim13-3xHA and the potential formation of Tim8-3xHA/Tim13-3xHA hexamers in *P. falciparum*.

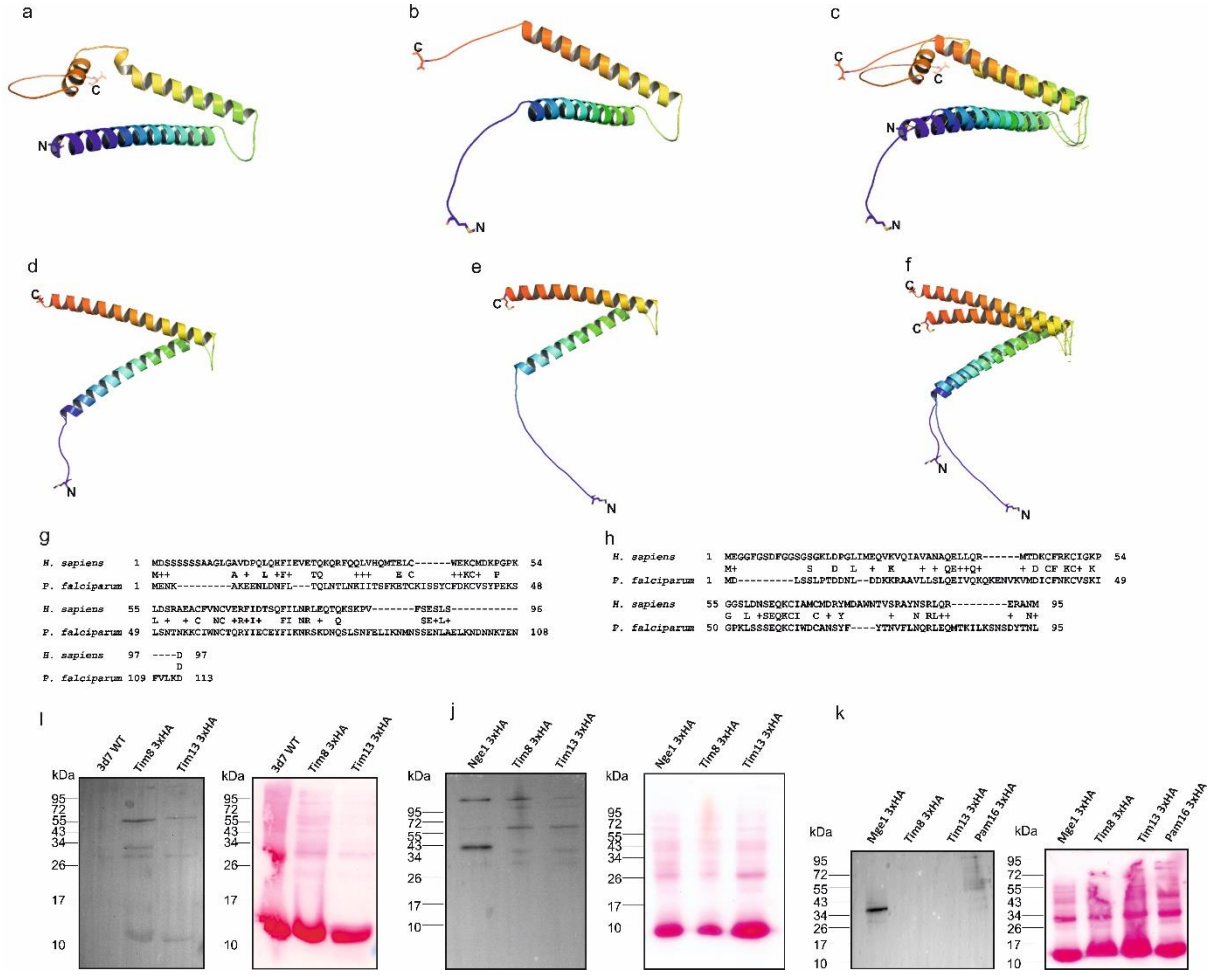

Figure 17 Analyses of *P. falciparum* Tim8 and Tim13. (a) Predicted AlphaFold structure of *Pf*Tim8. (b) Predicted AlphaFold structure of *Hs*Tim8. (c) Structural alignment of *Pf*Tim8 and *Hs*Tim8. (d) Sequence alignment of *Pf*Tim8 and *Hs*Tim8. (e) Predicted AlphaFold structure of *Pf*Tim13. (f) Predicted AlphaFold structure of *Hs*Tim13. (g) Structural alignment of *Pf*Tim13 and *Hs*Tim13. (h) Sequence alignment of *Pf*Tim13 and *Hs*Tim13. (I-k) Left: Western blot detection of *PFTIM8-3xHA* SLI and *PFTIM13-3xHA* SLI constructs that were successfully integrated into the endogenous loci of *Pf*Tim8 and *Pf*Tim13 expressed in blood-stage parasites. Proteins were separated using a 20% SDS PAGE gel and transferred to a PVDF membrane, and probed with rabbit anti-HA antibody. Right: Ponceau S staining of PVDF membrane as loading control.

.

3.3 Mitochondrial localization of tagged components of the protein import machineries in *P. falciparum*

Following the validation of the production of *P. falciparum* mitochondrial protein import machinery core components by Western blot analyses, the mitochondrial localization of these components was then analyzed by immunofluorescence microscopy. To achieve this objective, asynchronous cultures of 3xHA-tagged transgenic parasites were used for the immunofluorescence assay. Prior to the initial fixation step with paraformaldehyde, the

mitochondria were stained with MitoTracker Orange CM™ Ros (MTO) to visualize the mitochondria and determine the potential mitochondrial colocalization of the tagged proteins. The samples were then treated with α-HA primary antibody against the 3xHA and subsequently incubated with the fluorescent secondary antibody conjugate Alexa488 to visualize the 3xHA fusion proteins. The parasite nuclei were stained with DAPI to distinguish between infected and uninfected erythrocytes as well as the different asexual blood stages. The mitochondrial localization of the core components of the mitochondrial outer membrane, intermembrane space, inner membrane, and the matrix was analyzed for the ring, trophozoite, and schizont asexual blood stages of *P. falciparum.*

3.3.1 Mitochondrial localization of Tom40 and Sam50 in *P. falciparum*

Confocal immunofluorescence microscopy images for the strains of 3D7 *Pf*Tom40-3xHA and 3D7 *Pf*Sam50-3xHA are shown in Figure 18a and b, respectively. An α-HA signal of the Alexa 488 fluorophore was detected in both strains, confirming the production of *Pf*Tom40-3xHA and *Pf*Sam50-3xHA in all three asexual blood stages of *P. falciparum*. Merge I, which is an overlay of the MTO signal and the α-HA signal, produced a colocalization signal showing the mitochondrial localization of *Pf*Tom40 and *Pf*Sam50 in all three asexual blood stages of *P. falciparum.* An overlay of the MTO signal and the DAPI signal did not yield an overlapping signal, ruling out a “bleed-through” effect of the mitochondrial or nuclear signals and further validating the colocalization signal of the MTO and the α-HA signals for *Pf*Tom40-3xHA and *Pf*Sam50-3xHA. These results confirm that *P. falciparum* homologs of Tom40 and Sam50 localize to the mitochondrion.

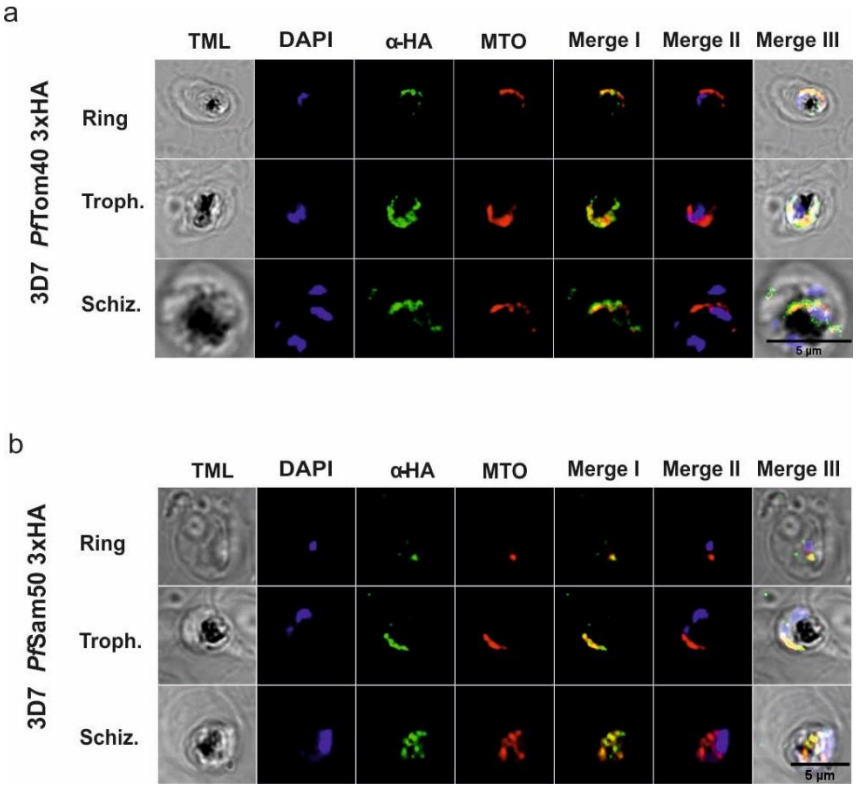

Figure 18 Localization of *Pf*Tom40 and *Pf*Sam50 Immunofluorescence staining of asynchronous cultures of asexual *P. falciparum* 3D7 SLI parasites with chromosomally-encoded (a) *Pf*Tom40-3xHA and (b) *Pf*Sam50-3xHA, respectively. Transmitted light (TML) shows the infected erythrocytes. DAPI shows the parasite nuclei stained with DAPI. α-HA is the signal of the secondary antibody Alexa488 against the α-HA primary antibody, which shows the production of *Pf*Tom40-3xHA and *Pf*Sam50-3xHA. MTO (MitoTracker orange CMTM Ros) shows the mitochondrial staining. Merge I is the overlay of the α-HA and MTO channels showing co-localization. Merge II combines the DAPI and MTO channels. Merge III combines all signals into a single image. Representative cells of the samples imaged are shown. All images were acquired using a confocal microscope in Z-stack format under identical parameters and analyzed identically for comparability. The same representative plane is shown for all channels from the Z-stack. The scale bar corresponds to 5 µm.

3.3.2 Mitochondrial localization of the PAM components in *P. falciparum*

Three components of the PAM complex analyzed by confocal microscopy are shown in Figure 19. Microscopy images of the immunofluorescence staining for the 3D7 strains *f*Hsp70-3xHA (a), 3D7 *Pf*Mge1-3xHA (b), and 3D7 *Pf*Pam16-3xHA (c) were analyzed. α-HA signals of the Alexa 488 fluorophore were detected in all three strains, demonstrating the production of *Pf*Hsp70-3xHA, *Pf*Mge1-3xHA, and *Pf*Pam16-3xHA in all three asexual blood stages of *P. falciparum*. Merge I, which is an overlay of the MTO signal and the α-HA signal, produced a colocalization signal confirming the mitochondrial localization of *Pf*Hsp70-3xHA, *Pf*Mge1-3xHA, and

*Pf*Pam16-3xHA in all three asexual blood stages of *P. falciparum.* An overlay of the MTO signal and the DAPI signal did not yield an overlapping signal, ruling out a “bleed-through” effect of the mitochondrial or nuclear signals. Taking the data altogether, the data indicate a localization of *P. falciparum* homologues of Hsp70, Mge1, and Pam16 in the mitochondrion.

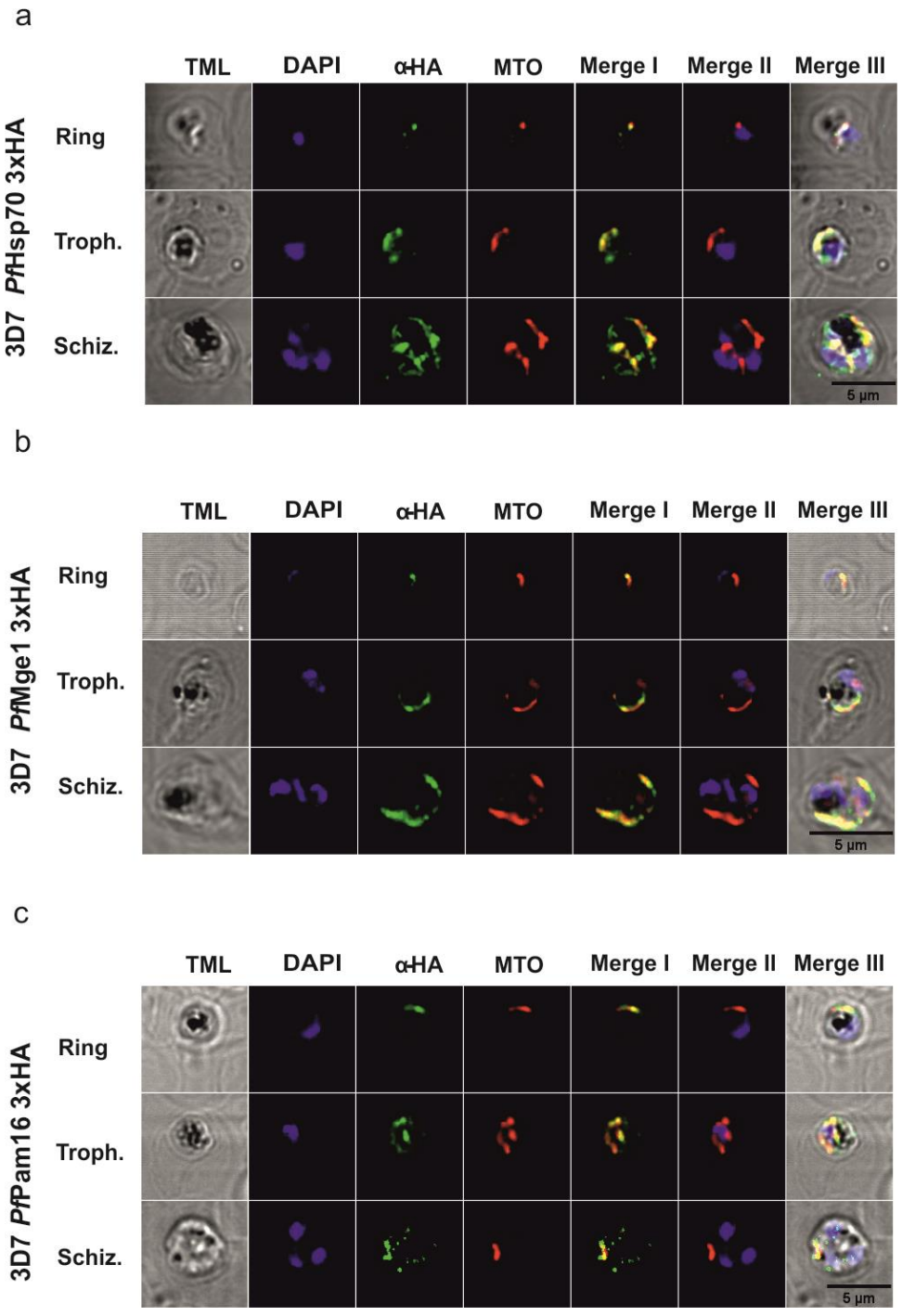

Figure 19 Localization of *Pf*Hsp70, *Pf*Mge1, and *Pf*Pam16. Immunofluorescence staining of asynchronous cultures of asexual *P. falciparum* 3D7 SLI parasites with chromosomally-encoded (a)*Pf*Hsp70-3xHA, (b) *Pf*Mge1-3xHA, and (c) *Pf*Pam16-3xHA, respectively. Transmitted light (TML) shows the infected erythrocytes in transmitted light, DAPI shows the parasite nuclei stained with DAPI, α-HA is the signal of the secondary antibody Alexa488 against the α-HA primary antibody, which shows the production of *Pf*Hsp70, *Pf*Mge1, and *Pf*Pam16, MTO (MitoTracker orange CMTM Ros) shows the mitochondrial staining. Merge I is the overlay of the α-HA and MTO channels showing co-localization. Merge II combines the DAPI and MTO channels. Merge III combines all signals into a single image. Representative cells of the samples imaged are shown. All images were acquired using a confocal microscope in Z-stack format under identical parameters and analyzed identically for comparability. The same representative plane is shown for all channels from the Z-stack. The scale bar corresponds to 5 µm.

3.3.3 Mitochondrial localization of Oxa1 in *P. falciparum*

Figure 20 shows the microscopy images of the immunofluorescence staining for the strain of 3D7 *Pf*Oxa1-3xHA. An α-HA signal of the Alexa 488 fluorophore was detected in all three asexual blood stages of *P. falciparum,* which confirmed the production of *Pf*Oxa1-3xHA. Merge I, which is an overlay of the MTO signal and the α-HA signal, produced a colocalization signal showing the mitochondrial localization of *Pf*Oxa1 in all three asexual blood stages of *P. falciparum*. It was also observed that parts of the α-HA signal did not show a colocalization signal after the overlay with the MTO signal. An overlay of the MTO signal and the DAPI signal did not yield an overlapping signal, ruling out a "bleed-through" effect of the mitochondrial or nuclear signals, further validating the colocalization signal of the MTO and the α-HA signals. The results indicate that the *P. falciparum* homologue of Oxa1 localizes to the mitochondrion and potentially dually localizes or targets to a neighboring organelle.

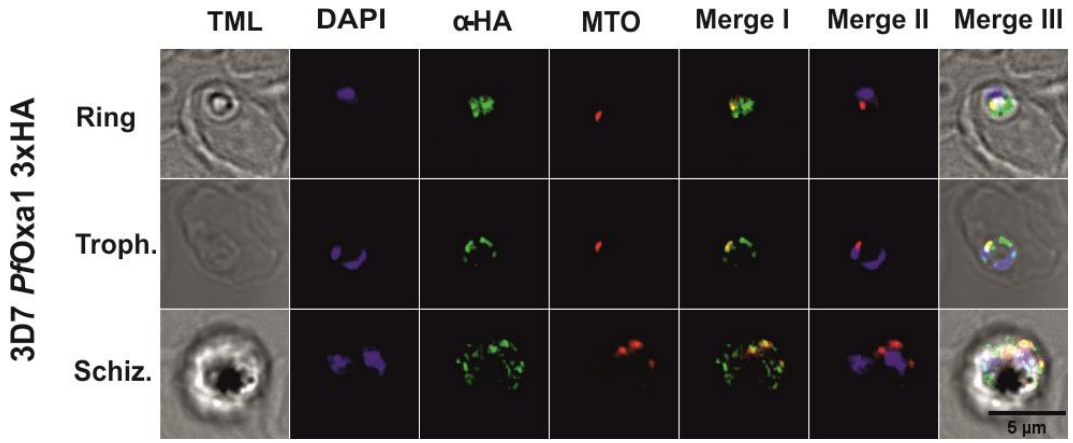

Figure 20 Localization of *Pf*Oxa1. Immunofluorescence staining of asynchronous culture of asexual *P. falciparum* 3D7 SLI parasites with chromosomally encoded *Pf*Oxa1-3xHA. Transmitted light (TML) shows the infected erythrocytes. DAPI shows the parasite nuclei stained with DAPI. α-HA is the signal of the secondary antibody Alexa488 against the α-HA primary

antibody, which shows the production of *Pf*Oxa1-3xHA. MTO (MitoTracker orange CMTM Ros) shows the mitochondrial staining. Merge I is the overlay of the α-HA and MTO channels showing co-localization. Merge II combines the DAPI and MTO channels. Merge III combines all signals into a single image. Representative cells of the samples imaged are shown. All images were acquired using a confocal microscope in Z-stack format under identical parameters and analyzed identically for comparability. The same representative plane is shown for all channels from the Z-stack. The scale bar corresponds to 5 µm.

3.3.4 Mitochondrial localization of small Tim proteins in *P. falciparum*

Two small Tim proteins, Tim8 and Tim13, were analyzed by confocal microscopy for their localization in the mitochondrion of *P. falciparum*. Figure 21 shows the microscopy images of the immunofluorescence staining for the strain 3D7 Tim13-3xHA (a) and 3D7 Tim8-3xHA (b). α-HA signals of the Alexa 488 fluorophore were detected in both strains across all three asexual blood stages of P. falciparum, which confirmed the production of *Pf*Tim13 3xHA and *Pf*Tim8-3xHA. Merge I, which is an overlay of the MTO signal and the α-HA signal, produced a colocalization signal showing the mitochondrial localization of *Pf*Tim13-3xHA and *Pf*Tim8-3xHA in all three asexual blood stages of *P. falciparum.* An overlay of the MTO signal and the DAPI signal did not yield an overlapping signal, ruling out a “bleed-through” effect of the mitochondrial or nuclear signals. These results indicate that *P. falciparum* homologs of Tim13 and Tim8 localize to the mitochondrion.

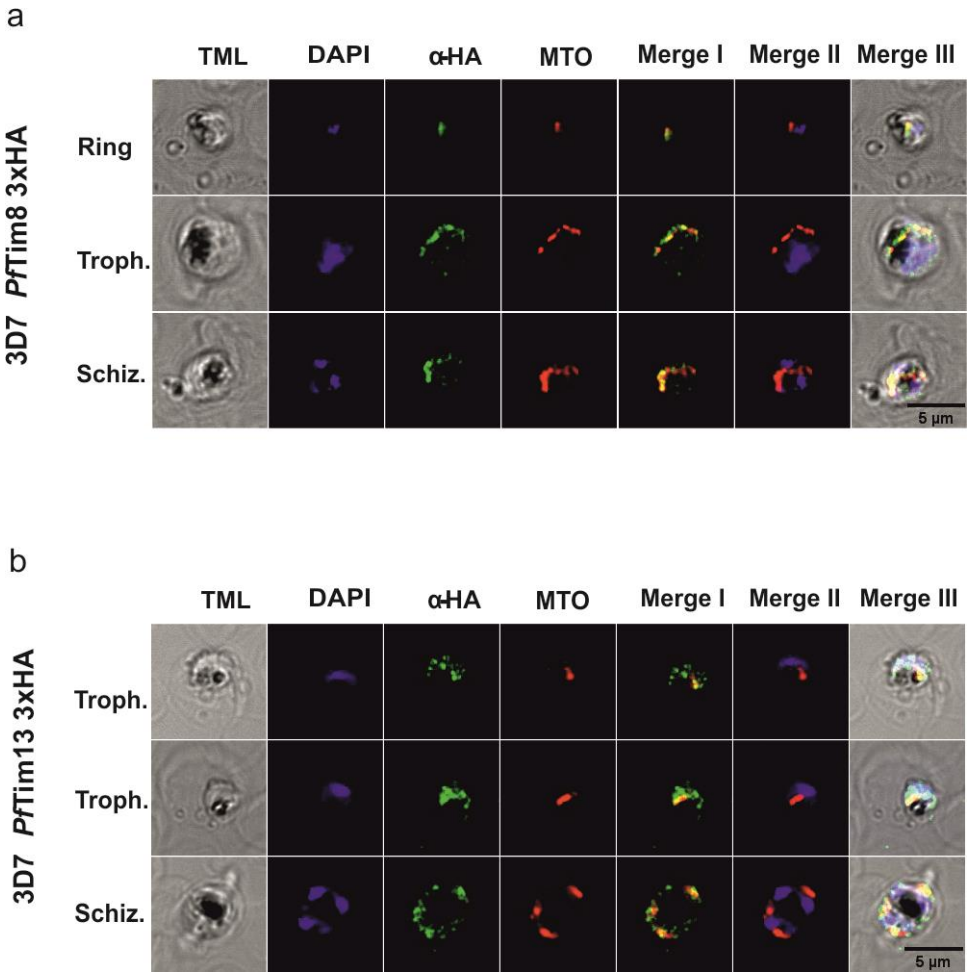

Figure 21 Localization of *Pf*Tim8 and *Pf*Tim13. Immunofluorescence staining of asynchronous cultures of asexual *P. falciparum* 3D7 SLI parasites with chromosomally encoded (a) *Pf*Tim8-3xHA and (b) *Pf*Tim13-3xHA, respectively. Transmitted light (TML) shows the infected erythrocytes. DAPI shows the parasite nuclei stained with DAPI. α-HA is the signal of the secondary antibody Alexa488 against the α-HA primary antibody, which shows the production of *Pf*Tim8 and *Pf*Pam16. MTO (MitoTracker orange CMTM Ros) shows the mitochondrial staining. Merge I is the overlay of the α-HA and MTO channels showing co-localization. Merge II combines the DAPI and MTO channels. Merge III combines all signals into a single image. Representative cells of the samples imaged are shown. All images were acquired using a confocal microscope in Z-stack format under identical parameters and analyzed identically for comparability. The same representative plane is shown for all channels from the Z-stack. The scale bar corresponds to 5 µm.

A summary of the western blot analyses and confocal immunofluorescence microscopy analyses of the tagged components of the mitochondrial protein import machineries of *P. falciparum* is shown in Table 20.

Table 20 Summary of 3xHA tagged components analyses.

Protein	Western blot signal	Immunofluorescence signal
*Pf*Tom40-3xHA	Positive	Positive
*Pf*TSam50-3xHA	Positive	Positive
*Pf*Tim8-3xHA	Positive	Positive
*Pf*Tim13-3xHA	positive	Positive
*Pf*mtHsp70-3xHA	Positive	Positive
*Pf*Mge1-3xHA	Positive	Positive
*Pf*Pam16-3xHA	Negative	Positive
*Pf*Oxa1-3xHA	Positive	Positive

3.4 Identification of protein–protein interaction partners of tagged components of the mitochondrial protein import machineries in *P. falciparum*.

Immunoblotting and confocal imaging confirmed for the first time the production and mitochondrial localization of the core components of the mitochondrial protein import machinery in *P. falciparum*. Building on these findings, the next objective was to characterize the interactome of selected import machineries of the core components of *P. falciparum*. To achieve this, pulldown assays were conducted using cell lysates of transgenic strains producing the 3xHA-tagged core components as bait proteins and magnetic beads that were coupled to HA antibodies. To confirm the success of pulldown assays, the lysates, hereby referred to as inputs (IN), and the eluates (EL) were resolved by SDS PAGE gel and transferred to a PVDF membrane. The membranes were decorated using a rabbit α-HA antibody. The pulldown assays were performed in three technical replicates for *Pf*Mge1-3xHA of the PAM complex, *Pf*Tom40-3xHA of the TOM complex, and *Pf*Sam50-3xHA of the SAM complex. The eluates were first purified and enriched using the SP3 assay and digested overnight with trypsin. The digested peptides were further purified on C18 tips and the eluted peptides sent directly for LC-MS/MS analyses. Data analyses was performed with Perseus software version 1.6.12.0.

Prior to the analyses of the MS results, the predicted protein interaction network of candidate bait proteins was analyzed in the String proteomic database.

The western blot analyses of the *Pf*Mge1-3xHA pulldown revealed a signal above 34 kDa (Figure 22a) in the eluate sample corresponding to the calculated molecular weight of processed *Pf*Mge1-3xHA of 3kDa, confirming the successful enrichment or pulldown of the bait protein. A 55 kDa band was detected in the eluate sample for *Pf*Tom40-3xHA, which did not correspond to the expected band size of the full-length *Pf*Tom40 (44kDa) or full-length *Pf*Tom40-3xHA (47kDa) (Figure 23a), while a similar band size corresponding to the expected band size of *Pf*SAM50 (54kDa) was detected in the eluate of the *Pf*Sam50-3xHA pulldown western blot (Figure 24) which could be a false positive or a band corresponding to the heavy chain of the HA antibody (which was detected in all sample lanes). Altogether, a successful pull-down was confirmed by Western blot analyses for *Pf*Mge1-3xHA, while no clear bands confirming the enrichment of *Pf*Tom40-3xHA and *Pf*Sam50-3xHA were detected.

3.4.1 Interactome analyses of *Pf*Mge1-3xHA in *P. falciparum*

Prior to the LC-MS/MS analyses, predicted protein-interacting partners of *Pf*Mge1 were retrieved from the STRING database, as shown in Table 21. A list of physical interactors was generated with medium to high confidence, and this included components of the PAM complex. Additionally, several core subunits of the TIM23 complex were identified, consistent with known physical associations between the opistokonts TIM23 and PAM complexes involved in translocating proteins to the mitochondrial matrix and inner membrane. Analyses of the interactome of *Pf*Mge1-3xHA from the pulldown confirmed significant enrichment of the bait protein. However, predicted interactors from the STRING database were not significantly enriched based on statistical testing (t-test, FDR<0.01, S0 = 1 for class A interactors and t-test, FDR<0.05, S0 =1 for class B interactors)(Figure 22b). Interestingly, proteins that were significantly enriched alongside *Pf*Mge1 during the pulldown did not correspond to known interactors listed in the STRING database (t-test, FDR<0.01, S0 = 1 for class A interactors and t-test, FDR<0.05, S0 =1 for class B interactors), suggesting possible nonspecific binding of unrelated proteins (Table 22).

Table 21 Predicted protein interactors of *Pf*Mge1

Gene ID	Protein
PF3D7_0309700	SECIS-binding protein 2, putative.
PF3D7_0513500	Mitochondrial import inner membrane translocase subunit TIM16, putative.
PF3D7_0627400	Mitochondrial import inner membrane translocase subunit TIM22, putative.
PF3D7_0629200	DnaJ protein, putative.
PF3D7_0724400	Mitochondrial import inner membrane translocase subunit TIM14, putative.
PF3D7_0726900	Mitochondrial import inner membrane translocase subunit TIM50
PF3D7_0730900	EMP1-traffickingprotein.
PF3D7_0827900	Protein disulfide-isomerase.
PF3D7_0917000	Merozoite organizing protein.
PF3D7_0919400	Protein disulfide isomerase.
PF3D7_1124700	GrpE protein homolog
PF3D7_1125400	Mitochondrial import inner membrane translocase subunit TIM44, putative.
PF3D7_1134000	Heat shock protein 70; Belongs to the heat shock protein 70 family.
PF3D7_1208600	Mitochondrial import inner membrane translocase subunit TIM10, putative.
PF3D7_1344200	Endoplasmic reticulum chaperone GRP170.
PF3D7_1353700	Reactive oxygen species modulator 1
PF3D7_1356200	Mitochondrial import inner membrane translocase subunit TIM23, putative.
PF3D7_1368600	Mitochondrial import inner membrane translocase subunit TIM9, putative.
PF3D7_1420300	DNL-type zinc finger protein.
PF3D7_1434700	Mitochondrial import inner membrane translocase subunit TIM17, putative.

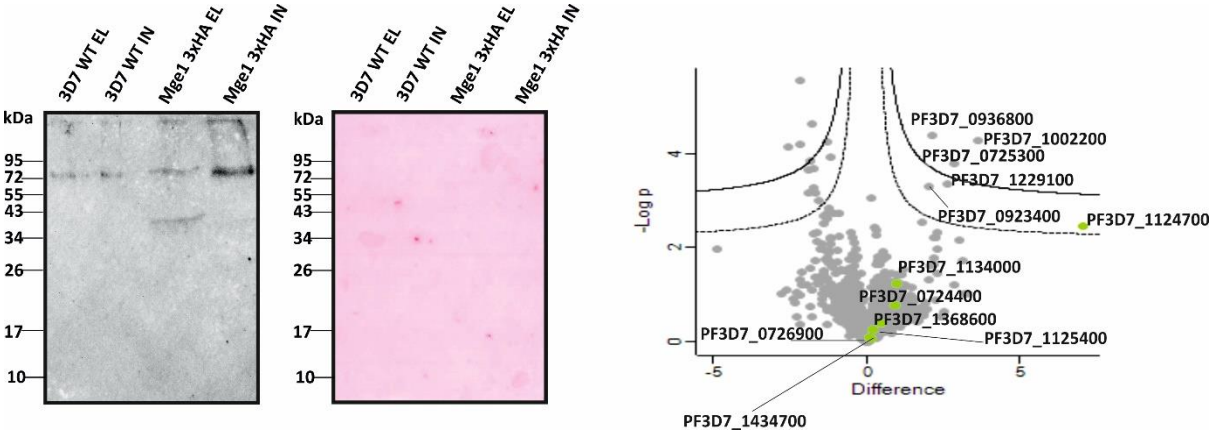

Figure 22 *Pf*Mge1 interactome analyses. (a) Left: Western blot detection of pulldown assay of *PFMGE1-3xHA* SLI construct that was successfully integrated into the endogenous locus of *Pf*Mge1 and expressed in blood-stage parasites. Parasite lysates, hereby referred to as input (IN) and eluted proteins (EL), were separated using a 12% SDS PAGE gel and transferred to a PVDF membrane. The blots were decorated using rabbit anti-HA antibody (b) Volcano plot representation of the outcome of *Pf*Mge1 interactome study conducted in blood stage *P. falciparum* 3D7 SLI parasites with chromosomally encoded *Pf*Mge1-3xHA. The proteins highlighted in green were identified as *Pf*Mge1 interacting partners in the STRING database. The figure also shows the identified interacting candidates of *Pf*Mge1 from the interactome analyses (t-test, FDR<0.01, S0 = 1 for class A interactors and t-test, FDR<0.05, S0 = 1 for class B interactors).

Table 22 Detected protein interactors of *Pf*Mge1

Gene ID	Protein
PF3D7_1124700	GrpE protein homolog (Mge1)
PF3D7_0936800	Plasmodium RESA N-terminal domain-containing protein
PF3D7_1002200	Tryptophan-rich antigen 3
PF3D7_1229100	Multidrug resistance-associated protein
PF3D7_0923400	Uncharacterized protein
PF3D7_0725300	WD repeat-containing protein

3.4.2 Interactome analyses of *Pf*Tom40-3xHA and *Pf*Sam50-3xHA components in *P. falciparum*

To explore the protein-protein interaction landscape of outer mitochondrial membrane components in *P. falciparum*, predicted interactors of *Pf*Tom40 and *Pf*Sam50 were retrieved

from the STRING database and are summarized in Tables 23 and 25, respectively. Two potential interactors of *Pf*Tom4 were retrieved from the STRING database: the sorting assembly machinery of the SAM complex (Sam50) and a cytosolic vacuolar protein-associated sorting protein 3. In contrast, only Tom40 of the TOM complex was predicted as a physical interactor for *Pf*Sam50. The list of physical interactors was generated with medium to high confidence. However, IP-MS analyses of *Pf*Tom40-3xHA (Figure 23b) and *Pf*Sam50-3xHA (Figure 24b) did not show significant enrichment of the bait proteins or their predicted interactors following statistical evaluation (t-test, FDR<0.01, S0 = 1 for class A interactors and t-test, FDR<0.05, S0 =1 for class B interactors). Although these criteria significantly enriched several other proteins, none aligned with known interactors of *Pf*Tom40 or *Pf*Sam50 based on STRING annotations (t-test, FDR<0.01, S0 = 1 for class A interactors and t-test, FDR<0.05, S0 =1 for class B interactors) (Table 24 and Table 26). This outcome likely reflects strong nonspecific binding by unrelated proteins during the pulldown process. Altogether, these results indicate neither the bait proteins nor their expected interacting partners were enriched in the eluate fraction to levels detectable by mass spectrometry. Therefore, the pulldown assays targeting the outer membrane proteins were unsuccessful.

Table 23 Predicted protein interactors of *Pf*Tom40.

Gene ID	Protein Name
PF3D7_0608310	Sorting assembly machinery 50 kDa subunit, putative.
PF3D7_0617000	Mitochondrial import receptor subunit TOM40, putative.
PF3D7_1423800	Vacuolar protein sorting-associated protein 3, putative.

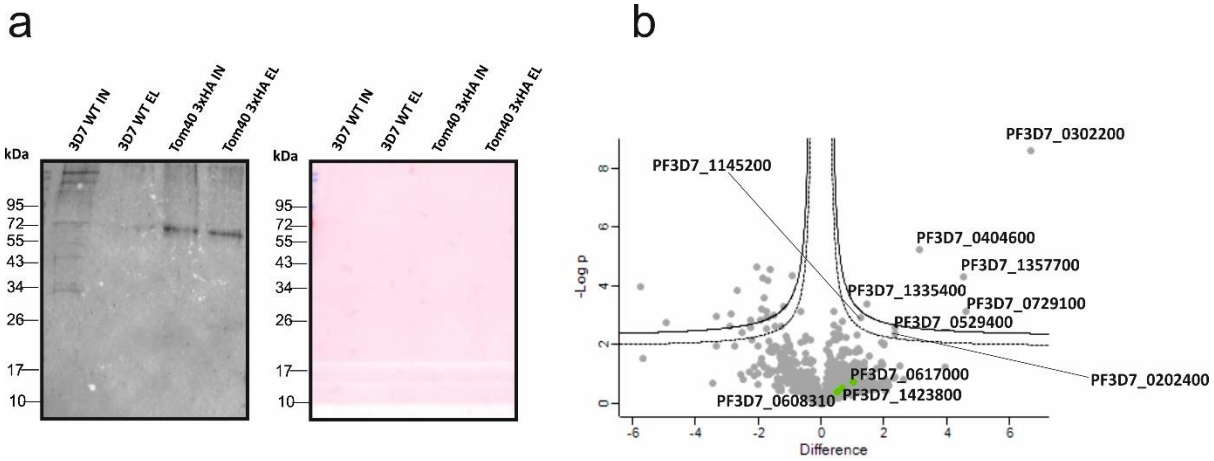

Figure 23 *Pf*Tom40 interactome analyses. (a) Left: Western blot detection of pulldown assay of *PFTOM40-3xHA* SLI construct that was successfully integrated into the endogenous locus of *Pf*Tom40 and expressed in blood-stage parasites. Parasite lysates, hereby referred to as input (IN) and eluted proteins (EL), were separated using a 12% SDS PAGE gel and transferred to a PVDF membrane. The blots were decorated using rabbit anti-HA antibody. (b) Volcano plot representation of the outcome of the *Pf*Tom40 interactome study conducted with blood-stage *P. falciparum* 3D7 SLI parasites with chromosomally-encoded *Pf*Tom40-3xHA. The proteins highlighted in green were identified as interacting partners of *Pf*Tom40 in the STRING database. The figure also shows the identified interacting candidates of *Pf*Tom40 from the interactome analyses (t-test, FDR<0.01, S0 = 1 for class A interactors and t-test, FDR<0.05, S0 1 for class B interactors).

Table 24 Detected protein interactors of *Pf*Tom40

Gene ID	Protein
PF3D7_0202400	Translation-enhancing factor
PF3D7_0529400	Uncharacterized protein
PF3D7_0729100	Allantoicase domain-containing protein
PF3D7_1335400	Reticulocyte-binding-like protein 2
PF3D7_1357700	U3 small nucleolar RNA-associated protein 21, putative
PF3D7_0404600	Uncharacterized protein
PF3D7_1145200	Serine/threonine protein kinase, putative
PF3D7_0302200	Cytoadherence-linked asexual protein 3.2

Table 25 Predicted protein interactors of *Pf*Sam50.

Gene ID	**Protein name**

PF3D7_0608310	Sorting assembly machinery 50 kDa subunit, putative.
PF3D7_0617000	Mitochondrial import receptor subunit TOM40, putative

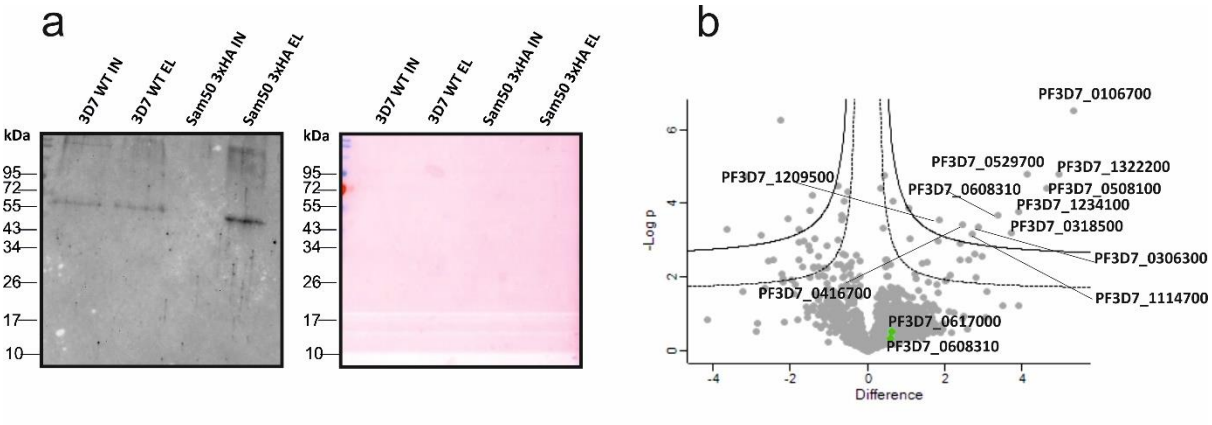

Figure 24 *Pf*Sam50 interactome analyses. (a) (a) Left: Western blot detection of pulldown assay of *PFSAM50-3xHA* SLI construct that was successfully integrated into the endogenous locus of *Pf*Sam50 and expressed in blood-stage parasites. Parasite lysates, hereby referred to as input (IN) and eluted proteins (EL), were separated using a 12% SDS PAGE gel and transferred to a PVDF membrane. The blots were decorated using rabbit anti-HA antibody (b) Volcano plot representation of the outcome *Pf*Sam50 interactome study conducted in blood-stage *P. falciparum* 3D7 SLI parasites with chromosomally-encoded *Pf*Sam50-3xHA. The proteins highlighted in green were identified as interacting partners of *Pf*Sam50 in the STRING database. The figure also shows the identified interacting candidates of *Pf*Sam50 from the interactome analyses (t-test, FDR<0.01, S0 = 1 for class A interactors and t-test, FDR<0.05, S0 1 for class B interactors) are listed in the top right corner.

Table 26 Detected protein interactors of *Pf*Sam50

Gene ID	Protein
PF3D7_0106700	Small ribosomal subunit assembling AARP2 protein
PF3D7_0529700	Heptatricopeptide repeat-containing protein, putative
PF3D7_1322200	TOG domain-containing protein
PF3D7_0508100	U3 small nucleolar RNA-associated protein 21, putative
PF3D7_1234100	Bromodomain protein, putative
PF3D7_0318500	Uncharacterized protein
PF3D7_0416700	CDGSH iron-sulfur domain-containing protein, putative
PF3D7_1209500	cGMP-specific 3',5'-cyclic phosphodiesterase alpha
PF3D7_0306300	Glutaredoxin-1

PF3D7_1114700	non-specific serine/threonine protein kinase

3.5 CRISPR-Cas9-mediated gene knockout of components of the mitochondrial protein import machineries in *P. falciparum*

To investigate the functional relevance and essentiality of selected components of the mitochondrial protein import machinery in *P. falciparum*, the CRISPR-Cas9 gene knockout strategy previously described by Ghorbal et al was adopted. In this method, the pUF1-Cas9 plasmid that encodes the gene of Cas9 enzyme and the pL7 plasmid were employed for the disruption of genes by double cross-over homologous recombination. In this work, the pL7 plasmids were generated by cloning the guide sequence and the flanking homology regions (HR) of target genes into the pL6 plasmid. The homology regions 3' HR and 5' HR were cloned to flank the expression cassette encoding the human dihydrofolate reductase (hDHFR) gene that confers resistance to WR99210, an antifolate drug of *P. falciparum* (Fidock & Wellems, 1997), serving as a positive selectable marker. Gene knockouts were conducted by co-transfection of the pUF1-Cas9 plasmid and the pL7 plasmid into *P. falciparum* 3D7 wild-type strains. Initial drug selection for expression of the pUF1-Cas9 plasmid and episomal uptake of the pL7 plasmid was carried out with DSM1 and WR99210, respectively. Transfectants were detected by Giemsa-stained blood smears four to six weeks post-positive selection with WR99210. Negative selection was carried out using 5-fluorocytosine (5-FC) to eliminate parasites carrying unintegrated pL7 plasmids or parasites in which only a single cross-over event occurred after transfection. Gene knockouts were checked with PCR to confirm successful disruption. The list of compled cloned contructs are shown in Table 27.

Table 27 Summary of CRISPR-Cas9 cloning

Protein candidate	PCR of the 5' &3' homology region (HR) of candidate genes	Cloning of the 5' &3' homology region (HR) of candidate genes into the pL6 plasmid	Cloning of sgRNA into the pL6 plasmid	Sequencing of pL7 plasmids
*Pf*Tom40	completed	completed	Completed	completed
*Pf*Tim9	completed	completed	Completed	completed
PfHsp70	completed	completed	Completed	completed
*Pf*Tim10	completed	completed	Completed	completed
*Pf*Tim13	completed	completed	Completed	completed

3.5.1 CRISPR-Cas9-mediated gene knockout attempt for *PFHSP70*

To assess successful disruption of the *PFHSP70* gene locus, multiple genotyping PCRs were performed for parasites generated after four knockout attempts and selection with with WR99210 and 5-FC. The first PCR (PCR1) targeted the whole *PFHSP70* locus to confirm the disruption of the locus and integration of the *hDHFR* cassette (Figure 25a). Analytic agarose gel electrophoresis of PCR products of Δ*PF3D7hsp70* strain revealed a band size of 1.6 kb corresponding to the band size of 3D7 wild-type *HSP70* (Figure 25b). The results, therefore, confirmed that the *PFHSP70* locus was not disrupted and there was no integration of the *hDHFR* expression cassette at the target locus. Further checks using specific primers targeting the hDHFR expression cassette and the 3' & 5' HRs of *PFHSP70* (PCR 2 &3), respectively, (Figure 25a), yielded a 1.9 kb and 2.7 kb band size, confirming the presence of the pL7 plasmid in the strain (Figure 25b). The results show that the plasmid might have only been taken up episomally or integrated into a different locus. Altogether, the PCR analyses revealed that the loci of *PFHSP70* were not disrupted, and the knockout attempt was unsuccessful suggeting potential essentialty of *PFHSP70*.

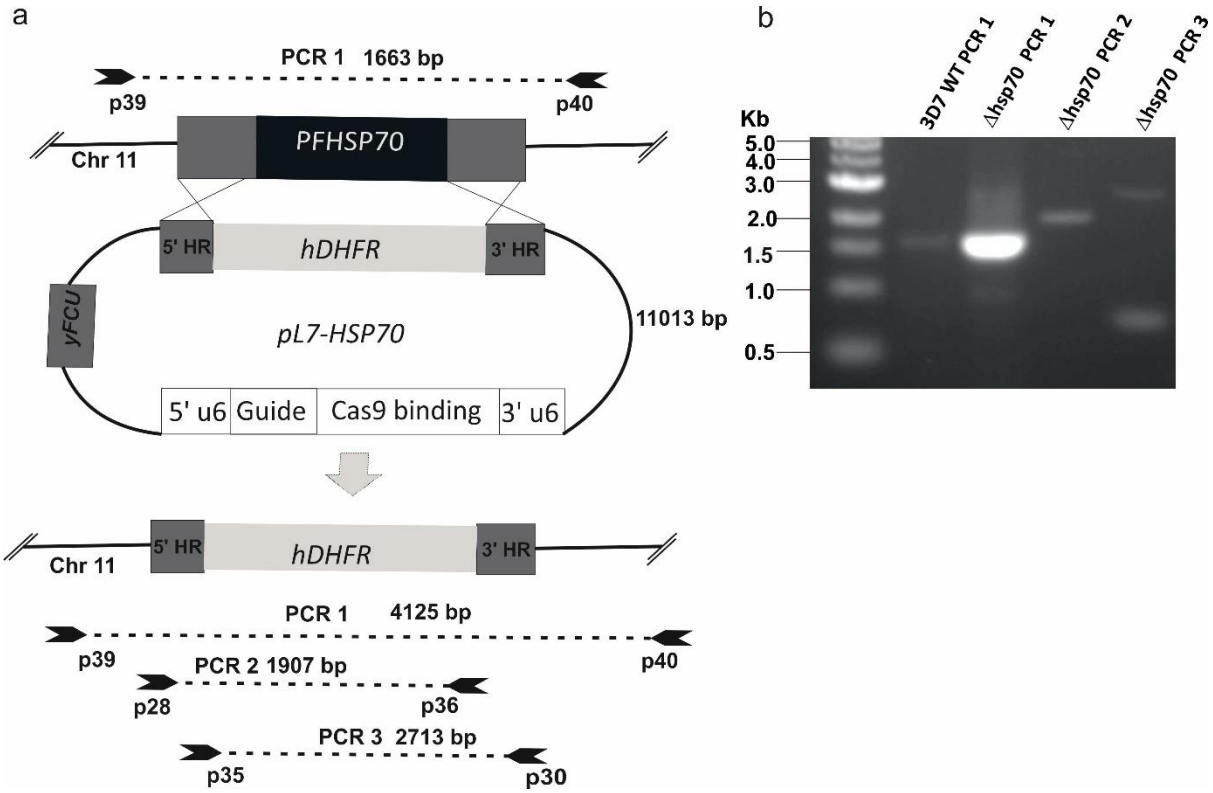

Figure 25 Attempted knockout of *PFHSP70*.(a) Knockout scheme for *PFHSP70*, adopting the CRISPR-Cas9 strategy (Ghorbal *et al.*, 2014). (b) PCR analyses of isolated genomic DNA from putative 3D7 Δ*hsp70* strains generated after transfection and selection. The results are compared with the 3D7 wild-type strain as a control.

3.5.2 CRISPR-Cas9-mediated gene knockout attempt of *PFTOM40* in *P. falciparum*

To validate successful disruption of the *PFTOM40* gene locus, multiple genotyping PCRs were performed for parasites generated after five knockout attempts and selection with with WR99210 and 5-FC. The first PCR (PCR1) targeted the whole *PFTOM40* locus to confirm the disruption of the locus and integration of the *hDHFR* cassette (Figure 26a). Analytic agarose gel electrophoresis of PCR products of the *PFΔtom40* strain revealed a band size of 1.5 kb corresponding to the band size of 3D7 wild-type *TOM40* (Figure 26b). The results therefore confirmed that the PFTOM40 locus was not disrupted and there was no integration of the hDHFR expression cassette at the target locus. Further checks using specific primers targeting the *hDHFR* expression cassette and the 3' & 5' HRs of *PFTOM40* (PCR 2 &3), respectively (Figure 26a) yielded a 1.8 kb and 2.3 kb band size, confirming the presence of the pL7 plasmid in the strain (Figure 26b) The results show that the plasmid might have only been taken up

episomally or integrated into a different locus. Altogether, the PCR analyses revealed that the locus of *PFTOM40* was not disrupted, and that the knockout attempt was unsuccessful indicating a potential essentiality of *PFTOM40*.

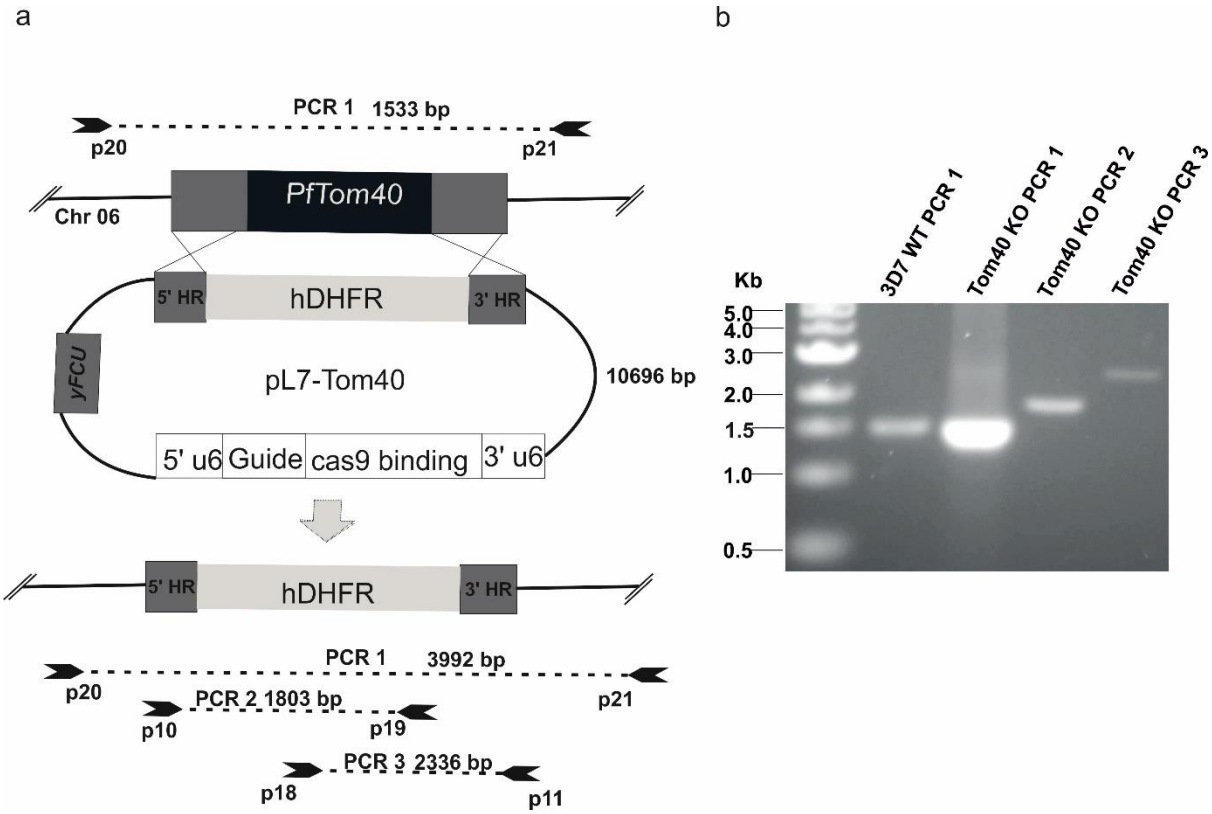

Figure 26 Attempted knockout of *PFTOM40*. (a) Knockout scheme for *PFTOM40*, adopting the CRISPR-Cas9 strategy (Ghorbal *et al.*, 2014). (b) PCR analyses of isolated genomic DNA from putative 3D7 *Δtom40*strains generated after trasfection and selection. The results are compared with the 3D7 wild-type strain as control.

4 Discussion

4.1 Predicted *N*-terminal presequences of the components of the mitochondrial protein import machineries in *P. falciparum*

Presequences are extensions of about 15 to 70 amino acid residues at the *N*-terminus of a protein, which is cleavable and required to direct proteins into the mitochondrial matrix sufficiently (Bykov et al., 2022; Hurt et al., 1984; Neupert, 1997). Membrane proteins that are also imported via the TIM23 complex pathway usually bear an *N*-terminal cleavable presequence, although exceptional cases exist (Habib et al., 2007). The mitochondrial processing peptidase (MPP), which is made of two subunits, α-MPP and β-MPP, is necessary for processing the cleavable presequences in the matrix (Emtage & Jensen, 1993; Geli & Glick, 1990; Glaser & Dessi, 1999; Hawlitschek et al., 1988; Kalousek et al., 1993). In this work, MitoProt II was able to predict the cleavable presequence for *Pf*Mge1, but not for *Pf*mtHsp70 (Table 18) even though both are soluble matrix proteins and are expected to contain an *N*-terminal presequence. In yeast, mtHsp70 is synthesized and imported as an unfolded precursor protein containing an *N*-terminal presequence that is cleaved off upon import into the matrix (Blamowska et al., 2012). The non-predictable *N*-terminal presequence of *Pf*mtHsp70 and other core components could be due to the rich A/T genome content, giving rise to proteins with modified or shorter *N*-terminal presequences, which makes it sometimes difficult to predict (Bender et al., 2003; Deponte et al., 2012). *Pf*Pam16 and *Pf*Pam18, which are subunits of the PAM complex, were also predicted to contain a cleavable *N*-terminal presequence in *P. falciparum*. Although Pam16 and Pam18 participate in the translocation of proteins with *N*-terminal presequence, they are not known to possess a cleavable *N*-terminal presequence in opisthokonts (P. D'Silva et al., 2004; P. R. D'Silva et al., 2008). Therefore, the predicted cleavable presequence could be another modification of the *P. falciparum* homologues. *Pf*Tom40 was also unexpectedly predicted to have a cleavable presequence, contrary to the characteristic outer membrane proteins.

4.2 Detection and localization of core subunits of the TOM and SAM complexes in the mitochondrial outer membrane of *P. falciparum*

The mechanisms of protein import to mitochondria have been well studied in yeast and related organisms, in contrast to other eukaryotic lineages. Although the fundamental biological process of mitochondrial protein import seems to be conserved, there are significant modifications or alterations in the import machinery of different eukaryotic lineages (Eckers et al., 2012; Van Dooren et al., 2006). For instance, plants lack homologues of Tom70 and Tom20 in the TOM complex, and lineage-specific receptor proteins have evolved instead (Lister et al., 2007; Rimmer et al., 2011). Similarly, *trypanosomatids* possess a divergent TOM complex, termed the archaic translocase of the mitochondrial outer membrane (ATOM), composed of subunits such as ATOM40, ATOM36, ATOM69, ATOM12, and ATOM14, which lack clear yeast homologs. (Mani et al., 2015, 2016; Pusnik et al., 2012; Zarsky et al., 2012). Mitochondrial protein import machinery of apicomplexan parasites, including malaria parasites and *T. gondii,* has mainly been analyzed with computational approaches, identifying putative homologs of the core components, including TOM, SAM, TIM23, TIM22, and PAM complexes (Alcock et al., 2012; Deponte, 2013; Deponte et al., 2012; Van Dooren et al., 2006). Within the TOM complex of *P. falciparum*, canonical receptor subunits are absent (Tom20) or highly divergent (Tom22), while the central pore-forming subunit Tom40 is conserved. This study demonstrates, for the first time, production of *Pf*Tom40-3xHA with a calculated molecular weight of 47 kDa in *P. falciparum* (Figure 11e), corroborating previous reports of a 48 kDa Tom40 homolog in *T. gondii*(Van Dooren et al., 2016). Confocal microscopy also revealed a colocalization of *Pf*Tom40 with the mitochondrion of *P. falciparum* (Figure 18a). The validation of the presence of the *Pf*Tom40 subunit confirms the potential role that it plays in the active TOM complex, which serves as the common entry point for proteins targeted to different compartments of the mitochondrion in *P. falciparum*.

The SAM complex of malaria parasites has been identified to contain a homologue of the central subunit Sam50. However, the adjacent opistokont receptor subunits of Sam35 and Sam37 are predicted to be absent (Deponte et al., 2012; Eckers et al., 2012). In this work, *Pf*Sam50-3xHA was shown to be produced with a calculated molecular weight of 57kDa in *P. falciparum* (Figure 12e). The ponceau staining showed an up-regulated protein at the same

size (Figure 12e), which could be a response to the tagging of the Sam50 subunit to compensate for its negative effect on its essential function. Confocal microscopy also revealed a colocalization signal showing the mitochondrial localization of *Pf*Sam50 in all three asexual blood stages of *P. falciparum* (Figure 18b). The results of the immunoblotting and confocal microscopy altogether validate the production and localization of *Pf*Sam50-3xHA in the mitochondria of *P. falciparum*. This confirms the predicted conservation of the Sam50 subunit in apicomplexan parasites as reported in *T. gondii*(Van Dooren et al., 2016). The validation of the presence of the *Pf*Sam50 subunit confirms its potentially significant role in the active SAM complex, which serves as the core subunit of the SAM complex for the insertion of β-barrel proteins into the mitochondrial outer membrane.

4.3 Detection and localization of the core components of the PAM complex in *P. falciparum*

In the presequence - or TIM23 pathway, the PAM complex or the import motor interacts with the TIM23 complex in an ATP-dependent manner driven by Hsp70 to complete the translocation of proteins into the mitochondrial matrix (Okamoto et al., 2002). Comparative genomics in apicomplexan parasites has identified homologues of several PAM components, suggesting a conservation of the TIM23 import pathway (Deponte et al., 2012; Eckers et al., 2012; Van Dooren et al., 2016). Only Pam18 of the PAM complex has been demonstrated to localize to the mitochondria of apicomplexan parasites, based on a study in *T. gondii* (Van Dooren et al., 2016). In this work, the core components of the PAM complex of *P. falciparum*, *Pf*Hsp70-3xHA, and the nucleotide exchange factor, *Pf*Mge1-3xHA (processed), were demonstrated to be produced in *P. falciparum* with calculated molecular weights of 75kDa (Figure 13e) and 37kDa (Figure 14e), respectively. Confocal microscopy also revealed a mitochondrial localization of *Pf*Hsp70-3xHA and *Pf*Mge-3xHA (Figure 19a and bFigure 19) in all three asexual blood stages of *P. falciparum*. Although no clear western blot signals were obtained for *Pf*Pam16-3xHA (Figure 15), confocal microscopy revealed a mitochondrial localization of *Pf*Pam16-3xHA in all three asexual blood stages of *P. falciparum* (Figure 19c). The results of the immunoblotting and confocal microscopy altogether validate the production and mitochondrial localization of *Pf*Hsp70-3xHA and *Pf*Mge1-3xHA, and *Pf*Pam16-3xHA for

the first time in *P. falciparum*. This confirms the predicted conservation of the presequence - or TIM23 pathway in apicomplexan parasites as demonstrated in *T. gondii* (Van Dooren et al., 2016).

4.4 Detection and localization of the small Tim protein components in *P. falciparum*

Although comparative genomic studies have found putative small Tim proteins in apicomplexan parasites, no study has demonstrated production and localizations to the mitochondria of apicomplexan parasites (Eckers et al., 2012; Mallo et al., 2018). Nonetheless, small Tim proteins have been identified and localized to the mitochondria of the kinetoplastids, *Trypanosoma brucei* (Eckers et al., 2012b; Joseph T Smith et al., 2018). Western blot analyses detected signals between 10kDa and 17kDa that likely correspond to the full-length untagged proteins for *Pf*Tim8 (13kDa) and PfTim13 (11kDa) (Figure 17i and j). On the other hand, the signals that were detected between 26kDa and 34kDa could reflect the formation of *Pf*Tim8-3xHA/*Pf*Tim13-3xHA hexamers of 31kDa (Figure 17i and j). The results suggest the production of *Pf*Tim8-3xHA and *Pf*Tim13-3xHA and the potential formation of Tim8-3xHA/Tim13-3xHA hexamers in *P. falciparum*. Confocal microscopy revealed a mitochondrial localization of *Pf*Tim8-3xHA and *Pf*Tim13-3xHA (Figure 21a and b) in all three asexual blood stages of *P. falciparum*. The result of confocal microscopy validates the production and localizations of PfTim8-3xHA and PfTim13-3xHA in *P. falciparum*.

4.5 Potential dual localization of Oxa1 in *P. falciparum*

The amino acid sequence of *P. falciparum* Oxa1, shown below (Figure 27), likely explains the observed double band western blot signals in Figure 16. The two bands could potentially be two isoforms of Oxa1 formed from alternative translational initiation sites. The upper bands migrating between 72kDa and 95kDa likely corresponds to the calculated molecular weight of *Pf*Oxa1-3xHA of 75kDa produced from the canonical translation initiation site at the beginning of the amino acid sequence (Methionine, M at position 1) (Figure 27). On the other hand, the additional lower bands migrating between 43kDa and 55kDa correspond to the calculated

molecular weight of *Pf*Oxa1-3xHA of ~50kDa, potentially produced from an alternative translation initiation start site at position 154 of the amino acid sequence of *Pf*Oxa1 (Figure 27). A study on translation initiation in *P. falciparum* shows that translation initiation sites are influenced by the presence of purines at positions -3 and +4 of the start codon. In contrast, the presence of a U at -1 increases the translation initiation by 2.5-fold (Patakottu et al., 2012). Therefore, the additional lower band size could be explained by the alternative translation initiation site that is more favorable, potentially, position 154 (Figure 27). Isoforms of Oxa1 were also identified in *Arabidopsis thaliana* (*At*Oxa1a and *At*Oxa1b), although this was attributed to single gene duplication (Benz et al., 2013). This report seems to agree with the initial results of this work, showing possible isoforms of the *PfOxa1 in P. falciparum*. Nevertheless, detecting western blot signals of the tagged full-length protein and the tagged truncated versions is needed to confirm this observation.

Confocal microscopy also revealed a possible dual localization of these isoforms of *Pf*Oxa1 to the mitochondrion and a nearby organelle, possibly the apicoplast. Image analyses shows that there was no complete colocalization of the MTO signal with the HA signal (Figure 20) which could indicate that the HA signal was detected in a very closely connected organelle, in this case, the apicoplast. However, further imaging analyses comparing localization signals of the mitochondrion and apicoplast is needed to confirm this assertion. Alternatively, conducting MS analyses of *Pf*Oxa1-3xHA pulldown samples could potentially reveal organelle-specific protein interactors of *Pf*Oxa1.

MFQQNNSLKCNFNIIFHHISFRTNKGEWTKGLSTNPNKINQIENNKSNINNTYYHIYQYDKSILVNKFIQMYIKMGYIKNKKN
KISIKQNNNIYNKHNINNIYNKHNINNIYNIYNIYYNTFICSTNNVRNKQSFCNNNVHDKFGGLALFSRFFFTMPINNINNYF
NKQHNDKNINDKFDTSHCEEDPDKGVSKNIDHLKREDEHGKALTNKEMNNNNNNNNNNDDNIYNDDNVYNDDNNYNDGNIYNN
NNDYAYNNKSNEGSTYPLNEEETNVNLTEDIYPYTDFIIEKCKLNIKSDVDIYENTWYVKLIYDLLNSTKLFFDCTWMSSIIM
TTLFMRIIILPLTISSERDRRKQKILSPLLKELTKKLKDNAQDGNIKKAVEFKKKILNIRNTHGISLIPKSIILMAFFQTPLF
FIFYFSMKRIASYPDIFKDFTFESPLWLDSLSLPDPYYILPILSSLLLLSNNELTLLIDKKINENNKQSNLNNQEETEFQKNM
KKITKLAMRLFYLSSVLFFKSMPSGLFIYFITNTFFQLFITQICKIKIIENFLDLPPLHSKGFITSTNTSQQQTTSQKKIIHM
NDLIKRKK

Figure 27 Amino acid sequence of *P. falciparum* Oxa1 Potential translation initiation sites marked in yellow and green**.** M at position 154 (marked green) represents the potential alternative translation initiation site for the observed lower western blot signal of *Pf*Oxa1 of ~50kDa.

4.5 Interactome Analyses of the PAM complex in *P. falciparum*

In opisthokonts, components of the presequence translocase-associated motor (PAM) complex have been shown to functionally and physically interact to facilitate the translocation of preproteins into the mitochondrial matrix and inner membrane. Multiple studies have demonstrated these interactions through co-immunoprecipitation assays or by isolating PAM subunits as part of stable protein complexes (Chacinska et al., 2003; Murcha et al., 2014. In contrast, within apicomplexan parasites, although orthologs of PAM components have been predicted bioinformatically, no experimental evidence has yet confirmed their physical or functional interactions. In this work, the production and localizations of three core components of the PAM complex (*Pf*Mge1, *Pf*Hsp70, and *Pf*Pam16) were demonstrated by western blot analyses (Figure 13 and Figure 14) and confocal microscopy (Figure 19). STRING proteomic database was also used to analyze the protein interaction network of the PAM complex *in P. falciparum* using *Pf*Mge1 as the search protein To identify potential interacting partners of *Pf*Mge1-3xHA and demonstrate the protein-protein interaction network of the PAM complex in *P. falciparum*, a pulldown assay coupled to LC-MS/MS was conducted using *Pf*Mge1-3xHA as the bait protein. Western blot analyses of the pulldown assay for *Pf*Mge1-3xHA confirmed the success of the pulldown, despite a weak signal Interactome analyses confirmed the identification of the bait, *Pf*Mge1, as it was significantly enriched (Figure 22). The potential interacting partners identified using the STRING network analyses were, however, not found to be significantly enriched after statistical analyses (t-test, FDR<0.01, S0 =1 for class A interactors and t-test, FDR<0.05, S0 =1 for class B interactors) (Figure 22). The nonstatistical significance of the potential interactors of *Pf*Mge1-3xHA could be due to the relatively low abundance or intensity of these proteins. This could have resulted from the multiple washing steps in the pulldown assay, leading to loss of weak binders or interactors and hence low enrichment. The candidates that were identified to be significantly enriched after statistical analyses were not found to belong to the PAM complex nor interact with the bait protein. They could therefore be nonspecific binders that were enriched in the pulldown.

4.6 Interactome analyses of the TOM and SAM complexes in *P. falciparum*

The TOM complex of apicomplexan parasites is highly modified, with the presequence receptors either missing or altered. In *P. falciparum*, only the central subunit Tom40 and an altered Tom22 without a cytosolic domain have been identified as components (Deponte et al., 2012; Eckers et al., 2012). This raises questions as to how precursors with presequences are recognized at the TOM complex and translocated to the compartments of the mitochondrion. Tom70 was also demonstrated to occur in apicomplexan parasites in *T. gondii* (Van Dooren et al., 2016). The β-barrel protein, Sam50, remains the only identified component of the SAM complex in apicomplexan parasites. No homologues of the receptor subunits Sam38 and Sam37 were identified (Deponte et al., 2012b; Eckers et al., 2012a; Van Dooren et al., 2016). In this work, *Pf*Tom40-3xHA and *Pf*Sam50-3xHA were shown to be produced and localized to the mitochondrion of *P. falciparum* (Figure 18). However, it was important to explore the interactome of the TOM and SAM complexes to identify potential interactors of *Pf*Tom40 and *Pf*Sam50 in *P. falciparum.* This was necessary to understand how presequence-bearing precursors are guided from the TOM complex to different compartments and which receptors interact with *Pf*Sam50 in the SAM complex to insert outer membrane precursor proteins. The STRING database was used to predict the potential interacting partners of the central subunit of the TOM complex, *Pf*Tom40 and *Pf*Sam50 of the SAM complex (Table 25) of *P. falciparum.* The results showed only an interaction with *Pf*Sam50 of the SAM complex for *Pf*Tom40 and *vice versa*. While vast studies done on the TOM and SAM complex of opisthokonts have elucidated other receptor subunits of the complexes in addition to the central subunit Tom40 (Tom70, Tom20, Tom22, Tom5, Tom6, and Tom7) and Sam50 (Sam35, Sam37, Sam38), fewer (receptor) subunits have been identified in apicomplexan parasites. So far only Tom40, truncated Tom22, Tom70, and Sam50 have been demonstrated in apicomplexan parasites by work done in *T. gondii* (Van Dooren et al., 2016). *Pf*Tom40 and *Pf*Sam50 were also detected in this current study in *P. falciparum*, but beyond that, no homologues of the small (receptor) subunits have been identified in the genomes of apicomplexan parasites. It was therefore not surprising that the STRING database could not retrieve potential interactors of *Pf*Tom40 other than *Pf*Sam50 which has been predicted to

facilitate the insertion of β-barrel proteins from the TOM complex into the outer mitochondrial membrane in yeasts. Further probing of the interactome of the TOM and SAM complexes using *Pf*Tom40-3xHA and *Pf*Sam50-3xHA respectively as bait proteins proved unsuccessful as no clear western blot signal was observed in the input lane or eluate lane of the western blot analyses of the pulldown assay. The interactome analyses of *Pf*Tom40-3xHA and *Pf*Sam50-3xHA did not show any of potential interacting partners identified using the STRING network and neither *Pf*Tom40 (Figure 23) nor *Pf*Sam50 (Figure 24) were found to be significantly enriched after statistical analyses t-test, FDR<0.01, S0 =1 for class A interactors and t-test, FDR<0.05, S0 =1 for class B interactors) further confirming the failed pulldown experiment.

4.7 Unsuccessful attempts to knockout *PFHSP70* and *PFTOM40* in *P. falciparum*.

In opisthokonts, both Tom40 and Hsp70 have been reported to be essential components of the mitochondrial import machineries, with knockout mutants showing deleterious effects (P. D'Silva et al., 2004; Hill et al., 1998). It was therefore hypothesized in this work that *Pf*Tom40 and *Pf*Hsp70 were essential for the blood-stage survival of malaria parasites. To evaluate this hypothesis, the CRISPR-Cas9 system described by Ghorbal *et al.* was adopted to conduct gene knockout studies for *PFHSP70* and *PFTOM40*. Analytical PCR of both revealed that the knockout attempts were not successful as the wild-type loci were not disrupted and there was no confirmed integration of the *hDHFR* expression cassette at the target loci of *PFHSP70* (Figure 25) and *PFTOM40* (Figure 26). The CRISPR-Cas9 strategy described by Ghorbal *et al.* was previously used to successfully disrupt the genes encoding *P. falciparum* cytosolic glyoxalases in the Deponte lab (Wezena et al., 2018), confirming the adaptation of this method in our lab and the robustness of the strategy. Nevertheless, several attempts in this current work to disrupt the genes encoding *Pf*Hsp70 and *Pf*Tom40 were not successful using the same CRISPR strategy. Results in this work show that attempts to generate 3D7 *PFΔhsp*70 (four attempts) and 3D7 *PFΔtom*40 (five attempts) strains failed even though transfectants were observed by Giemsa-stained smears after both positive and negative selection with WR99210 and 5-FC, respectively. This observed outcome could be caused by an off-target integration of

the *hDHFR* expression cassette (positive selectable marker) into the genome of the parasite. The CRISPR-Cas9 strategy used in this current work employed the use of a circular plasmid (pL7) to deliver homologous regions for double-crossover repair. A limitation associated with this approach is the possibility of an unwanted insertion of the plasmid into the genome via a single crossover event (Duraisingh et al., 2002). In addition, off-target insertion could have also been influenced by a non-specific guide RNA sequence, which is required for targeted double-strand break by the Cas9 enzyme, or due to the high A/T content of the homology regions of *PFHSP70* and *PFTOM40*. Also, there could be an episomal uptake of the pL7 plasmid without insertion or integration into the target loci due to an inactive CRISPR-Cas9 vector. A possible solution for reducing off-target integration is to adopt the use of linearized plasmids for the delivery of homologous regions for double recombination(Crawford et al., 2017; Ghorbal et al., 2014). An added advantage of this approach is the avoidance of a negative selection step in the generation of knockout phenotypes. Therefore, the use of linearized plasmid in future knockout experiments may prevent the episomal maintenance of the plasmid and reduce off-target effects (Crawford et al., 2017). The several unsuccessful attempts to knockout both genes could also suggest the essentiality of *PFHSP70* and *PFTOM40.*

4.8 Conclusion and recommendation

Although the fundamental process of mitochondrial protein import has been conserved throughout evolution, recent reports have shown that components of the import machineries are significantly altered among the major eukaryotic lineages. In malaria parasites, these changes range from the replacement of a single component to completely new import machineries. These changes and variations present opportunities to target the mitochondria of the malaria parasite for selective intervention strategies. The results from this thesis present, for the first time, the production and mitochondrial localizations of core components of mitochondrial import machineries in malaria parasites. The core subunits of the TOM and SAM complex of the outer mitochondrial membrane were validated successfully with confocal microscopy and western blot analyses. Similarly, two subunits of the PAM complex (*Pf*Hsp70 and *Pf*Mge1) and the central subunit of the OXA pathway, *Pf*Oxa1, were demonstrated in this

thesis to be produced and localized to the mitochondrion of malaria parasites. Also, western blot analyses suggest the potential production and formation of Tim8/Tim13 hexamers in *P. falciparum*. Confocal microscopy also revealed that Tim8, Tim13, and Pam16 are localized to the mitochondrion of malaria parasites. To enhance the detection of elusive proteins as encountered with Pam16-3xHA, future experiments could involve isolating purified mitochondria and applying a TCA precipitation to improve protein yields for western analyses. While *Pf*Mge1 was successfully enriched in interactome studies, its predicted interaction partners were not identifiable using the current methods. Similarly, although mass spectrometry detected *Pf*Tom40 and *Pf*Sam50 in pulldown assays, neither protein appeared to be substantially enriched, indicating inefficient recovery of their complexes. Future strategies might benefit from chemical crosslinking and denaturing affinity-purification techniques to capture transient interactors better and to improve solubilization of integral membrane proteins.

Additionally, gene knockout attempts using circular pL7 plasmids suggested a risk of unintended insertions or single-crossover events. Therefore, adopting linearized plasmids in future gene editing efforts may enhance the knockout efficiency in *P. falciparum*. to confirm the potentiality of the candidate genes knockout experiments with recue plasmids or inducible knockdown experiments should be conducted.

5. Supplements (S)

5.1 SLI Plasmids

S1 pSLI-*TOM40*-3xHA

GGATATGGCAGCTTAATGTTCGTTTTTCTTATTTATATATTTATACCAATTGATTGTATTTATAACTGTAAAAATGTGTATGTTGTGTGCAT
ATTTTTTTTTTGTGCATGCACATGCATGTAAATAGCTAAAATTATGAACATTTTATTTTTTGTTCAGAAAAAAAAAACTTTACACACATAAAA
TGGCTAGTATGAATAGCCATATTTTATATAAATTAAATCCTATGAATTTATGACCATATTAAAAATTTAGATATTTATGGAACATAATATG
TTTGAAACAATAAGACAAAATTATTATTATTATTATTTTTACTGTTATAATTATGTGTCTCCTTCAATGATTCATAAATAGTTGGACTTG
ATTTTTAAAATGTTTATAATATGATTAGCATAGTTAAATAAAAAAAGTTGAAAAATTAAAAAAAAACATATAAACACAAATGATGGTTTTT
CCTTCAATTTCGATATCAATTTATAGAAACAAAATATATACTTGTATAATTTTATTTTTTTATATAAATCATTACATATATAATTATACAATA
TTTTTTCTAAGAGATAATTATATATTAATATATATAAAAAAAGGTGTTTTTTTTTTTTTTTTTATTTTTATTTTTATTTTATGGTAATATTTTA
TTTTCCTTATTTTATAAATTATATTAGTTTATATGTGATTAATTTTATATATTATCAATTTATATATTTTTAAATGCTTACTTAATTATCTTTTT
TTTTTTTTTTTTTTTTTTTCCCCTCTTTTTATATTAATTTATTTTTGAAAAAATTGATATATATATATATATATAATATATATATATACATGTA
GTAGTATTAAACAATGTATAATATATATAAATAATATATTTATATATTTCATTTCAATTTTAATTTTTTTTGGTTTTTTTTTTTTTTCTTTTTGT
CATATTTAAAAAAAATTATATTCATATAAGTTATGCATTTTTTATAAACATTATTCAATATATGTATAATATAATATATATATATATATTTAAT
GTATTATTCCAATGTGCATGATAAAAGAAAAAAATAATATTTATAAAAAAAAAGAAAAATAAAACAAAAAAAGAAAAAAAAAAAAAAA
AAAAAAAAAATACAAAAATAAATAATATAATTTATAATTATATATTCTTGTCACAATAAAAATATATATATATATATATATTTATAATAT
GTATATTTTAAACTAGAAAAGGAATAACTAATATTTTATTTATTATCATTCAAGATTTATATTTTATAATAATAAATACCTAATAGAAATAT
ATCAGGATCCATGCATGGTTCGCTAAACTGCATCGTCGCTGTGTCCCAGAACATGGGCATCGGCAAGAACGGGGACTACCCCTGGCCAC
CGCTCAGGAACGAATTTAGATATTTCCAGAGAATGACCACAACCTCTTCAGTAGAAGGTAAACAGAATCTGGTGATTATGGGTAAGAAG
ACCTGGTTCTCCATTCCTGAGAAGAATCGACCTTTAAAGGGTAGAATTAATTTAGTTCTCAGCAGAGAACTCAAGGAACCTCCACAAGGA
GCTCATTTTCTTTCCAGAAGTCTAGATGATGCCTTAAAACTTACTGAACAACCAGAATTAGCAAATAAAGTAGACATGGTCTGGATAGTT
GGTGGCAGTTCTGTTTATAAGGAAGCCATGAATCACCCAGGCCATCTTAAACTATTTGTGACAAGGATCATGCAAGACTTTGAAAGTGA
CACGTTTTTTCCAGAAATTGATTTGGAGAAATATAAACTTCTGCCAGAATACCCAGGTGTTCTCTCTGATGTCCAGGAGGAGAAAGGCAT
TAAGTACAAATTTGAAGTATATGAGAAGAATGATTAAGCTTATTTAATAATAGATTAAAAATATTATAAAAATAAAAACATAAACACAGA
AATTACAAAAAAAAATACATATGAATTTTTTTTTTGTAATCTTCCTTATAAATATAGAATAATGAATCATATAAAACATATCATTATTCATTTA
TTTACATTTAAAATTATTGTTTCAGTATCTTTAATTTATTATGTATATATAAAAATAACTTACAATTTTATTAATAAACAATATATGTTTATTA
ATTCATGTTTTGTAATTTATGGGATAGCGATTTTTTTTACTGTCTGTATTTTTCTTTTTTAATTATGTTTTAATTGTATTTTATTTTTATTATTG
TTCTTTTTATAGTATTATTTTAAAACAAAATGTATTTTCTAAGAACTTATAATAATAATAAATATAAATTTTAATAAAAATTATATTTATCTT
TTACAATATGAACATAAAGTACAACATTAATATATAGCTTTTAATATTTTTATTCCTAATCATGTAAATCTTAAATTTTTCTTTTTAAACATA
TGTTAAATATTTATTTCTCATTATATATAAGAACATATTTATTAAATCTAGAATTCTATAGTGAGTCGTATTACAATTCACTGGCCGTCGTT
TTACAACGTCGTGACTGGGAAAACCCTGGCGTTACCCAACTTAATCGCCTTGCAGCACATCCCCCTTTCGCCAGCTGGCGTAATAGCGAA
GAGGCCCGCACCGATCGCCCTTCCCAACAGTTGCGCAGCCTGAATGGCGAATGGCGCCTGATGCGGTATTTTCTCCTTACGCATCTGTGC
GGTATTTCACACCGCATATGGTGCACTCTCAGTACAATCTGCTCTGATGCCGCATAGTTAAGCCAGCCCCGACACCCGCCAACACCCGCT
GACGCGCCCTGACGGGCTTGTCTGCTCCCGGCATCCGCTTACAGACAAGCTGTGACCGTCTCCGGGAGCTGCATGTGTCAGAGGTTTTC
ACCGTCATCACCGAAACGCGCGAGACGAAAGGGCCTCGTGATACGCCTATTTTTATAGGTTAATGTCATGATAATAATGGTTTCTTAGAC
GTCAGGTGGCACTTTTCGGGGAAATGTGCGCGGAACCCCTATTTGTTTATTTTTC

AAATACATTCAAATATGTATCCGCTCATGAGACAATAACCCTGATAAATGCTTCAATAATATTGAAAAAGGAAGAGTATGAGTATTCAAC
ATTTCCGTGTCGCCCTTATTCCCTTTTTTGCGGCATTTTGCCTTCCTGTTTTTGCTCACCCAGAAACGCTGGTGAAAGTAAAAGATGCTGAA
GATCAGTTGGGTGCACGAGTGGGTTACATCGAACTGGATCTCAACAGCGGTAAGATCCTTGAGAGTTTTCGCCCCGAAGAACGTTTTCC
AATGATGAGCACTTTTAAAGTTCTGCTATGTGGCGCGGTATTATCCCGTATTGACGCCGGGCAAGAGCAACTCGGTCGCCGCATACACT
ATTCTCAGAATGACTTGGTTGAGTACTCACCAGTCACAGAAAAGCATCTTACGGATGGCATGACAGTAAGAGAATTATGCAGTGCTGCC
ATAACCATGAGTGATAACACTGCGGCCAACTTACTTCTGACAACGATCGGAGGACCGAAGGAGCTAACCGCTTTTTTGCACAACATGGG
GGATCATGTAACTCGCCTTGATCGTTGGGAACCGGAGCTGAATGAAGCCATACCAAACGACGAGCGTGACACCACGATGCCTGTAGCA
ATGCCAACAACGTTGCGCAAACTATTAACTGGCGAACTACTTACTCTAGCTTCCCGGCAACAATTAATAGACTGGATGGAGGCGGATAA
AGTTGCAGGACCACTTCTGCGCTCGGCCCTTCCGGCTGGCTGGTTTATTGCTGATAAATCTGGAGCCGGTGAGCGTGGGTCTCGCGGTA
TCATTGCAGCACTGGGGCCAGATGGTAAGCCCTCCCGTATCGTAGTTATCTACACGACGGGGAGTCAGGCAACTATGGATGAACGAAAT
AGACAGATCGCTGAGATAGGTGCCTCACTGATTAAGCATTGGTAACTGTCAGACCAAGTTTACTCATATATACTTTAGATTGATTTAAAA
CTTCATTTTTAATTTAAAAGGATCTAGGTGAAGATCCTTTTTGATAATCTCATGACCAAAATCCCTTAACGTGAGTTTTCGTTCCACTGAGC
GTCAGACCCCGTAGAAAAGATCAAAGGATCTTCTTGAGATCCTTTTTTTCTGCGCGTAATCTGCTGCTTGCAAACAAAAAAACCACCGCT
ACCAGCGGTGGTTTGTTTGCCGGATCAAGAGCTACCAACTCTTTTTCCGAAGGTAACTGGCTTCAGCAGAGCGCAGATACCAAATACTGT
CCTTCTAGTGTAGCCGTAGTTAGGCCACCACTTCAAGAACTCTGTAGCACCGCCTACATACCTCGCTCTGCTAATCCTGTTACCAGTGGCT
GCTGCCAGTGGCGATAAGTCGTGTCTTACCGGGTTGGACTCAAGACGATAGTTACCGGATAAGGCGCAGCGGTCGGGCTGAACGGGG
GGTTCGTGCACACAGCCCAGCTTGGAGCGAACGACCTACACCGAACTGAGATACCTACAGCGTGAGCTATGAGAAAGCGCCACGCTTCC
CGAAGGGAGAAAGGCGGACAGGTATCCGGTAAGCGGCAGGGTCGGAACAGGAGAGCGCACGAGGGAGCTTCCAGGGGGAAACGCC
TGGTATCTTTATAGTCCTGTCGGGTTTCGCCACCTCTGACTTGAGCGTCGATTTTTGTGATGCTCGTCAGGGGGGCGGAGCCTATCGAAA
AACGCCAGCAACGCGGCCTTTTTACGGTTCCTGGCCTTTTGCTGGCCTTTTGCTCACATGTTCTTTCCTGCGTTATCCCCTGATTCTGTGGA
TAACCGTATTACCGCCTTTGAGTGAGCTGATACCGCTCGCCGCAGCCGAACGACCGAGCGCAGCGAGTCAGTGAGCGAGGAAGCGGAA
GAGCGCCCAATACGCAAACCGCCTCTCCCCGCGCGTTGGCCGATTCATTAATGCAGCTGGCACGACAGGTTTCCCGACTGGAAAGCGGG
CAGTGAGCGCAACGCAATTAATGTGAGTTAGCTCACTCATTAGGCACCCCAGGCTTTACACTTTATGCTTCCGGCTCGTATGTTGTGTGG
AATTGTGAGCGGATAACAATTTCACACAGGAAACAGCTATGACCATGATTACGCCAAGCTATTTAGGTGACACTATAGAATACTCGCGG
CCGCTAAATATGGCAAGGAGCATGGATATTTAATACTTCATATACACAATTATTAACAAAGAAATTACAAGCAGGTGTAGATCTAACATA
TATTGCTTCCAATTGTGCTTCCATAGGATCTTTTGGTTTAAGATATAATCATAAAAATAATGTTTTAACCATGCAAATTGTTAGACAACCCA
ACTTTAAATCACCCGAGTTTATGTTAAACCAAACTCATTTATATAAAATACAATATGCCAAAAAAATATCAGACCGTTTATCCTTAGGAAC
AGAATTAGAAATTACACCACAAACAAAAGAATCAGCTATGAGACTTGGTTGGGATTATTCTTTCAGACATGCAAAAGTACAAGGCTCTAT
TGATACCAGTGGAAAAATTTCCGTCTTCACACAAGACTATTCAGGTTTTGGTGTCAGTGGATATATAGATTATTTGAATAATGATTATAA
GTTTGGATTCATGATGCACATATCTCCTTCACAAGAGCAACCACAGACAGCAGCAACGCGTGGATCCTATCCTTATGATGTTCCAGATTA
TGCAGGTTATCCTTATGATGTACCAGATTATGCTGGTTATCCTTATGATGTTCCTGATTATGCAGTCGACGGAGAAGGAAGAGGAAGTTT
ATTAACATGTGGAGATGTAGAAGAAAATCCAGGACCAATGATTGAACAAGATGGATTGCACGCAGGTTCTCCGGCCGCTTGGGTGGAG
AGGCTATTCGGCTATGACTGGGCACAACAGACAATCGGCTGCTCTGATGCCGCCGTGTTCCGGCTGTCAGCGCAGGGGCGCCCGGTTCT

TTTTGTCAAGACCGACCTGTCCGGTGCCCTGAATGAACTGCAGGACGAGGCAGCGCGGCTATCGTGGCTGGCCACGACGGGCGTTCCTT
GCGCAGCTGTGCTCGACGTTGTCACTGAAGCGGGAAGGGACTGGCTGCTATTGGGCGAAGTGCCGGGGCAGGATCTCCTGTCATCTCA
CCTTGCTCCTGCCGAGAAAGTATCCATCATGGCTGATGCAATGCGGCGGCTGCATACGCTTGATCCGGCTACCTGCCCATTCGACCACCA
AGCGAAACATCGCATCGAGCGAGCACGTACTCGGATGGAAGCCGGTCTTGTCGATCAGGATGATCTGGACGAAGAGCATCAGGGGCTC
GCGCCAGCCGAACTGTTCGCCAGGCTCAAGGCGCGCATGCCCGACGGCGAGGATCTCGTCGTGACCCATGGCGATGCCTGCTTGCCGA
ATATCATGGTGGAAAATGGCCGCTTTTCTGGATTCATCGACTGTGGCCGGCTGGGTGTGGCGGACCGCTATCAGGACATAGCGTTGGCT
ACCCGTGATATTGCTGAAGAGCTTGGCGGCGAATGGGCTGACCGCTTCCTCGTGCTTTACGGTATCGCCGCTCCCGATTCGCAGCGCAT
CGCCTTCTATCGCCTTCTTGACGAGTTCTTCTAACTCGAG

Expected without intron

ATATGGCAAGGAGCATGGATATTTAATACTTCATATACACAATTATTAACAAAGAAATTACAAGCAGGTGTAGATCTAACATATATTGCT
TCCAATTGTGCTTCCATAGGATCTTTTGGTTTAAGATATAATCATAAAAATAATGTTTTAACCATGCAAATTGTTAGACAACCCAACTTTAA
ATCACCCGAGTTTATGTTAAACCAAACTCATTTATATAAAATACAATATGCCAAAAAAATATCAGACCGTTTATCCTTAGGAACAGAATTA
GAAATTACACCACAAACAAAAGAATCAGCTATGAGACTTGGTTGGGATTATTCTTTCAGACATGCAAAAGTACAAGGCTCTATTGATACC
AGTGGAAAAATTTCCGTCTTCACACAAGACTATTCAGGTTTTGGTGTCAGTGGATATATAGATTATTTGAATAATGATTATAAGTTTGGAT
TCATGATGCACATATCTCCTTCACAAGA***GCAACCACAGACAGCAGCA***ACGCGTGGATCCT***ATCCTTATGATGTTC****CAGATTATG*CAGGTT
ATCCTTATGATGTACCAGATTATGCTGGTTATC***CTTATGATGTTCCTGATTATGCA***GTCGACGGAGAAGGAAGAGGAAGTTTATTAACAT
GTGGAGATGTAGAAGAAAATCCAGGACCA**ATG**ATTGAACAAGATGGATTGCACGCAGGTTCTCCGGCCGCTTGGGTGGAGAGGCTATT
CGGCTATGACTGGGCACAACAGACAATCGGCTGCTCTGATGCCGCCGTGTTCCGGCTGTCAGCGCAGGGGCGCCCGGTTCTTTTTGTCA
AGACCGACCTGTCCGGTGCCCTGAATGAACTGCAGGACGAGGCAGCGCGGCTATCGTGGCTGGCCACGACGGGCGTTCCTTGCGCAGC
TGTGCTCGACGTTGTCACTGAAGCGGGAAGGGACTGGCTGCTATTGGGCGAAGTGCCGGGGCAGGATCTCCTGTCATCTCACCTTGCTC
CTGCCGAGAAAGTATCCATCATGGCTGATGCAATGCGGCGGCTGCATACGCTTGATCCGGCTACCTGCCCATTCGACCACCAAGCGAAA
CATCGCATCGAGCGAGCACGTACTCGGATGGAAGCCGGTCTTGTCGATCAGGATGATCTGGACGAAGAGCATCAGGGGCTCGCGCCAG
CCGAACTGTTCGCCAGGCTCAAGGCGCGCATGCCCGACGGCGAGGATCTCGTCGTGACCCATGGCGATGCCTGCTTGCCGAATATCATG
GTGGAAAATGGCCGCTTTTCTGGATTCATCGACTGTGGCCGGCTGGGTGTGGCGGACCGCTATCAGGACATAGCGTTGGCTACCCGTG
ATATTGCTGAAGAGCTTGGCGGCGAATGGGCTGACCGCTTCCTCGTGCTTTACGGTATCGCCGCTCCCGATTCGCAGCGCATCGCCTTCT
ATCGCCTTCTTGACGAGTTCTTC**TAA**

Expected translation product

IWQGAWIFNTSYTQLLTKKLQAGVDLTYIASNCASIGSFGLRYNHKNNVLTMQIVRQPNFKSPEFMLNQTHLYKIQYAKKISDRLSLGTELEITP
QTKESAMRLGWDYSFRHAKVQGSIDTSGKISVFTQDYSGFGVSGYIDYLNNDYKFGFMMMHISPSQEQPQTAATRGSYPYDVPDYAGYPYDV
PDYAGYPYDVPDYAVDGEGRGSLLTCGDVEENPGPMIEQDGLHAGSPAAWVERLFGYDWAQQTIGCSDAAVFRLSAQGRPVLFVKTDLSG
ALNELQDEAARLSWLATTGVPCAAVLDVVTEAGRDWLLLGEVPGQDLLSSHLAPAEKVSIMADAMRRLHTLDPATCPFDHQAKHRIERARTR
MEAGLVDQDDLDEEHQGLAPAELFARLKARMPDGEDLVVTHGDACLPNIMVENGRFSGFIDCGRLGVADRYQDIALATRDIAEELGGEWA
DRFLVLYGIAAPDSQRIAFYRLLDEFFX

hDHFR

PfTOM40

3xHA tag

Neo-R

Skip peptide (skip between G and P, GGA-CCA)

S2 pSLI- *PFSAM50*-3xHA

GGATATGGCAGCTTAATGTTCGTTTTTCTTATTTATATATTTATACCAATTGATTGTATTTATAACTGTAAAAATGTGTATGTTGTGTGCAT
ATTTTTTTTTGTGCATGCACATGCATGTAAATAGCTAAAATTATGAACATTTTATTTTTTGTTCAGAAAAAAAAAACTTTACACACATAAAA
TGGCTAGTATGAATAGCCATATTTTATATAAATTAAATCCTATGAATTTATGACCATATTAAAAATTTAGATATTTATGGAACATAATATG
TTTGAAACAATAAGACAAAATTATTATTATTATTATTTTTACTGTTATAATTATGTGTCTCCTTCAATGATTCATAAATAGTTGGACTTG
ATTTTTAAAATGTTTATAATATGATTAGCATAGTTAAATAAAAAAAGTTGAAAAATTAAAAAAAAACATATAAACACAAATGATGGTTTTT
CCTTCAATTTCGATATCAATTTATAGAAACAAAATATATACTTGTATAATTTTATTTTTTTATATAAATCATTACATATATAATTATACAATA
TTTTTTCTAAGAGATAATTATATATTAATATATATAAAAAAAGGTGTTTTTTTTTTTTTTTTTTATTTTTATTTTTATTTTATGGTAATATTTTA
TTTTCCTTATTTTATAAATTATATTAGTTTATATGTGATTAATTTTATATATTATCAATTTATATATTTTTAAATGCTTACTTAATTATCTTTTT
TTTTTTTTTTTTTTTTTTTTCCCCTCTTTTTATATTAATTTATTTTTGAAAAAATTGATATATATATATATATATAATATATATATATACATGTA
GTAGTATTAAACAATGTATAATATATATAAATAATATATTTATATATTTCATTTCAATTTTAATTTTTTTTGGTTTTTTTTTTTTTTCTTTTTGT
CATATTTAAAAAAAATTATATTCATATAAGTTATGCATTTTTTATAAACATTATTCAATATATGTATAATATAATATATATATATATATTAAT
GTATTATTCCAATGTGCATGATAAAAGAAAAAAATAATATTTATAAAAAAAAAGAAAAATAAAACAAAAAAAGAAAAAAAAAAAAAAA
AAAAAAAAAATACAAAAATAAATAATATAATTTATAATTATATATTCTTGTCACAATAAAAATATATATATATATATATATTTATAATAT
GTATATTTTAAACTAGAAAAGGAATAACTAATATTTTATTTATTATCATTCAAGATTTATATTTTATAATAATAAATACCTAATAGAAATAT
ATCA**GGATCCATG**CATGGTTCGCTAAACTGCATCGTCGCTGTGTCCCAGAACATGGGCATCGGCAAGAACGGGGACTACCCCTGGCCAC
CGCTCAGGAACGAATTTAGATATTTCCAGAGAATGACCACAACCTCTTCAGTAGAAGGTAAACAGAATCTGGTGATTATGGGTAAGAAG
ACCTGGTTCTCCATTCCTGAGAAGAATCGACCTTTAAAGGGTAGAATTAATTTAGTTCTCAGCAGAGAACTCAAGGAACCTCCACAAGGA
GCTCATTTTCTTTCCAGAAGTCTAGATGATGCCTTAAAACTTACTGAACAACCAGAATTAGCAAATAAAGTAGACATGGTCTGGATAGTT
GGTGGCAGTTCTGTTTATAAGGAAGCCATGAATCACCCAGGCCATCTTAAACTATTTGTGACAAGGATCATGCAAGACTTTGAAAGTGA
CACGTTTTTTCCAGAAATTGATTTGGAGAAATATAAACTTCTGCCAGAATACCCAGGTGTTCTCTCTGATGTCCAGGAGGAGAAAGGCAT
TAAGTACAAATTTGAAGTATATGAGAAGAATGAT**TAAGCTT**ATTTAATAATAGATTAAAAATATTATAAAAATAAAAACATAAACACAGA
AATTACAAAAAAAAATACATATGAATTTTTTTTTTGTAATCTTCCTTATAAATATAGAATAATGAATCATATAAAACATATCATTATTCATTTA
TTTACATTTAAAATTATTGTTTCAGTATCTTTAATTTATTATGTATATATAAAAATAACTTACAATTTTATTAATAAACAATATATGTTTATTA
ATTCATGTTTTGTAATTTATGGGATAGCGATTTTTTTTACTGTCTGTATTTTTCTTTTTTAATTATGTTTTAATTGTATTTTATTTTTATTATTG
TTCTTTTTATAGTATTATTTTAAAACAAAATGTATTTTCTAAGAACTTATAATAATAATAAATATAAATTTTAATAAAAATTATATTTATCTT
TTACAATATGAACATAAAGTACAACATTAATATATAGCTTTTAATATTTTTATTCCTAATCATGTAAATCTTAAATTTTTCTTTTTAAACATA
TGTTAAATATTTATTTCTCATTATATATAAGAACATATTTATTAAATCTAGAATTCTATAGTGAGTCGTATTACAATTCACTGGCCGTCGTT
TTACAACGTCGTGACTGGGAAAACCCTGGCGTTACCCAACTTAATCGCCTTGCAGCACATCCCCCTTTCGCCAGCTGGCGTAATAGCGAA
GAGGCCCGCACCGATCGCCCTTCCCAACAGTTGCGCAGCCTGAATGGCGAATGGCGCCTGATGCGGTATTTTCTCCTTACGCATCTGTGC
GGTATTTCACACCGCATATGGTGCACTCTCAGTACAATCTGCTCTGATGCCGCATAGTTAAGCCAGCCCCGACACCCGCCAACACCCGCT
GACGCGCCCTGACGGGCTTGTCTGCTCCCGGCATCCGCTTACAGACAAGCTGTGACCGTCTCCGGGAGCTGCATGTGTCAGAGGTTTTC
ACCGTCATCACCGAAACGCGCGAGACGAAAGGGCCTCGTGATACGCCTATTTTTATAGGTTAATGTCATGATAATAATGGTTTCTTAGAC
GTCAGGTGGCACTTTTCGGGGAAATGTGCGCGGAACCCCTATTTGTTTATTTTTCTAAATACATTCAAATATGTATCCGCTCATGAGACAA
TAACCCTGATAAATGCTTCAATAATATTGAAAAAGGAAGAGTATGAGTATTCAACATTTCCGTGTCGCCCTTATTCCCTTTTTTGCGGCAT
TTTGCCTTCCTGTTTTTGCTCACCCAGAAACGCTGGTGAAAGTAAAAGATGCTGAAGATCAGTTGGGTGCACGAGTGGGTTACATCGAA

CTGGATCTCAACAGCGGTAAGATCCTTGAGAGTTTTCGCCCCGAAGAACGTTTTCCAATGATGAGCACTTTTAAAGTTCTGCTATGTGGC
GCGGTATTATCCCGTATTGACGCCGGGCAAGAGCAACTCGGTCGCCGCATACACTATTCTCAGAATGACTTGGTTGAGTACTCACCAGTC
ACAGAAAAGCATCTTACGGATGGCATGACAGTAAGAGAATTATGCAGTGCTGCCATAACCATGAGTGATAACACTGCGGCCAACTTACT
TCTGACAACGATCGGAGGACCGAAGGAGCTAACCGCTTTTTTGCACAACATGGGGGATCATGTAACTCGCCTTGATCGTTGGGAACCGG
AGCTGAATGAAGCCATACCAAACGACGAGCGTGACACCACGATGCCTGTAGCAATGCCAACAACGTTGCGCAAACTATTAACTGGCGA
ACTACTTACTCTAGCTTCCCGGCAACAATTAATAGACTGGATGGAGGCGGATAAAGTTGCAGGACCACTTCTGCGCTCGGCCCTTCCGGC
TGGCTGGTTTATTGCTGATAAATCTGGAGCCGGTGAGCGTGGGTCTCGCGGTATCATTGCAGCACTGGGGCCAGATGGTAAGCCCTCCC
GTATCGTAGTTATCTACACGACGGGGAGTCAGGCAACTATGGATGAACGAAATAGACAGATCGCTGAGATAGGTGCCTCACTGATTAA
GCATTGGTAACTGTCAGACCAAGTTTACTCATATATACTTTAGATTGATTTAAAACTTCATTTTTAATTTAAAAGGATCTAGGTGAAGATC
CTTTTTGATAATCTCATGACCAAAATCCCTTAACGTGAGTTTTCGTTCCACTGAGCGTCAGACCCCGTAGAAAAGATCAAAGGATCTTCTT
GAGATCCTTTTTTTCTGCGCGTAATCTGCTGCTTGCAAACAAAAAAACCACCGCTACCAGCGGTGGTTTGTTTGCCGGATCAAGAGCTAC
CAACTCTTTTTCCGAAGGTAACTGGCTTCAGCAGAGCGCAGATACCAAATACTGTCCTTCTAGTGTAGCCGTAGTTAGGCCACCACTTCA
AGAACTCTGTAGCACCGCCTACATACCTCGCTCTGCTAATCCTGTTACCAGTGGCTGCTGCCAGTGGCGATAAGTCGTGTCTTACCGGGT
TGGACTCAAGACGATAGTTACCGGATAAGGCGCAGCGGTCGGGCTGAACGGGGGGTTCGTGCACACAGCCCAGCTTGGAGCGAACGA
CCTACACCGAACTGAGATACCTACAGCGTGAGCTATGAGAAAGCGCCACGCTTCCCGAAGGGAGAAAGGCGGACAGGTATCCGGTAAG
CGGCAGGGTCGGAACAGGAGAGCGCACGAGGGAGCTTCCAGGGGGAAACGCCTGGTATCTTTATAGTCCTGTCGGGTTTCGCCACCTC
TGACTTGAGCGTCGATTTTTGTGATGCTCGTCAGGGGGGCGGAGCCTATCGAAAAACGCCAGCAACGCGGCCTTTTTACGGTTCCTGGC
CTTTTGCTGGCCTTTTGCTCACATGTTCTTTCCTGCGTTATCCCCTGATTCTGTGGATAACCGTATTACCGCCTTTGAGTGAGCTGATACCG
CTCGCCGCAGCCGAACGACCGAGCGCAGCGAGTCAGTGAGCGAGGAAGCGGAAGAGCGCCCAATACGCAAACCGCCTCTCCCCGCGC
GTTGGCCGATTCATTAATGCAGCTGGCACGACAGGTTTCCCGACTGGAAAGCGGGCAGTGAGCGCAACGCAATTAATGTGAGTTAGCT
CACTCATTAGGCACCCCAGGCTTTACACTTTATGCTTCCGGCTCGTATGTTGTGTGGAATTGTGAGCGGATAACAATTTCACACAGGAAA
CAGCTATGACCATGATTACGCCAAGCTATTTAGGTGACACTATAGAATACTC**GCGGCCGCTAA*TACATATATTAATATTAGTAATGG***AA
TCAAATATGATTATAATCAACACAAACCATACACACTAAATAATTTTAATTTTACTGGTAGTATAGGTAGCTCATTAGTTTTAAGAGGTTT
TGAATATAATAGTATTGGTCAACCTGAACATTGTTATAAGTTTCATAAAAACAAAAACGATTATAAAATAACATATAATTATCTTGGTGCT
AACTTTTTTACAAATATTCAACTCATATTTAAATATATACTTAACATTCAAAATATGAACCCTATGGTATTCTTTTATATACACCTAGGAAG
ACTCAGTAATCATTTTTATTCATCTATTAATCAATTAATTAAAGATACAAGAATATCAACAGGTATTGGTATTATGGCATATATTCAAAAA
AACATTTCTCTAGAACTATTTTTTAATTATCCTATCTTATATCATATAACGGATAAAACCAAATTTTTTCAAGTCG***GCTTGAATTTTAAGGG***
AATCTTA**ACGCGT**GGATCCT***ATCCTTATGATGTTC****CAGATTATG*CAGGTTATCCTTATGATGTACCAGATTATGCTGGTTATC***CTTATGAT***
GTTCCTGATTATGCAGTCGACGGAGAAGGAAGAGGAAGTTTATTAACATGTGGAGATGTAGAAGAAAATCCAGGACCA**ATG**ATTGAAC
AAGATGGATTGCACGCAGGTTCTCCGGCCGCTTGGGTGGAGAGGCTATTCGGCTATGACTGGGCACAACAGACAATCGGCTGCTCTGA
TGCCGCCGTGTTCCGGCTGTCAGCGCAGGGGCGCCCGGTTCTTTTTGTCAAGACCGACCTGTCCGGTGCCCTGAATGAACTGCAGGACG
AGGCAGCGCGGCTATCGTGGCTGGCCACGACGGGCGTTCCTTGCGCAGCTGTGCTCGACGTTGTCACTGAAGCGGGAAGGGACTGGCT
GCTATTGGGCGAAGTGCCGGGGCAGGATCTCCTGTCATCTCACCTTGCTCCTGCCGAGAAAGTATCCATCATGGCTGATGCAATGCGGC
GGCTGCATACGCTTGATCCGGCTACCTGCCCATTCGACCACCAAGCGAAACATCGCATCGAGCGAGCACGTACTCGGATGGAAGCCGGT
CTTGTCGATCAGGATGATCTGGACGAAGAGCATCAGGGGCTCGCGCCAGCCGAACTGTTCGCCAGGCTCAAGGCGCGCATGCCCGACG
GCGAGGATCTCGTCGTGACCCATGGCGATGCCTGCTTGCCGAATATCATGGTGGAAAATGGCCGCTTTTCTGGATTCATCGACTGTGGC
CGGCTGGGTGTGGCGGACCGCTATCAGGACATAGCGTTGGCTACCCGTGATATTGCTGAAGAGCTTGGCGGCGAATGGGCTGACCGCT
TCCTCGTGCTTTACGGTATCGCCGCTCCCGATTCGCAGCGCATCGCCTTCTATCGCCTTCTTGACGAGTTCTTC**TAA**CTCGAG

Expected without intron

TACATATATTAATATTAGTAATGGAATCAAATATGATTATAATCAACACAAACCATACACACTAAATAATTTTAATTTTACTGGTAGTATA
GGTAGCTCATTAGTTTTAAGAGGTTTTGAATATAATAGTATTGGTCAACCTGAACATTGTTATAAGTTTCATAAAAACAAAAACGATTATA
AAATAACATATAATTATCTTGGTGCTAACTTTTTTACAAATATTCAACTCATATTTAAATATATACTTAACATTCAAAATATGAACCCTATG
GTATTCTTTTATATACACCTAGGAAGACTCAGTAATCATTTTTATTCATCTATTAATCAATTAATTAAAGATACAAGAATATCAACAGGTAT
TGGTATTATGGCATATATTCAAAAAAACATTTCTCTAGAACTATTTTTTAATTATCCTATCTTATATCATATAACGGATAAAACCAAATTTTT
TCAAGTCG***GCTTGAATTTTAAGGGAATCTTA***ACGCGTGGATCCT***ATCCTTATGATGTTC****CAGATTATG*CAGGTTATCCTTATGATGTACC
AGATTATGCTGGTTATC***CTTATGATGTTCCTGATTATGCA***GTCGACGGAGAAGGAAGAGGAAGTTTATTAACATGTGGAGATGTAGAA
GAAAATCCAGGACCA**ATG**ATTGAACAAGATGGATTGCACGCAGGTTCTCCGGCCGCTTGGGTGGAGAGGCTATTCGGCTATGACTGGG
CACAACAGACAATCGGCTGCTCTGATGCCGCCGTGTTCCGGCTGTCAGCGCAGGGGCGCCCGGTTCTTTTTGTCAAGACCGACCTGTCC
GGTGCCCTGAATGAACTGCAGGACGAGGCAGCGCGGCTATCGTGGCTGGCCACGACGGGCGTTCCTTGCGCAGCTGTGCTCGACGTTG
TCACTGAAGCGGGAAGGGACTGGCTGCTATTGGGCGAAGTGCCGGGGCAGGATCTCCTGTCATCTCACCTTGCTCCTGCCGAGAAAGT
ATCCATCATGGCTGATGCAATGCGGCGGCTGCATACGCTTGATCCGGCTACCTGCCCATTCGACCACCAAGCGAAACATCGCATCGAGC
GAGCACGTACTCGGATGGAAGCCGGTCTTGTCGATCAGGATGATCTGGACGAAGAGCATCAGGGGCTCGCGCCAGCCGAACTGTTCGC
CAGGCTCAAGGCGCGCATGCCCGACGGCGAGGATCTCGTCGTGACCCATGGCGATGCCTGCTTGCCGAATATCATGGTGGAAAATGGC
CGCTTTTCTGGATTCATCGACTGTGGCCGGCTGGGTGTGGCGGACCGCTATCAGGACATAGCGTTGGCTACCCGTGATATTGCTGAAGA
GCTTGGCGGCGAATGGGCTGACCGCTTCCTCGTGCTTTACGGTATCGCCGCTCCCGATTCGCAGCGCATCGCCTTCTATCGCCTTCTTGA
CGAGTTCTTC**TAA**

Expected translation product

TYINISNGIKYDYNQHKPYTLNNFNFTGSIGSSLVLRGFEYNSIGQPEHCYKFHKNKNDYKITYNYLGANFFTNIQLIFKYILNIQNMNPMVFFYIH
LGRLSNHFYSSINQLIKDTRISTGIGIMAYIQKNISLELFFNYPILYHITDKTKFFQVGLNFKGILTRGSYPYDVPDYAGYPYDVPDYAGYPYDVPDY
AVDGEGRGSLLTCGDVEENPGPMIEQDGLHAGSPAAWVERLFGYDWAQQTIGCSDAAVFRLSAQGRPVLFVKTDLSGALNELQDEAARLS
WLATTGVPCAAVLDVVTEAGRDWLLLGEVPGQDLLSSHLAPAEKVSIMADAMRRLHTLDPATCPFDHQAKHRIERARTRMEAGLVDQDDL
DEEHQGLAPAELFARLKARMPDGEDLVVTHGDACLPNIMVENGRFSGFIDCGRLGVADRYQDIALATRDIAEELGGEWADRFLVLYGIAAPD
SQRIAFYRLLDEFF*X

hDHFR

PfSAM50

3xHA tag

Neo-R

Skip peptide (skip between G and P, GGA-CCA)

S3 pSLI-*PFHSP70*-3xHA

GGATATGGCAGCTTAATGTTCGTTTTTCTTATTTATATATTTATACCAATTGATTGTATTTATAACTGTAAAAATGTGTATGTTGTGTGCAT
ATTTTTTTTTGTGCATGCACATGCATGTAAATAGCTAAAATTATGAACATTTTATTTTTTGTTCAGAAAAAAAAAACTTTACACACATAAAA
TGGCTAGTATGAATAGCCATATTTTATATAAATTAAATCCTATGAATTTATGACCATATTAAAAATTTAGATATTTATGGAACATAATATG
TTTGAAACAATAAGACAAAATTATTATTATTATTATTTTTACTGTTATAATTATGTGTCTCCTTCAATGATTCATAAATAGTTGGACTTG
ATTTTTAAAATGTTTATAATATGATTAGCATAGTTAAATAAAAAAAGTTGAAAAATTAAAAAAAAACATATAAACACAAATGATGGTTTTT
CCTTCAATTTCGATATCAATTTATAGAAACAAAATATATACTTGTATAATTTTATTTTTTTATATAAATCATTACATATATAATTATACAATA
TTTTTTCTAAGAGATAATTATATATTAATATATATAAAAAAAGGTGTTTTTTTTTTTTTTTTTATTTTTATTTTTATTTTATGGTAATATTTTA
TTTTCCTTATTTTATAAATTATATTAGTTTATATGTGATTAATTTTATATATTATCAATTTATATATTTTTAAATGCTTACTTAATTATCTTTTT

TTTTTTTTTTTTTTTTTTTCCCCTCTTTTTATATTAATTTATTTTTGAAAAAATTGATATATATATATATATATAATATATATATATACATGTA
GTAGTATTAAACAATGTATAATATATATAAATAATATATTTATATATTTCATTTCAATTTTAATTTTTTTTGGTTTTTTTTTTTTTTCTTTTTGT
CATATTTAAAAAAAATTATATTCATATAAGTTATGCATTTTTTATAAACATTATTCAATATATGTATAATATAATATATATATATATATTTAAT
GTATTATTCCAATGTGCATGATAAAAGAAAAAAATAATATTTATAAAAAAAAAGAAAAATAAAACAAAAAAAGAAAAAAAAAAAAAAA
AAAAAAAAAATACAAAAATAAATAATATAATTTATAATTATATATTCTTGTCACAATAAAAATATATATATATATATATATTTATAATAT
GTATATTTTAAACTAGAAAAGGAATAACTAATATTTTATTTATTATCATTCAAGATTTATATTTTATAATAATAAATACCTAATAGAAATAT
ATCA**GGATCC****ATG**CATGGTTCGCTAAACTGCATCGTCGCTGTGTCCCAGAACATGGGCATCGGCAAGAACGGGGACTACCCCTGGCCAC
CGCTCAGGAACGAATTTAGATATTTCCAGAGAATGACCACAACCTCTTCAGTAGAAGGTAAACAGAATCTGGTGATTATGGGTAAGAAG
ACCTGGTTCTCCATTCCTGAGAAGAATCGACCTTTAAAGGGTAGAATTAATTTAGTTCTCAGCAGAGAACTCAAGGAACCTCCACAAGGA
GCTCATTTTCTTTCCAGAAGTCTAGATGATGCCTTAAAACTTACTGAACAACCAGAATTAGCAAATAAAGTAGACATGGTCTGGATAGTT
GGTGGCAGTTCTGTTTATAAGGAAGCCATGAATCACCCAGGCCATCTTAAACTATTTGTGACAAGGATCATGCAAGACTTTGAAAGTGA
CACGTTTTTTCCAGAAATTGATTTGGAGAAATATAAACTTCTGCCAGAATACCCAGGTGTTCTCTCTGATGTCCAGGAGGAGAAAGGCAT
TAAGTACAAATTTGAAGTATATGAGAAGAATGAT**TAA****GCTT**ATTTAATAATAGATTAAAAATATTATAAAAATAAAAACATAAACACAGA
AATTACAAAAAAAAATACATATGAATTTTTTTTTTGTAATCTTCCTTATAAATATAGAATAATGAATCATATAAAACATATCATTATTCATTTA
TTTACATTTAAAATTATTGTTTCAGTATCTTTAATTTATTATGTATATATAAAAATAACTTACAATTTTATTAATAAACAATATATGTTTATTA
ATTCATGTTTTGTAATTTATGGGATAGCGATTTTTTTTACTGTCTGTATTTTTCTTTTTTAATTATGTTTTAATTGTATTTTATTTTTATTATTG
TTCTTTTTATAGTATTATTTTAAAACAAAATGTATTTTCTAAGAACTTATAATAATAATAAATATAAATTTTAATAAAAATTATATTTATCTT
TTACAATATGAACATAAAGTACAACATTAATATATAGCTTTTAATATTTTTATTCCTAATCATGTAAATCTTAAATTTTTCTTTTTAAACATA
TGTTAAATATTTATTTCTCATTATATATAAGAACATATTTATTAAATCTAGAATTCTATAGTGAGTCGTATTACAATTCACTGGCCGTCGTT
TTACAACGTCGTGACTGGGAAAACCCTGGCGTTACCCAACTTAATCGCCTTGCAGCACATCCCCCTTTCGCCAGCTGGCGTAATAGCGAA
GAGGCCCGCACCGATCGCCCTTCCCAACAGTTGCGCAGCCTGAATGGCGAATGGCGCCTGATGCGGTATTTTCTCCTTACGCATCTGTGC
GGTATTTCACACCGCATATGGTGCACTCTCAGTACAATCTGCTCTGATGCCGCATAGTTAAGCCAGCCCCGACACCCGCCAACACCCGCT
GACGCGCCCTGACGGGCTTGTCTGCTCCCGGCATCCGCTTACAGACAAGCTGTGACCGTCTCCGGGAGCTGCATGTGTCAGAGGTTTTC
ACCGTCATCACCGAAACGCGCGAGACGAAAGGGCCTCGTGATACGCCTATTTTTATAGGTTAATGTCATGATAATAATGGTTTCTTAGAC
GTCAGGTGGCACTTTTCGGGGAAATGTGCGCGGAACCCCTATTTGTTTATTTTTCTAAATACATTCAAATATGTATCCGCTCATGAGACAA
TAACCCTGATAAATGCTTCAATAATATTGAAAAAGGAAGAGTATGAGTATTCAACATTTCCGTGTCGCCCTTATTCCCTTTTTTGCGGCAT
TTTGCCTTCCTGTTTTTGCTCACCCAGAAACGCTGGTGAAAGTAAAAGATGCTGAAGATCAGTTGGGTGCACGAGTGGGTTACATCGAA
CTGGATCTCAACAGCGGTAAGATCCTTGAGAGTTTTCGCCCCGAAGAACGTTTTCCAATGATGAGCACTTTTAAAGTTCTGCTATGTGGC
GCGGTATTATCCCGTATTGACGCCGGGCAAGAGCAACTCGGTCGCCGCATACACTATTCTCAGAATGACTTGGTTGAGTACTCACCAGTC
ACAGAAAAGCATCTTACGGATGGCATGACAGTAAGAGAATTATGCAGTGCTGCCATAACCATGAGTGATAACACTGCGGCCAACTTACT
TCTGACAACGATCGGAGGACCGAAGGAGCTAACCGCTTTTTTGCACAACATGGGGGATCATGTAACTCGCCTTGATCGTTGGGAACCGG
AGCTGAATGAAGCCATACCAAACGACGAGCGTGACACCACGATGCCTGTAGCAATGCCAACAACGTTGCGCAAACTATTAACTGGCGA
ACTACTTACTCTAGCTTCCCGGCAACAATTAATAGACTGGATGGAGGCGGATAAAGTTGCAGGACCACTTCTGCGCTCGGCCCTTCCGGC
TGGCTGGTTTATTGCTGATAAATCTGGAGCCGGTGAGCGTGGGTCTCGCGGTATCATTGCAGCACTGGGGCCAGATGGTAAGCCCTCCC
GTATCGTAGTTATCTACACGACGGGGAGTCAGGCAACTATGGATGAACGAAATAGACAGATCGCTGAGATAGGTGCCTCACTGATTAA
GCATTGGTAACTGTCAGACCAAGTTTACTCATATATACTTTAGATTGATTTAAAACTTCATTTTTAATTTAAAAGGATCTAGGTGAAGATC
CTTTTTGATAATCTCATGACCAAAATCCCTTAACGTGAGTTTTCGTTCCACTGAGCGTCAGACCCCGTAGAAAAGATCAAAGGATCTTCTT
GAGATCCTTTTTTTCTGCGCGTAATCTGCTGCTTGCAAACAAAAAAACCACCGCTACCAGCGGTGGTTTGTTTGCCGGATCAAGAGCTAC
CAACTCTTTTTCCGAAGGTAACTGGCTTCAGCAGAGCGCAGATACCAAATACTGTCCTTCTAGTGTAGCCGTAGTTAGGCCACCACTTCA
AGAACTCTGTAGCACCGCCTACATACCTCGCTCTGCTAATCCTGTTACCAGTGGCTGCTGCCAGTGGCGATAAGTCGTGTCTTACCGGGT
TGGACTCAAGACGATAGTTACCGGATAAGGCGCAGCGGTCGGGCTGAACGGGGGGTTCGTGCACACAGCCCAGCTTGGAGCGAACGA
CCTACACCGAACTGAGATACCTACAGCGTGAGCTATGAGAAAGCGCCACGCTTCCCGAAGGGAGAAAGGCGGACAGGTATCCGGTAAG

CGGCAGGGTCGGAACAGGAGAGCGCACGAGGGAGCTTCCAGGGGGAAACGCCTGGTATCTTTATAGTCCTGTCGGGTTTCGCCACCTC
TGACTTGAGCGTCGATTTTTGTGATGCTCGTCAGGGGGGCGGAGCCTATCGAAAAACGCCAGCAACGCGGCCTTTTTACGGTTCCTGGC
CTTTTGCTGGCCTTTTGCTCACATGTTCTTTCCTGCGTTATCCCCTGATTCTGTGGATAACCGTATTACCGCCTTTGAGTGAGCTGATACCG
CTCGCCGCAGCCGAACGACCGAGCGCAGCGAGTCAGTGAGCGAGGAAGCGGAAGAGCGCCCAATACGCAAACCGCCTCTCCCCGCGC
GTTGGCCGATTCATTAATGCAGCTGGCACGACAGGTTTCCCGACTGGAAAGCGGGCAGTGAGCGCAACGCAATTAATGTGAGTTAGCT
CACTCATTAGGCACCCCAGGCTTTACACTTTATGCTTCCGGCTCGTATGTTGTGTGGAATTGTGAGCGGATAACAATTTCACACAGGAAA
CAGCTATGACCATGATTACGCCAAGCTATTTAGGTGACACTATAGAATACTC**GCGGCCGCTAA*CACCAGCACCAAGAGGTGTACCACAA***
ATTGAAGTTACCTTTGATGTTGATGCCAATGCTATTATTAACATATCAGCTATTGATAAAATGACTAACAAAAAACAACAAATTACTAT
ACAAAGTAGTGGTGGTTTAAGCAAGGAAGAAATTGAAAAAATGGTTCAAGAAGCTGAATTAAACAGAGAAAAAGATCAACTCAAG
AAAAATTTAACTGATTCTAAAAATGAAGCTGAAACACTTATTTATAGTTCTGAAAAACAATTGGAAGATTTCAAAGATAAAATTTCCG
ATTCTGATAAAGATGAATTAAGACAAAAAATTACAGTATTAAGAGAAAAGTTGACATCTGAAGATTTAGATTCTATTAAAGATGCCA
CTAAGCAGTTACAAGAAAAATCATGGGCCATATCGCAAGAAATGTACAAAAATAATGCTCAACAAGGAGCCCAACAAGAACAACCA
AATAATGAAAATAAAGCTGAAGAAAATAAAGATAATGCA**ACGCGT**GGATCCT***ATCCTTATGATGTTC****CAGATTATG***CAGGTTATCCTT
ATGATGTACCAGATTATGCTGGTTATC***CTTATGATGTTCCTGATTATGCA*****GTCGAC**GGAGAAGGAAGAGGAAGTTTATTAACATGTGGA
GATGTAGAAGAAAATCCAGGACCA**ATG**ATTGAACAAGATGGATTGCACGCAGGTTCTCCGGCCGCTTGGGTGGAGAGGCTATTCGGCT
ATGACTGGGCACAACAGACAATCGGCTGCTCTGATGCCGCCGTGTTCCGGCTGTCAGCGCAGGGGCGCCCGGTTCTTTTTGTCAAGACC
GACCTGTCCGGTGCCCTGAATGAACTGCAGGACGAGGCAGCGCGGCTATCGTGGCTGGCCACGACGGGCGTTCCTTGCGCAGCTGTGC
TCGACGTTGTCACTGAAGCGGGAAGGGACTGGCTGCTATTGGGCGAAGTGCCGGGGCAGGATCTCCTGTCATCTCACCTTGCTCCTGCC
GAGAAAGTATCCATCATGGCTGATGCAATGCGGCGGCTGCATACGCTTGATCCGGCTACCTGCCCATTCGACCACCAAGCGAAACATCG
CATCGAGCGAGCACGTACTCGGATGGAAGCCGGTCTTGTCGATCAGGATGATCTGGACGAAGAGCATCAGGGGCTCGCGCCAGCCGA
ACTGTTCGCCAGGCTCAAGGCGCGCATGCCCGACGGCGAGGATCTCGTCGTGACCCATGGCGATGCCTGCTTGCCGAATATCATGGTGG
AAAATGGCCGCTTTTCTGGATTCATCGACTGTGGCCGGCTGGGTGTGGCGGACCGCTATCAGGACATAGCGTTGGCTACCCGTGATATT
GCTGAAGAGCTTGGCGGCGAATGGGCTGACCGCTTCCTCGTGCTTTACGGTATCGCCGCTCCCGATTCGCAGCGCATCGCCTTCTATCGC
CTTCTTGACGAGTTCTT

Expected without intron

CACCAGCACCAAGAGGTGTACCACAAATTGAAGTTACCTTTGATGTTGATGCCAATGCTATTATTAACATATCAGCTATTGATAAAATG
ACTAACAAAAAACAACAAATTACTATACAAAGTAGTGGTGGTTTAAGCAAGGAAGAAATTGAAAAAATGGTTCAAGAAGCTGAATT
AAACAGAGAAAAAGATCAACTCAAGAAAAATTTAACTGATTCTAAAAATGAAGCTGAAACACTTATTTATAGTTCTGAAAAACAATT
GGAAGATTTCAAAGATAAAATTTCCGATTCTGATAAAGATGAATTAAGACAAAAAATTACAGTATTAAGAGAAAAGTTGACATCTGA
AGATTTAGATTCTATTAAAGATGCCACTAAGCAGTTACAAGAAAAATCATGGGCCATATCGCAAGAAATGTACAAAAATAATGCTCA
ACAAGGAGCCCAACAAGAACAACCAAATAATGAAAATAAAGCTGAAGAAAATAAAGATAATGCAACGCGTGGATCCT***ATCCTTATG***
ATGTTC*CAGATTATG*CAGGTTATCCTTATGATGTACCAGATTATGCTGGTTATC***CTTATGATGTTCCTGATTATGCA***GTCGACGGAGAAG
GAAGAGGAAGTTTATTAACATGTGGAGATGTAGAAGAAAATCCAGGACCA**ATG**ATTGAACAAGATGGATTGCACGCAGGTTCTCCGGC
CGCTTGGGTGGAGAGGCTATTCGGCTATGACTGGGCACAACAGACAATCGGCTGCTCTGATGCCGCCGTGTTCCGGCTGTCAGCGCAG
GGGCGCCCGGTTCTTTTTGTCAAGACCGACCTGTCCGGTGCCCTGAATGAACTGCAGGACGAGGCAGCGCGGCTATCGTGGCTGGCCA
CGACGGGCGTTCCTTGCGCAGCTGTGCTCGACGTTGTCACTGAAGCGGGAAGGGACTGGCTGCTATTGGGCGAAGTGCCGGGGCAGG
ATCTCCTGTCATCTCACCTTGCTCCTGCCGAGAAAGTATCCATCATGGCTGATGCAATGCGGCGGCTGCATACGCTTGATCCGGCTACCT
GCCCATTCGACCACCAAGCGAAACATCGCATCGAGCGAGCACGTACTCGGATGGAAGCCGGTCTTGTCGATCAGGATGATCTGGACGA
AGAGCATCAGGGGCTCGCGCCAGCCGAACTGTTCGCCAGGCTCAAGGCGCGCATGCCCGACGGCGAGGATCTCGTCGTGACCCATGGC
GATGCCTGCTTGCCGAATATCATGGTGGAAAATGGCCGCTTTTCTGGATTCATCGACTGTGGCCGGCTGGGTGTGGCGGACCGCTATCA

GGACATAGCGTTGGCTACCCGTGATATTGCTGAAGAGCTTGGCGGCGAATGGGCTGACCGCTTCCTCGTGCTTTACGGTATCGCCGCTC
CCGATTCGCAGCGCATCGCCTTCTATCGCCTTCTTGACGAGTTCTTCTAA

Expected translation product

PAPRGVPQIEVTFDVDANAIINISAIDKMTNKKQQITIQSSGGLSKEEIEKMVQEAELNREKDQLKKNLTDSKNEAETLIYSSEKQLEDFKDKISDS
DKDELRQKITVLREKLTSEDLDSIKDATKQLQEKSWAISQEMYKNNAQQGAQQEQPNNENKAEENKDNATRGSYPYDVPDYAGYPYDVPDY
AGYPYDVPDYAVDGEGRGSLLTCGDVEENPGPMIEQDGLHAGSPAAWVERLFGYDWAQQTIGCSDAAVFRLSAQGRPVLFVKTDLSGALN
ELQDEAARLSWLATTGVPCAAVLDVVTEAGRDWLLLGEVPGQDLLSSHLAPAEKVSIMADAMRRLHTLDPATCPFDHQAKHRIERARTRME
AGLVDQDDLDEEHQGLAPAELFARLKARMPDGEDLVVTHGDACLPNIMVENGRFSGFIDCGRLGVADRYQDIALATRDIAEELGGEWADRF
LVLYGIAAPDSQRIAFYRLLDEFFX

hDHFR

PfHSP70

3xHA tag

Neo-R

Skip peptide (skip between G and P, GGA-CCA)

S4 pSLI- *PAM16*-3xHA

GGATATGGCAGCTTAATGTTCGTTTTTCTTATTTATATATTTATACCAATTGATTGTATTTATAACTGTAAAAATGTGTATGTTGTGTGCAT
ATTTTTTTTTGTGCATGCACATGCATGTAAATAGCTAAAATTATGAACATTTTATTTTTTGTTCAGAAAAAAAAAACTTTACACACATAAAA
TGGCTAGTATGAATAGCCATATTTTATATAAATTAAATCCTATGAATTTATGACCATATTAAAAATTTAGATATTTATGGAACATAATATG
TTTGAAACAATAAGACAAAATTATTATTATTATTATTTTTACTGTTATAATTATGTGTCTCCTTCAATGATTCATAAATAGTTGGACTTG
ATTTTTAAAATGTTTATAATATGATTAGCATAGTTAAATAAAAAAAGTTGAAAAATTAAAAAAAAACATATAAACACAAATGATGGTTTTT
CCTTCAATTTCGATATCAATTTATAGAAACAAAATATATACTTGTATAATTTTATTTTTTTATATAAATCATTACATATATAATTATACAATA
TTTTTTCTAAGAGATAATTATATATTAATATATATAAAAAAAGGTGTTTTTTTTTTTTTTTTTTATTTTTATTTTTATTTTATGGTAATATTTTA
TTTTCCTTATTTTATAAATTATATTAGTTTATATGTGATTAATTTTATATATTATCAATTTATATATTTTTAAATGCTTACTTAATTATCTTTTT
TTTTTTTTTTTTTTTTTTTTCCCCTCTTTTTATATTAATTTATTTTTGAAAAAATTGATATATATATATATATATAATATATATATATACATGTA
GTAGTATTAAACAATGTATAATATATATAAATAATATATTTATATATTTCATTTCAATTTTAATTTTTTTTGGTTTTTTTTTTTTTTCTTTTTGT
CATATTTAAAAAAAATTATATTCATATAAGTTATGCATTTTTTATAAACATTATTCAATATATGTATAATATAATATATATATATATATTAAT
GTATTATTCCAATGTGCATGATAAAAGAAAAAAATAATATTTATAAAAAAAAAGAAAAATAAAACAAAAAAAGAAAAAAAAAAAAAAA
AAAAAAAAAATACAAAAATAAATAATATAATTTATAATTATATATTCTTGTCACAATAAAAATATATATATATATATATATTTATAATAT
GTATATTTTAAACTAGAAAAGGAATAACTAATATTTTATTTATTATCATTCAAGATTTATATTTTATAATAATAAATACCTAATAGAAATAT
ATCAGGATCCATGCATGGTTCGCTAAACTGCATCGTCGCTGTGTCCCAGAACATGGGCATCGGCAAGAACGGGGACTACCCCTGGCCAC
CGCTCAGGAACGAATTTAGATATTTCCAGAGAATGACCACAACCTCTTCAGTAGAAGGTAAACAGAATCTGGTGATTATGGGTAAGAAG
ACCTGGTTCTCCATTCCTGAGAAGAATCGACCTTTAAAGGGTAGAATTAATTTAGTTCTCAGCAGAGAACTCAAGGAACCTCCACAAGGA
GCTCATTTTCTTTCCAGAAGTCTAGATGATGCCTTAAAACTTACTGAACAACCAGAATTAGCAAATAAAGTAGACATGGTCTGGATAGTT
GGTGGCAGTTCTGTTTATAAGGAAGCCATGAATCACCCAGGCCATCTTAAACTATTTGTGACAAGGATCATGCAAGACTTTGAAAGTGA
CACGTTTTTTCCAGAAATTGATTTGGAGAAATATAAACTTCTGCCAGAATACCCAGGTGTTCTCTCTGATGTCCAGGAGGAGAAAGGCAT
TAAGTACAAATTTGAAGTATATGAGAAGAATGATTAAGCTTATTTAATAATAGATTAAAAATATTATAAAAATAAAAACATAAACACAGA
AATTACAAAAAAAAATACATATGAATTTTTTTTTTGTAATCTTCCTTATAAATATAGAATAATGAATCATATAAAACATATCATTATTCATTTA
TTTACATTTAAAATTATTGTTTCAGTATCTTTAATTTATTATGTATATATAAAAATAACTTACAATTTTATTAATAAACAATATATGTTTATTA

ATTCATGTTTTGTAATTTATGGGATAGCGATTTTTTTTACTGTCTGTATTTTTCTTTTTTAATTATGTTTTAATTGTATTTTATTTTTATTATTG
TTCTTTTTATAGTATTATTTTAAAACAAAATGTATTTTCTAAGAACTTATAATAATAATAAATATAAATTTTAATAAAAATTATATTTATCTT
TTACAATATGAACATAAAGTACAACATTAATATATAGCTTTTAATATTTTTATTCCTAATCATGTAAATCTTAAATTTTTCTTTTTAAACATA
TGTTAAATATTTATTTCTCATTATATATAAGAACATATTTATTAAATCTAGAATTCTATAGTGAGTCGTATTACAATTCACTGGCCGTCGTT
TTACAACGTCGTGACTGGGAAAACCCTGGCGTTACCCAACTTAATCGCCTTGCAGCACATCCCCCTTTCGCCAGCTGGCGTAATAGCGAA
GAGGCCCGCACCGATCGCCCTTCCCAACAGTTGCGCAGCCTGAATGGCGAATGGCGCCTGATGCGGTATTTTCTCCTTACGCATCTGTGC
GGTATTTCACACCGCATATGGTGCACTCTCAGTACAATCTGCTCTGATGCCGCATAGTTAAGCCAGCCCCGACACCCGCCAACACCCGCT
GACGCGCCCTGACGGGCTTGTCTGCTCCCGGCATCCGCTTACAGACAAGCTGTGACCGTCTCCGGGAGCTGCATGTGTCAGAGGTTTTC
ACCGTCATCACCGAAACGCGCGAGACGAAAGGGCCTCGTGATACGCCTATTTTTATAGGTTAATGTCATGATAATAATGGTTTCTTAGAC
GTCAGGTGGCACTTTTCGGGGAAATGTGCGCGGAACCCCTATTTGTTTATTTTTCTAAATACATTCAAATATGTATCCGCTCATGAGACAA
TAACCCTGATAAATGCTTCAATAATATTGAAAAAGGAAGAGTATGAGTATTCAACATTTCCGTGTCGCCCTTATTCCCTTTTTTGCGGCAT
TTTGCCTTCCTGTTTTTGCTCACCCAGAAACGCTGGTGAAAGTAAAAGATGCTGAAGATCAGTTGGGTGCACGAGTGGGTTACATCGAA
CTGGATCTCAACAGCGGTAAGATCCTTGAGAGTTTTCGCCCCGAAGAACGTTTTCCAATGATGAGCACTTTTAAAGTTCTGCTATGTGGC
GCGGTATTATCCCGTATTGACGCCGGGCAAGAGCAACTCGGTCGCCGCATACACTATTCTCAGAATGACTTGGTTGAGTACTCACCAGTC
ACAGAAAAGCATCTTACGGATGGCATGACAGTAAGAGAATTATGCAGTGCTGCCATAACCATGAGTGATAACACTGCGGCCAACTTACT
TCTGACAACGATCGGAGGACCGAAGGAGCTAACCGCTTTTTTGCACAACATGGGGGATCATGTAACTCGCCTTGATCGTTGGGAACCGG
AGCTGAATGAAGCCATACCAAACGACGAGCGTGACACCACGATGCCTGTAGCAATGCCAACAACGTTGCGCAAACTATTAACTGGCGA
ACTACTTACTCTAGCTTCCCGGCAACAATTAATAGACTGGATGGAGGCGGATAAAGTTGCAGGACCACTTCTGCGCTCGGCCCTTCCGGC
TGGCTGGTTTATTGCTGATAAATCTGGAGCCGGTGAGCGTGGGTCTCGCGGTATCATTGCAGCACTGGGGCCAGATGGTAAGCCCTCCC
GTATCGTAGTTATCTACACGACGGGGAGTCAGGCAACTATGGATGAACGAAATAGACAGATCGCTGAGATAGGTGCCTCACTGATTAA
GCATTGGTAACTGTCAGACCAAGTTTACTCATATATACTTTAGATTGATTTAAAACTTCATTTTTAATTTAAAAGGATCTAGGTGAAGATC
CTTTTTGATAATCTCATGACCAAAATCCCTTAACGTGAGTTTTCGTTCCACTGAGCGTCAGACCCCGTAGAAAAGATCAAAGGATCTTCTT
GAGATCCTTTTTTTCTGCGCGTAATCTGCTGCTTGCAAACAAAAAAACCACCGCTACCAGCGGTGGTTTGTTTGCCGGATCAAGAGCTAC
CAACTCTTTTTCCGAAGGTAACTGGCTTCAGCAGAGCGCAGATACCAAATACTGTCCTTCTAGTGTAGCCGTAGTTAGGCCACCACTTCA
AGAACTCTGTAGCACCGCCTACATACCTCGCTCTGCTAATCCTGTTACCAGTGGCTGCTGCCAGTGGCGATAAGTCGTGTCTTACCGGGT
TGGACTCAAGACGATAGTTACCGGATAAGGCGCAGCGGTCGGGCTGAACGGGGGGTTCGTGCACACAGCCCAGCTTGGAGCGAACGA
CCTACACCGAACTGAGATACCTACAGCGTGAGCTATGAGAAAGCGCCACGCTTCCCGAAGGGAGAAAGGCGGACAGGTATCCGGTAAG
CGGCAGGGTCGGAACAGGAGAGCGCACGAGGGAGCTTCCAGGGGGAAACGCCTGGTATCTTTATAGTCCTGTCGGGTTTCGCCACCTC
TGACTTGAGCGTCGATTTTTGTGATGCTCGTCAGGGGGGCGGAGCCTATCGAAAAACGCCAGCAACGCGGCCTTTTTACGGTTCCTGGC
CTTTTGCTGGCCTTTTGCTCACATGTTCTTTCCTGCGTTATCCCCTGATTCTGTGGATAACCGTATTACCGCCTTTGAGTGAGCTGATACCG
CTCGCCGCAGCCGAACGACCGAGCGCAGCGAGTCAGTGAGCGAGGAAGCGGAAGAGCGCCCAATACGCAAACCGCCTCTCCCCGCGC
GTTGGCCGATTCATTAATGCAGCTGGCACGACAGGTTTCCCGACTGGAAAGCGGGCAGTGAGCGCAACGCAATTAATGTGAGTTAGCT
CACTCATTAGGCACCCCAGGCTTTACACTTTATGCTTCCGGCTCGTATGTTGTGTGGAATTGTGAGCGGATAACAATTTCACACAGGAAA
CAGCTATGACCATGATTACGCCAAGCTATTTAGGTGACACTATAGAATACTCGCGGCCGCTAAGCTTATAGAGAAATAATAAAAAATAA
ACACAATACACATTTTATAAAAGAAAAATACAACCCTTGTATGAATATAGAAGAAGCTTTAAATATATTAAACGTCGATAAAACAAAAAT
ATATAAAAATTTAAATAAAGAAGAATTAATGTCTTTAAAAGATGAAATAACAAATAGACACTTGATTTTAAATAAATTAAATGAGAAAAA
TGGTCCATATAATGGTTCTGCCTATATACAAAAAAAGGCCAGAATTGCAAAGGATATATTGTTTCAGCATTTAAAATTACAAACGCGTGG
ATCCTATCCTTATGATGTTCCAGATTATGCAGGTTATCCTTATGATGTACCAGATTATGCTGGTTATCCTTATGATGTTCCTGATTATGCAG
TCGACGGAGAAGGAAGAGGAAGTTTATTAACATGTGGAGATGTAGAAGAAAATCCAGGACCAATGATTGAACAAGATGGATTGCACG
CAGGTTCTCCGGCCGCTTGGGTGGAGAGGCTATTCGGCTATGACTGGGCACAACAGACAATCGGCTGCTCTGATGCCGCCGTGTTCCGG
CTGTCAGCGCAGGGGCGCCCGGTTCTTTTTGTCAAGACCGACCTGTCCGGTGCCCTGAATGAACTGCAGGACGAGGCAGCGCGGCTATC
GTGGCTGGCCACGACGGGCGTTCCTTGCGCAGCTGTGCTCGACGTTGTCACTGAAGCGGGAAGGGACTGGCTGCTATTGGGCGAAGTG

CCGGGGCAGGATCTCCTGTCATCTCACCTTGCTCCTGCCGAGAAAGTATCCATCATGGCTGATGCAATGCGGCGGCTGCATACGCTTGAT
CCGGCTACCTGCCCATTCGACCACCAAGCGAAACATCGCATCGAGCGAGCACGTACTCGGATGGAAGCCGGTCTTGTCGATCAGGATGA
TCTGGACGAAGAGCATCAGGGGCTCGCGCCAGCCGAACTGTTCGCCAGGCTCAAGGCGCGCATGCCCGACGGCGAGGATCTCGTCGTG
ACCCATGGCGATGCCTGCTTGCCGAATATCATGGTGGAAAATGGCCGCTTTTCTGGATTCATCGACTGTGGCCGGCTGGGTGTGGCGGA
CCGCTATCAGGACATAGCGTTGGCTACCCGTGATATTGCTGAAGAGCTTGGCGGCGAATGGGCTGACCGCTTCCTCGTGCTTTACGGTA
TCGCCGCTCCCGATTCGCAGCGCATCGCCTTCTATCGCCTTCTTGACGAGTTCTTCTAACTCGAG

Expected without intron

GCTTATAGAGAAATAATAAAAAATAAACACAATACACATTTTATAAAAGAAAAATACAACCCTTGTATGAATATAGAAGAAGCTTTAAAT
ATATTAAACGTCGATAAAACAAAAATATATAAAAATTTAAATAAAGAAGAATTAATGTCTTTAAAAGATGAAATAACAAATAGACACTTG
ATTTTAAATAAATTAAATGAGAAAAATGGTCCATATAATGGTTCTGCCTATATACAAAAAAAGGCCAGAATTGCAAAG***GATATATTGTTT***
CAGCATTTAAAATTACAAACGCGTGGATCCT***ATCCTTATGATGTTC****CAGATTATG*CAGGTTATCCTTATGATGTACCAGATTATGCTGGTT
ATC***CTTATGATGTTCCTGATTATGCA***GTCGACGGAGAAGGAAGAGGAAGTTTATTAACATGTGGAGATGTAGAAGAAAATCCAGGACC
A**ATG**ATTGAACAAGATGGATTGCACGCAGGTTCTCCGGCCGCTTGGGTGGAGAGGCTATTCGGCTATGACTGGGCACAACAGACAATC
GGCTGCTCTGATGCCGCCGTGTTCCGGCTGTCAGCGCAGGGGCGCCCGGTTCTTTTTGTCAAGACCGACCTGTCCGGTGCCCTGAATGA
ACTGCAGGACGAGGCAGCGCGGCTATCGTGGCTGGCCACGACGGGCGTTCCTTGCGCAGCTGTGCTCGACGTTGTCACTGAAGCGGGA
AGGGACTGGCTGCTATTGGGCGAAGTGCCGGGGCAGGATCTCCTGTCATCTCACCTTGCTCCTGCCGAGAAAGTATCCATCATGGCTGA
TGCAATGCGGCGGCTGCATACGCTTGATCCGGCTACCTGCCCATTCGACCACCAAGCGAAACATCGCATCGAGCGAGCACGTACTCGGA
TGGAAGCCGGTCTTGTCGATCAGGATGATCTGGACGAAGAGCATCAGGGGCTCGCGCCAGCCGAACTGTTCGCCAGGCTCAAGGCGCG
CATGCCCGACGGCGAGGATCTCGTCGTGACCCATGGCGATGCCTGCTTGCCGAATATCATGGTGGAAAATGGCCGCTTTTCTGGATTCA
TCGACTGTGGCCGGCTGGGTGTGGCGGACCGCTATCAGGACATAGCGTTGGCTACCCGTGATATTGCTGAAGAGCTTGGCGGCGAATG
GGCTGACCGCTTCCTCGTGCTTTACGGTATCGCCGCTCCCGATTCGCAGCGCATCGCCTTCTATCGCCTTCTTGACGAGTTCTTC**TAA**

Expected translation product

AYREIIKNKHNTHFIKEKYNPCMNIEEALNILNVDKTKIYKNLNKEELMSLKDEITNRHLILNKLNEKNGPYNGSAYIQKKARIAKDILFQHLKLQT
RGSYPYDVPDYAGYPYDVPDYAGYPYDVPDYAVDGEGRGSLLTCGDVEENPGPMIEQDGLHAGSPAAWVERLFGYDWAQQTIGCSDAAVF
RLSAQGRPVLFVKTDLSGALNELQDEAARLSWLATTGVPCAAVLDVVTEAGRDWLLLGEVPGQDLLSSHLAPAEKVSIMADAMRRLHTLDPA
TCPFDHQAKHRIERARTRMEAGLVDQDDLDEEHQGLAPAELFARLKARMPDGEDLVVTHGDACLPNIMVENGRFSGFIDCGRLGVADRYQ
DIALATRDIAEELGGEWADRFLVLYGIAAPDSQRIAFYRLLDEFF*X

hDHFR

PfPAM16

3xHA tag

Neo-R

Skip peptide (skip between G and P, GGA-CCA)

S5 pSLI- *PFMGE1*-3xHA

GGATATGGCAGCTTAATGTTCGTTTTTCTTATTTATATATTTATACCAATTGATTGTATTTATAACTGTAAAAATGTGTATGTTGTGTGCAT
ATTTTTTTTTGTGCATGCACATGCATGTAAATAGCTAAAATTATGAACATTTTATTTTTTGTTCAGAAAAAAAAAACTTTACACACATAAAA
TGGCTAGTATGAATAGCCATATTTTATATAAATTAAATCCTATGAATTTATGACCATATTAAAAATTTAGATATTTATGGAACATAATATG
TTTGAAACAATAAGACAAAATTATTATTATTATTATTTTTACTGTTATAATTATGTGTCTCCTTCAATGATTCATAAATAGTTGGACTTG

ATTTTTAAAATGTTTATAATATGATTAGCATAGTTAAATAAAAAAAGTTGAAAAATTAAAAAAAAACATATAAACACAAATGATGGTTTTT
CCTTCAATTTCGATATCAATTTATAGAAACAAAATATATACTTGTATAATTTTATTTTTTTATATAAATCATTACATATATAATTATACAATA
TTTTTTCTAAGAGATAATTATATATTAATATATATAAAAAAAGGTGTTTTTTTTTTTTTTTTTTATTTTTATTTTTATTTTATGGTAATATTTTA
TTTTCCTTATTTTATAAATTATATTAGTTTATATGTGATTAATTTTATATATTATCAATTTATATATTTTTAAATGCTTACTTAATTATCTTTTT
TTTTTTTTTTTTTTTTTTTTCCCCTCTTTTTATATTAATTTATTTTTGAAAAAATTGATATATATATATATATATAATATATATATATACATGTA
GTAGTATTAAACAATGTATAATATATATAAATAATATATTTATATATTTCATTTCAATTTTAATTTTTTTTGGTTTTTTTTTTTTTTCTTTTTGT
CATATTTAAAAAAAATTATATTCATATAAGTTATGCATTTTTTATAAACATTATTCAATATATGTATAATATAATATATATATATATTTAAT
GTATTATTCCAATGTGCATGATAAAAGAAAAAAATAATATTTATAAAAAAAAAGAAAAATAAAACAAAAAAAGAAAAAAAAAAAAAAA
AAAAAAAAAATACAAAAATAAATAATATAATTTATAATTATATATTCTTGTCACAATAAAAATATATATATATATATATATTTATAATAT
GTATATTTTAAACTAGAAAAGGAATAACTAATATTTTATTTATTATCATTCAAGATTTATATTTTATAATAATAAATACCTAATAGAAATAT
ATCAGGATCCATGCATGGTTCGCTAAACTGCATCGTCGCTGTGTCCCAGAACATGGGCATCGGCAAGAACGGGGACTACCCCTGGCCAC
CGCTCAGGAACGAATTTAGATATTTCCAGAGAATGACCACAACCTCTTCAGTAGAAGGTAAACAGAATCTGGTGATTATGGGTAAGAAG
ACCTGGTTCTCCATTCCTGAGAAGAATCGACCTTTAAAGGGTAGAATTAATTTAGTTCTCAGCAGAGAACTCAAGGAACCTCCACAAGGA
GCTCATTTTCTTTCCAGAAGTCTAGATGATGCCTTAAAACTTACTGAACAACCAGAATTAGCAAATAAAGTAGACATGGTCTGGATAGTT
GGTGGCAGTTCTGTTTATAAGGAAGCCATGAATCACCCAGGCCATCTTAAACTATTTGTGACAAGGATCATGCAAGACTTTGAAAGTGA
CACGTTTTTTCCAGAAATTGATTTGGAGAAATATAAACTTCTGCCAGAATACCCAGGTGTTCTCTCTGATGTCCAGGAGGAGAAAGGCAT
TAAGTACAAATTTGAAGTATATGAGAAGAATGATTAAGCTTATTTAATAATAGATTAAAAATATTATAAAAATAAAAACATAAACACAGA
AATTACAAAAAAAAATACATATGAATTTTTTTTTTGTAATCTTCCTTATAAATATAGAATAATGAATCATATAAAACATATCATTATTCATTTA
TTTACATTTAAAATTATTGTTTCAGTATCTTTAATTTATTATGTATATATAAAAATAACTTACAATTTTATTAATAAACAATATATGTTTATTA
ATTCATGTTTTGTAATTTATGGGATAGCGATTTTTTTTACTGTCTGTATTTTTCTTTTTTAATTATGTTTTAATTGTATTTTATTTTTATTATTG
TTCTTTTTATAGTATTATTTTAAAACAAAATGTATTTTCTAAGAACTTATAATAATAATAAATATAAATTTTAATAAAAATTATATTTATCTT
TTACAATATGAACATAAAGTACAACATTAATATATAGCTTTTAATATTTTTATTCCTAATCATGTAAATCTTAAATTTTTCTTTTTAAACATA
TGTTAAATATTTATTTCTCATTATATATAAGAACATATTTATTAAATCTAGAATTCTATAGTGAGTCGTATTACAATTCACTGGCCGTCGTT
TTACAACGTCGTGACTGGGAAAACCCTGGCGTTACCCAACTTAATCGCCTTGCAGCACATCCCCCTTTCGCCAGCTGGCGTAATAGCGAA
GAGGCCCGCACCGATCGCCCTTCCCAACAGTTGCGCAGCCTGAATGGCGAATGGCGCCTGATGCGGTATTTTCTCCTTACGCATCTGTGC
GGTATTTCACACCGCATATGGTGCACTCTCAGTACAATCTGCTCTGATGCCGCATAGTTAAGCCAGCCCCGACACCCGCCAACACCCGCT
GACGCGCCCTGACGGGCTTGTCTGCTCCCGGCATCCGCTTACAGACAAGCTGTGACCGTCTCCGGGAGCTGCATGTGTCAGAGGTTTTC
ACCGTCATCACCGAAACGCGCGAGACGAAAGGGCCTCGTGATACGCCTATTTTTATAGGTTAATGTCATGATAATAATGGTTTCTTAGAC
GTCAGGTGGCACTTTTCGGGGAAATGTGCGCGGAACCCCTATTTGTTTATTTTTCTAAATACATTCAAATATGTATCCGCTCATGAGACAA
TAACCCTGATAAATGCTTCAATAATATTGAAAAAGGAAGAGTATGAGTATTCAACATTTCCGTGTCGCCCTTATTCCCTTTTTTGCGGCAT
TTTGCCTTCCTGTTTTTGCTCACCCAGAAACGCTGGTGAAAGTAAAAGATGCTGAAGATCAGTTGGGTGCACGAGTGGGTTACATCGAA
CTGGATCTCAACAGCGGTAAGATCCTTGAGAGTTTTCGCCCCGAAGAACGTTTTCCAATGATGAGCACTTTTAAAGTTCTGCTATGTGGC
GCGGTATTATCCCGTATTGACGCCGGGCAAGAGCAACTCGGTCGCCGCATACACTATTCTCAGAATGACTTGGTTGAGTACTCACCAGTC
ACAGAAAAGCATCTTACGGATGGCATGACAGTAAGAGAATTATGCAGTGCTGCCATAACCATGAGTGATAACACTGCGGCCAACTTACT
TCTGACAACGATCGGAGGACCGAAGGAGCTAACCGCTTTTTTGCACAACATGGGGGATCATGTAACTCGCCTTGATCGTTGGGAACCGG
AGCTGAATGAAGCCATACCAAACGACGAGCGTGACACCACGATGCCTGTAGCAATGCCAACAACGTTGCGCAAACTATTAACTGGCGA
ACTACTTACTCTAGCTTCCCGGCAACAATTAATAGACTGGATGGAGGCGGATAAAGTTGCAGGACCACTTCTGCGCTCGGCCCTTCCGGC
TGGCTGGTTTATTGCTGATAAATCTGGAGCCGGTGAGCGTGGGTCTCGCGGTATCATTGCAGCACTGGGGCCAGATGGTAAGCCCTCCC
GTATCGTAGTTATCTACACGACGGGGAGTCAGGCAACTATGGATGAACGAAATAGACAGATCGCTGAGATAGGTGCCTCACTGATTAA
GCATTGGTAACTGTCAGACCAAGTTTACTCATATATACTTTAGATTGATTTAAAACTTCATTTTTAATTTAAAAGGATCTAGGTGAAGATC
CTTTTTGATAATCTCATGACCAAAATCCCTTAACGTGAGTTTTCGTTCCACTGAGCGTCAGACCCCGTAGAAAAGATCAAAGGATCTTCTT
GAGATCCTTTTTTTCTGCGCGTAATCTGCTGCTTGCAAACAAAAAAACCACCGCTACCAGCGGTGGTTTGTTTGCCGGATCAAGAGCTAC

CAACTCTTTTTCCGAAGGTAACTGGCTTCAGCAGAGCGCAGATACCAAATACTGTCCTTCTAGTGTAGCCGTAGTTAGGCCACCACTTCA
AGAACTCTGTAGCACCGCCTACATACCTCGCTCTGCTAATCCTGTTACCAGTGGCTGCTGCCAGTGGCGATAAGTCGTGTCTTACCGGGT
TGGACTCAAGACGATAGTTACCGGATAAGGCGCAGCGGTCGGGCTGAACGGGGGGTTCGTGCACACAGCCCAGCTTGGAGCGAACGA
CCTACACCGAACTGAGATACCTACAGCGTGAGCTATGAGAAAGCGCCACGCTTCCCGAAGGGAGAAAGGCGGACAGGTATCCGGTAAG
CGGCAGGGTCGGAACAGGAGAGCGCACGAGGGAGCTTCCAGGGGGAAACGCCTGGTATCTTTATAGTCCTGTCGGGTTTCGCCACCTC
TGACTTGAGCGTCGATTTTTGTGATGCTCGTCAGGGGGGCGGAGCCTATCGAAAAACGCCAGCAACGCGGCCTTTTTACGGTTCCTGGC
CTTTTGCTGGCCTTTTGCTCACATGTTCTTTCCTGCGTTATCCCCTGATTCTGTGGATAACCGTATTACCGCCTTTGAGTGAGCTGATACCG
CTCGCCGCAGCCGAACGACCGAGCGCAGCGAGTCAGTGAGCGAGGAAGCGGAAGAGCGCCCAATACGCAAACCGCCTCTCCCCGCGC
GTTGGCCGATTCATTAATGCAGCTGGCACGACAGGTTTCCCGACTGGAAAGCGGGCAGTGAGCGCAACGCAATTAATGTGAGTTAGCT
CACTCATTAGGCACCCCAGGCTTTACACTTTATGCTTCCGGCTCGTATGTTGTGTGGAATTGTGAGCGGATAACAATTTCACACAGGAAA
CAGCTATGACCATGATTACGCCAAGCTATTTAGGTGACACTATAGAATACTCGCGGCCGCTAAGCTTATAGAGAAATAATAAAAAATAA
ACACAATACACATTTTATAAAAGAAAAATACAACCCTTGTATGAATATAGAAGAAGCTTTAAATATATTAAACGTCGATAAAACAAAAAT
ATATAAAAATTTAAATAAAGAAGAATTAATGTCTTTAAAAGATGAAATAACAAATAGACACTTGATTTTAAATAAATTAAATGAGAAAAA
TGGTCCATATAATGGTTCTGCCTATATACAAAAAAAGGCCAGAATTGCAAAGGATATATTGTTTCAGCATTTAAAATTACAAACGCGTGG
ATCCTATCCTTATGATGTTCCAGATTATGCAGGTTATCCTTATGATGTACCAGATTATGCTGGTTATCCTTATGATGTTCCTGATTATGCAG
TCGACGGAGAAGGAAGAGGAAGTTTATTAACATGTGGAGATGTAGAAGAAAATCCAGGACCAATGATTGAACAAGATGGATTGCACG
CAGGTTCTCCGGCCGCTTGGGTGGAGAGGCTATTCGGCTATGACTGGGCACAACAGACAATCGGCTGCTCTGATGCCGCCGTGTTCCGG
CTGTCAGCGCAGGGGCGCCCGGTTCTTTTTGTCAAGACCGACCTGTCCGGTGCCCTGAATGAACTGCAGGACGAGGCAGCGCGGCTATC
GTGGCTGGCCACGACGGGCGTTCCTTGCGCAGCTGTGCTCGACGTTGTCACTGAAGCGGGAAGGGACTGGCTGCTATTGGGCGAAGTG
CCGGGGCAGGATCTCCTGTCATCTCACCTTGCTCCTGCCGAGAAAGTATCCATCATGGCTGATGCAATGCGGCGGCTGCATACGCTTGAT
CCGGCTACCTGCCCATTCGACCACCAAGCGAAACATCGCATCGAGCGAGCACGTACTCGGATGGAAGCCGGTCTTGTCGATCAGGATGA
TCTGGACGAAGAGCATCAGGGGCTCGCGCCAGCCGAACTGTTCGCCAGGCTCAAGGCGCGCATGCCCGACGGCGAGGATCTCGTCGTG
ACCCATGGCGATGCCTGCTTGCCGAATATCATGGTGGAAAATGGCCGCTTTTCTGGATTCATCGACTGTGGCCGGCTGGGTGTGGCGGA
CCGCTATCAGGACATAGCGTTGGCTACCCGTGATATTGCTGAAGAGCTTGGCGGCGAATGGGCTGACCGCTTCCTCGTGCTTTACGGTA
TCGCCGCTCCCGATTCGCAGCGCATCGCCTTCTATCGCCTTCTTGACGAGTTCTTCTAACTCGAG

ATAGAAACTAGTAAATTATATTGTATTAGTAATTTTGCAAAATCATTACTTGATGTAGCAGACAATTTATCATTAGCTATTAAAAATATAA
ATGAAGAATCTTTAAAAACAAATGAAGAAATTAATAATATATACAAAGGTATAGAAATGACTGAAACGATTCTTCATAATATTTTTAATA
AATATGGAATTGATAAATATAATCCTATAAATGAAAAATTTAATCCACAATTACATGAAGCAATATTTGAAATTAATGACAGTACAAAAG
AAAAGGGAACCGTAGCAACTGTTATTCAGCATGGATATAAAATAAAGGACCGAATATTAAGAGCTG***CCAAAGTTGGAGTGGTTAAAAA***
TACGCGTGGATCCT***ATCCTTATGATGTTC****CAGATTATG*CAGGTTATCCTTATGATGTACCAGATTATGCTGGTTATC***CTTATGATGTTCCT***
GATTATGCAGTCGACGGAGAAGGAAGAGGAAGTTTATTAACATGTGGAGATGTAGAAGAAAATCCAGGACCA**ATG**ATTGAACAAGAT
GGATTGCACGCAGGTTCTCCGGCCGCTTGGGTGGAGAGGCTATTCGGCTATGACTGGGCACAACAGACAATCGGCTGCTCTGATGCCG
CCGTGTTCCGGCTGTCAGCGCAGGGGCGCCCGGTTCTTTTTGTCAAGACCGACCTGTCCGGTGCCCTGAATGAACTGCAGGACGAGGCA
GCGCGGCTATCGTGGCTGGCCACGACGGGCGTTCCTTGCGCAGCTGTGCTCGACGTTGTCACTGAAGCGGGAAGGGACTGGCTGCTAT
TGGGCGAAGTGCCGGGGCAGGATCTCCTGTCATCTCACCTTGCTCCTGCCGAGAAAGTATCCATCATGGCTGATGCAATGCGGCGGCTG
CATACGCTTGATCCGGCTACCTGCCCATTCGACCACCAAGCGAAACATCGCATCGAGCGAGCACGTACTCGGATGGAAGCCGGTCTTGT
CGATCAGGATGATCTGGACGAAGAGCATCAGGGGCTCGCGCCAGCCGAACTGTTCGCCAGGCTCAAGGCGCGCATGCCCGACGGCGA
GGATCTCGTCGTGACCCATGGCGATGCCTGCTTGCCGAATATCATGGTGGAAAATGGCCGCTTTTCTGGATTCATCGACTGTGGCCGGC
TGGGTGTGGCGGACCGCTATCAGGACATAGCGTTGGCTACCCGTGATATTGCTGAAGAGCTTGGCGGCGAATGGGCTGACCGCTTCCT
CGTGCTTTACGGTATCGCCGCTCCCGATTCGCAGCGCATCGCCTTCTATCGCCTTCTTGACGAGTTCTTC**TAA**

Expected translation product

IETSKLYCISNFAKSLLDVADNLSLAIKNINEESLKTNEEINNIYKGIEMTETILHNIFNKYGIDKYNPINEKFNPQLHEAIFEINDSTKEKGTVATVIQ

HGYKIKDRILRAAKVGVVKNTRGSYPYDVPDYAGYPYDVPDYAGYPYDVPDYAVDGEGRGSLLTCGDVEENPGPMIEQDGLHAGSPAAWVE

RLFGYDWAQQTIGCSDAAVFRLSAQGRPVLFVKTDLSGALNELQDEAARLSWLATTGVPCAAVLDVVTEAGRDWLLLGEVPGQDLLSSHLAP

AEKVSIMADAMRRLHTLDPATCPFDHQAKHRIERARTRMEAGLVDQDDLDEEHQGLAPAELFARLKARMPDGEDLVVTHGDACLPNIMVE

NGRFSGFIDCGRLGVADRYQDIALATRDIAEELGGEWADRFLVLYGIAAPDSQRIAFYRLLDEFF*

hDHFR

PfMGE1

3xHA tag

Neo-R

Skip peptide (skip between G and P, GGA-CCA)

S6 pSLI-*PFOXA1*-3xHA

GGATATGGCAGCTTAATGTTCGTTTTTCTTATTTATATATTTATACCAATTGATTGTATTTATAACTGTAAAAATGTGTATGTTGTGTGCAT

ATTTTTTTTTGTGCATGCACATGCATGTAAATAGCTAAAATTATGAACATTTTATTTTTTGTTCAGAAAAAAAAAACTTTACACACATAAAA

TGGCTAGTATGAATAGCCATATTTTATATAAATTAAATCCTATGAATTTATGACCATATTAAAAATTTAGATATTTATGGAACATAATATG

TTTGAAACAATAAGACAAAATTATTATTATTATTATTTTTACTGTTATAATTATGTGTCTCCTTCAATGATTCATAAATAGTTGGACTTG

ATTTTTAAAATGTTTATAATATGATTAGCATAGTTAAATAAAAAAAGTTGAAAAATTAAAAAAAAACATATAAACACAAATGATGGTTTTT

CCTTCAATTTCGATATCAATTTATAGAAACAAAATATATACTTGTATAATTTTATTTTTTTATATAAATCATTACATATATAATTATACAATA

TTTTTTCTAAGAGATAATTATATATTAATATATATAAAAAAAGGTGTTTTTTTTTTTTTTTTTTATTTTTATTTTTATTTTATGGTAATATTTTA

TTTTCCTTATTTTATAAATTATATTAGTTTATATGTGATTAATTTTATATATTATCAATTTATATATTTTTAAATGCTTACTTAATTATCTTTTT

TTTTTTTTTTTTTTTTTTTCCCCTCTTTTTATATTAATTTATTTTTGAAAAAATTGATATATATATATATATATAATATATATATATACATGTA

GTAGTATTAAACAATGTATAATATATATAAATAATATATTTATATATTTCATTTCAATTTTAATTTTTTTTGGTTTTTTTTTTTTTTCTTTTTGT

CATATTTAAAAAAAATTATATTCATATAAGTTATGCATTTTTTATAAACATTATTCAATATATGTATAATATAATATATATATATATTAAT

GTATTATTCCAATGTGCATGATAAAAGAAAAAAATAATATTTATAAAAAAAAAGAAAAATAAAACAAAAAAAGAAAAAAAAAAAAAAA

AAAAAAAAAATACAAAAATAAATAATATAATTTATAATTATATATTCTTGTCACAATAAAAATATATATATATATATATATATTTATAATAT

GTATATTTTAAACTAGAAAAGGAATAACTAATATTTTATTTATTATCATTCAAGATTTATATTTTATAATAATAAATACCTAATAGAAATAT

ATCA**GGATCC****ATG**CATGGTTCGCTAAACTGCATCGTCGCTGTGTCCCAGAACATGGGCATCGGCAAGAACGGGGACTACCCCTGGCCAC

CGCTCAGGAACGAATTTAGATATTTCCAGAGAATGACCACAACCTCTTCAGTAGAAGGTAAACAGAATCTGGTGATTATGGGTAAGAAG

ACCTGGTTCTCCATTCCTGAGAAGAATCGACCTTTAAAGGGTAGAATTAATTTAGTTCTCAGCAGAGAACTCAAGGAACCTCCACAAGGA

GCTCATTTTCTTTCCAGAAGTCTAGATGATGCCTTAAAACTTACTGAACAACCAGAATTAGCAAATAAAGTAGACATGGTCTGGATAGTT

GGTGGCAGTTCTGTTTATAAGGAAGCCATGAATCACCCAGGCCATCTTAAACTATTTGTGACAAGGATCATGCAAGACTTTGAAAGTGA

CACGTTTTTTCCAGAAATTGATTTGGAGAAATATAAACTTCTGCCAGAATACCCAGGTGTTCTCTCTGATGTCCAGGAGGAGAAAGGCAT

TAAGTACAAATTTGAAGTATATGAGAAGAATGAT**TAA****GCTT**ATTTAATAATAGATTAAAAATATTATAAAAATAAAAACATAAACACAGA

AATTACAAAAAAAAATACATATGAATTTTTTTTTTGTAATCTTCCTTATAAATATAGAATAATGAATCATATAAAACATATCATTATTCATTTA

TTTACATTTAAAATTATTGTTTCAGTATCTTTAATTTATTATGTATATATAAAAATAACTTACAATTTTATTAATAAACAATATATGTTTATTA

ATTCATGTTTTGTAATTTATGGGATAGCGATTTTTTTTACTGTCTGTATTTTTCTTTTTTAATTATGTTTTAATTGTATTTTATTTTTATTATTG

TTCTTTTTATAGTATTATTTTAAAACAAAATGTATTTTCTAAGAACTTATAATAATAATAAATATAAATTTTAATAAAAATTATATTTATCTT

TTACAATATGAACATAAAGTACAACATTAATATATAGCTTTTAATATTTTTATTCCTAATCATGTAAATCTTAAATTTTTCTTTTTAAACATA

TGTTAAATATTTATTTCTCATTATATATAAGAACATATTTATTAAATCTAGAATTCTATAGTGAGTCGTATTACAATTCACTGGCCGTCGTT

TTACAACGTCGTGACTGGGAAAACCCTGGCGTTACCCAACTTAATCGCCTTGCAGCACATCCCCCTTTCGCCAGCTGGCGTAATAGCGAA

GAGGCCCGCACCGATCGCCCTTCCCAACAGTTGCGCAGCCTGAATGGCGAATGGCGCCTGATGCGGTATTTTCTCCTTACGCATCTGTGC

GGTATTTCACACCGCATATGGTGCACTCTCAGTACAATCTGCTCTGATGCCGCATAGTTAAGCCAGCCCCGACACCCGCCAACACCCGCT
GACGCGCCCTGACGGGCTTGTCTGCTCCCGGCATCCGCTTACAGACAAGCTGTGACCGTCTCCGGGAGCTGCATGTGTCAGAGGTTTTC
ACCGTCATCACCGAAACGCGCGAGACGAAAGGGCCTCGTGATACGCCTATTTTTATAGGTTAATGTCATGATAATAATGGTTTCTTAGAC
GTCAGGTGGCACTTTTCGGGGAAATGTGCGCGGAACCCCTATTTGTTTATTTTTCTAAATACATTCAAATATGTATCCGCTCATGAGACAA
TAACCCTGATAAATGCTTCAATAATATTGAAAAAGGAAGAGTATGAGTATTCAACATTTCCGTGTCGCCCTTATTCCCTTTTTTGCGGCAT
TTTGCCTTCCTGTTTTTGCTCACCCAGAAACGCTGGTGAAAGTAAAAGATGCTGAAGATCAGTTGGGTGCACGAGTGGGTTACATCGAA
CTGGATCTCAACAGCGGTAAGATCCTTGAGAGTTTTCGCCCCGAAGAACGTTTTCCAATGATGAGCACTTTTAAAGTTCTGCTATGTGGC
GCGGTATTATCCCGTATTGACGCCGGGCAAGAGCAACTCGGTCGCCGCATACACTATTCTCAGAATGACTTGGTTGAGTACTCACCAGTC
ACAGAAAAGCATCTTACGGATGGCATGACAGTAAGAGAATTATGCAGTGCTGCCATAACCATGAGTGATAACACTGCGGCCAACTTACT
TCTGACAACGATCGGAGGACCGAAGGAGCTAACCGCTTTTTTGCACAACATGGGGGATCATGTAACTCGCCTTGATCGTTGGGAACCGG
AGCTGAATGAAGCCATACCAAACGACGAGCGTGACACCACGATGCCTGTAGCAATGCCAACAACGTTGCGCAAACTATTAACTGGCGA
ACTACTTACTCTAGCTTCCCGGCAACAATTAATAGACTGGATGGAGGCGGATAAAGTTGCAGGACCACTTCTGCGCTCGGCCCTTCCGGC
TGGCTGGTTTATTGCTGATAAATCTGGAGCCGGTGAGCGTGGGTCTCGCGGTATCATTGCAGCACTGGGGCCAGATGGTAAGCCCTCCC
GTATCGTAGTTATCTACACGACGGGGAGTCAGGCAACTATGGATGAACGAAATAGACAGATCGCTGAGATAGGTGCCTCACTGATTAA
GCATTGGTAACTGTCAGACCAAGTTTACTCATATATACTTTAGATTGATTTAAAACTTCATTTTTAATTTAAAAGGATCTAGGTGAAGATC
CTTTTTGATAATCTCATGACCAAAATCCCTTAACGTGAGTTTTCGTTCCACTGAGCGTCAGACCCCGTAGAAAAGATCAAAGGATCTTCTT
GAGATCCTTTTTTTCTGCGCGTAATCTGCTGCTTGCAAACAAAAAAACCACCGCTACCAGCGGTGGTTTGTTTGCCGGATCAAGAGCTAC
CAACTCTTTTTCCGAAGGTAACTGGCTTCAGCAGAGCGCAGATACCAAATACTGTCCTTCTAGTGTAGCCGTAGTTAGGCCACCACTTCA
AGAACTCTGTAGCACCGCCTACATACCTCGCTCTGCTAATCCTGTTACCAGTGGCTGCTGCCAGTGGCGATAAGTCGTGTCTTACCGGGT
TGGACTCAAGACGATAGTTACCGGATAAGGCGCAGCGGTCGGGCTGAACGGGGGGTTCGTGCACACAGCCCAGCTTGGAGCGAACGA
CCTACACCGAACTGAGATACCTACAGCGTGAGCTATGAGAAAGCGCCACGCTTCCCGAAGGGAGAAAGGCGGACAGGTATCCGGTAAG
CGGCAGGGTCGGAACAGGAGAGCGCACGAGGGAGCTTCCAGGGGGAAACGCCTGGTATCTTTATAGTCCTGTCGGGTTTCGCCACCTC
TGACTTGAGCGTCGATTTTTGTGATGCTCGTCAGGGGGGCGGAGCCTATCGAAAAACGCCAGCAACGCGGCCTTTTTACGGTTCCTGGC
CTTTTGCTGGCCTTTTGCTCACATGTTCTTTCCTGCGTTATCCCCTGATTCTGTGGATAACCGTATTACCGCCTTTGAGTGAGCTGATACCG
CTCGCCGCAGCCGAACGACCGAGCGCAGCGAGTCAGTGAGCGAGGAAGCGGAAGAGCGCCCAATACGCAAACCGCCTCTCCCCGCGC
GTTGGCCGATTCATTAATGCAGCTGGCACGACAGGTTTCCCGACTGGAAAGCGGGCAGTGAGCGCAACGCAATTAATGTGAGTTAGCT
CACTCATTAGGCACCCCAGGCTTTACACTTTATGCTTCCGGCTCGTATGTTGTGTGGAATTGTGAGCGGATAACAATTTCACACAGGAAA
CAGCTATGACCATGATTACGCCAAGCTATTTAGGTGACACTATAGAATACTC**GCGGCCGCTAA*AAAGAATAGCATCTTATCCTG***ATATTT
TTAAAGACTTTACTTTTGAATCCCCATTGTGGTTAGATAGTCTATCCTTACCAGACCCATATTACATTCTTCCTATCTTATCATCACTCTTGT
TATTATCAAATAATGAATTAACATTATTAATAGATAAAAAAATCAATGAAAATAATAAACAATCAAATTTAAATAACCAAGAAGAAACAG
AGTTTCAAAAAAATATGAAAAAAATTACAAAACTTGCTATGCGCTTATTCTATTTATCCTCTGTACTTTTCTTTAAATCCATGCCATCTGGA
CTTTTTATATATTTTATTACAAATACATTTTTTCAATTATTCATAACACAAATATGTAAAATTAAAATTATAGAAAATTTCCTTGACCTACCA
CCCTTACATTCGAAGGGATTTATAACGAGTACTAACACATCACAACAGCAAACAACTTCACAAAAAAAAAATAATACACAT***GAATGATTTA***
ATCAAAAGGAAAAAA**ACGCGT**GGATCCT***ATCCTTATGATGTTC****CAGATTATG*CAGGTTATCCTTATGATGTACCAGATTATGCTGGTTAT
C***CTTATGATGTTCCTGATTATGCA*****GTCGAC**GGAGAAGGAAGAGGAAGTTTATTAACATGTGGAGATGTAGAAGAAAATCCAGGACCAA
TGATTGAACAAGATGGATTGCACGCAGGTTCTCCGGCCGCTTGGGTGGAGAGGCTATTCGGCTATGACTGGGCACAACAGACAATCGG
CTGCTCTGATGCCGCCGTGTTCCGGCTGTCAGCGCAGGGGCGCCCGGTTCTTTTTGTCAAGACCGACCTGTCCGGTGCCCTGAATGAACT
GCAGGACGAGGCAGCGCGGCTATCGTGGCTGGCCACGACGGGCGTTCCTTGCGCAGCTGTGCTCGACGTTGTCACTGAAGCGGGAAG
GGACTGGCTGCTATTGGGCGAAGTGCCGGGGCAGGATCTCCTGTCATCTCACCTTGCTCCTGCCGAGAAAGTATCCATCATGGCTGATG
CAATGCGGCGGCTGCATACGCTTGATCCGGCTACCTGCCCATTCGACCACCAAGCGAAACATCGCATCGAGCGAGCACGTACTCGGATG
GAAGCCGGTCTTGTCGATCAGGATGATCTGGACGAAGAGCATCAGGGGCTCGCGCCAGCCGAACTGTTCGCCAGGCTCAAGGCGCGCA
TGCCCGACGGCGAGGATCTCGTCGTGACCCATGGCGATGCCTGCTTGCCGAATATCATGGTGGAAAATGGCCGCTTTTCTGGATTCATC

GACTGTGGCCGGCTGGGTGTGGCGGACCGCTATCAGGACATAGCGTTGGCTACCCGTGATATTGCTGAAGAGCTTGGCGGCGAATGGG
CTGACCGCTTCCTCGTGCTTTACGGTATCGCCGCTCCCGATTCGCAGCGCATCGCCTTCTATCGCCTTCTTGACGAGTTCTTC**TAA**CTCGA
G

Expected without intron

RIASYPDIFKDFTFESPLWLDSLSLPDPYYILPILSSLLLLSNNELTLLIDKKINENNKQSNLNNQEETEFQKNMKKITKLAMRLFYLSSVLFFKSMPS
GLFIYFITNTFFQLFITQICKIKIIENFLDLPPLHSKGFITSTNTSQQQTTSQKKIIHMNDLIKRKKTRGSYPYDVPDYAGYPYDVPDYAGYPYDVPDY
AVDGEGRGSLLTCGDVEENPGPMIEQDGLHAGSPAAWVERLFGYDWAQQTIGCSDAAVFRLSAQGRPVLFVKTDLSGALNELQDEAARLS
WLATTGVPCAAVLDVVTEAGRDWLLLGEVPGQDLLSSHLAPAEKVSIMADAMRRLHTLDPATCPFDHQAKHRIERARTRMEAGLVDQDDL
DEEHQGLAPAELFARLKARMPDGEDLVVTHGDACLPNIMVENGRFSGFIDCGRLGVADRYQDIALATRDIAEELGGEWADRFLVLYGIAAPD
SQRIAFYRLLDEFF

hDHFR
PFOXA1
3xHA tag
Neo-R
Skip peptide (skip between G and P, GGA-

S7 pSLI- *PFTIM8*-3xHA

GGATATGGCAGCTTAATGTTCGTTTTTCTTATTTATATATTTATACCAATTGATTGTATTTATAACTGTAAAAATGTGTATGTTGTGTGCAT
ATTTTTTTTTGTGCATGCACATGCATGTAAATAGCTAAAATTATGAACATTTTATTTTTTGTTCAGAAAAAAAAAACTTTACACACATAAAA
TGGCTAGTATGAATAGCCATATTTTATATAAATTAAATCCTATGAATTTATGACCATATTAAAAATTTAGATATTTATGGAACATAATATG
TTTGAAACAATAAGACAAAATTATTATTATTATTATTTTTACTGTTATAATTATGTGTCTCCTTCAATGATTCATAAATAGTTGGACTTG
ATTTTTAAAATGTTTATAATATGATTAGCATAGTTAAATAAAAAAAGTTGAAAAATTAAAAAAAAACATATAAACACAAATGATGGTTTTT
CCTTCAATTTCGATATCAATTTATAGAAACAAAATATATACTTGTATAATTTTATTTTTTTATATAAATCATTACATATATAATTATACAATA
TTTTTTCTAAGAGATAATTATATATTAATATATATAAAAAAAGGTGTTTTTTTTTTTTTTTTTTATTTTTATTTTTATTTTATGGTAATATTTTA
TTTTCCTTATTTTATAAATTATATTAGTTTATATGTGATTAATTTTATATATTATCAATTTATATATTTTTAAATGCTTACTTAATTATCTTTTT
TTTTTTTTTTTTTTTTTTTTCCCCTCTTTTTATATTAATTTATTTTTGAAAAAATTGATATATATATATATATATAATATATATATATACATGTA
GTAGTATTAAACAATGTATAATATATATAAATAATATATTTATATATTTCATTTCAATTTTAATTTTTTTTGGTTTTTTTTTTTTTTCTTTTTGT
CATATTTAAAAAAAATTATATTCATATAAGTTATGCATTTTTTATAAACATTATTCAATATATGTATAATATAATATATATATATATATTAAT
GTATTATTCCAATGTGCATGATAAAAGAAAAAAATAATATTTATAAAAAAAAAGAAAAATAAAACAAAAAAAGAAAAAAAAAAAAAAA
AAAAAAAAAATACAAAAATAAATAATATAATTTATAATTATATATTCTTGTCACAATAAAAATATATATATATATATATATTTATAATAT
GTATATTTTAAACTAGAAAAGGAATAACTAATATTTTATTTATTATCATTCAAGATTTATATTTTATAATAATAAATACCTAATAGAAATAT
ATCAGGATCCATGCATGGTTCGCTAAACTGCATCGTCGCTGTGTCCCAGAACATGGGCATCGGCAAGAACGGGGACTACCCCTGGCCAC
CGCTCAGGAACGAATTTAGATATTTCCAGAGAATGACCACAACCTCTTCAGTAGAAGGTAAACAGAATCTGGTGATTATGGGTAAGAAG
ACCTGGTTCTCCATTCCTGAGAAGAATCGACCTTTAAAGGGTAGAATTAATTTAGTTCTCAGCAGAGAACTCAAGGAACCTCCACAAGGA
GCTCATTTTCTTTCCAGAAGTCTAGATGATGCCTTAAAACTTACTGAACAACCAGAATTAGCAAATAAAGTAGACATGGTCTGGATAGTT
GGTGGCAGTTCTGTTTATAAGGAAGCCATGAATCACCCAGGCCATCTTAAACTATTTGTGACAAGGATCATGCAAGACTTTGAAAGTGA

CACGTTTTTTCCAGAAATTGATTTGGAGAAATATAAACTTCTGCCAGAATACCCAGGTGTTCTCTCTGATGTCCAGGAGGAGAAAGGCAT
TAAGTACAAATTTGAAGTATATGAGAAGAATGATTAAGCTTATTTAATAATAGATTAAAAATATTATAAAAATAAAAACATAAACACAGA
AATTACAAAAAAAAATACATATGAATTTTTTTTTTGTAATCTTCCTTATAAATATAGAATAATGAATCATATAAAACATATCATTATTCATTTA
TTTACATTTAAAATTATTGTTTCAGTATCTTTAATTTATTATGTATATATAAAAATAACTTACAATTTTATTAATAAACAATATATGTTTATTA
ATTCATGTTTTGTAATTTATGGGATAGCGATTTTTTTTACTGTCTGTATTTTTCTTTTTTAATTATGTTTTAATTGTATTTTATTTTTATTATTG
TTCTTTTTATAGTATTATTTTAAAACAAAATGTATTTTCTAAGAACTTATAATAATAATAAATATAAATTTTAATAAAAATTATATTTATCTT
TTACAATATGAACATAAAGTACAACATTAATATATAGCTTTTAATATTTTTATTCCTAATCATGTAAATCTTAAATTTTTCTTTTTAAACATA
TGTTAAATATTTATTTCTCATTATATATAAGAACATATTTATTAAATCTAGAATTCTATAGTGAGTCGTATTACAATTCACTGGCCGTCGTT
TTACAACGTCGTGACTGGGAAAACCCTGGCGTTACCCAACTTAATCGCCTTGCAGCACATCCCCCTTTCGCCAGCTGGCGTAATAGCGAA
GAGGCCCGCACCGATCGCCCTTCCCAACAGTTGCGCAGCCTGAATGGCGAATGGCGCCTGATGCGGTATTTTCTCCTTACGCATCTGTGC
GGTATTTCACACCGCATATGGTGCACTCTCAGTACAATCTGCTCTGATGCCGCATAGTTAAGCCAGCCCCGACACCCGCCAACACCCGCT
GACGCGCCCTGACGGGCTTGTCTGCTCCCGGCATCCGCTTACAGACAAGCTGTGACCGTCTCCGGGAGCTGCATGTGTCAGAGGTTTTC
ACCGTCATCACCGAAACGCGCGAGACGAAAGGGCCTCGTGATACGCCTATTTTTATAGGTTAATGTCATGATAATAATGGTTTCTTAGAC
GTCAGGTGGCACTTTTCGGGGAAATGTGCGCGGAACCCCTATTTGTTTATTTTTCTAAATACATTCAAATATGTATCCGCTCATGAGACAA
TAACCCTGATAAATGCTTCAATAATATTGAAAAAGGAAGAGTATGAGTATTCAACATTTCCGTGTCGCCCTTATTCCCTTTTTTGCGGCAT
TTTGCCTTCCTGTTTTTGCTCACCCAGAAACGCTGGTGAAAGTAAAAGATGCTGAAGATCAGTTGGGTGCACGAGTGGGTTACATCGAA
CTGGATCTCAACAGCGGTAAGATCCTTGAGAGTTTTCGCCCCGAAGAACGTTTTCCAATGATGAGCACTTTTAAAGTTCTGCTATGTGGC
GCGGTATTATCCCGTATTGACGCCGGGCAAGAGCAACTCGGTCGCCGCATACACTATTCTCAGAATGACTTGGTTGAGTACTCACCAGTC
ACAGAAAAGCATCTTACGGATGGCATGACAGTAAGAGAATTATGCAGTGCTGCCATAACCATGAGTGATAACACTGCGGCCAACTTACT
TCTGACAACGATCGGAGGACCGAAGGAGCTAACCGCTTTTTTGCACAACATGGGGGATCATGTAACTCGCCTTGATCGTTGGGAACCGG
AGCTGAATGAAGCCATACCAAACGACGAGCGTGACACCACGATGCCTGTAGCAATGCCAACAACGTTGCGCAAACTATTAACTGGCGA
ACTACTTACTCTAGCTTCCCGGCAACAATTAATAGACTGGATGGAGGCGGATAAAGTTGCAGGACCACTTCTGCGCTCGGCCCTTCCGGC
TGGCTGGTTTATTGCTGATAAATCTGGAGCCGGTGAGCGTGGGTCTCGCGGTATCATTGCAGCACTGGGGCCAGATGGTAAGCCCTCCC
GTATCGTAGTTATCTACACGACGGGGAGTCAGGCAACTATGGATGAACGAAATAGACAGATCGCTGAGATAGGTGCCTCACTGATTAA
GCATTGGTAACTGTCAGACCAAGTTTACTCATATATACTTTAGATTGATTTAAAACTTCATTTTTAATTTAAAAGGATCTAGGTGAAGATC
CTTTTTGATAATCTCATGACCAAAATCCCTTAACGTGAGTTTTCGTTCCACTGAGCGTCAGACCCCGTAGAAAAGATCAAAGGATCTTCTT
GAGATCCTTTTTTTCTGCGCGTAATCTGCTGCTTGCAAACAAAAAAACCACCGCTACCAGCGGTGGTTTGTTTGCCGGATCAAGAGCTAC
CAACTCTTTTTCCGAAGGTAACTGGCTTCAGCAGAGCGCAGATACCAAATACTGTCCTTCTAGTGTAGCCGTAGTTAGGCCACCACTTCA
AGAACTCTGTAGCACCGCCTACATACCTCGCTCTGCTAATCCTGTTACCAGTGGCTGCTGCCAGTGGCGATAAGTCGTGTCTTACCGGGT
TGGACTCAAGACGATAGTTACCGGATAAGGCGCAGCGGTCGGGCTGAACGGGGGGTTCGTGCACACAGCCCAGCTTGGAGCGAACGA
CCTACACCGAACTGAGATACCTACAGCGTGAGCTATGAGAAAGCGCCACGCTTCCCGAAGGGAGAAAGGCGGACAGGTATCCGGTAAG
CGGCAGGGTCGGAACAGGAGAGCGCACGAGGGAGCTTCCAGGGGGAAACGCCTGGTATCTTTATAGTCCTGTCGGGTTTCGCCACCTC
TGACTTGAGCGTCGATTTTTGTGATGCTCGTCAGGGGGGCGGAGCCTATCGAAAAACGCCAGCAACGCGGCCTTTTTACGGTTCCTGGC
CTTTTGCTGGCCTTTTGCTCACATGTTCTTTCCTGCGTTATCCCCTGATTCTGTGGATAACCGTATTACCGCCTTTGAGTGAGCTGATACCG
CTCGCCGCAGCCGAACGACCGAGCGCAGCGAGTCAGTGAGCGAGGAAGCGGAAGAGCGCCCAATACGCAAACCGCCTCTCCCCGCGC
GTTGGCCGATTCATTAATGCAGCTGGCACGACAGGTTTCCCGACTGGAAAGCGGGCAGTGAGCGCAACGCAATTAATGTGAGTTAGCT
CACTCATTAGGCACCCCAGGCTTTACACTTTATGCTTCCGGCTCGTATGTTGTGTGGAATTGTGAGCGGATAACAATTTCACACAGGAAA
CAGCTATGACCATGATTACGCCAAGCTATTTAGGTGACACTATAGAATACTCGCGGCCGCTAA*GCTTATAGAGAAATAATAAAAAATAA*
ACACAATACACATTTTATAAAAGAAAAATACAACCCTTGTATGAATATAGAAGAAGCTTTAAATATATTAAACGTCGATAAAACAAAAAT
ATATAAAAATTTAAATAAAGAAGAATTAATGTCTTTAAAAGATGAAATAACAAATAGACACTTGATTTTAAATAAATTAAATGAGAAAAA
*TGGTCCATATAATGGTTCTGCCTATATACAAAAAAAGGCCAGAATTGCAAAGGATATATTGTTTCAGCATTTAAAATTACAA*ACGCGTGG
ATCCT*ATCCTTATGATGTTCCAGATTATG*CAGGTTATCCTTATGATGTACCAGATTATGCTGGTTATC*CTTATGATGTTCCTGATTATGCA*G

TCGACGGAGAAGGAAGAGGAAGTTTATTAACATGTGGAGATGTAGAAGAAAATCCAGGACCAATGATTGAACAAGATGGATTGCACG
CAGGTTCTCCGGCCGCTTGGGTGGAGAGGCTATTCGGCTATGACTGGGCACAACAGACAATCGGCTGCTCTGATGCCGCCGTGTTCCGG
CTGTCAGCGCAGGGGCGCCCGGTTCTTTTTGTCAAGACCGACCTGTCCGGTGCCCTGAATGAACTGCAGGACGAGGCAGCGCGGCTATC
GTGGCTGGCCACGACGGGCGTTCCTTGCGCAGCTGTGCTCGACGTTGTCACTGAAGCGGGAAGGGACTGGCTGCTATTGGGCGAAGTG
CCGGGGCAGGATCTCCTGTCATCTCACCTTGCTCCTGCCGAGAAAGTATCCATCATGGCTGATGCAATGCGGCGGCTGCATACGCTTGAT
CCGGCTACCTGCCCATTCGACCACCAAGCGAAACATCGCATCGAGCGAGCACGTACTCGGATGGAAGCCGGTCTTGTCGATCAGGATGA
TCTGGACGAAGAGCATCAGGGGCTCGCGCCAGCCGAACTGTTCGCCAGGCTCAAGGCGCGCATGCCCGACGGCGAGGATCTCGTCGTG
ACCCATGGCGATGCCTGCTTGCCGAATATCATGGTGGAAAATGGCCGCTTTTCTGGATTCATCGACTGTGGCCGGCTGGGTGTGGCGGA
CCGCTATCAGGACATAGCGTTGGCTACCCGTGATATTGCTGAAGAGCTTGGCGGCGAATGGGCTGACCGCTTCCTCGTGCTTTACGGTA
TCGCCGCTCCCGATTCGCAGCGCATCGCCTTCTATCGCCTTCTTGACGAGTTCTTCTAACTCGAG

ATTATTACTTCTTTTAAAGAAACGTGTAAGATTTCATCCTACTGTTTTGATAAATGTGTTAGCTATCCAGAAAAAAGTTTAAGCAATACAA
ATAAAAAGTGCATATGGAATTGTACACAAAGATATATTGAATGTGAATATTTTATAAAGAATCGTTCAAAAGATAATCAGAGCTTATCTA
ATTTTGAATTGATTAAAAATATGAATAGTTCAGAAAATTTAGCTGAACTGAAGAA***CGATAATAATAAAACAGAAAATTTTG***TTTTAAAA
GATACGCGTGGATCCT***ATCCTTATGATGTTC****CAGATTATG*CAGGTTATCCTTATGATGTACCAGATTATGCTGGTTATC***CTTATGATGTTC***
CTGATTATGCAGTCGACGGAGAAGGAAGAGGAAGTTTATTAACATGTGGAGATGTAGAAGAAAATCCAGGACCA**ATG**ATTGAACAAG
ATGGATTGCACGCAGGTTCTCCGGCCGCTTGGGTGGAGAGGCTATTCGGCTATGACTGGGCACAACAGACAATCGGCTGCTCTGATGCC
GCCGTGTTCCGGCTGTCAGCGCAGGGGCGCCCGGTTCTTTTTGTCAAGACCGACCTGTCCGGTGCCCTGAATGAACTGCAGGACGAGGC
AGCGCGGCTATCGTGGCTGGCCACGACGGGCGTTCCTTGCGCAGCTGTGCTCGACGTTGTCACTGAAGCGGGAAGGGACTGGCTGCTA
TTGGGCGAAGTGCCGGGGCAGGATCTCCTGTCATCTCACCTTGCTCCTGCCGAGAAAGTATCCATCATGGCTGATGCAATGCGGCGGCT
GCATACGCTTGATCCGGCTACCTGCCCATTCGACCACCAAGCGAAACATCGCATCGAGCGAGCACGTACTCGGATGGAAGCCGGTCTTG
TCGATCAGGATGATCTGGACGAAGAGCATCAGGGGCTCGCGCCAGCCGAACTGTTCGCCAGGCTCAAGGCGCGCATGCCCGACGGCG
AGGATCTCGTCGTGACCCATGGCGATGCCTGCTTGCCGAATATCATGGTGGAAAATGGCCGCTTTTCTGGATTCATCGACTGTGGCCGG
CTGGGTGTGGCGGACCGCTATCAGGACATAGCGTTGGCTACCCGTGATATTGCTGAAGAGCTTGGCGGCGAATGGGCTGACCGCTTCC
TCGTGCTTTACGGTATCGCCGCTCCCGATTCGCAGCGCATCGCCTTCTATCGCCTTCTTGACGAGTTCTTC**TAA**

Expected translation product

IITSFKETCKISSYCFDKCVSYPEKSLSNTNKKCIWNCTQRYIECEYFIKNRSKDNQSLSNFELIKNMNSSENLAELKNDNNKTENFVLKDTRGSYP
YDVPDYAGYPYDVPDYAGYPYDVPDYAVDGEGRGSLLTCGDVEENPGPMIEQDGLHAGSPAAWVERLFGYDWAQQTIGCSDAAVFRLSAQ
GRPVLFVKTDLSGALNELQDEAARLSWLATTGVPCAAVLDVVTEAGRDWLLLGEVPGQDLLSSHLAPAEKVSIMADAMRRLHTLDPATCPFD
HQAKHRIERARTRMEAGLVDQDDLDEEHQGLAPAELFARLKARMPDGEDLVVTHGDACLPNIMVENGRFSGFIDCGRLGVADRYQDIALAT
RDIAEELGGEWX

hDHFR

PFTIM8

3xHA tag

Neo-R

Skip peptide (skip between G and P, GGA

S8 pSLI-*TIM13*-3xHA

GGATATGGCAGCTTAATGTTCGTTTTTCTTATTTATATATTTATACCAATTGATTGTATTTATAACTGTAAAAATGTGTATGTTGTGTGCAT
ATTTTTTTTTGTGCATGCACATGCATGTAAATAGCTAAAATTATGAACATTTTATTTTTTGTTCAGAAAAAAAAAACTTTACACACATAAAA
TGGCTAGTATGAATAGCCATATTTTATATAAATTAAATCCTATGAATTTATGACCATATTAAAAATTTAGATATTTATGGAACATAATATG
TTTGAAACAATAAGACAAAATTATTATTATTATTATTTTTACTGTTATAATTATGTGTCTCCTTCAATGATTCATAAATAGTTGGACTTG
ATTTTTAAAATGTTTATAATATGATTAGCATAGTTAAATAAAAAAAGTTGAAAAATTAAAAAAAAACATATAAACACAAATGATGGTTTTT
CCTTCAATTTCGATATCAATTTATAGAAACAAAATATATACTTGTATAATTTTATTTTTTTATATAAATCATTACATATATAATTATACAATA
TTTTTTCTAAGAGATAATTATATATTAATATATATAAAAAAAGGTGTTTTTTTTTTTTTTTTTTATTTTTATTTTTATTTTATGGTAATATTTTA
TTTTCCTTATTTTATAAATTATATTAGTTTATATGTGATTAATTTTATATATTATCAATTTATATATTTTTAAATGCTTACTTAATTATCTTTTT
TTTTTTTTTTTTTTTTTTTTCCCCTCTTTTTATATTAATTTATTTTTGAAAAAATTGATATATATATATATATATAATATATATATATACATGTA
GTAGTATTAAACAATGTATAATATATATAAATAATATATTTATATATTTCATTTCAATTTTAATTTTTTTTGGTTTTTTTTTTTTTTCTTTTTGT
CATATTTAAAAAAAATTATATTCATATAAGTTATGCATTTTTTATAAACATTATTCAATATATGTATAATATAATATATATATATATATTAAT
GTATTATTCCAATGTGCATGATAAAAGAAAAAAATAATATTTATAAAAAAAAAGAAAAATAAAACAAAAAAAGAAAAAAAAAAAAAAA
AAAAAAAAAATACAAAAATAAATAATATAATTTATAATTATATATTCTTGTCACAATAAAAATATATATATATATATATATATTTATAATAT
GTATATTTTAAACTAGAAAAGGAATAACTAATATTTTATTTATTATCATTCAAGATTTATATTTTATAATAATAAATACCTAATAGAAATAT
ATCAGGATCCATGCATGGTTCGCTAAACTGCATCGTCGCTGTGTCCCAGAACATGGGCATCGGCAAGAACGGGGACTACCCCTGGCCAC
CGCTCAGGAACGAATTTAGATATTTCCAGAGAATGACCACAACCTCTTCAGTAGAAGGTAAACAGAATCTGGTGATTATGGGTAAGAAG
ACCTGGTTCTCCATTCCTGAGAAGAATCGACCTTTAAAGGGTAGAATTAATTTAGTTCTCAGCAGAGAACTCAAGGAACCTCCACAAGGA
GCTCATTTTCTTTCCAGAAGTCTAGATGATGCCTTAAAACTTACTGAACAACCAGAATTAGCAAATAAAGTAGACATGGTCTGGATAGTT
GGTGGCAGTTCTGTTTATAAGGAAGCCATGAATCACCCAGGCCATCTTAAACTATTTGTGACAAGGATCATGCAAGACTTTGAAAGTGA
CACGTTTTTTCCAGAAATTGATTTGGAGAAATATAAACTTCTGCCAGAATACCCAGGTGTTCTCTCTGATGTCCAGGAGGAGAAAGGCAT
TAAGTACAAATTTGAAGTATATGAGAAGAATGATTAAGCTTATTTAATAATAGATTAAAAATATTATAAAAATAAAAACATAAACACAGA
AATTACAAAAAAAAATACATATGAATTTTTTTTTTGTAATCTTCCTTATAAATATAGAATAATGAATCATATAAAACATATCATTATTCATTTA
TTTACATTTAAAATTATTGTTTCAGTATCTTTAATTTATTATGTATATATAAAAATAACTTACAATTTTATTAATAAACAATATATGTTTATTA
ATTCATGTTTTGTAATTTATGGGATAGCGATTTTTTTTACTGTCTGTATTTTTCTTTTTTAATTATGTTTTAATTGTATTTTATTTTTATTATTG
TTCTTTTTATAGTATTATTTTAAAACAAAATGTATTTTCTAAGAACTTATAATAATAATAAATATAAATTTTAATAAAAATTATATTTATCTT
TTACAATATGAACATAAAGTACAACATTAATATATAGCTTTTAATATTTTTATTCCTAATCATGTAAATCTTAAATTTTTCTTTTTAAACATA
TGTTAAATATTTATTTCTCATTATATATAAGAACATATTTATTAAATCTAGAATTCTATAGTGAGTCGTATTACAATTCACTGGCCGTCGTT
TTACAACGTCGTGACTGGGAAAACCCTGGCGTTACCCAACTTAATCGCCTTGCAGCACATCCCCCTTTCGCCAGCTGGCGTAATAGCGAA
GAGGCCCGCACCGATCGCCCTTCCCAACAGTTGCGCAGCCTGAATGGCGAATGGCGCCTGATGCGGTATTTTCTCCTTACGCATCTGTGC
GGTATTTCACACCGCATATGGTGCACTCTCAGTACAATCTGCTCTGATGCCGCATAGTTAAGCCAGCCCCGACACCCGCCAACACCCGCT
GACGCGCCCTGACGGGCTTGTCTGCTCCCGGCATCCGCTTACAGACAAGCTGTGACCGTCTCCGGGAGCTGCATGTGTCAGAGGTTTTC
ACCGTCATCACCGAAACGCGCGAGACGAAAGGGCCTCGTGATACGCCTATTTTTATAGGTTAATGTCATGATAATAATGGTTTCTTAGAC
GTCAGGTGGCACTTTTCGGGGAAATGTGCGCGGAACCCCTATTTGTTTATTTTTCTAAATACATTCAAATATGTATCCGCTCATGAGACAA
TAACCCTGATAAATGCTTCAATAATATTGAAAAAGGAAGAGTATGAGTATTCAACATTTCCGTGTCGCCCTTATTCCCTTTTTTGCGGCAT
TTTGCCTTCCTGTTTTTGCTCACCCAGAAACGCTGGTGAAAGTAAAAGATGCTGAAGATCAGTTGGGTGCACGAGTGGGTTACATCGAA
CTGGATCTCAACAGCGGTAAGATCCTTGAGAGTTTTCGCCCCGAAGAACGTTTTCCAATGATGAGCACTTTTAAAGTTCTGCTATGTGGC
GCGGTATTATCCCGTATTGACGCCGGGCAAGAGCAACTCGGTCGCCGCATACACTATTCTCAGAATGACTTGGTTGAGTACTCACCAGTC
ACAGAAAAGCATCTTACGGATGGCATGACAGTAAGAGAATTATGCAGTGCTGCCATAACCATGAGTGATAACACTGCGGCCAACTTACT
TCTGACAACGATCGGAGGACCGAAGGAGCTAACCGCTTTTTTGCACAACATGGGGGATCATGTAACTCGCCTTGATCGTTGGGAACCGG
AGCTGAATGAAGCCATACCAAACGACGAGCGTGACACCACGATGCCTGTAGCAATGCCAACAACGTTGCGCAAACTATTAACTGGCGA
ACTACTTACTCTAGCTTCCCGGCAACAATTAATAGACTGGATGGAGGCGGATAAAGTTGCAGGACCACTTCTGCGCTCGGCCCTTCCGGC
TGGCTGGTTTATTGCTGATAAATCTGGAGCCGGTGAGCGTGGGTCTCGCGGTATCATTGCAGCACTGGGGCCAGATGGTAAGCCCTCCC

GTATCGTAGTTATCTACACGACGGGGAGTCAGGCAACTATGGATGAACGAAATAGACAGATCGCTGAGATAGGTGCCTCACTGATTAA
GCATTGGTAACTGTCAGACCAAGTTTACTCATATATACTTTAGATTGATTTAAAACTTCATTTTTAATTTAAAAGGATCTAGGTGAAGATC
CTTTTTGATAATCTCATGACCAAAATCCCTTAACGTGAGTTTTCGTTCCACTGAGCGTCAGACCCCGTAGAAAAGATCAAAGGATCTTCTT
GAGATCCTTTTTTTCTGCGCGTAATCTGCTGCTTGCAAACAAAAAAACCACCGCTACCAGCGGTGGTTTGTTTGCCGGATCAAGAGCTAC
CAACTCTTTTTCCGAAGGTAACTGGCTTCAGCAGAGCGCAGATACCAAATACTGTCCTTCTAGTGTAGCCGTAGTTAGGCCACCACTTCA
AGAACTCTGTAGCACCGCCTACATACCTCGCTCTGCTAATCCTGTTACCAGTGGCTGCTGCCAGTGGCGATAAGTCGTGTCTTACCGGGT
TGGACTCAAGACGATAGTTACCGGATAAGGCGCAGCGGTCGGGCTGAACGGGGGGTTCGTGCACACAGCCCAGCTTGGAGCGAACGA
CCTACACCGAACTGAGATACCTACAGCGTGAGCTATGAGAAAGCGCCACGCTTCCCGAAGGGAGAAAGGCGGACAGGTATCCGGTAAG
CGGCAGGGTCGGAACAGGAGAGCGCACGAGGGAGCTTCCAGGGGGAAACGCCTGGTATCTTTATAGTCCTGTCGGGTTTCGCCACCTC
TGACTTGAGCGTCGATTTTTGTGATGCTCGTCAGGGGGGCGGAGCCTATCGAAAAACGCCAGCAACGCGGCCTTTTTACGGTTCCTGGC
CTTTTGCTGGCCTTTTGCTCACATGTTCTTTCCTGCGTTATCCCCTGATTCTGTGGATAACCGTATTACCGCCTTTGAGTGAGCTGATACCG
CTCGCCGCAGCCGAACGACCGAGCGCAGCGAGTCAGTGAGCGAGGAAGCGGAAGAGCGCCCAATACGCAAACCGCCTCTCCCCGCGC
GTTGGCCGATTCATTAATGCAGCTGGCACGACAGGTTTCCCGACTGGAAAGCGGGCAGTGAGCGCAACGCAATTAATGTGAGTTAGCT
CACTCATTAGGCACCCCAGGCTTTACACTTTATGCTTCCGGCTCGTATGTTGTGTGGAATTGTGAGCGGATAACAATTTCACACAGGAAA
CAGCTATGACCATGATTACGCCAAGCTATTTAGGTGACACTATAGAATACTCGCGGCCGCTAA*GCTTATAGAGAAATAATAAAAAATAA*
ACACAATACACATTTTATAAAAGAAAAATACAACCCTTGTATGAATATAGAAGAAGCTTTAAATATATTAAACGTCGATAAAACAAAAAT
ATATAAAAAATTTAAATAAAGAAGAATTAATGTCTTTAAAAGATGAAATAACAAATAGACACTTGATTTTAAATAAATTAAATGAGAAAAA
*TGGTCCATATAATGGTTCTGCCTATATACAAAAAAAGGCCAGAATTGCAAAGGATATATTGTTTCAGCATTTAAAATTACAA*ACGCGTGG
ATCCT*ATCCTTATGATGTTCCAGATTATG*CAGGTTATCCTTATGATGTACCAGATTATGCTGGTTATC*CTTATGATGTTCCTGATTATGCA*G
TCGACGGAGAAGGAAGAGGAAGTTTATTAACATGTGGAGATGTAGAAGAAAATCCAGGACCAATGATTGAACAAGATGGATTGCACG
CAGGTTCTCCGGCCGCTTGGGTGGAGAGGCTATTCGGCTATGACTGGGCACAACAGACAATCGGCTGCTCTGATGCCGCCGTGTTCCGG
CTGTCAGCGCAGGGGCGCCCGGTTCTTTTTGTCAAGACCGACCTGTCCGGTGCCCTGAATGAACTGCAGGACGAGGCAGCGCGGCTATC
GTGGCTGGCCACGACGGGCGTTCCTTGCGCAGCTGTGCTCGACGTTGTCACTGAAGCGGGAAGGGACTGGCTGCTATTGGGCGAAGTG
CCGGGGCAGGATCTCCTGTCATCTCACCTTGCTCCTGCCGAGAAAGTATCCATCATGGCTGATGCAATGCGGCGGCTGCATACGCTTGAT
CCGGCTACCTGCCCATTCGACCACCAAGCGAAACATCGCATCGAGCGAGCACGTACTCGGATGGAAGCCGGTCTTGTCGATCAGGATGA
TCTGGACGAAGAGCATCAGGGGCTCGCGCCAGCCGAACTGTTCGCCAGGCTCAAGGCGCGCATGCCCGACGGCGAGGATCTCGTCGTG
ACCCATGGCGATGCCTGCTTGCCGAATATCATGGTGGAAAATGGCCGCTTTTCTGGATTCATCGACTGTGGCCGGCTGGGTGTGGCGGA
CCGCTATCAGGACATAGCGTTGGCTACCCGTGATATTGCTGAAGAGCTTGGCGGCGAATGGGCTGACCGCTTCCTCGTGCTTTACGGTA
TCGCCGCTCCCGATTCGCAGCGCATCGCCTTCTATCGCCTTCTTGACGAGTTCTTCTAACTCGAG

Expected without intron

TGTGTTTCAAAAATTGGACCAAAATTAAGTTCAAGTGAACAAAAATGTATATGGGATTGTGCAAATAGCTATTTTTATACTAACGTTTTCT
TAAATCAGCGCTTGGAACAGATGACAAAGATTTTAAAATCAAATAGTGACTACACAAACTTAACGCGTGGATCCTATCCTTATGATGTTC
CAGATTATGCAGGTTATCCTTATGATGTACCAGATTATGCTGGTTATCCTTATGATGTTCCTGATTATGCAGTCGACGGAGAAGGAAGAG
GAAGTTTATTAACATGTGGAGATGTAGAAGAAAATCCAGGACCAATGATTGAACAAGATGGATTGCACGCAGGTTCTCCGGCCGCTTG
GGTGGAGAGGCTATTCGGCTATGACTGGGCACAACAGACAATCGGCTGCTCTGATGCCGCCGTGTTCCGGCTGTCAGCGCAGGGGCGC
CCGGTTCTTTTTGTCAAGACCGACCTGTCCGGTGCCCTGAATGAACTGCAGGACGAGGCAGCGCGGCTATCGTGGCTGGCCACGACGG
GCGTTCCTTGCGCAGCTGTGCTCGACGTTGTCACTGAAGCGGGAAGGGACTGGCTGCTATTGGGCGAAGTGCCGGGGCAGGATCTCCT
GTCATCTCACCTTGCTCCTGCCGAGAAAGTATCCATCATGGCTGATGCAATGCGGCGGCTGCATACGCTTGATCCGGCTACCTGCCCATT
CGACCACCAAGCGAAACATCGCATCGAGCGAGCACGTACTCGGATGGAAGCCGGTCTTGTCGATCAGGATGATCTGGACGAAGAGCAT
CAGGGGCTCGCGCCAGCCGAACTGTTCGCCAGGCTCAAGGCGCGCATGCCCGACGGCGAGGATCTCGTCGTGACCCATGGCGATGCCT

GCTTGCCGAATATCATGGTGGAAAATGGCCGCTTTTCTGGATTCATCGACTGTGGCCGGCTGGGTGTGGCGGACCGCTATCAGGACATA
GCGTTGGCTACCCGTGATATTGCTGAAGAGCTTGGCGGCGAATGGGCTGACCGCTTCCTCGTGCTTTACGGTATCGCCGCTCCCGATTC
GCAGCGCATCGCCTTCTATCGCCTTCTTGACGAGTTCTTCTAA

Expected translation product

CVSKIGPKLSSSEQKCIWDCANSYFYTNVFLNQRLEQMTKILKSNSDYTNLTRGSYPYDVPDYAGYPYDVPDYAGYPYDVPDYAVDGEGRGSLL
TCGDVEENPGPMIEQDGLHAGSPAAWVERLFGYDWAQQTIGCSDAAVFRLSAQGRPVLFVKTDLSGALNELQDEAARLSWLATTGVPCAA
VLDVVTEAGRDWLLLGEVPGQDLLSSHLAPAEKVSIMADAMRRLHTLDPATCPFDHQAKHRIERARTRMEAGLVDQDDLDEEHQGLAPAEL
FARLKARMPDGEDLVVTHGDACLPNIMVENGRFSGFIDCGRLGVADRYQDIALATRDIAEELGGEWADRFLVLYGIAAPDSQRIAFYRLLDEFF
X

hDHFR

PFTIM13

3xHA tag

Neo-R

Skip peptide (skip between G and P, GGA

6 References

Abe, Y., Shodai, T., Muto, T., Mihara, K., Torii, H., Nishikawa, S. ichi, Endo, T., & Kohda, D. (2000). Structural basis of presequence recognition by the mitochondrial protein import receptor Tom20. *Cell*, *100*(5), 551–560. https://doi.org/10.1016/S0092-8674(00)80691-1

Aikawa, M., Huff, C. G., & Sprinz, H. (1967). Fine structure of the asexual stages of Plasmodium elongatum. *The Journal of Cell Biology*, *34*(1), 229–249. https://doi.org/10.1083/JCB.34.1.229

Alcock, F., Webb, C. T., Dolezal, P., Hewitt, V., Shingu-Vasquez, M., Likić, V. A., Traven, A., & Lithgow, T. (2012). A small Tim homohexamer in the relict mitochondrion of Cryptosporidium. *Molecular Biology and Evolution*, *29*(1), 113–122. https://doi.org/10.1093/MOLBEV/MSR165

Alternative and Novel Drug Based Prevention Approaches | Malaria | CDC. (n.d.). Retrieved June 16, 2025, from https://www.cdc.gov/malaria/php/public-health-strategy/alternative-drug-prevention.html?CDC_AAref_Val=https://www.cdc.gov/malaria/diagnosis_treatment/clinicians1.html

Amino, R., Thiberge, S., Martin, B., Celli, S., Shorte, S., Frischknecht, F., & Ménard, R. (2006). Quantitative imaging of Plasmodium transmission from mosquito to mammal. *Nature Medicine*, *12*(2), 220–224. https://doi.org/10.1038/nm1350

Araiso, Y., & Endo, T. (2022). Structural overview of the translocase of the mitochondrial outer membrane complex. In *Biophysics and physicobiology* (Vol. 19). Biophysical Society of Japan. https://doi.org/10.2142/biophysico.bppb-v19.0022

Ashley, E. A., Pyae Phyo, A., & Woodrow, C. J. (2018). Malaria. In *The Lancet* (Vol. 391, Issue 10130, pp. 1608–1621). Lancet Publishing Group. https://doi.org/10.1016/S0140-6736(18)30324-6

Autino, B., Noris, A., Russo, R., & Castelli, F. (2012). Epidemiology of malaria in endemic areas. In *Mediterranean Journal of Hematology and Infectious Diseases* (Vol. 4, Issue 1). https://doi.org/10.4084/MJHID.2012.060

Bartoloni, A., & Zammarchi, L. (2012). Clinical aspects of uncomplicated and severe malaria. In *Mediterranean Journal of Hematology and Infectious Diseases* (Vol. 4, Issue 1). https://doi.org/10.4084/MJHID.2012.026

Bauer, M., Behrens, M., Esser, K., Michaelis, G., & Pratje, E. (1994). PET1402, a nuclear gene required for proteolytic processing of cytochrome oxidase subunit 2 in yeast. *MGG Molecular & General Genetics*, *245*(3), 272–278. https://doi.org/10.1007/BF00290106/METRICS

Becker, T., Pfannschmidt, S., Guiard, B., Stojanovski, D., Milenkovic, D., Kutik, S., Pfanner, N., Meisinger, C., & Wiedemann, N. (2008). Biogenesis of the mitochondrial TOM complex: Mim1 promotes insertion and assembly of signal-anchored receptors. *Journal of Biological Chemistry*, *283*(1), 120–127. https://doi.org/10.1074/JBC.M706997200;

Bender, A., Van Dooren, G. G., Ralph, S. A., McFadden, G. I., & Schneider, G. (2003). Properties and prediction of mitochondrial transit peptides from Plasmodium falciparum. *Molecular and Biochemical Parasitology*, *132*(2), 59–66. https://doi.org/10.1016/J.MOLBIOPARA.2003.07.001

Benz, M., Soll, J., & Ankele, E. (2013). Arabidopsis thaliana Oxa proteins locate to mitochondria and fulfill essential roles during embryo development. *Planta*, *237*(2), 573–588. https://doi.org/10.1007/S00425-012-1793-9/FIGURES/6

Bhatt, S., Weiss, D. J., Cameron, E., Bisanzio, D., Mappin, B., Dalrymple, U., Battle, K. E., Moyes, C. L., Henry, A., Eckhoff, P. A., Wenger, E. A., Briët, O., Penny, M. A., Smith, T. A., Bennett, A., Yukich, J., Eisele, T. P., Griffin, J. T., Fergus, C. A., … Gething, P. W. (2015). The effect of malaria control on Plasmodium falciparum in Africa between 2000 and 2015. *Nature*, *526*(7572), 207–211. https://doi.org/10.1038/NATURE15535

Bimboim, H. C., & Doly, J. (1979). A rapid alkaline extraction procedure for screening recombinant plasmid DNA. *Nucleic Acids Research*, *7*(6), 1513–1523. https://doi.org/10.1093/NAR/7.6.1513,

Birnbaum, J., Flemming, S., Reichard, N., Soares, A. B., Mesén-Ramírez, P., Jonscher, E., Bergmann, B., & Spielmann, T. (2017). A genetic system to study Plasmodium falciparum protein function. *Nature Methods*, *14*(4), 450–456. https://doi.org/10.1038/nmeth.4223

Blamowska, M., Neupert, W., & Hell, K. (2012). Biogenesis of the mitochondrial Hsp70 chaperone. *Journal of Cell Biology*, *199*(1), 125–135. https://doi.org/10.1083/JCB.201205012

Bonnefoy, N., Chalvet, F., Hamel, P., Slonimski, P. P., & Dujardin, G. (1994). OXA1, a Saccharomyces cerevisiae nuclear gene whose sequence is conserved from prokaryotes to eukaryotes controls cytochrome oxidase biogenesis. *Journal of Molecular Biology*, *239*(2), 201–212. https://doi.org/10.1006/jmbi.1994.1363

Bykov, Y. S., Flohr, T., Boos, F., Zung, N., Herrmann, J. M., & Schuldiner, M. (2022). Widespread use of unconventional targeting signals in mitochondrial ribosome proteins. *The EMBO Journal*, *41*(1). https://doi.org/10.15252/EMBJ.2021109519,

Chacinska, A., Koehler, C. M., Milenkovic, D., Lithgow, T., & Pfanner, N. (2009). Importing Mitochondrial Proteins: Machineries and Mechanisms. *Cell*, *138*(4), 628–644. https://doi.org/10.1016/J.CELL.2009.08.005;

Chacinska, A., Lind, M., Frazier, A. E., Dudek, J., Meisinger, C., Geissler, A., Sickmann, A., Meyer, H. E., Truscott, K. N., Guiard, B., Pfanner, N., & Rehling, P. (2005). Mitochondrial

presequence translocase: Switching between TOM tethering and motor recruitment involves Tim21 and Tim17. *Cell*, *120*(6), 817–829. https://doi.org/10.1016/J.CELL.2005.01.011

Chacinska, A., Pfannschmidt, S., Wiedemann, N., Kozjak, V., Sanjuán Szklarz, L. K., Schulze-Specking, A., Truscott, K. N., Guiard, B., Meisinger, C., & Pfanner, N. (2004). Essential role of Mia40 in import and assembly of mitochondrial intermembrane space proteins. *EMBO Journal*, *23*(19), 3735–3746. https://doi.org/10.1038/SJ.EMBOJ.7600389;

Chatzi, A., Manganas, P., & Tokatlidis, K. (2016). Oxidative folding in the mitochondrial intermembrane space: A regulated process important for cell physiology and disease. *Biochimica et Biophysica Acta - Molecular Cell Research*, *1863*(6), 1298–1306. https://doi.org/10.1016/j.bbamcr.2016.03.023

Chen, I., Clarke, S. E., Gosling, R., Hamainza, B., Killeen, G., Magill, A., O'Meara, W., Price, R. N., & Riley, E. M. (2016). "Asymptomatic" Malaria: A Chronic and Debilitating Infection That Should Be Treated. *PLoS Medicine*, *13*(1). https://doi.org/10.1371/journal.pmed.1001942

Conroy, A. L., Hawkes, M., Elphinstone, R. E., Morgan, C., Hermann, L., Barker, K. R., Namasopo, S., Opoka, R. O., John, C. C., Liles, W. C., & Kain, K. C. (2016). Acute kidney injury is common in pediatric severe malaria and is associated with increased mortality. *Open Forum Infectious Diseases*, *3*(2). https://doi.org/10.1093/ofid/ofw046

Cooper, D. J., Rajahram, G. S., William, T., Jelip, J., Mohammad, R., Benedict, J., Alaza, D. A., Malacova, E., Yeo, T. W., Grigg, M. J., Anstey, N. M., & Barber, B. E. (2020). Plasmodium knowlesi Malaria in Sabah, Malaysia, 2015-2017: Ongoing increase in incidence despite nearelimination of the human-only plasmodium species. *Clinical Infectious Diseases*, *70*(3), 361–367. https://doi.org/10.1093/cid/ciz237

Cowman, A. F., Healer, J., Marapana, D., & Marsh, K. (2016). Malaria: Biology and Disease. In *Cell* (Vol. 167, Issue 3, pp. 610–624). Cell Press. https://doi.org/10.1016/j.cell.2016.07.055

Crawford, E. D., Quan, J., Horst, J. A., Ebert, D., Wu, W., & DeRisi, J. L. (2017). Plasmid-free CRISPR/Cas9 genome editing in Plasmodium falciparum confirms mutations conferring resistance to the dihydroisoquinolone clinical candidate SJ733. *PLoS ONE*, *12*(5). https://doi.org/10.1371/JOURNAL.PONE.0178163

Crompton, P. D., Moebius, J., Portugal, S., Waisberg, M., Hart, G., Garver, L. S., Miller, L. H., Barillas, C., & Pierce, S. K. (2014). Malaria immunity in man and mosquito: Insights into unsolved mysteries of a deadly infectious disease. In *Annual Review of Immunology* (Vol. 32, pp. 157–187). Annual Reviews Inc. https://doi.org/10.1146/annurev-immunol-032713-120220

Curran, S. P., Leuenberger, D., Schmidt, E., & Koehler, C. M. (2002). The role of the Tim8p-Tim13p complex in a conserved import pathway for mitochondrial polytopic inner

membrane proteins. *Journal of Cell Biology*, *158*(6), 1017–1027. https://doi.org/10.1083/JCB.200205124

Daily, J. P., Minuti, A., & Khan, N. (2022). Diagnosis, Treatment, and Prevention of Malaria in the US: A Review. *JAMA*, *328*(5), 460–471. https://doi.org/10.1001/JAMA.2022.12366

Datoo, M. S., Dicko, A., Tinto, H., Ouédraogo, J. B., Hamaluba, M., Olotu, A., Beaumont, E., Ramos Lopez, F., Natama, H. M., Weston, S., Chemba, M., Compaore, Y. D., Issiaka, D., Salou, D., Some, A. M., Omenda, S., Lawrie, A., Bejon, P., Rao, H., … Valea, I. (2024). Safety and efficacy of malaria vaccine candidate R21/Matrix-M in African children: a multicentre, double-blind, randomised, phase 3 trial. *The Lancet*, *403*(10426), 533–544. https://doi.org/10.1016/S0140-6736(23)02511-4

Datoo, M. S., Natama, H. M., Somé, A., Bellamy, D., Traoré, O., Rouamba, T., Tahita, M. C., Ido, N. F. A., Yameogo, P., Valia, D., Millogo, A., Ouedraogo, F., Soma, R., Sawadogo, S., Sorgho, F., Derra, K., Rouamba, E., Ramos-Lopez, F., Cairns, M., … Tinto, H. (2022). Efficacy and immunogenicity of R21/Matrix-M vaccine against clinical malaria after 2 years' follow-up in children in Burkina Faso: a phase 1/2b randomised controlled trial. *The Lancet Infectious Diseases*, *22*(12), 1728–1736. https://doi.org/10.1016/S1473-3099(22)00442-X

Dayananda, K. K., Achur, R. N., & Gowda, D. C. (2018). Epidemiology, drug resistance, and pathophysiology of *Plasmodium vivax malaria*. In *Journal of Vector Borne Diseases* (Vol. 55, Issue 1, pp. 1–8). Wolters Kluwer Medknow Publications. https://doi.org/10.4103/0972-9062.234620

Deponte, M. (2013). Mitochondrial Protein Import in Malaria Parasites. *Encyclopedia of Malaria*, 1–13. https://doi.org/10.1007/978-1-4614-8757-9_95-1

Deponte, M., & Hell, K. (2009). Disulfide bond formation in the intermembrane space of mitochondria. *Journal of Biochemistry*, *146*(5), 599–608. https://doi.org/10.1093/JB/MVP133

Deponte, M., Hoppe, H. C., Lee, M. C. S., Maier, A. G., Richard, D., Rug, M., Spielmann, T., & Przyborski, J. M. (2012). Wherever i may roam: Protein and membrane trafficking in P. falciparum-infected red blood cells. *Molecular and Biochemical Parasitology*, *186*(2), 95–116. https://doi.org/10.1016/J.MOLBIOPARA.2012.09.007

Di Cristina, M., & Carruthers, V. B. (2018). New and emerging uses of CRISPR/Cas9 to genetically manipulate apicomplexan parasites. *Parasitology*, *145*(9), 1119. https://doi.org/10.1017/S003118201800001X

Dolezal, P., Likic, V., Tachezy, J., & Lithgow, T. (2006). Evolution of the molecular machines for protein import into mitochondria. *Science*, *313*(5785), 314–318. https://doi.org/10.1126/SCIENCE.1127895;

D'Silva, P., Liu, Q., Walter, W., & Craig, E. A. (2004). Regulated interactions of mtHsp70 with Tim44 at the translocon in the mitochondrial inner membrane. *Nature Structural and Molecular Biology*, *11*(11), 1084–1091. https://doi.org/10.1038/NSMB846,

D'Silva, P. R., Schilke, B., Hayashi, M., & Craig, E. A. (2008). Interaction of the J-protein heterodimer Pam18/Pam16 of the mitochondrial import motor with the translocon of the inner membrane. *Molecular Biology of the Cell*, *19*(1), 424–432. https://doi.org/10.1091/MBC.E07-08-0748

Dudek, J., Rehling, P., & van der Laan, M. (2013a). Mitochondrial protein import: Common principles and physiological networks. *Biochimica et Biophysica Acta - Molecular Cell Research*, *1833*(2), 274–285. https://doi.org/10.1016/J.BBAMCR.2012.05.028

Dukanovic, J., & Rapaport, D. (2011). Multiple pathways in the integration of proteins into the mitochondrial outer membrane. *Biochimica et Biophysica Acta - Biomembranes*, *1808*(3), 971–980. https://doi.org/10.1016/J.BBAMEM.2010.06.021

Duraisingh, M. T., Triglia, T., & Cowman, A. F. (2002). Negative selection of Plasmodium falciparum reveals targeted gene deletion by double crossover recombination. *International Journal for Parasitology*, *32*(1), 81–89. https://doi.org/10.1016/S0020-7519(01)00345-9

Eckers, E., Cyrklaff, M., Simpson, L., & Deponte, M. (2012). Mitochondrial protein import pathways are functionally conserved among eukaryotes despite compositional diversity of the import machineries. *Biological Chemistry*, *393*(6), 513–524. https://doi.org/10.1515/HSZ-2011-0255

Emtage, J. L. T., & Jensen, R. E. (1993). MAS6 encodes an essential inner membrane component of the yeast mitochondrial protein import pathway. *Journal of Cell Biology*, *122*(5), 1003–1012. https://doi.org/10.1083/JCB.122.5.1003,

Endo, T., & Yamano, K. (2009). Multiple pathways for mitochondrial protein traffic. *Biological Chemistry*, *390*(8), 723–730. https://doi.org/10.1515/BC.2009.087

Fairhurst, R. M., & Wellems, T. E. (n.d.). *Modulation of malaria virulence by determinants of Plasmodium falciparum erythrocyte membrane protein-1 display*.

Fidock, D. A., & Wellems, T. E. (1997). Transformation with human dihydrofolate reductase renders malaria parasites insensitive to WR99210 but does not affect the intrinsic activity of proguanil. *Proceedings of the National Academy of Sciences of the United States of America*, *94*(20), 10931–10936. https://doi.org/10.1073/PNAS.94.20.10931

Fischer, M., & Riemer, J. (2013). The mitochondrial disulfide relay system: Roles in oxidative protein folding and beyond. *International Journal of Cell Biology*, *2013*. https://doi.org/10.1155/2013/742923,

Fowkes, F. J. I., Boeuf, P., & Beeson, J. G. (2016). Immunity to malaria in an era of declining malaria transmission. In *Parasitology* (Vol. 143, Issue 2, pp. 139–153). Cambridge University Press. https://doi.org/10.1017/S0031182015001249

Frazier, A. E., Dudek, J., Guiard, B., Voos, W., Li, Y., Lind, M., Meisinger, C., Geissler, A., Sickmann, A., Meyer, H. E., Bilanchone, V., Cumsky, M. G., Truscott, K. N., Pfanner, N., & Rehling, P. (2004). Pam16 has an essential role in the mitochondrial protein import motor. *Nature Structural and Molecular Biology*, *11*(3), 226–233. https://doi.org/10.1038/NSMB735;

Fry, M., & Beesley, J. E. (1991). Mitochondria of mammalian Plasmodium spp. *Parasitology*, *102*(1), 17–26. https://doi.org/10.1017/S0031182000060297

Gabriel, K., Egan, B., & Lithgow, T. (2003). Tom40, the import channel of the mitochondrial outer membrane, plays an active role in sorting imported proteins. *EMBO Journal*, *22*(10), 2380–2386. https://doi.org/10.1093/EMBOJ/CDG229,

Geli, V., & Glick, B. (1990). Mitochondrial protein import. *Journal of Bioenergetics and Biomembranes*, *22*(6), 725–751. https://doi.org/10.1007/BF00786928/METRICS

Gentle, I. E., Perry, A. J., Alcock, F. H., Likić, V. A., Dolezal, P., Ng, E. T., Purcell, A. W., McConnville, M., Naderer, T., Chanez, A. L., Charrière, F., Aschinger, C., Schneider, A., Tokatlidis, K., & Lithgow, T. (2007). Conserved motifs reveal details of ancestry and structure in the small TIM chaperones of the mitochondrial intermembrane space. *Molecular Biology and Evolution*, *24*(5), 1149–1160. https://doi.org/10.1093/MOLBEV/MSM031

Ghorbal, M., Gorman, M., MacPherson, C. R., Martins, R. M., Scherf, A., & Lopez-Rubio, J. J. (2014). Genome editing in the human malaria parasite Plasmodium falciparum using the CRISPR-Cas9 system. *Nature Biotechnology*, *32*(8), 819–821. https://doi.org/10.1038/nbt.2925

Glaser, E., & Dessi, P. (1999). Integration of the mitochondrial-processing peptidase into the cytochrome bc1 complex in plants. *Journal of Bioenergetics and Biomembranes*, *31*(3), 259–274. https://doi.org/10.1023/A:1005475930477,

Grau, G. E. R., & Craig, A. G. (2012). Cerebral malaria pathogenesis: Revisiting parasite and host contributions. In *Future Microbiology* (Vol. 7, Issue 2, pp. 291–302). Future Medicine Ltd. https://doi.org/10.2217/fmb.11.155

Gross, J., & Bhattacharya, D. (2009). Mitochondrial and plastid evolution in eukaryotes: An outsiders' perspective. *Nature Reviews Genetics*, *10*(7), 495–505. https://doi.org/10.1038/NRG2610

Grüring, C., Heiber, A., Kruse, F., Ungefehr, J., Gilberger, T. W., & Spielmann, T. (2011). Development and host cell modifications of Plasmodium falciparum blood stages in four dimensions. *Nature Communications*, *2*(1). https://doi.org/10.1038/ncomms1169

Habib, S. J., Neupert, W., & Rapaport, D. (2007). Analyses and Prediction of Mitochondrial Targeting Signals. *Methods in Cell Biology*, *80*, 761–781. https://doi.org/10.1016/S0091-679X(06)80035-X

Hawlitschek, G., Schneider, H., Schmidt, B., Tropschug, M., Hartl, F. U., & Neupert, W. (1988). Mitochondrial protein import: Identification of processing peptidase and of PEP, a processing enhancing protein. *Cell*, *53*(5), 795–806. https://doi.org/10.1016/0092-8674(88)90096-7,

Hemmer, C. J., Holst, F. G. E., Kern, P., Chiwakata, C. B., Dietrich, M., & Reisinger, E. C. (2006). Stronger host response per parasitized erythrocyte in Plasmodium vivax or ovale than in Plasmodium falciparum malaria. *Tropical Medicine and International Health*, *11*(6), 817–823. https://doi.org/10.1111/j.1365-3156.2006.01635.x

Hill, K., Model, K., Ryan, M. T., Dietmeier, K., Martint, F., Wagner, R., & Pfanner, N. (1998). Tom40 forms the hydrophilic channel of the mitochondrial import pore for preproteins. *Nature*, *395*(6701), 516–521. https://doi.org/10.1038/26780,

Hino, A., Hirai, M., Tanaka, T. Q., Watanabe, Y. I., Matsuoka, H., & Kita, K. (2012). Critical roles of the mitochondrial complex II in oocyst formation of rodent malaria parasite Plasmodium berghei. *Journal of Biochemistry*, *152*(3), 259–268. https://doi.org/10.1093/JB/MVS058

Homberg, B., Rehling, P., & Cruz-Zaragoza, L. D. (2023). The multifaceted mitochondrial OXA insertase. *Trends in Cell Biology*, *33*(9), 765–772. https://doi.org/10.1016/J.TCB.2023.02.001

Hoppins, S. C., & Nargang, F. E. (2004). The Tim8-Tim13 Complex of Neurospora crassa Functions in the Assembly of Proteins into Both Mitochondrial Membranes. *Journal of Biological Chemistry*, *279*(13), 12396–12405. https://doi.org/10.1074/JBC.M313037200

Horst, M., Oppliger, W., Rospert, S., Schönfeld, H. J., Schatz, G., & Azem, A. (1997). Sequential action of two hsp70 complexes during protein import into mitochondria. *The EMBO Journal*, *16*(8), 1842. https://doi.org/10.1093/EMBOJ/16.8.1842

Hughes, C. S., Moggridge, S., Müller, T., Sorensen, P. H., Morin, G. B., & Krijgsveld, J. (2019). Single-pot, solid-phase-enhanced sample preparation for proteomics experiments. *Nature Protocols*, *14*(1), 68–85. https://doi.org/10.1038/S41596-018-0082-X,

Hulett, J. M., Lueder, F., Chan, N. C., Perry, A. J., Wolynec, P., Likić, V. A., Gooley, P. R., & Lithgow, T. (2008). The Transmembrane Segment of Tom20 Is Recognized by Mim1 for Docking to the Mitochondrial TOM Complex. *Journal of Molecular Biology*, *376*(3), 694–704. https://doi.org/10.1016/J.JMB.2007.12.021;

Hurt, E. C., Pesold-Hurt, B., & Schatz, G. (1984). The amino-terminal region of an imported mitochondrial precursor polypeptide can direct cytoplasmic dihydrofolate reductase into the mitochondrial matrix. *The EMBO Journal*, *3*(13), 3149–3156. https://doi.org/10.1002/J.1460-2075.1984.TB02272.X;WGROUP:STRING:EMBO

Hussin, N., Lim, Y. A. L., Goh, P. P., William, T., Jelip, J., & Mudin, R. N. (2020). Updates on malaria incidence and profile in Malaysia from 2013 to 2017. *Malaria Journal*, *19*(1). https://doi.org/10.1186/s12936-020-3135-x

Idro, R., Jenkins, N. E., & Newton, C. R. J. (2005). Pathogenesis, clinical features, and neurological outcome of cerebral malaria. *Lancet Neurology*, *4*(12), 827–840. https://doi.org/10.1016/S1474-4422(05)70247-7

Ieva, R., Schrempp, S. G., Opaliński, Ł., Wollweber, F., Höß, P., Heißwolf, A. K., Gebert, M., Zhang, Y., Guiard, B., Rospert, S., Becker, T., Chacinska, A., Pfanner, N., & vanderLaan, M. (2014). Mgr2 Functions as Lateral Gatekeeper for Preprotein Sorting in the Mitochondrial Inner Membrane. *Molecular Cell*, *56*(5), 641–652. https://doi.org/10.1016/J.MOLCEL.2014.10.010

Introini, V., Govendir, M. A., Rayner, J. C., Cicuta, P., & Bernabeu, M. (2022). Biophysical Tools and Concepts Enable Understanding of Asexual Blood Stage Malaria. *Frontiers in Cellular and Infection Microbiology*, *12*. https://doi.org/10.3389/FCIMB.2022.908241

John, C. C., Kutamba, E., Mugarura, K., & Opoka, R. O. (2010). Adjunctive therapy for cerebral malaria and other severe forms of Plasmodium falciparum malaria. *Expert Review of Anti-Infective Therapy*, *8*(9), 997–1008. https://doi.org/10.1586/ERI.10.90

Jores, T., Klinger, A., Groß, L. E., Kawano, S., Flinner, N., Duchardt-Ferner, E., Wöhnert, J., Kalbacher, H., Endo, T., Schleiff, E., & Rapaport, D. (2016). Characterization of the targeting signal in mitochondrial β-barrel proteins. *Nature Communications*, *7*. https://doi.org/10.1038/NCOMMS12036,

Joseph T Smith, J., Singha, U. K., Misra, S., & Chaudhuri, M. (2018). Divergent Small Tim Homologues Are Associated with TbTim17 and Critical for the Biogenesis of TbTim17 Protein Complexes in Trypanosoma brucei. *MSphere*, *3*(3), e00204-18. https://doi.org/10.1128/MSPHERE.00204-18

Kafsack, B. F. C., Rovira-Graells, N., Clark, T. G., Bancells, C., Crowley, V. M., Campino, S. G., Williams, A. E., Drought, L. G., Kwiatkowski, D. P., Baker, D. A., Cortés, A., & Llinás, M. (2014). A transcriptional switch underlies commitment to sexual development in malaria parasites. *Nature*, *507*(7491), 248–252. https://doi.org/10.1038/nature12920

Kalousek, F., Neupert, W., Omura, T., Schatz, G., & Schmitz, U. K. (1993). Uniform nomenclature for the mitochondrial peptidases cleaving precursors of mitochondrial proteins. *Trends in Biochemical Sciences*, *18*(7), 249. https://doi.org/10.1016/0968-0004(93)90174-L

Kang, P. J., Ostermann, J., Shilling, J., Neupert, W., Craig, E. A., & Pfanner, N. (1990). Requirement for hsp70 in the mitochondrial matrix for translocation and folding of precursor proteins. *Nature*, *348*(6297), 137–143. https://doi.org/10.1038/348137A0

Keeling, P. J., & Palmer, J. D. (2008). Horizontal gene transfer in eukaryotic evolution. *Nature Reviews Genetics*, *9*(8), 605–618. https://doi.org/10.1038/NRG2386

Kiebler, M., Pfaller, R., Söllner, T., Griffiths, G., Horstmann, H., Pfanner, N., & Neupert, W. (1990). Identification of a mitochondrial receptor complex required for recognition and

membrane insertion of precursor proteins. *Nature*, *348*(6302), 610–616. https://doi.org/10.1038/348610A0;KWRD=SCIENCE

Killeen, G. F., Tatarsky, A., Diabate, A., Chaccour, C. J., Marshall, J. M., Okumu, F. O., Brunner, S., Newby, G., Williams, Y. A., Malone, D., Tusting, L. S., & Gosling, R. D. (2017). Developing an expanded vector control toolbox for malaria elimination. *BMJ Global Health*, *2*(2). https://doi.org/10.1136/BMJGH-2016-000211

Koehler, C. M. (2000). Protein translocation pathways of the mitochondrion. *FEBS Lett.*, *476*, 27–31.

Kotepui, M., Kotepui, K. U., Milanez, G. D., & Masangkay, F. R. (2020). Global prevalence and mortality of severe Plasmodium malariae infection: A systematic review and meta-analyses. *Malaria Journal*, *19*(1). https://doi.org/10.1186/s12936-020-03344-z

Kovermann, P., Truscott, K. N., Guiard, B., Rehling, P., Sepuri, N. B., Müller, H., Jensen, R. E., Wagner, R., & Pfanner, N. (2002). Tim22, the essential core of the mitochondrial protein insertion complex, forms a voltage-activated and signal-gated channel. *Molecular Cell*, *9*(2), 363–373. https://doi.org/10.1016/S1097-2765(02)00446-X

Krishna, S., Wailer, D. W., Ter Kuile, F., Kwiatkowski, D., Crawley, J., Craddock, C. F. C., Nosten, F., Chapman, D., Brewster, D., Holloway, P. A., & White, N. J. (1994). Lactic acidosis and hypoglycaemia in children with severe malaria: Pathophysiological and prognostic significance. *Transactions of the Royal Society of Tropical Medicine and Hygiene*, *88*(1), 67–73. https://doi.org/10.1016/0035-9203(94)90504-5

Krungkrai, J., Prapunwattana, P., & Krungkrai, S. R. (2000). Ultrastructure and function of mitochondria in gametocytic stage of Plasmodium falciparum. *Parasite*, *7*(1), 19–26. https://doi.org/10.1051/PARASITE/2000071019

Kutik, S., Stojanovski, D., Becker, L., Becker, T., Meinecke, M., Krüger, V., Prinz, C., Meisinger, C., Guiard, B., Wagner, R., Pfanner, N., & Wiedemann, N. (2008). Dissecting Membrane Insertion of Mitochondrial β-Barrel Proteins. *Cell*, *132*(6), 1011–1024. https://doi.org/10.1016/J.CELL.2008.01.028;

Laloraya, S., Gambill, B. D., & Craig, E. A. (1994). A role for a eukaryotic GrpE-related protein, Mgelp, in protein translocation. *Cell Biology*, *91*, 6481–6485. https://www.pnas.org

Lambros, C., & Vanderberg, J. P. (1979). Synchronization of Plasmodium falciparum erythrocytic stages in culture. *Journal of Parasitology*, *65*(3), 418–420. https://doi.org/10.2307/3280287

Leech, J. H., Barnwell, J. W., Aikawa, M., Miller, L. H., & Howard, R.]. (1995). *Plasmodium falciparum Malaria : Association of Knobs on the Surface of Infected Erythrocytes with a Histidine-rich Protein and the Erythrocyte Skeleton 1256*.

Lister, R., Carrie, C., Duncan, O., Ho, L. H. M., Howell, K. A., Murcha, M. W., & Whelan, J. (2007). Functional definition of outer membrane proteins involved in preprotein import

into mitochondria. *Plant Cell*, *19*(11), 3739–3759. https://doi.org/10.1105/TPC.107.050534

Lithgow, T., & Schneider, A. (2010). Evolution of macromolecular import pathways in mitochondria, hydrogenosomes and mitosomes. *Philosophical Transactions of the Royal Society B: Biological Sciences*, *365*(1541), 799–817. https://doi.org/10.1098/RSTB.2009.0167;

Lo, E., Yewhalaw, D., Zhong, D., Zemene, E., Degefa, T., Tushune, K., Ha, M., Lee, M. C., James, A. A., & Yan, G. (2015). Molecular epidemiology of Plasmodium vivax and Plasmodium falciparum malaria among duffy-positive and Duffy-negative populations in Ethiopia. *Malaria Journal*, *14*(1). https://doi.org/10.1186/s12936-015-0596-4

Mallo, N., Fellows, J., Johnson, C., & Sheiner, L. (2018). Protein Import into the Endosymbiotic Organelles of Apicomplexan Parasites. *Genes 2018, Vol. 9, Page 412*, *9*(8), 412. https://doi.org/10.3390/GENES9080412

Mani, J., Desy, S., Niemann, M., Chanfon, A., Oeljeklaus, S., Pusnik, M., Schmidt, O., Gerbeth, C., Meisinger, C., Warscheid, B., & Schneider, A. (2015). Mitochondrial protein import receptors in Kinetoplastids reveal convergent evolution over large phylogenetic distances. *Nature.ComJ Mani, S Desy, M Niemann, A Chanfon, S Oeljeklaus, M Pusnik, O Schmidt, C GerbethNature Communications, 2015•nature.Com*, *6*. https://doi.org/10.1038/ncomms7646

Mayer, M. P., & Bukau, B. (2005). Hsp70 chaperones: Cellular functions and molecular mechanism. *Cellular and Molecular Life Sciences*, *62*(6), 670–684. https://doi.org/10.1007/S00018-004-4464-6,

Milner, D. A. (2018). Malaria pathogenesis. *Cold Spring Harbor Perspectives in Medicine*, *8*(1). https://doi.org/10.1101/cshperspect.a025569

Mokranjac, D., & Neupert, W. (2015). Cell biology: Architecture of a protein entry gate. *Nature*, *528*(7581), 201–202. https://doi.org/10.1038/NATURE16318;SUBJMETA=45,535,631,80;KWRD=BIOCHEMISTRY,CELL+BIOLOGY,STRUCTURAL+BIOLOGY

Moody, A. (2002). Rapid diagnostic tests for malaria parasites. *Clinical Microbiology Reviews*, *15*(1), 66–78. https://doi.org/10.1128/CMR.15.1.66-78.2002

Moreno-Pérez, D. A., Ruíz, J. A., & Patarroyo, M. A. (2013). Reticulocytes: Plasmodium vivax target cells. In *Biology of the Cell* (Vol. 105, Issue 6, pp. 251–260). https://doi.org/10.1111/boc.201200093

Mota, M. M., Vanderberg, J. P., R Hafalla, J. C., Frevert, U., & Nussenmeig, V. (1997). Migration of Plasmodium Sporozoites Through Cells Before Infection. In *P. Fatt, I. Neurophysiol* (Vol. 20). www.sciencemag.org/cgi/content/fulV291/5501/138/

Murphy, M. P., Leuenberger, D., Curran, S. P., Oppliger, W., & Koehler, C. M. (2001). The Essential Function of the Small Tim Proteins in the TIM22 Import Pathway Does Not

Depend on Formation of the Soluble 70-Kilodalton Complex. *Molecular and Cellular Biology*, *21*(18), 6132–6138. https://doi.org/10.1128/MCB.21.18.6132-6138.2001

Murphy, S. C., & Breman, J. G. (2001). GAPS in the childhood malaria burden in Africa: Cerebral malaria, neurological sequelae, anemia, respiratory distress, hypoglycemia, and complications of pregnancy. *American Journal of Tropical Medicine and Hygiene*, *64*(1-2 SUPPL.), 57–67. https://doi.org/10.4269/AJTMH.2001.64.57

Murray, C. K., Gasser, R. A., Magill, A. J., & Miller, R. S. (2008). Update on rapid diagnostic testing for malaria. *Clinical Microbiology Reviews*, *21*(1), 97–110. https://doi.org/10.1128/CMR.00035-07

Nagaraj, V. A., Arumugam, R., Prasad, D., Rangarajan, P. N., & Padmanaban, G. (2010). Protoporphyrinogen IX oxidase from Plasmodium falciparum is anaerobic and is localized to the mitochondrion. *Molecular and Biochemical Parasitology*, *174*(1), 44–52. https://doi.org/10.1016/J.MOLBIOPARA.2010.06.012

Nagaraj, V. A., Prasad, D., Arumugam, R., Rangarajan, P. N., & Padmanaban, G. (2010). Characterization of coproporphyrinogen III oxidase in Plasmodium falciparum cytosol. *Parasitology International*, *59*(2), 121–127. https://doi.org/10.1016/J.PARINT.2009.12.001

Naing, C., Whittaker, M. A., Nyunt Wai, V., & Mak, J. W. (2014). Is Plasmodium vivax Malaria a Severe Malaria?: A Systematic Review and Meta-Analyses. *PLoS Neglected Tropical Diseases*, *8*(8). https://doi.org/10.1371/journal.pntd.0003071

Nair, S. C., Munro, J. T., Mann, A., Llinás, M., & Prigge, S. T. (2023). The mitochondrion of Plasmodium falciparum is required for cellular acetyl-CoA metabolism and protein acetylation. *Proceedings of the National Academy of Sciences of the United States of America*, *120*(17), e2210929120. https://doi.org/10.1073/PNAS.2210929120/SUPPL_FILE/PNAS.2210929120.SD02.XLSX

Naoé, M., Ohwa, Y., Ishikawa, D., Ohshima, C., Nishikawa, S. I., Yamamoto, H., & Endo, T. (2004). Identification of Tim40 that mediates protein sorting to the mitochondrial intermembrane space. *Journal of Biological Chemistry*, *279*(46), 47815–47821. https://doi.org/10.1074/JBC.M410272200;

Neupert, W. (1997). Protein import into mitochondria. *Annual Review of Biochemistry*, *66*, 863–917. https://doi.org/10.1146/ANNUREV.BIOCHEM.66.1.863

Okamoto, K., Brinker, A., Paschen, S. A., Moarefi, I., Hayer-Hartl, M., Neupert, W., & Brunner, M. (2002). The protein import motor of mitochondria: A targeted molecular ratchet driving unfolding and translocation. *EMBO Journal*, *21*(14), 3659–3671. https://doi.org/10.1093/EMBOJ/CDF358

Painter, H. J., Morrisey, J. M., Mather, M. W., & Vaidya, A. B. (2007). Specific role of mitochondrial electron transport in blood-stage Plasmodium falciparum. *Nature*, *446*(7131), 88–91. https://doi.org/10.1038/NATURE05572

Paschen, S. A., & Neupert, W. (2001). Protein import into mitochondria. *IUBMB Life*, *52*, 101–112.

Paschen, S. A., Rothbauer, U., Káldi, K., Bauer, M. F., Neupert, W., & Brunner, M. (2000). The role of the TIM8-13 complex in the import of Tim23 into mitochondria. *EMBO Journal*, *19*(23), 6392–6400. https://doi.org/10.1093/EMBOJ/19.23.6392

Paschen, S. A., Waizenegger, T., Stan, T., Preuss, M., Cyrklaff, M., Hell, K., Rapaport, D., & Neupert, W. (2003). Evolutionary conservation of biogenesis of β-barrel membrane proteins. *Nature*, *426*(6968), 862–866. https://doi.org/10.1038/NATURE02208

Patakottu, B. R., Singh, P. K., Malhotra, P., Chauhan, V. S., & Patankar, S. (2012). In vivo analyses of translation initiation sites in Plasmodium falciparum. *Molecular Biology Reports*, *39*(3), 2225–2232. https://doi.org/10.1007/S11033-011-0971-3/TABLES/3

Pfanner, N., Warscheid, B., & Wiedemann, N. (2019). Mitochondrial proteins: from biogenesis to functional networks. In *Nature Reviews Molecular Cell Biology* (Vol. 20, Issue 5, pp. 267–284). Nature Publishing Group. https://doi.org/10.1038/s41580-018-0092-0

Popov-Čeleketić, J., Waizenegger, T., & Rapaport, D. (2008). Mim1 Functions in an Oligomeric Form to Facilitate the Integration of Tom20 into the Mitochondrial Outer Membrane. *Journal of Molecular Biology*, *376*(3), 671–680. https://doi.org/10.1016/J.JMB.2007.12.006

Pusnik, M., Mani, J., Schmidt, O., Niemann, M., Oeljeklaus, S., Schnarwiler, F., Warscheid, B., Lithgow, T., Meisinger, C., & Schneider, A. (2012). An essential novel component of the noncanonical mitochondrial outer membrane protein import system of trypanosomatids. *Molecular Biology of the Cell*, *23*(17), 3420–3428. https://doi.org/10.1091/MBC.E12-02-0107

Qiu, J., Wenz, L. S., Zerbes, R. M., Oeljeklaus, S., Bohnert, M., Stroud, D. A., Wirth, C., Ellenrieder, L., Thornton, N., Kutik, S., Wiese, S., Schulze-Specking, A., Zufall, N., Chacinska, A., Guiard, B., Hunte, C., Warscheid, B., Van Der Laan, M., Pfanner, N., … Becker, T. (2013). XCoupling of mitochondrial import and export translocases by receptor-mediated supercomplex formation. *Cell*, *154*(3). https://doi.org/10.1016/j.cell.2013.06.033

Ranson, H., & Lissenden, N. (2016). Insecticide Resistance in African Anopheles Mosquitoes: A Worsening Situation that Needs Urgent Action to Maintain Malaria Control. *Trends in Parasitology*, *32*(3), 187–196. https://doi.org/10.1016/j.pt.2015.11.010

Rapaport, D., Neupert, W., & Lill, R. (1997). Mitochondrial protein import. Tom40 plays a major role in targeting and translocation of preproteins by forming a specific binding site for the presequence. *Journal of Biological Chemistry*, *272*(30), 18725–18731. https://doi.org/10.1074/JBC.272.30.18725

Rimmer, K. A., Foo, J. H., Ng, A., Petrie, E. J., Shilling, P. J., Perry, A. J., Mertens, H. D. T., Lithgow, T., Mulhern, T. D., & Gooley, P. R. (2011). Recognition of mitochondrial targeting sequences by the import receptors Tom20 and Tom22. *Journal of Molecular Biology*, *405*(3), 804–818. https://doi.org/10.1016/J.JMB.2010.11.017

Roise, D., Horvath, S. J., Tomich, J. M., Richards, J. H., & Schatz, G. (1986). A chemically synthesized pre-sequence of an imported mitochondrial protein can form an amphiphilic helix and perturb natural and artificial phospholipid bilayers. *The EMBO Journal*, *5*(6), 1327–1334. https://doi.org/10.1002/J.1460-2075.1986.TB04363.X,

Schmidt, O., Pfanner, N., & Meisinger, C. (2010). Mitochondrial protein import: From proteomics to functional mechanisms. In *Nature Reviews Molecular Cell Biology* (Vol. 11, Issue 9, pp. 655–667). https://doi.org/10.1038/nrm2959

Schneider, H. C., Westermann, B., Neupert, W., & Brunner, M. (1996). The nucleotide exchange factor MGE exerts a key function in the ATP-dependent cycle of mt-Hsp70-Tim44 interaction driving mitochondrial protein import. *EMBO Journal*, *15*(21), 5796–5803. https://doi.org/10.1002/J.1460-2075.1996.TB00966.X

Seesui, K., Imtawil, K., Chanetmahun, P., Laummaunwai, P., & Boonmars, T. (2018). An Alternative Method for Extracting Plasmodium DNA from EDTA Whole Blood for Malaria Diagnosis. *The Korean Journal of Parasitology*, *56*(1), 25. https://doi.org/10.3347/KJP.2018.56.1.25

Setoguchi, K., Otera, H., & Mihara, K. (2006). Cytosolic factor- and TOM-independent import of C-tail-anchored mitochondrial outer membrane proteins. *The EMBO Journal*, *25*(24), 5635. https://doi.org/10.1038/SJ.EMBOJ.7601438

Shikani, H. J., Freeman, B. D., Lisanti, M. P., Weiss, L. M., Tanowitz, H. B., & Desruisseaux, M. S. (2012). Cerebral malaria: We have come a long way. *American Journal of Pathology*, *181*(5), 1484–1492. https://doi.org/10.1016/j.ajpath.2012.08.010

Shiota, T., Imai, K., Qiu, J., Hewitt, V. L., Tan, K., Shen, H. H., Sakiyama, N., Fukasawa, Y., Hayat, S., Kamiya, M., Elofsson, A., Tomii, K., Horton, P., Wiedemann, N., Pfanner, N., Lithgow, T., & Endo, T. (2015). Molecular architecture of the active mitochondrial protein gate. *Science*, *349*(6255), 1544–1548. https://doi.org/10.1126/SCIENCE.AAC6428

Sinclair, D., Donegan, S., Isba, R., & Lalloo, D. G. (2012). Artesunate versus quinine for treating severe malaria. *Cochrane Database of Systematic Reviews*, *2019*(5). https://doi.org/10.1002/14651858.CD005967.PUB4

Singer, M., Marshall, J., Heiss, K., Mair, G. R., Grimm, D., Mueller, A. K., & Frischknecht, F. (2015). Zinc finger nuclease-based double-strand breaks attenuate malaria parasites and reveal rare microhomology-mediated end joining. *Genome Biology*, *16*(1). https://doi.org/10.1186/S13059-015-0811-1

Sirrenberg, C., Bauer, M. F., Guiard, B., Neupert, W., & Brunner, M. (1996). Import of carrier proteins into the mitochondrial inner membrane mediated by Tim22. *Nature*, *384*(6609), 582–585. https://doi.org/10.1038/384582A0,

Sirrenberg, C., Endres, M., Folsch, H., Stuart, R. A., Neupert, W., & Brunner, M. (1998). Carrier protein import into mitochondria mediated by the intermembrane proteins Tim10/Mrs11 and Tim12/Mrs5. *Nature*, *391*(6670), 912–915. https://doi.org/10.1038/36136

Slomianny, C., & Prensier, G. (1986). Application of the serial sectioning and tridimensional reconstruction techniques to the morphological study of the Plasmodium falciparum mitochondrion. *Journal of Parasitology*, *72*(4), 595–598. https://doi.org/10.2307/3281516

Smith, J. D., Rowe, J. A., Higgins, M. K., & Lavstsen, T. (2013). Malaria's deadly grip: Cytoadhesion of Plasmodium falciparum-infected erythrocytes. In *Cellular Microbiology* (Vol. 15, Issue 12, pp. 1976–1983). https://doi.org/10.1111/cmi.12183

Spinelli, J. B., & Haigis, M. C. (2018). The multifaceted contributions of mitochondria to cellular metabolism. *Nature Cell Biology*, *20*(7), 745–754. https://doi.org/10.1038/S41556-018-0124-1,

Stanway, R. R., Mueller, N., Zobiak, B., Graewe, S., Froehlke, U., Zessin, P. J. M., Aepfelbacher, M., & Heussler, V. T. (2011). Organelle segregation into Plasmodium liver stage merozoites. *Cellular Microbiology*, *13*(11), 1768–1782. https://doi.org/10.1111/j.1462-5822.2011.01657.x

Stauffer, W. M., Cartwright, C. P., Olson, D. A., Juni, B. A., Taylor, C. M., Bowers, S. H., Hanson, K. L., Rosenblatt, J. E., & Boulware, D. R. (2009). Diagnostic performance of rapid diagnostic tests versus blood smears for malaria in US clinical practice. *Clinical Infectious Diseases*, *49*(6), 908–913. https://doi.org/10.1086/605436

Stojanovski, D., Bohnert, M., Pfanner, N., & van der Laan, M. (2012). Mechanisms of protein sorting in mitochondria. *Cold Spring Harbor Perspectives in Biology*, *4*(10). https://doi.org/10.1101/CSHPERSPECT.A011320

Stoldt, S., Wenzel, D., Hildenbeutel, M., Wurm, C. A., Herrmann, J. M., & Jakobs, S. (2012). The inner-mitochondrial distribution of Oxa1 depends on the growth conditions and on the availability of substrates. *Molecular Biology of the Cell*, *23*(12), 2292–2301. https://doi.org/10.1091/MBC.E11-06-0538/ASSET/IMAGES/LARGE/2292FIG6.JPEG

Straimer, J., Lee, M. C. S., Lee, A. H., Zeitler, B., Williams, A. E., Pearl, J. R., Zhang, L., Rebar, E. J., Gregory, P. D., Llinás, M., Urnov, F. D., & Fidock, D. A. (2012). Site-specific genome editing in Plasmodium falciparum using engineered zinc-finger nucleases. *Nature Methods*, *9*(10), 993–998. https://doi.org/10.1038/NMETH.2143

Tavares, J., Formaglio, P., Thiberge, S., Mordelet, E., Van Rooijen, N., Medvinsky, A., Ménard, R., & Amino, R. (2013). Role of host cell traversal by the malaria sporozoite during liver

infection. *Journal of Experimental Medicine*, *210*(5), 905–915. https://doi.org/10.1084/jem.20121130

Taylor, W. R. J., Hanson, J., Turner, G. D. H., White, N. J., & Dondorp, A. M. (2012). Respiratory manifestations of malaria. *Chest*, *142*(2), 492–505. https://doi.org/10.1378/chest.11-2655

Trager, W., & Jensen, J. B. (1976). Human malaria parasites in continuous culture. *Science*, *193*(4254), 673–675. https://doi.org/10.1126/SCIENCE.781840,

Truscott, K. N., Wiedemann, N., Rehling, P., Müller, H., Meisinger, C., Pfanner, N., & Guiard, B. (2002). Mitochondrial Import of the ADP/ATP Carrier: the Essential TIM Complex of the Intermembrane Space Is Required for Precursor Release from the TOM Complex. *Molecular and Cellular Biology*, *22*(22), 7780–7789. https://doi.org/10.1128/MCB.22.22.7780-7789.2002

Ulrich, T., Oberhettinger, P., Schütz, M., Holzer, K., Ramms, A. S., Linke, D., Autenrieth, I. B., & Rapaport, D. (2014). Evolutionary conservation in biogenesis of β-barrel proteins allows mitochondria to assemble a functional bacterial trimeric autotransporter protein. *Journal of Biological Chemistry*, *289*(43), 29457–29470. https://doi.org/10.1074/jbc.M114.565655

Vaidya, A. B., & Mather, M. W. (2009). Mitochondrial evolution and functions in malaria parasites. *Annual Review of Microbiology*, *63*, 249–267. https://doi.org/10.1146/ANNUREV.MICRO.091208.073424

Van Dooren, G. G., Marti, M., Tonkin, C. J., Stimmler, L. M., Cowman, A. F., & McFadden, G. I. (2005). Development of the endoplasmic reticulum, mitochondrion and apicoplast during the asexual life cycle of Plasmodium falciparum. *Molecular Microbiology*, *57*(2), 405–419. https://doi.org/10.1111/J.1365-2958.2005.04699.X

Van Dooren, G. G., Stimmler, L. M., & McFadden, G. I. (2006). Metabolic maps and functions of the Plasmodium mitochondrion. *FEMS Microbiology Reviews*, *30*(4), 596–630. https://doi.org/10.1111/J.1574-6976.2006.00027.X

Van Dooren, G. G., Yeoh, L. M., Striepen, B., & McFadden, G. I. (2016). The Import of Proteins into the Mitochondrion of Toxoplasma gondii. *The Journal of Biological Chemistry*, *291*(37), 19335. https://doi.org/10.1074/JBC.M116.725069

Varo, R., Chaccour, C., & Bassat, Q. (2020). Update on malaria. In *Medicina Clinica* (Vol. 155, Issue 9, pp. 395–402). Ediciones Doyma, S.L. https://doi.org/10.1016/j.medcli.2020.05.010

Veiga, M. I., Dhingra, S. K., Henrich, P. P., Straimer, J., Gnädig, N., Uhlemann, A. C., Martin, R. E., Lehane, A. M., & Fidock, D. A. (2016). Globally prevalent PfMDR1 mutations modulate Plasmodium falciparum susceptibility to artemisinin-based combination therapies. *Nature Communications*, *7*. https://doi.org/10.1038/NCOMMS11553

Venugopal, K., Hentzschel, F., Valkiūnas, G., & Marti, M. (2020). Plasmodium asexual growth and sexual development in the haematopoietic niche of the host. In *Nature Reviews Microbiology* (Vol. 18, Issue 3, pp. 177–189). Nature Research. https://doi.org/10.1038/s41579-019-0306-2

Vögtle, F. N., Wortelkamp, S., Zahedi, R. P., Becker, D., Leidhold, C., Gevaert, K., Kellermann, J., Voos, W., Sickmann, A., Pfanner, N., & Meisinger, C. (2009). Global Analyses of the Mitochondrial N-Proteome Identifies a Processing Peptidase Critical for Protein Stability. *Cell*, *139*(2), 428–439. https://doi.org/10.1016/J.CELL.2009.07.045

Voos, W. (2009). Mitochondrial protein homeostasis: the cooperative roles of chaperones and proteases. *Research in Microbiology*, *160*(9), 718–725. https://doi.org/10.1016/j.resmic.2009.08.003

Voos, W. (2013). Chaperone–protease networks in mitochondrial protein homeostasis. *Biochimica et Biophysica Acta (BBA) - Molecular Cell Research*, *1833*(2), 388–399. https://doi.org/10.1016/J.BBAMCR.2012.06.005

Voos, W., Gambill, B. D., Laloraya, S., Ang, D., Craig, E. A., & Pfanner, N. (1994). Mitochondrial GrpE is present in a complex with hsp70 and preproteins in transit across membranes. *Molecular and Cellular Biology*, *14*(10), 6627–6634. https://doi.org/10.1128/MCB.14.10.6627-6634.1994

Wagner, J. C., Platt, R. J., Goldfless, S. J., Zhang, F., & Niles, J. C. (2014). Efficient CRISPR-Cas9-mediated genome editing in Plasmodium falciparum. *Nature Methods*, *11*(9), 915–918. https://doi.org/10.1038/NMETH.3063

Walliker, D., Quakyi, I. A., Wellems, T. E., McCutchan, T. F., Szarfman, A., London, W. T., Corcoran, L. M., Burkot, T. R., & Carter, R. (1987). Genetic analyses of the human malaria parasite Plasmodium falciparum. *Science*, *236*(4809), 1661–1666. https://doi.org/10.1126/SCIENCE.3299700,

Walther, D. M., Papic, D., Bos, M. P., Tommassen, J., & Rapaport, D. (2009). Signals in bacterial β-barrel proteins are functional in eukaryotic cells for targeting to and assembly in mitochondria. *Proceedings of the National Academy of Sciences of the United States of America*, *106*(8), 2531–2536. https://doi.org/10.1073/PNAS.0807830106;

Walther, D. M., Rapaport, D., & Tommassen, J. (2009). Biogenesis of β-barrel membrane proteins in bacteria and eukaryotes: evolutionary conservation and divergence. *Cellular and Molecular Life Sciences: CMLS*, *66*(17), 2789. https://doi.org/10.1007/S00018-009-0029-Z

Weiland, A. S. (2023). Recent Advances in Imported Malaria Pathogenesis, Diagnosis, and Management. *Current Emergency and Hospital Medicine Reports*, *11*(2), 49–57. https://doi.org/10.1007/s40138-023-00264-5

Wenz, L. S., Ellenrieder, L., Qiu, J., Bohnert, M., Zufall, N., van der Laan, M., Pfanner, N., Wiedemann, N., & Becker, T. (2015). Sam37 is crucial for formation of the mitochondrial TOM-SAM supercomplex, thereby promoting ß-barrel biogenesis. *Journal of Cell Biology*, *210*(7), 1047–1054. https://doi.org/10.1083/JCB.201504119,

Westermann, B., Prip-Buus, C., Neupert, W., & Schwarz, E. (1995). The role of the GrpE homologue, Mge1p, in mediating protein import and protein folding in mitochondria. *EMBO Journal*, *14*(14), 3452–3460. https://doi.org/10.1002/J.1460-2075.1995.TB07351.X

Wezena, C. A., Alisch, R., Golzmann, A., Liedgens, L., Staudacher, V., Pradel, G., & Deponte, M. (2017). The cytosolic glyoxalases of *Plasmodium falciparum* are dispensable during asexual blood-stage development. *Microbial cell (Graz, Austria)*, *5*(1), 32–41. https://doi.org/10.15698/mic2018.01.608

White, N. J. (2018). Anaemia and malaria. *Malaria Journal*, *17*(1), 371. https://doi.org/10.1186/S12936-018-2509-9

WHO guidelines for malaria, 30 November 2024. (2024). https://doi.org/10.2471/B09146

Wiedemann, N., Kozjak, V., Chacinska, A., Schönfisch, B., Rospert, S., Ryan, M. T., Pfanner, N., & Meisinger, C. (2003). Machinery for protein sorting and assembly in the mitochondrial outer membrane. *Nature*, *424*(6948), 565–571. https://doi.org/10.1038/NATURE01753;

Wiedemann, N., & Pfanner, N. (2017). Mitochondrial machineries for protein import and assembly. *Annual Review of Biochemistry*, *86*, 685–714. https://doi.org/10.1146/ANNUREV-BIOCHEM-060815-014352

Wiedemann, N., & Pfanner, N. (2024). *BI86CH28-Pfanner ARI Mitochondrial Machineries for Protein Import and Assembly BI86CH28-Pfanner ARI*. 19. https://doi.org/10.1146/annurev

World Health Organization (2023).

Wu, C. C., Naveen, V., Chien, C. H., Chang, Y. W., & Hsiaos, C. D. (2012). Crystal structure of DnaK protein complexed with nucleotide exchange factor GrpE in DnaK chaperone system: Insight into intermolecular communication. *Journal of Biological Chemistry*, *287*(25), 21461–21470. https://doi.org/10.1074/JBC.M112.344358/ATTACHMENT/F945EFE7-0C2C-4616-B2BB-461E827B8781/MMC1.PDF

Zarsky, V., Tachezy, J., & Dolezal, P. (2012). Tom40 is likely common to all mitochondria. *Current Biology*, *22*(12). https://doi.org/10.1016/J.CUB.2012.03.057

Zimmerman, G. A., & Castro-Faria-Neto, H. (2010). Persistent cognitive impairment after cerebral malaria: Models, mechanisms and adjunctive therapies. *Expert Review of Anti-Infective Therapy*, *8*(11), 1209–1212. https://doi.org/10.1586/ERI.10.117

***Curriculum vitae* – Felix Alexander Ayelazuno**

Personal Details

Surname/first name	Ayelazuno, Felix Alexander
Titles/degrees	M.Sc., B.Sc.
E-mail	ayelazunofelix@gmail.com
Current position/status:	Cand. Dr. rer. nat. at the RPTU Kaiserslautern

Education

2020 – 2025	**PhD** Molecular Parasitology- RPTU Kaiserslautern
2015 – 2017	**M.Sc.** Molecular Cell Biology of Infectious Disease University of Ghana, Legon CGPA: 3.39 out of 4.00
2015 – 2014	**B.Sc.** Biochemistry Kwame Nkrumah University of Science and Technology Second class upper, CWA: 63.84